

Summer–Fall Habitat Actions for Delta Smelt—Report on Effectiveness of Actions Taken Between 2011 and 2024



State of California
California Natural Resources Agency



Department of Water Resources

The Delta Coordination Group Science
and Monitoring Work Group

April 2026

Summer–Fall Habitat Actions for Delta Smelt—Report on Effectiveness of Actions Taken Between 2011 and 2024

California Department of Water Resources

Prepared by:
The Delta Coordination Group Science
and Monitoring Work Group

Contributing Authors:

- Rosemary Hartman, California Department of Water Resources
- Brittany Davis, California Department of Water Resources
- Trinh Nguyen, California Department of Fish and Wildlife
- Celeste Dodge, California Department of Fish and Wildlife
- Trishelle Tempel, California Department of Water Resources
- Daniel O’Donnell, California Department of Fish and Wildlife
- Nick Rasmussen, California Department of Water Resources
- Lily Tomkovic, California Department of Water Resources
- John Schiff, Contra Costa Water District
- Shey Rajagopal, California Department of Water Resources
- Shawn Acuña, Metropolitan Water District
- Eli Ateljevich, California Department of Water Resources
- Christina Burdi, California Department of Water Resources
- Ching-Fu Chang, Contra Costa Water District

Acknowledgments for review and assistance to:

- April Hennessy, California Department of Fish and Wildlife
- Gabriel Ng, California Department of Fish and Wildlife
- Steve Micko, Metropolitan Water District
- Kristi Arend, US Fish and Wildlife Service

Acknowledgments

This report could not have been written without the tireless work of countless scientists from the Interagency Ecological Program, UC Davis, ICF International, Inc., and many others. In particular, we would like to thank the staff of the California Department of Fish and Wildlife (CDFW) (Stockton) who run the Summer Townet Survey, Fall Midwater Trawl, Spring Kodiak Trawl, 20 mm Survey, Diet and Condition Study, and EMP Zooplankton Survey. We would also like to thank the staff of the US Fish and Wildlife Service (USFWS; Lodi office) who run the Delta Juvenile Fish Monitoring Program and Enhanced Delta Smelt Monitoring Program. Special thanks also go to Will Smith, Leo Polansky, and Matt Nobriga of the USFWS for their invaluable assistance in developing and sharing the Delta Smelt Life Cycle Model and Delta Smelt Bioenergetics Model. We would like to thank Drs. Bruce Hammock and Levi Lewis for generously sharing their data on Delta smelt health and growth rates. We would like to thank Brian Mahardja, Leo Polansky, Will Smith, Louise Conrad, Gabriel Ng, Michael Eakin, and Bruce Hammock for their helpful reviews on earlier drafts of this document.

Executive Summary

This report describes the science behind the Delta Smelt Summer–Fall Habitat Action (SFHA), including Fall X2 and the operation of the Suisun Marsh Salinity Control Gates (SMSCG). It provides a weight-of-evidence approach to evaluate the effectiveness of the actions intended to improve Delta smelt habitat, survival, and recruitment. The overall finding of this report supports recent findings of the USFWS life cycle model; **higher Delta outflow and lower salinity in Suisun Bay and Suisun Marsh during summer showed stronger correlations to improved Delta smelt condition and survival than higher outflow and lower salinity during fall.** Specific findings for X2 (i.e., the distance from the Golden Gate Bridge to location of 2 PSU) and SMSCG operations to habitat, food supply, and Delta smelt growth are as follows:

Lower X2 and SMSCG operation increased Delta smelt physical habitat availability in both summer and fall.

- Suisun Bay and Grizzly Bay provide higher turbidity and cooler temperatures than upstream regions and become most accessible to Delta smelt at lower X2 values.
- Suisun Marsh provides higher turbidity than upstream regions, though temperatures may be either warmer or cooler, depending on the year. Low Salinity Zone (LSZ) habitat in Suisun Marsh can be increased with either lower X2 or SMSCG operations, though SMSCG operations are more effective when salinity is not already low.
- SMSCG operations only increase LSZ habitat in Grizzly Bay when combined with an X2 action or when salinity is already low.
- SMSCG operations also decrease chlorophyll concentration in Montezuma Slough.

Lower X2 and SMSCG operations also increase Delta smelt food supply in the LSZ, though this effect is greater in summer than in fall.

- The calanoid copepod *Pseudodiaptomus* spp. dominates Delta smelt diets during the summer and fall, and abundances of *Pseudodiaptomus* spp. in the LSZ increase with increased flow.
- Abundance of *Pseudodiaptomus* spp. is generally greater in upstream regions (i.e., Sacramento River) than in Suisun Bay or Suisun Marsh, except at very high-flow conditions.
- Average abundance of *Pseudodiaptomus* spp. peaks in June and July in all regions and at all levels of outflow. Therefore, decreased X2 during summer has a greater potential to transport *Pseudodiaptomus* spp. into the LSZ than during fall.

- Higher outflow conditions result in greater abundances of *Pseudodiaptomus* spp. than would be expected from lower salinity alone.
- Existing zooplankton biomass in Suisun Bay is generally much less than what would cause food saturation for Delta smelt. Any increase in zooplankton will increase Delta smelt growth. Bioenergetic modeling suggests it would take a 50% increase in both adult and juvenile *Pseudodiaptomus* spp. across the entire summer–fall time period to increase the growth of Delta smelt by a total of 0.1 g.

Delta smelt growth rates were generally higher with lower X2 in summer, but there was no relationship in fall, and the relationship between smelt condition and X2 was mixed.

- Delta smelt liver weights increased with lower X2 at higher temperatures (such as seen in summer) but not at lower temperatures (such as seen in fall). Higher weights are suggestive of better health.
- There was a significant relationship between higher growth rates (based on otoliths) and lower average X2 in summer but not in fall.
- There was a significant relationship between higher growth rate potential (using the bioenergetic model) and lower average X2 in summer but not in fall.
- Limitations on growth rate potential varied between seasons and from year to year, but changes in zooplankton drove most of the differences between years in summer, with higher growth rates associated with higher zooplankton density.
- 2011 was a particularly good year for Delta smelt, due to the combination of higher flows, higher zooplankton, and cooler temperatures.

These findings support work from Polansky et al. (2024), which used a life cycle model to demonstrate that high outflow in summer was the strongest predictor of summer survival and positive population growth. This report uses more recent data to explore potential mechanisms behind that finding and identifies higher food availability in summer as more important than area of appropriate habitat in predicting Delta smelt condition and growth rate. However, years when cool temperatures, high zooplankton availability, and high summer outflow all overlap (such as 2011) show the highest Delta smelt condition, growth, and survival. As the climate continues to change, conditions like those in 2011 will likely become less frequent.

Contents

Acknowledgments	iii
Background	1
Scientific Basis	1
Regulations	3
Implementation of Actions	4
Analysis to Date	5
Fall Flow	5
Suisun Marsh	8
Population Models	8
Hypotheses	9
Smelt Habitat	11
Introduction	11
Hypotheses	13
Methods	13
Continuous Water Quality	13
Aquatic Vegetation	18
Habitat Area Modeling	19
Chlorophyll	21
Results	22
Continuous Water Quality	22
Aquatic Vegetation	28
Habitat Area Modeling	29
Chlorophyll	34
Discussion	38
Temperature, Turbidity, Salinity	38
Aquatic Vegetation	40
Chlorophyll	40
Conclusions	41
Smelt Food	44
Introduction	44
Hypotheses	45
Methods	46
Data Access	46

Flow-Abundance Relationships of Major Zooplankton Taxa	46
<i>Pseudodiaptomus spp.</i> Abundance	47
Relative Importance of Each Taxon in the Diet.....	50
Bioenergetic Model of Prey Saturation Point.....	51
Results	53
Flow-Abundance Relationships of Zooplankton Taxa	53
<i>Pseudodiaptomus spp.</i> Abundance	55
Relative Importance of Each Taxon in the Diet.....	67
Bioenergetic Model	70
Discussion	72
What Do Smelt Eat Anyway?	72
Flow-Abundance Relationships.....	73
Impact of X2 and SMSCG on <i>Pseudodiaptomus spp.</i>	74
Benefits to Delta Smelt	75
Conclusions	76
Smelt Growth—Wild Fish	78
Introduction	78
Hypotheses	80
Methods.....	80
Bioenergetic Modeling of Potential Growth.....	80
Comparing Growth Rate Metrics.....	83
Results	84
Otolith Analysis.....	84
Bioenergetic Modeling.....	86
Discussion	94
Good Years and Bad Years	94
Summer Versus Fall	95
Conclusions	96
Smelt Health—Wild Fish	98
Introduction	98
Hypotheses	98
Methods.....	98
Data Access	98
Statistical Analysis	101
Results	107

Discussion 115

 Nutritionally Healthier Fish in More Turbid Water..... 115

 Nutritionally Healthier Fish in Low X2 When Water Temperature is High 116

 Nutritionally Healthier Fish in Low X2 Are More Important for Larger Individuals..... 117

 Nutritionally Healthiest Fish in Low X2 When Temperature is High for the Largest Individuals 118

 Limitations and Future Efforts..... 119

 Conclusions 120

Smelt Growth and Survival—Enclosures 121

 Introduction 121

 Hypotheses 122

 Methods 123

 Enclosure Deployments..... 123

 Habitat Conditions..... 124

 Delta Smelt Responses 126

 Bioenergetic Growth Modeling 127

 Results 128

 Habitat Conditions..... 128

 Bioenergetics..... 139

 Discussion 142

 Differences in Space and Time..... 142

 Enclosure Effects..... 144

 Conclusions 145

Synthesis..... 147

 Conclusions 150

References 154

Tables

Table 1.....5

Table 2..... 15

Table 3..... 21

Table 4..... 24

Table 5.....	24
Table 6.....	25
Table 7.....	37
Table 8.....	57
Table 9.....	58
Table 10.....	60
Table 11.....	62
Table 12.....	65
Table 13.....	65
Table 14.....	66
Table 15.....	86
Table 16.....	93
Table 17.....	105
Table 18.....	109
Table 19.....	124
Table 20.....	125
Table 21.....	134
Table 22.....	135
Table 23.....	136
Table 24.....	137
Table 25.....	152

Figures

Figure 1.. ..	2
Figure 2.. ..	14
Figure 3.. ..	16
Figure 4.. ..	17
Figure 5.. ..	19
Figure 6.. ..	22
Figure 7.. ..	23
Figure 8.. ..	26
Figure 9.. ..	27
Figure 10.....	28
Figure 11.....	30
Figure 12.....	31

Figure 13..... 32

Figure 14..... 34

Figure 15..... 36

Figure 16..... 37

Figure 17..... 47

Figure 18..... 54

Figure 19..... 55

Figure 20..... 56

Figure 21..... 60

Figure 22..... 63

Figure 23..... 64

Figure 24..... 68

Figure 25..... 69

Figure 26..... 70

Figure 27..... 71

Figure 28..... 81

Figure 29..... 84

Figure 30..... 85

Figure 31..... 87

Figure 32..... 88

Figure 33..... 89

Figure 34..... 90

Figure 35..... 91

Figure 36..... 92

Figure 37..... 93

Figure 38..... 99

Figure 39..... 108

Figure 40..... 110

Figure 41..... 111

Figure 42..... 112

Figure 43..... 113

Figure 44..... 114

Figure 45..... 123

Figure 46..... 130

Figure 47..... 131

Figure 48..... 132

Figure 49..... 133

Figure 50..... 134

Figure 51..... 135

Figure 52..... 138

Figure 53..... 140

Figure 54..... 140

Figure 55..... 141

Figure 56..... 141

Figure 57..... 150

Figure 58..... 182

Figure 59..... 183

Figure 60..... 183

Figure 61..... 184

Figure 62..... 184

Figure 63..... 185

Figure 64..... 185

Figure 65..... 186

Figure 66..... 186

Figure 67..... 187

Figure 68..... 189

Appendices

Appendix A. Additional Graphs

Suggested Citation

Delta Coordination Group Science and Monitoring Workgroup. 2026. Summer–Fall Habitat Actions for Delta Smelt—Report on Effectiveness of Actions Taken Between 2011 and 2024. [Report.] California Department of Water Resources.

Abbreviations and Acronyms

Term	Definition
ANOVA	analysis of variance
BIC	Bayesian information criterion
BiOp	biological opinion
CDFW	California Department of Fish and Wildlife
CF	condition factor
CSAMP	Collaborative Science and Adaptive Management Team
CVP	Central Valley Project
df	degrees of freedom
DOP	Directed Outflow Project
DWR	California Department of Water Resources
EDSM	Enhanced Delta Smelt Monitoring Program
EMP	Environmental Monitoring Program
FLOAT-MAST	Flow Alteration Management Analysis and Synthesis Team
FMWT	Fall Midwater Trawl Survey
FNU	formazin nephelometric unit
GAM	Generalized Additive Model
HSI	hepatosomatic index
IEP	Interagency Ecological Program
IRI	index of relative importance
ITP	Incidental Take Permit
LASSO	least absolute shrinkage and selection operator
LSZ	low salinity zone – 0.5–6 PSU
MAST	Management, Analysis, and Synthesis Team of the Interagency Ecological Program
NTU	nephelometric turbidity units
PERMANOVA	permutational multivariate analysis of variance
PSU	practical salinity units
Reclamation	US Bureau of Reclamation
SAV	submerged aquatic vegetation
SCHISM	Semi-Implicit Cross-scale Hydroscience Integrated System Model
SE	standard error

Term	Definition
SFHA	Summer–Fall Habitat Action
SKT	Spring Kodiak Trawl
SMSCG	Suisun Marsh Salinity Control Gates
STN	Summer Towntet Survey
SWP	State Water Project
TAF	thousand acre-feet
USFWS	United States Fish and Wildlife Service
USGS	United States Geological Survey
X2	distance between the Golden Gate Bridge and the position of the 2 PSU isohaline (in kilometers)

Background

Delta smelt (*Hypomesus transpacificus*) are a small, pelagic fish endemic to the San Francisco Bay – Sacramento-San Joaquin Delta. The species was listed as threatened and endangered under federal and state Endangered Species Acts in 1993 and 2009, respectively (United States Fish and Wildlife Service [USFWS] 1993; California Department of Fish and Wildlife [CDFW] 2025). Since their listing, Delta smelt have become an integral consideration in state and federal water management and policies for California (Moyle et al. 2018). In this report, prepared by the Delta Coordination Group’s Science and Monitoring Work Group, an interagency team of government scientists and resource managers, we summarize the science behind water management actions designed to improve habitat conditions for Delta smelt in the summer and fall and analyze available data on the effectiveness of these management actions.

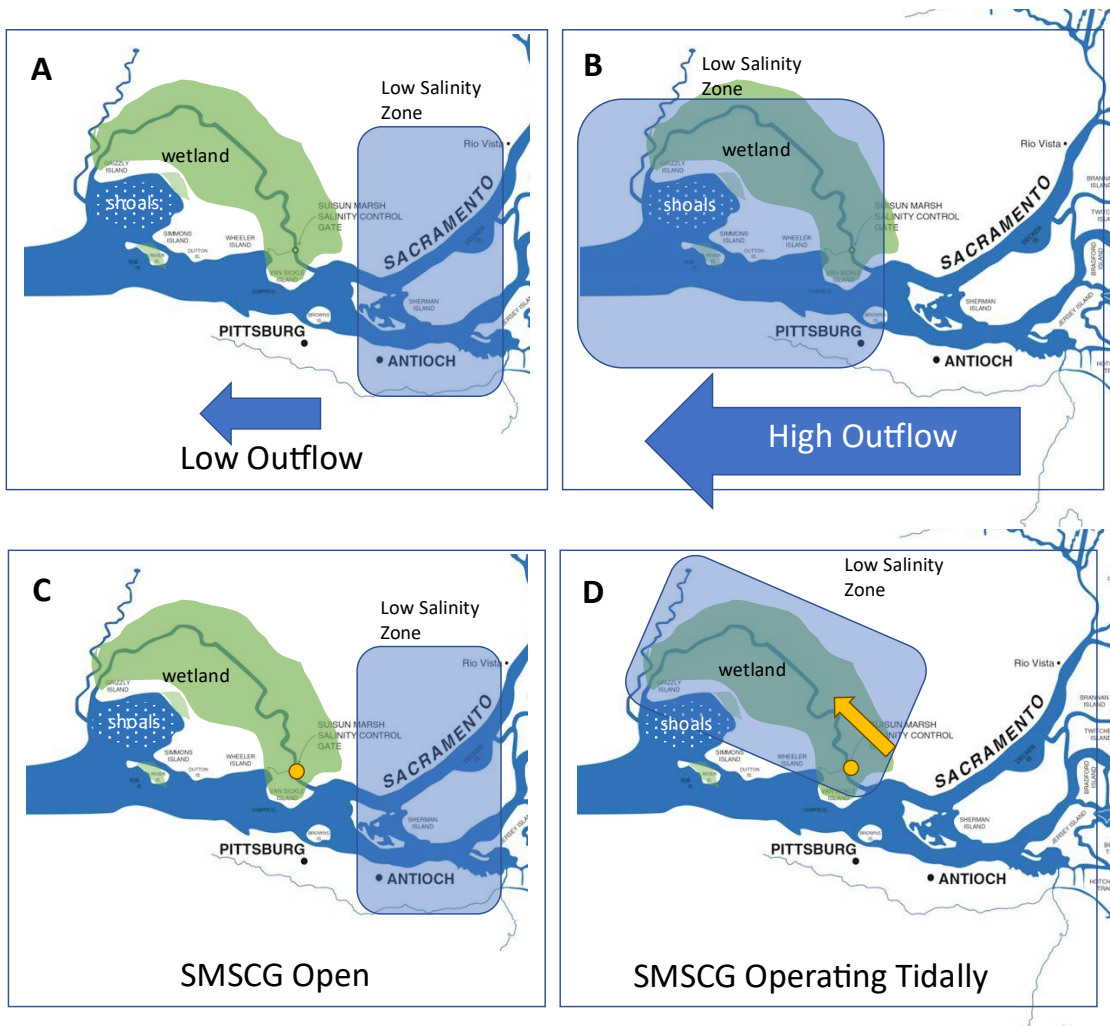
Scientific Basis

Most Delta smelt juveniles migrate and rear in the San Francisco Estuary’s low salinity zone (LSZ, 0.5–6 PSU) during the summer and fall (Hobbs, Lewis et al. 2019) June through October (Merz et al. 2011). Due to the high inter-annual and intra-annual variability in freshwater flow caused by California’s Mediterranean climate, the geographic location of the LSZ may vary significantly within and between years (Hutton and Roy 2019; Feyrer et al. 2007). During lower outflow years the LSZ may occur as far upstream as the lower Sacramento and San Joaquin Rivers, whereas in higher outflow years the LSZ may remain farther downstream in Suisun Bay throughout most of the summer and fall (Figure 1).

Analyses in the early 2000s identified the summer and fall as particularly stressful time periods in the Delta smelt life cycle and documented decreases in the area of appropriate Delta smelt habitat in the fall (Feyrer et al. 2007; Nobriga et al. 2008; Feyrer et al. 2011). Habitat in Suisun Bay is thought to be beneficial for the Delta smelt during the fall due to increased population distribution, greater foraging opportunities, and greater habitat complexity (Sommer and Mejia 2013). Suisun Bay is generally cooler than upstream areas in the Delta (Bashevkin, Mahardja et al. 2022; Pien et al. 2025), providing Delta smelt a thermal refuge during stressful periods of high temperature. Suisun Bay is also generally higher in turbidity, supporting the potential for increased feeding (Hasenbein et al. 2013), decreased stress, and decreased predation risk (Pasparakis et al. 2023; Ferrari et al. 2014). Suisun Marsh is also associated with reduced toxicity as evidenced by decreasing levels of liver and gill lesions (Hammock et al. 2015). Both Suisun Marsh and Suisun Bay have more tidal wetlands than the Delta, which have been correlated with higher feeding success (Hammock, Hartman et al. 2019).

Together, these analyses suggest that having the LSZ overlap with Suisun Bay and Suisun Marsh would provide access to higher-quality habitat for rearing Delta smelt (Figure 1), which is hypothesized to increase their growth, survival, and recruitment (Feyrer et al. 2011; Feyrer et al. 2007). This conceptual model of improving Delta smelt habitat via increased outflow directly informed regulations requiring flow management actions during the summer and fall.

Figure 1. Conceptual model demonstrating higher outflow or Suisun Marsh Salinity Control Gate (SMSCG) operation in summer and fall provides greater access to high quality habitat for Delta smelt. Modified from Brown et al. (2014). A) During a low outflow scenario, the LSZ is centered on the lower Sacramento River, a region with narrow, rip-rapped channels, clear water, and high temperatures. B) When outflow is higher, such as during a Fall X2 action, the LSZ is centered on Suisun Bay, where extensive shallow shoals and high turbidity provide better habitat. C) If outflow is low and the SMSCG are held open, salinity in Suisun Marsh is high, and the LSZ is in the Sacramento River. D) When the SMSCG are operating tidally, the LSZ moves into Suisun Marsh, where extensive tidal wetlands and higher turbidity are thought to provide better Delta smelt habitat.



Regulations

In 2008, the biological opinion (BiOp) for the State Water Project (SWP) and Central Valley Project (CVP), together “Projects” included a condition that the California Department of Water Resources (DWR) and the US Bureau of Reclamation (Reclamation) must maintain Fall X2, the point at which the bottom salinity is 2 PSU, at 74 km or less from the Golden Gate in September and October of Above Normal and Wet water years (Based on the Sacramento Valley Water Year Hydrologic Classification Index; USFWS 2008). This condition was developed through analyses showing that Projects operations caused X2 to be 10–15% higher in the early 2000s than it was under historical conditions (Feyrer et al. 2007; USFWS 2008), causing low-flow periods every fall, whereas historically wetter years had higher flows during the fall. The Fall X2 standard was only in effect in Above Normal and Wet years because enough water was available to push the LSZ into Suisun Bay. While Projects operations also increased X2 in the fall of Below Normal, Dry, and Critically Dry years, it would not be feasible to decrease X2 enough to provide habitat in Suisun Bay.

New permits issued by the US Fish and Wildlife Service (USFWS) and CDFW in 2019 and 2020 changed the Fall X2 standard from 74 km to 80 km and included operations of the Suisun Marsh Salinity Control Gates (SMSCG) as an additional habitat action to convey freshwater from the Sacramento River into Montezuma Slough. Together with several food subsidy actions still in development, Fall X2 and SMSCG comprised the Delta Smelt Summer–Fall Habitat Action (SFHA). Leading up to this, the Projects reinitiated consultation on the BiOps with USFWS, and, for the first time, the State of California started a separate consultation process for an Incidental Take Permit (ITP) with the CDFW. The Projects requested a change in the Fall X2 standard because “lower fall outflows would better mimic historical (pre-project) conditions, and analyses indicate that the CVP and SWP have had negligible effects on fall outflows measured using X2 as a proxy (Hutton et al. 2017).” (USFWS 2019).

The 2019 BiOp also required the SMSCG to be operated for 60 days in Above Normal, Below Normal, and some Dry years. This SMSCG action was developed as part of the Delta Smelt Resiliency Strategy (California Natural Resources Agency 2016), because it would increase the overlap of the LSZ and Suisun Marsh while requiring much less water than moving the location of X2. The action was piloted in 2018, and the pilot action achieved its goals of improving Delta smelt habitat in the Marsh (Sommer et al. 2020). Delta smelt populations in 2018 were already critically low, so it was difficult to conclude that the action improved the individual growth or population growth of smelt, but several smelt were captured in the Marsh during the action (Sommer et al. 2020). The success of the pilot action led to inclusion of SMSCG operation in the 2019 BiOp and 2020 ITP, but the lack of certainty in the outcomes of the actions also led to inclusion of the action in the adaptive

management plan for the Projects and requirements for independent science reviews of the summer–fall action.

To offset the change in the X2 standard included in the 2020 ITP, in Wet and Above Normal years, the 2020 ITP included an additional 100 thousand acre-feet (TAF) block of water to supplement Delta outflow. The 100 TAF block could either be deployed in the year it was created or deferred and redeployed the following year. Modeling of operation scenarios showed that using the 100 TAF to increase the SMSCG action beyond the required operations would improve Delta smelt habitat more than deploying the 100 TAF as outflow (DWR 2023).

In 2024 DWR and Reclamation reinitiated consultation again and new BiOps and ITP were issued by USFWS and CDFW. The updated regulations also included a Fall X2 action and the SMSCG action, with a stronger emphasis on adaptive management (CDFW 2024). The ITP Adaptive Management Program highlighted new scientific findings from life cycle modeling efforts that demonstrated Delta outflow in summer had stronger effects on Delta smelt survival and population growth rates than outflow in fall (Polansky et al. 2024) and mentioned potential mechanisms (e.g., temperature differences, prey subsidies, etc.). The Program identified the development of a comprehensive synthesis of summer–fall habitat conditions (this current report), to inform the development of a larger adaptive management plan for summer–fall and future considerations of alternative actions. This report, along with previous Structured Decision-Making reports on SFHA, are intended to inform adaptive management of summer–fall habitat for Delta smelt.

Implementation of Actions

Since 2008, DWR and Reclamation have implemented Fall X2 actions five times, and SMSCG actions four times (Table 1). Each implementation has been slightly different, and each was conducted in a different hydrologic backdrop and does not represent replications of a controlled experiment. Therefore, while this report will be comparing years with X2 or SMSCG actions to years without actions, it will be difficult to make conclusions that apply to all action years. The SMSCG actions that occurred during the summer of 2025 were used in analysis of Delta smelt habitat, but not all of the data on smelt food or smelt catch were available by the time the report was finalized in April 2026 and are not included here.

Table 1. Summer–Fall Habitat Actions taken since 2008, with Sacramento Valley Water Year Type, the legally mandated X2 action, the monthly average X2 achieved in September and October, the SMSCG action description, and the salinity achieved at Belden’s Landing (BDL) during the action.

Year	Water Year Type	X2 Action	Sept. X2	Oct. X2	SMSCG Action	Salinity at BDL During Action
2011	Wet	X2 at or below 74 km for September and October	72.9	72.6	None	NA
2017	Wet	X2 at or below 74 km for September and October	73.1	76.1	None	NA
2018	Below Normal	None	>81	>81	Gates operating Aug. 2–Sept. 7	3.54
2019	Wet	X2 at or below 74 km for September and October	72.3	72.6	None	NA
2023	Wet	X2 at or below 80 km for September and October	78.8	80.7	Gates operating Aug. 15–Oct. 17	1.58
2024	Above Normal	X2 at or below 80 km for September	80.3	>81	Gates operating July 1–Aug. 29 and Sept. 6–Sept. 30	1.51
2025	Above Normal	None	>81	>81	Gates operating June 23–Aug. 25 and Sep. 5–12	1.84

Analysis to Date

Fall Flow

The Fall X2 action included in the 2008 BiOp was based on research hypothesizing that fall habitat was important to the success of the Delta smelt population. However, later analyses of the results of the actions were inconclusive. The hypothesis began with an analysis by Feyrer et al. (2007), which linked Delta smelt abundance in fall to lower temperatures, low salinity, and low Secchi depth habitat and demonstrated that these habitat features have declined over time. Feyrer et al. (2007) also implicated changes to Projects operations as the cause of that decline. This work was expanded on by Nobriga et al. (2008), who used similar methods to link summertime abundance to salinity, Secchi depth, and temperature. The authors found a decline in summertime habitat suitability over time, though this was most discernable at smaller spatial scales, rather than estuary-wide, because habitat suitability declines over the course of the year. Feyrer et al. (2011) extended the previous analysis of long-term declines in Delta smelt habitat by adding additional years of data and incorporating future predictions of habitat under

climate change. They found significant declines in area of suitable habitat and Fall X2 over time, as well as a significant correlation between habitat index and Delta smelt abundance (with higher variance at higher habitat indices). They hypothesized that increased habitat area, as indexed by temperature, salinity, and Secchi depth, could bolster Delta smelt populations through increased resiliency to extreme events and decreased potential for density dependence (Feyrer et al. 2011).

This work was not without controversy. Miller et al. (2012) investigated factors impacting Delta smelt abundance and found no correlation with the abiotic habitat factors identified by Feyrer et al. (2011) nor Fall X2 (which was included in the 2008 BiOp). Instead, they found that food availability (as indexed by zooplankton abundance) was one of the strongest predictors of Delta smelt populations. Manly et al. (2015) were openly critical of the work of Feyrer et al. (2011) and applied a slightly different statistical methodology to the same data. This showed a much lower correlation between Delta smelt populations and abiotic habitat variables. Feyrer et al. (2016) responded in turn, criticizing their analysis. There were clear disagreements between scientists about the role of habitat quality and quantity in driving Delta smelt decline, resulting in legal and scientific debates.

While the controversy regarding the foundational research behind the fall habitat hypothesis was occurring, DWR and Reclamation implemented the first Fall X2 action in 2011. The 2011 water year was a very Wet year with low temperatures and a late spring, and Delta smelt populations rebounded to levels not seen since 2001 (IEP-MAST et al. 2015). To better learn from the 2011 X2 action, a team of Interagency Ecological Program (IEP) scientists conducted an intensive series of investigations into the effects of fall low salinity habitat (known as the "FLASH" report) (Brown et al. 2014). They evaluated flow, water quality, nutrients, phytoplankton, zooplankton, and fish abundance during 2011, comparing it with other Wet and Dry years to evaluate the effect of the action. They also began several special studies on contaminant concentrations, Delta smelt diets, and Delta smelt health and condition. In their final report, they found they could not make any conclusive statements regarding connections between the Fall X2 action and the increased abundance in Delta smelt. They did find that Delta smelt habitat, population indices, survival, and individual growth rates in the fall improved. However, they did not find increases in zooplankton or Delta smelt recruitment the following spring) (Brown et al. 2014). In many cases, data were insufficient to address their hypotheses, did not support their hypothesis, or were inconclusive (Brown et al. 2014).

The results of the 2011 synthesis also contributed to the IEP Management Analysis and Synthesis (MAST) report of 2015 (IEP-MAST et al. 2015). The MAST team used all the available Delta smelt data across their entire life cycle to determine how differences in conditions in two Wet years (2006 and 2011) resulted in different smelt population responses. They concluded that high temperatures reduce juvenile

growth, so low temperatures in 2011 may have contributed to high population growth. They also found that food resources frequently limit summertime growth, so high copepod abundance may have contributed as well. The greatest LSZ area and lowest X2 occurred in September and October 2011 and were associated with a high Fall Midwater Trawl (FMWT) index, which was followed by the highest Spring Kodiak Trawl (SKT) index on record, although survival from subadults to adults was actually lower in 2011 than in 2010 and 2006.

The next Fall X2 action, in 2017, was another opportunity to test the hypotheses behind the idea that improved fall habitat improves Delta smelt population growth. The IEP Flow Alteration Management Analysis and Synthesis (FLOAT-MAST) was formed to assess the hypotheses behind the Fall X2 action. Similar to the FLASH report of 2014, the FLOAT-MAST report was inconclusive regarding the effectiveness of the Fall X2 action (FLOAT-MAST 2021). While 2017 was one of the wettest years on record in the Sacramento Valley, Delta smelt populations did not rebound as they did in 2011. The FLOAT-MAST report found a significant negative correlation between X2 and summer to fall survival for years 2002-2014, but this correlation was not significant with the addition of 2017 (a very low outlier). High water temperatures, particularly the extended periods of water temperature above 22°C, were implicated in low fall Delta smelt abundance in that year (FLOAT-MAST 2021).

At the same time the FLOAT-MAST were conducting their synthesis, the Directed Outflow Project (DOP), led by Reclamation, began an intensive study of habitat conditions and Delta smelt health metrics to improve our understanding of fall outflow effects on smelt. This project included intensive phytoplankton and zooplankton sampling coupled with the Enhanced Delta Smelt Monitoring Program (EDSM), detailed analysis of gill lesions, liver lesions, glycogen concentration, growth rates, diet, and life history for all Delta smelt captured, as well as contaminant analyses across the smelt habitat range. The resulting report reinforced the theory that high temperatures in 2017 reduced any benefit of increased freshwater flow and noted that low zooplankton in the Suisun Bay region (due partly to grazing by invasive clams) generally reduces habitat suitability when compared to upstream regions (Schultz et al. 2019).

Further research found that, while more Delta smelt were caught in freshwater regions during recent flow actions, smelt growth (based on otolith analyses) tended to be lower in freshwater residents than in fish that migrated to the LSZ (Lewis et al. 2021). Otolith analyses also identified lower growth associated with higher temperatures (Lewis et al. 2021). While zooplankton biomass in the Suisun Bay tends to be lower than upstream regions, there are significantly more zooplankton (in particular the important copepod, *Pseudodiaptomus forbesi*) in Suisun Bay during high-flow falls than lower flow falls (Lee et al. 2023) due to subsidies from upstream areas (Hassrick et al. 2023).

Suisun Marsh

Much of the early work on fall habitat for Delta smelt focused on Suisun Bay, due to its cool temperatures, high turbidity, extended shallow shoals, and history of Delta smelt catch. However, there was increasing appreciation of the habitat value of Suisun Marsh for Delta smelt as well. Suisun Marsh was identified as part of the “arc of connected habitat” for native fish species (including Delta smelt) (Moyle et al. 2012) and was targeted as a priority for habitat restoration due to its higher pelagic productivity (when compared to Suisun Bay), dead-end sloughs, and extensive wetlands (Moyle et al. 2014). Analysis of Delta smelt health, condition, and diet found that fish caught in Suisun Marsh had higher stomach fullness and decreased contaminant stress when compared to fish caught upstream in the Delta (Hammock et al. 2015; Hammock et al. 2017; Hammock, Hartman et al. 2019).

In 2016, the Delta Smelt Resiliency Strategy first proposed operation of the SMSCG to lower salinity in Suisun Marsh during the summer and fall to increase the extent and duration of Delta smelt habitat. Operation of the SMSCG does require increased net Delta outflow in order to offset changes to salinity in the Confluence, but it requires much less water than changes to X2. Therefore, it was seen as a way to increase Delta smelt habitat with less water. In 2018, the SMSCG were operated for the month of August, and an associated monitoring plan tracked the physical and biological responses in ecosystem conditions. Sommer et al. (2020) found that the August operation (during a relatively dry summer) resulted in salinity conditions in the Marsh similar to those in previous wet Augusts, and the reduction in salinity continued for several weeks after operations ceased. They also caught several Delta smelt in Suisun Marsh during the action and none before or after the action. They also expected that the lowered salinity and increased flow into Suisun Marsh would increase biomass of *Pseudodiaptomus forbesi* (*P. forbesi*), similar to a Fall X2 action. However, they did not see the predicted increase in zooplankton in the Marsh during the action, and the zooplankton there was lower than that in the Sacramento River in all months. They also found that temperatures in Suisun Marsh were similar to, or higher than, temperatures upstream (Sommer et al. 2020).

Population Models

The empirical studies and syntheses listed above were accompanied by quantitative modeling of Delta smelt populations. One of the first models was developed by Maunder and Deriso (2011), who used a stage-space multistage life cycle model to identify which environmental variables were most important to Delta smelt population dynamics. They found that density dependence had a large role in population dynamics, with temperature, zooplankton, and predation being the most important environmental variables (Maunder and Deriso 2011).

Rose et al. (2013b; 2013a) developed an individual-based model based on bioenergetic parameters. They found growth of larvae, growth of juveniles in the

fall, temperature, zooplankton, and hydrodynamics were some of the most important contributors to population growth, but no single factor could explain the resulting population trends on its own. They disagreed with Maunder and Deriso regarding density dependence. The model was used again by Kimmerer and Rose (2018) to highlight the importance of zooplankton abundance and the negative effect of changes to zooplankton density and community composition on Delta smelt. A later sensitivity analysis of the Rose et al. model found that population growth rates were most responsive to changes in juvenile mortality and changes to juvenile food supply during the summer and fall (Zhang et al. 2022).

Further efforts to model Delta smelt population by USFWS used spatiotemporal models to develop design-based or model-based abundance estimates. This was followed by a state-space model to identify the most important correlates of population growth (Polansky et al. 2021). Polansky et al. (2021) found that recruitment was negatively correlated with temperature and the location of Fall X2 from the previous year. However, expanded analyses of this work found that summer outflow was more important than fall outflow for population growth, such that summer outflow actions might have been more effective than Fall X2 (Polansky et al. 2024; Smith et al. 2021).

Another approach to life cycle modeling conducted by Hamilton and Murphy (2018) used a stage-structured mechanistic model where life stage transitions were modeled as functions of hypothesized limiting factors. This approach ranked candidate models using Akaike's Information Criterion (AIC) to determine the most probable limiting factors. The top-ranked model included prior abundance, abundance of silversides (*Menidia audens*), food availability in summer, entrainment in power plants, and a recruitment parameter. Similar to Smith and Nobriga (2023), Hamilton and Murphy (2028) found that food limitation in the summer was a major factor in Delta smelt population growth. However, unlike other models, they found entrainment in power plants (rather than the Projects) and abundance of the predator/competitor silversides were some of the most important factors.

Hypotheses

The goal of this current report is to collate the data from previous summer and fall flow actions and evaluate the importance of habitat in Suisun Bay and Suisun Marsh during the summer and fall in driving Delta smelt survival. We use a hypothesis-based approach to evaluate the effect of salinity in Suisun Marsh and the position of X2 on Delta smelt habitat, food supply, and individual growth and health. We also review existing research on the connection between conditions for individual fish and population-level effects. We did not explicitly separate the effectiveness of specific management actions (Fall X2 and SMSCG operations) from similar conditions that occur during Wet years without management actions, as we did not have enough comparable situations without specific management actions. However,

the relationship between X2 or salinity and Delta smelt should be the same regardless of how the X2 condition was achieved, so understanding the relationship between habitat conditions and smelt responses should inform future management actions.

Our hypotheses are as follows:

- Lower X2 in the summer and fall, and lower salinity in Belden's Landing, will increase the extent and duration of suitable turbidity, temperature, and salinity habitat in Suisun Marsh, Suisun Bay, and Grizzly Bay.
- Lower X2 in the summer and fall, and lower salinity in Belden's Landing, will increase the abundance of the calanoid copepod *Pseudodiaptomus* spp. in Suisun Marsh, Suisun Bay, and Grizzly Bay.
- Years with lower X2 in the summer and fall, and lower salinity at Belden's Landing, will have higher Delta smelt growth, health, and condition in the summer and fall.
- Years with lower X2 in the summer and fall, and lower salinity in Belden's Landing, will increase the percentage of the population surviving at the end of the season.
- The influence of X2 and salinity in Suisun Marsh on Delta smelt habitat, food, growth, and survival will be greater in summer than in fall.

Smelt Habitat

Introduction

When assessing the effectiveness of a management action for a rare species, such as Delta smelt, it is difficult to measure the changes caused by the action (e.g. average body condition, overall abundance) due to the rarity of the target individuals. However, habitat restoration is frequently assessed based on the capacity of the habitat to support the target species and where the species has the opportunity to access the habitat (Simenstad and Cordell 2000). These assessments provide lines of evidence to show benefits of the action even if assessments of fish presence are difficult due to (lack of) fish catch.

This assessment of habitat capacity has long been the basis of evaluating the SFHA for Delta smelt. Feyrer et al. (2011) found a positive correlation between area of habitat (as indexed by turbidity, temperature, and salinity) and Delta smelt abundance, so similar habitat indices have been used to evaluate potential for increased abundance indices. Salinity less than six practical salinity units (PSU) was used to designate Delta smelt habitat in the BiOps and ITP in 2019/2020 and 2024 (CDFW 2020; 2024). Six PSU was also used in Bever et al. (2016) and Sommer and Mejia (2013), though some researchers suggest a lower salinity would be more appropriate, with Smith and Nobriga (2023) and Hendrix et al. (2023) using 5.5 PSU as the upper limit and Bennett (2005) pointing out that over 70% of juvenile and 60% of sub-adult Delta smelt are caught in less than 2 PSU. Turbidity thresholds are somewhat less clearly defined, with Sommer and Mejia (2013) using 12 nephelometric turbidity units (NTU) as the cutoff below which Delta smelt are less likely to be detected. Grimaldo et al. (2009) found that Delta smelt entrainment increased above a threshold of approximately 10 NTU. Many other analyses used a more continuous relationship, with Smith and Nobriga (2023) using an exponential relationship between turbidity and feeding up to a maximum of 35 NTU, Polansky et al. (2021 and 2024) found a roughly linear relationship between Delta smelt vital rates and Secchi depth, rather than a strict threshold.

Salinity and turbidity (or Secchi depth) have been the most widely used indices of abiotic Delta smelt habitat, but many other factors can contribute to whether smelt occur in a given location. Bever et al. (2016) found that Delta smelt were more likely to occur with lower current speeds, though this was not as strong a relationship as salinity or turbidity. Temperature is also commonly cited as a predictor of Delta smelt presence and has received more attention as increased frequency and severity of heat waves have decreased summer habitat suitability (Brown et al. 2013; Mahardja et al. 2025). Delta smelt can tolerate being in 24°C water or warmer under laboratory conditions when acclimated appropriately (Swanson et al. 2000; Komoroske et al. 2014; Komoroske et al. 2015; Komoroske et al. 2021), and sometimes in field conditions as well (Davis et al. 2024), but

metrics indicative of their physiological and ecological performance decline, and indicators of stress increase at temperatures above 21-22°C (Komoroske et al. 2015; Komoroske et al. 2021; Lewis et al. 2021; Davis et al. 2019; Hammock et al. 2022). Furthermore, all of the long-term trawl surveys show that catch peaks at approximately 20–21°C and declines in warmer water (Komoroske et al. 2014).

Biotic factors also impact how Delta smelt relate to their environment, though these will be discussed more extensively in later chapters. High zooplankton abundance is one of the most important predictors of Delta smelt abundance and condition (Tillotson et al. 2025; Hamilton and Murphy 2018; Hammock et al. 2015; Polansky et al. 2021), and smelt presence is also positively correlated with the presence of other small pelagic fishes (Tillotson et al. 2025). Proximity to tidal wetlands is also thought to increase foraging opportunities (Hammock, Hartman et al. 2019), and higher chlorophyll was correlated with higher health metrics (Hammock et al. 2022), though the mechanism behind this relationship is unclear. The presence of submerged or floating aquatic vegetation is also thought to negatively impact Delta smelt habitat quality, creating a physical impediment to swimming, decreasing turbidity, and providing refuge for predatory fishes (Ferrari et al. 2014; Boyer et al. 2013; Conrad et al. 2016; Hestir et al. 2016).

Taken together, previous research identifies ideal abiotic summer and fall habitat for Delta smelt to be areas where water temperature is less than 22°C, turbidity is greater than 12 NTU, and salinity is less than 6 PSU. However, these basic water quality parameters are only the first step in fully describing suitable habitat availability for Delta smelt, and biotic interactions may make conclusions based on abiotic parameters alone problematic.

Increased outflow in summer and fall has been conclusively tied to an increase in area of LSZ habitat in multiple previous publications (Kimmerer et al. 2009; Kimmerer et al. 2013; Feyrer et al. 2007), and this relationship holds in both summer and fall (Nobriga et al. 2008; Feyrer et al. 2011). Fewer analyses have been conducted on the impacts of SMSCG operations on LSZ habitat, but increased LSZ habitat with SMSCG operations can be expected based on the physics of the system and has been demonstrated empirically by Sommer et al. (2020). However, impacts of these actions on other aspects of water quality and physical habitat are less well understood. In particular, decreasing salinity may increase the prevalence of invasive aquatic vegetation that require lower salinity water (Borgnis and Boyer 2015; Kring et al. 2014; Boyer and Sutula 2015). Submerged aquatic vegetation (SAV) degrades the open-water habitat preferred by Delta smelt, so determining the extent of SAV in Suisun Marsh is an important part of the integrated approach for evaluating the availability of suitable smelt habitat. Suisun Marsh has exhibited less cover of invasive SAV compared to the Delta, likely because most of these plant species cannot tolerate the brackish conditions that are typical of the Marsh (Christman et al. 2023). The SMSCG are operated to move more fresh water from the Delta into Suisun Marsh during the summer and fall months, which could

increase the cover of SAV in the Marsh by two mechanisms: (1) increasing the transport of SAV propagules from the highly infested Delta and (2) reducing the salinity of the Marsh to levels amenable to these plants during their peak months for growth and reproduction.

Also, actions that increase flow, including SMSCG operations, can also be expected to decrease residence time, limiting chlorophyll and zooplankton biomass accumulation (Hartman et al. 2024; Hammock, Moose et al. 2019).

Hypotheses

In this section of the report, we further explore the main hypothesis that lower X2 and lower salinity will improve Delta smelt habitat availability (stated above). To further explore the importance of differences between SMSCG actions, Fall X2 actions, and hydrologic differences between water years, we explored several ancillary hypotheses:

- There will be more days of overlapping suitable salinity, temperature, and turbidity, as well as a greater area of the LSZ in Suisun Bay during years with Fall X2 actions.
- There will be more days of overlapping suitable salinity, temperature, and turbidity, as well as a greater area of the LSZ in Suisun Marsh during years with Fall X2 actions or SMSCG actions.
- SMSCG operations will cause a greater increase in LSZ area in Suisun Marsh in drier years, but LSZ area in Grizzly Bay will only increase when SMSCG actions occur in wetter years.
- Multiple (consecutive?) years with low X2 and lower salinity in Suisun Marsh will result in increased prevalence of submerged aquatic vegetation in Suisun Marsh and Suisun Bay.
- Operation of the SMSCG will decrease concentration of phytoplankton in Montezuma Slough.
- Abiotic habitat improvements with lower X2 will be similar in summer and fall.

Methods

Continuous Water Quality

Water quality monitoring relies on the network of high-frequency, telemetered, water quality instruments (sondes) distributed throughout the region (Figure 2). These sondes collect water temperature, specific conductance, and/or turbidity. DWR, UGSGS, and Reclamation deployed these sondes at various dates, as listed in Table 2. We compiled data from these stations either by direct correspondence with the data owners (for DWR data) or from CDEC (Reclamation data). Because water temperature and turbidity data were not available in all regions from earlier years,

we used data from discrete measurements collected by IEP's long-term fish, zooplankton, and water quality monitoring surveys compiled in the discretewq package (Bashevkin, Perry et al. 2023). We used daily averages of these discrete measurements by the subregions defined by the Delta Smelt Individual-Based Model (Rose et al. 2013a) and used linear interpolation to fill in averages for days in between the discrete measurements. This method is likely to overestimate average daily temperatures, because surveys only sample during the day, and will most likely miss short-term extremes in temperature, turbidity, or salinity. However, it provides an estimate of water quality conditions when no other data sources are available. Water quality trends (June–October only) in each region are shown in Figure 4.

Figure 2. Map of water quality sampling stations within each of the regions used for our analysis.

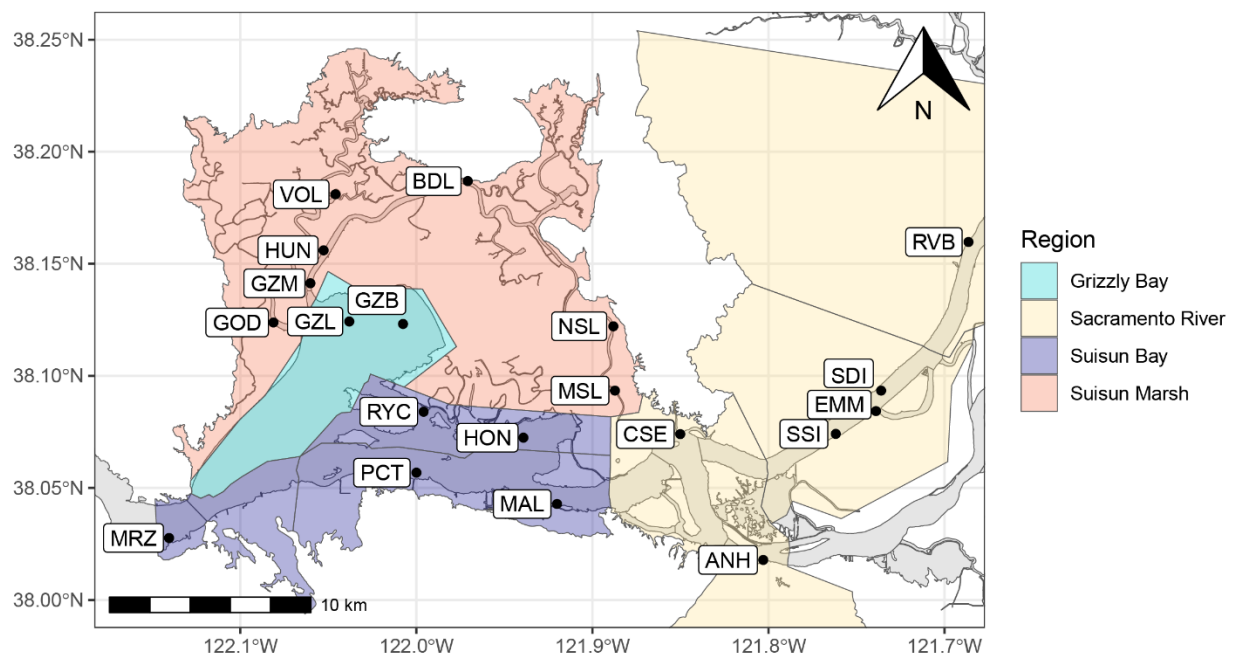


Table 2. Water quality stations used for analysis. The three-letter Station ID code is used for querying data from CDEC's and DWR's internal databases.

Station ID	Station Name	Region	Latitude	Longitude	Start Date	End Date	Parameters
GZB	Grizzly Bay Bouy	Grizzly Bay	38.12315	-122.0076	2018-07-05	2024-12-30	EC, Temp, Turbidity
GZL	Grizzly Bay Pile	Grizzly Bay	38.12425	-122.0380	2015-06-19	Present	EC, Temp, Turbidity
GZM	Grizzly Bay at Montezuma	Grizzly Bay	38.14130	-122.0602	2020-12-02	2024-12-30	EC, Temp, Turbidity
ANH	Antioch	Sac. River	38.01783	-121.8030	2008-10-16	Present	EC, Temp
CSE	Collinsville	Sac. River	38.0740	-121.8501	2009-02-19	Present	EC, Temp, Turbidity (turbidity since 2018 only)
MAL	Mallard Island	Sac. River	38.04281	-121.9201	2008-10-03	Present	EC, Temp, Turbidity
RVB	Rio Vista Bridge	Sac. River	38.15974	-121.6864	2008-09-23	Present	EC, Temp, Turbidity
SDI	Sacramento River at Decker	Sac. River	38.0934	-121.736	2010-01-20	2020-12-31	EC, Temp, Turbidity
SSI	Sacramento River near Sherman	Sac. River	38.0741	-121.7617	2015-06-19	Present	EC, Temp, Turbidity
HON	Honker Bay	Suisun Bay	38.0724	-121.9392	2015-06-19	Present	EC, Temp, Turbidity
MRZ	Martinez	Suisun Bay	38.02764	-122.1405	2008-08-21	Present	EC, Temp, Turbidity
PCT	Port Chicago	Suisun Bay	38.05679	-121.9999	1999-02-09	Present	EC
RYC	Suisun Bay Cutoff near Ryer	Suisun Bay	38.08397	-121.9958	2015-06-09	Present	EC, Temp, Turbidity
BDL	Belden's Landing	Suisun Marsh	38.1869	-121.9708	2009-05-27	Present	EC, Temp, Turbidity (turbidity since 2018 only)
GOD	Godfather II on Suisun Slough	Suisun Marsh	38.1238	-122.0812	2009-02-19	Present	EC, Temp, Turbidity (turbidity since 2018 only)
HUN	Hunter Cut	Suisun Marsh	38.156	-122.0527	2009-02-19	Present	EC, Temp, Turbidity (turbidity since 2018 only)
MSL	Montezuma Slough at Roaring River	Suisun Marsh	38.0934	-121.8872	2009-02-12	Present	EC, Temp, Turbidity (turbidity since 2018 only)
NSL	National Steel	Suisun Marsh	38.1221	-121.8881	2009-05-21	Present	EC, Temp, Turbidity
VOL	Volanti	Suisun Marsh	38.181	-122.046	2009-05-15	Present	EC, Temp, Turbidity (turbidity since 2020 only)

Figure 3. Data availability from continuous sondes in each region. Where data were present, all values for each day were averaged across stations within a region. Where no continuous data were present, data from discrete measurements were averaged and interpolated between discrete points.

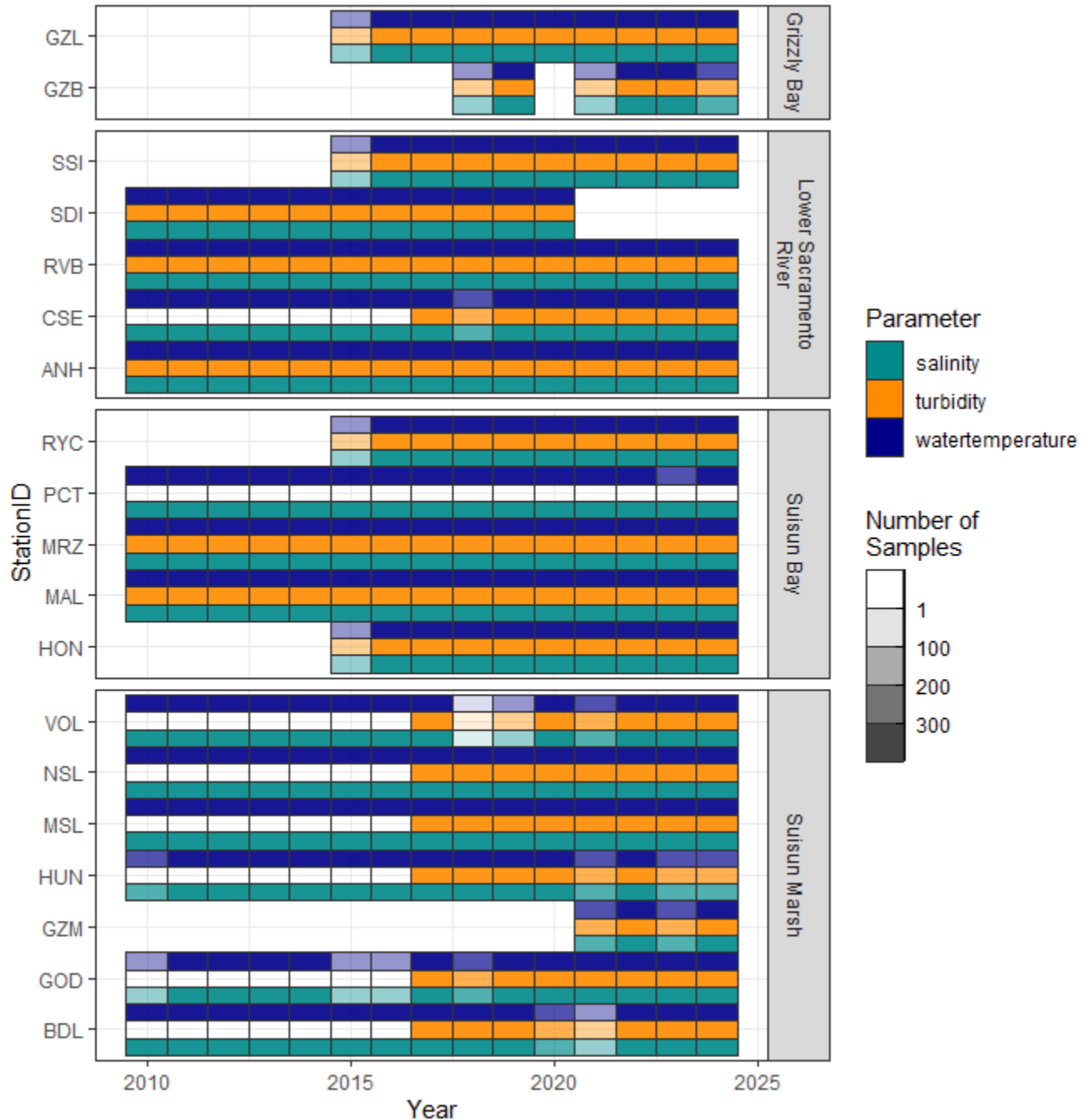
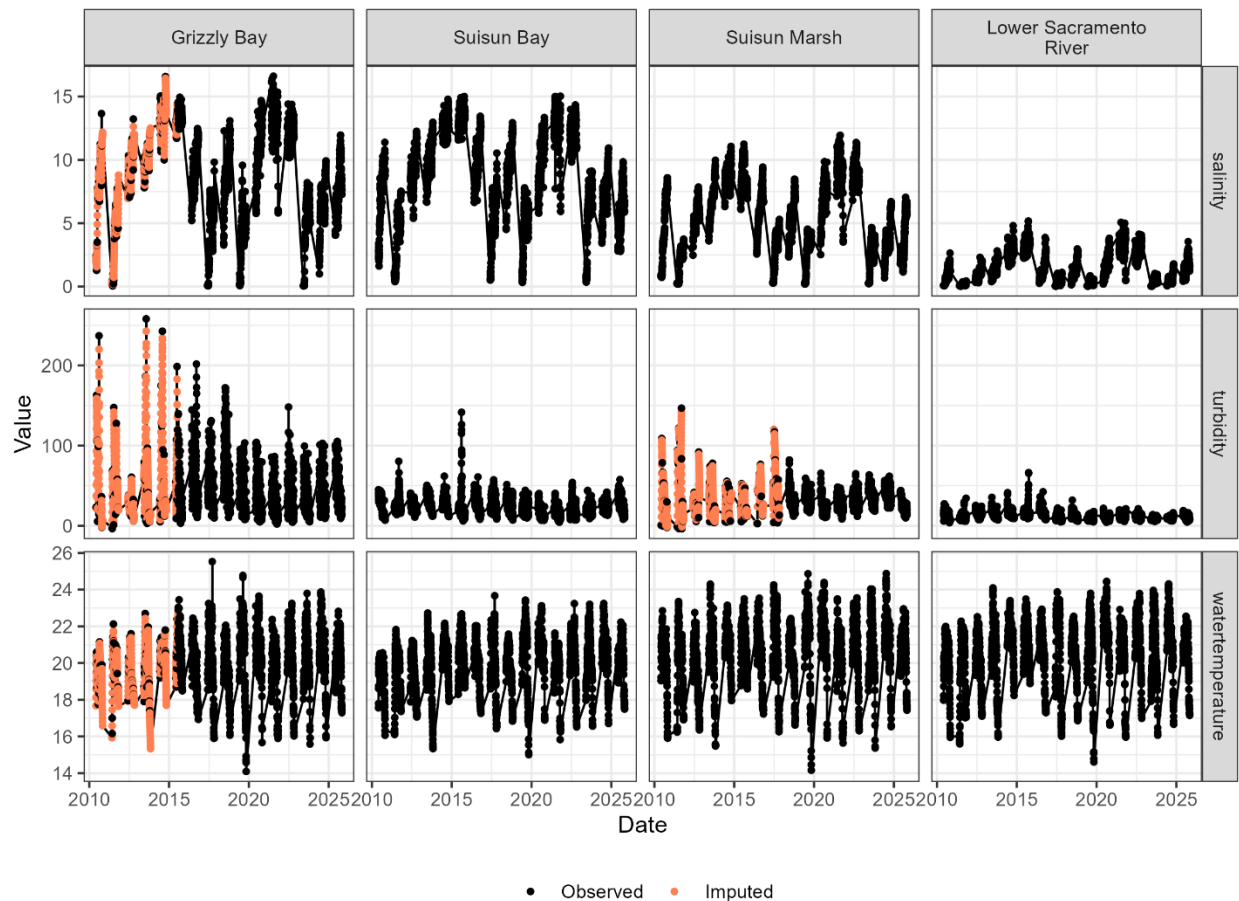


Figure 4. Average daily salinity, temperature, and turbidity for each of the regions used in this analysis (June–October only). Data from continuous sondes or discrete measurements (black points) were used when possible, and values were imputed between discrete measurements (orange points) when necessary.



We converted specific conductance to salinity using the `wql` R package (Jassby et al. 2017) and calculated daily averages for water temperature, turbidity, and salinity. We then compared the number of days each region had suitable habitat, defined as salinities below 6 PSU, turbidities above 12 NTU, and temperatures below 22°C from June–October of each year using a beta-binomial model (formula: $P = (\text{Suitable Days} : \text{Unsuitable Days}) = \text{SMSCG} * \text{Region} + \text{X2} * \text{Region}$) using the `'glmmTMB'` function in R (Brooks et al. 2025). This model structure assumes the effect of SMSCG and X2 actions are additive, but we did not have enough years with SMSCG actions without X2 actions to test the interaction between the two terms. In this case, the terms SMSCG and X2 indicate whether or not a SMSCG action or a Fall X2 action occurred. This only included SMSCG and X2 actions taken specifically to benefit Delta smelt and did not include cases where SMSCG started operating in fall of Dry years to comply with D-1641 or the Suisun Marsh Preservation Agreement (SMPA) because the SMPA operations have a much higher salinity trigger than the Delta smelt actions. The beta-binomial model was used

because a model using a binomial distribution was overdispersed. We followed the main model with pairwise comparisons of the X2 and SMSCG terms by region using the emmeans function from the emmeans package (Lenth et al. 2024). This function uses the Tukey method for multiple comparisons. We visualized the number of suitable turbidity days, the number of suitable temperature days, and the number of suitable salinity days, but only conducted statistical analyses on the number of days suitable in all three variables because we assume that if any one of these variables is unsuitable, Delta smelt are unlikely to occupy the area.

We also extracted the daily average position of X2 from DWR's Dayflow Model (DWR 2002) and conducted a linear model of proportion of time with suitable habitat versus the interaction of region and X2 position, plus season. We also investigated the three-way interaction between region, X2, and season, but it was not significant, so it was not included in the final model.

In Dayflow, X2 is estimated using the Autoregressive Lag Model: $X2(t) = 10.16 + 0.945 * X2(t-1) - 1.487 \log(\text{Outflow}(t))$ where $t = \text{current day}$ $t-1 = \text{previous day}$ (DWR 2002). The X2 calculation to be used in Dayflow should not be confused with the position of X2 needed to ensure compliance with the Habitat Protection Outflow standard of D-1641 and the ITP and BiOps, which interpolates the location of X2 based on salinity measurements from stations Martinez (MRZ, 56 km), Port Chicago (PCT, 64 km), Chipp's Island (PTS 74 km), and Collinsville (CSE, 81km).

Increased duration of suitable temperature, turbidity, and salinity in Suisun Marsh during SMSCG actions would support the hypothesis that the SMSCG action increased Delta smelt habitat. Increased duration and/or area of suitable temperature, turbidity, and salinity in Suisun Bay during X2 actions would support the hypothesis that the X2 action increased Delta smelt habitat.

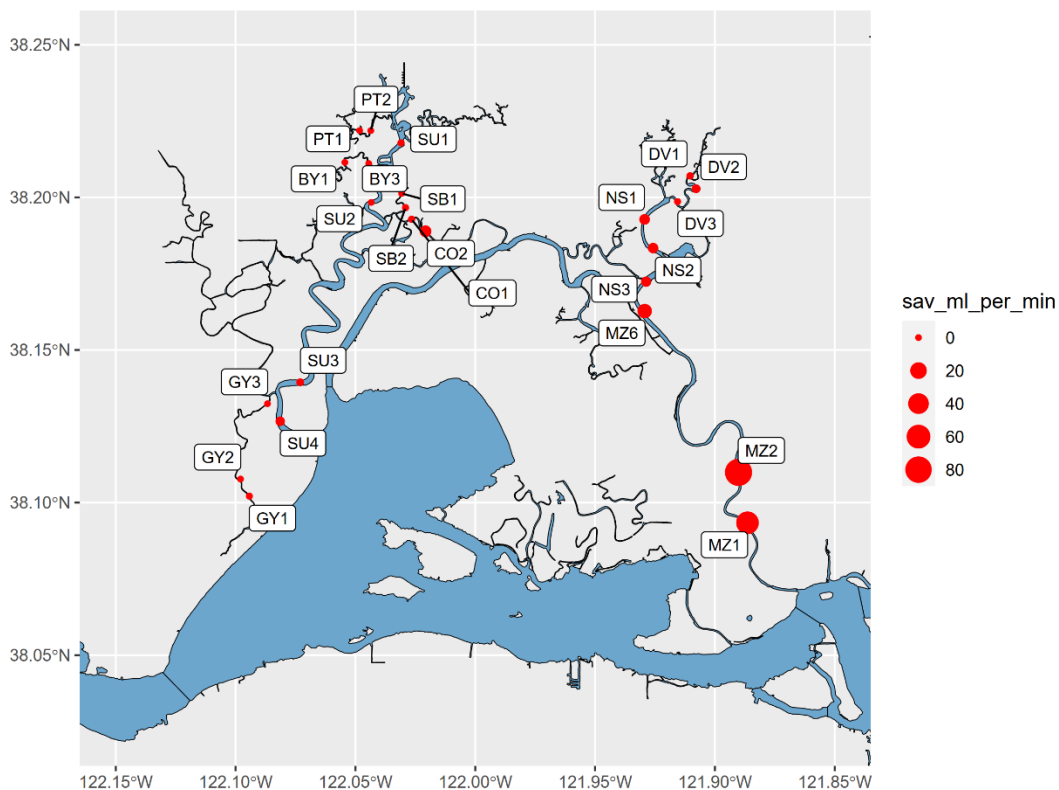
Aquatic Vegetation

We hypothesized that there would be more SAV in Suisun Marsh during years with increased freshwater flows created either by high precipitation or by management actions (X2 and/or SMSCG actions).

Tracking changes in SAV over time is difficult because the high turbidity of water in Suisun Marsh makes monitoring SAV with remote sensing (as is done in the Delta; e.g. Riaño et al. 2025) difficult. However, the Suisun Marsh Fish Survey, conducted by UC Davis, has quantified SAV "bycatch" in its monthly fish trawls since 2014 (Durand et al. 2025) and may provide valuable insight into trends in SAV abundance. We examined data from the 24 stations that had GPS coordinates and total sampling effort greater than 50 min of trawling across the time series. We focused the analysis of the summer and fall months only (July–October). Given the preference of Delta smelt for open water, we assumed that all SAV species negatively affected habitat quality, and therefore, we summed the volume of all

SAV species within a sample. Total SAV volume was divided by the duration of the tow (range: 2.5 – 10 min), resulting in a rate metric of total SAV volume (mL) per minute of trawling. Of these 24 stations, most had either no SAV ($n = 8$) or < 1 L total of SAV across the time series ($n = 13$, Figure 5). All three stations with > 1 L of SAV were in eastern Montezuma Slough (i.e., MZ1, MZ2, MZ6 in Figure 5). We plotted annual means based on data from these three stations for July–October as an indicator of patterns through time. We conducted multiple comparison tests with p-values adjusted with the Benjamini-Hochberg procedure to determine which years differed significantly from one another.

Figure 5. Map showing amount of submerged aquatic vegetation (SAV) bycatch at otter trawling stations of the University of California – Davis Suisun Marsh Fish Survey. Values represent the total volume (mL) of all SAV species collected July to October across all years of the time series (2014–2024) divided by total trawling time (min) for the same period.



Habitat Area Modeling

We modeled the area of habitat with appropriate salinity for Delta smelt (< 6 PSU) using the Bay-Delta Semi-Implicit Cross-scale Hydroscience Integrated System Model (SCHISM) model, which is based on the model developed by Zhang et al. (2016). The SCHISM hydrodynamic algorithm is based on mixed triangular-quadrangular unstructured grids in the horizontal plane and a flexible coordinate system in the vertical plane (Zhang et al. 2015). The DWR application of SCHISM to

the Bay-Delta as well as a regional description of performance is described in Ateljevich et al. (2015) and Ateljevich et al. (2014). We used the SCHISM model to produce the area below 6 PSU in Suisun Bay and Suisun Marsh for May–October of 2011–2024, adjusting the bathymetric grid to account for intentional restoration and unintentional levee breaches that occurred during this time frame. Only areas that were inundated for more than 80% of the tidal cycle were included in the final analysis of habitat area. We also used previous modeling conducted after the SMSCG and Fall X2 actions in 2023 and 2024 to compare area of the LSZ observed with the actions to what would have occurred without the actions.

To explore potential benefits of different timing of the SMSCG, we conducted a series of simulations of different gate actions for representative Wet, Above Normal, Below Normal, and Dry years. Hydrology from 2020 was used for the Dry year simulations, hydrology from 2016 was used for the Below Normal year simulations, hydrology from 2010 (which was classified as Below Normal) was used with operational conditions required by an Above Normal year for the Above Normal scenarios, and hydrology from 2017 was used for the Wet year scenarios.

The 2019/2024 ITP required 60-day operations in Dry, Below Normal, and Above Normal years, and each 60-day ITP operational scenario was modeled with two different scenarios. In the “continuous” scenario, SMSCG were operated tidally for 60 days. In the “7-days tidal, 7-days open” scenario, the 60 days of operation were spread over 120 days by operating the gates tidally for 7 days and leaving them open for 7 days. This allowed us to explore the trade-off between creating LSZ habitat in Suisun Marsh for longer and extending the spatial extent of the LSZ into Grizzly Bay. Operations began on July 1 in each scenario. While the ITP did not require SMSCG operations in Wet years, the 2019 ITP included the provision for 100 TAF of water that could be used for SMSCG operations if requested by CDFW. This generally provides approximately 60 days of compensating flow in Wet years. Because Belden’s Landing frequently does not reach 4 PSU until very late in the year during Wet years, we modeled a gate action starting July 1 and August 15 to compare the effect of different starting dates on the acreage of habitat created. Each year also included modeling of a base case with no SMSCG operations. This analysis was originally conducted in Summer 2023 to analyze the potential benefit of the 100 TAF block of water, and it is repeated here to provide a more comprehensive view of the SMSCG benefits.

Table 3. Scenarios used for modeling to assess benefits of different types of SMSCG actions for Delta smelt. Compensating flow indicates additional outflow required to meet D-1641 or Fall X2 standards.

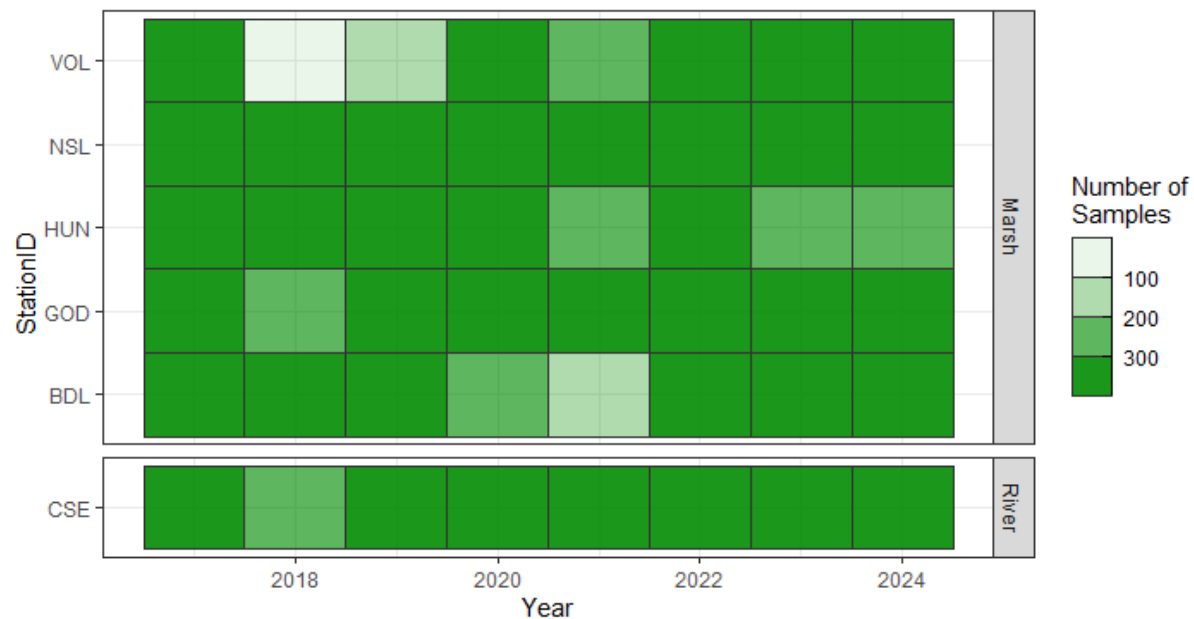
Scenario	Compensating Flow	Year Modeled	X2	SMSCG Operational Scenario
Dry Base	NA	2020	None	None
Dry 7-7	300 cfs	2020	None	60 days of operation non-consecutively, 7 days tidal, 7 days open, starting July 1
Dry 60d	300 cfs	2020	None	60 days of continuous operation, starting July 1
Below Normal Base	450 cfs	2016	None	None
Below Normal 7-7	NA	2016	None	60 days of operation non-consecutively, 7 days tidal, 7 days open, starting July 1
Below Normal 60d	450 cfs	2016	None	60 days of continuous operation, starting July 1
Above Normal Base	NA	2010	80km Sep.+Oct.	None
Above Normal 7-7	650 cfs (July), 850 cfs (Aug.)	2010	80km Sep.+Oct.	60 days of operation non-consecutively, 7 days tidal, 7 days open, starting July 1
Above Normal 60d	650 cfs (July), 850 cfs (Aug.)	2010	80km Sep.+Oct.	60 days of continuous operation, starting July 1
Wet Base	NA	2017	80km Sep.+Oct.	None
Wet 100TAF July 1	650 cfs (July), 850 cfs (Aug.-Oct.)	2017	80km Sep.+Oct.	Continuous operation, starting July 1 until additional 100 TAF is used
Wet 100TAF Aug. 15	850 cfs (Aug.-Oct.)	2017	80km Sep.+Oct.	Continuous operation, starting Aug. 15 until additional 100 TAF is used

Chlorophyll

To assess the impact of SMSCG operations on chlorophyll in Suisun Marsh, we used a subset of continuous sondes (analyzed in the continuous data analysis described above) that included chlorophyll fluorescence sensors. The number of sondes with chlorophyll sensors was low before 2017, so we only analyzed data from 2017–2024 (Figure 6). We visually compared trends in chlorophyll for the 10 days before and 10 days after the start of SMSCG operation, then used a generalized linear model of chlorophyll fluorescence versus time period (before or after gates started operating).

We used a lognormal generalized linear mixed model of log-transformed daily mean chlorophyll fluorescence versus an interaction of station and time period (before/after start of SMSCG operations) with year as a random effect. The previous day's chlorophyll was also included as a predictor term to account for temporal autocorrelation. This model was run using the glmmTMB package in R (Brooks et al. 2025). Models were checked for assumptions using the DHARMA package (Hartig 2022), and model diagnostic plots are included in Appendix A.

Figure 6. Chlorophyll data availability from 2017–2024, with color indicating number of days of data (out of a total of 365). Station IDs correspond to Table 2.



Results

Continuous Water Quality

As predicted, the number of days of suitable Delta smelt habitat in Suisun Marsh were higher during years with either SMSCG actions, X2 actions, or both, though X2 provides a greater improvement in conditions in Suisun Marsh than the SMSCG (Figure 7). An analysis of variance (ANOVA) comparing percent time with suitable habitat between regions in years with and without X2 and SMSCG actions found that years with X2 actions had more days with suitable habitat than years without X2 actions (Table 4; Figure 7), amounting to 50% more time in Grizzly Bay, 39% more time in Suisun Bay, and 30% more time in Suisun Marsh. The effect in the Sacramento River was weaker, with only 15% more time suitable and a marginally significant statistical test (Table 5; $P = 0.047$). Diagnostic plots for this model are available in Appendix A (Figure 58) and show no major deviations from the assumptions of a linear model.

Figure 7. Number of days from June 1–October 31 (153 total) where the average water quality parameters (salinity, temperature, turbidity, or all three) were within Delta smelt thresholds. No visible bar indicates there were no days of suitable habitat.

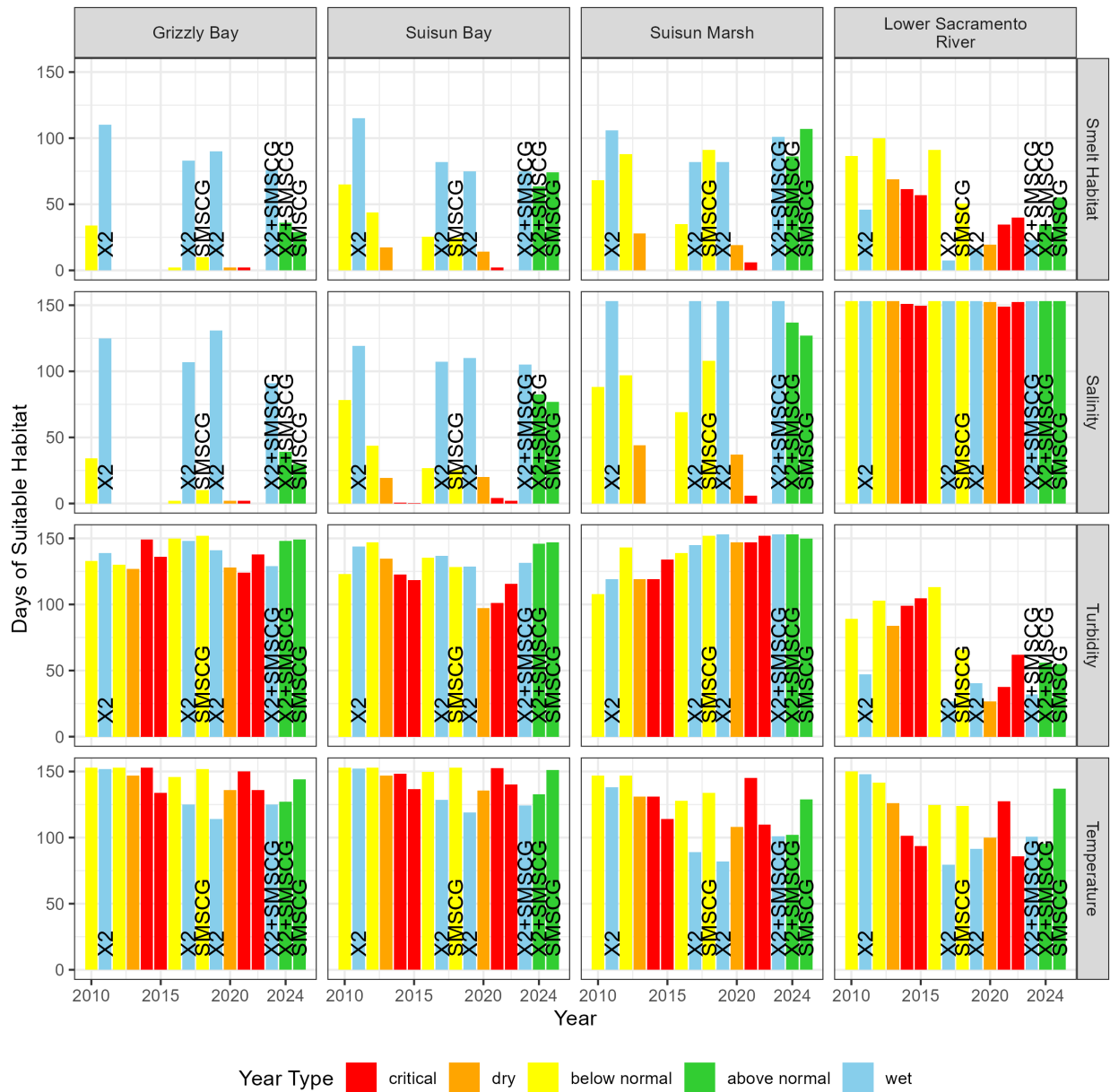


Table 4. Analysis of Deviance Table (Type II Wald chi square tests) of a beta-binomial regression of days with suitable habitat versus action type (SMSCG or X2), region, and the interaction between region and each action type. This table presents the overall significance of model terms, but results from the main effects of region, X2, and SMSCG operations should not be used except in light of the significant interaction between region and X2. See Table 5 for more detailed analysis of the interaction terms.

Predictor	Chisq	Df	Pr(>Chisq)
Region	8.29	3	0.040
X2	19.78	1	<0.0001
SMSCG	3.51	1	0.061
Region:X2	31.45	3	<0.0001
Region:SMSCG	4.80	3	0.187

Table 5. Post-hoc pairwise comparisons of the interaction terms from the model in Table 4 showing the significance of the X2 or SMSCG term in each region. Results for X2 were controlled for the effect of SMSCG operations and results for SMSCG were averaged across X2 actions. Results are given on the log odds ratio (not the response) scale.

Predictor	Region	Estimate	SE	z-ratio	p-value
X2	Grizzly Bay	-3.098	0.614	- 5.045	<.0001
X2	Suisun Bay	-2.056	0.528	-3.891	0.0001
X2	Suisun Marsh	-1.642	0.524	-3.131	0.0017
X2	Sacramento River	0.964	0.485	1.989	0.0467
SMSCG	Grizzly Bay	-0.0616	0.690	-0.089	0.9289
SMSCG	Suisun Bay	-0.5443	0.617	-0.882	0.3778
SMSCG	Suisun Marsh	-1.5955	0.583	-2.737	0.0062
SMSCG	Sacramento River	-0.0124	0.506	-0.025	0.9804

The linear model of average X2 position versus proportion of time that habitat is suitable for all three water quality variables showed a significant negative relationship between X2 and percent time with suitable habitat in Suisun Marsh (Table 5), Grizzly Bay, and Suisun Bay, and the trends in each of these regions were not significantly different from each other (Table 6, top row of Figure 8). The slope of the trend line between X2 and suitable habitat in the Sacramento River was significantly lower than the other regions and not statistically different from zero. Habitat was suitable for a slightly higher percentage of the time in fall than summer, but there was no significant relationship between season, region, and X2 (results of three-way interaction not shown). There does appear to be a slightly steeper relationship between habitat and X2 in Suisun Marsh in the fall than in the summer, but this difference was not clear enough for statistical significance.

Diagnostic plots for this model are available in Appendix A (Figure 59) and show minor quantile deviations but otherwise fit the assumptions of a linear model.

When looking at suitable habitat across the years (Figure 9), there were no consistent trends in overall habitat suitability, turbidity, or salinity over time (nonsignificant linear model results not shown); however, there was a significant decrease in the percent time water temperature was suitable across all regions during the summer but not the fall (beta-binomial model of time with suitable temperature in summer versus region and year estimate -0.097, SE 0.023, t-value -4.12, $p < 0.0001$). There was no significant interaction between region and year (analysis not shown).

Table 6. Analysis of deviance table from a generalized linear model (beta-binomial distribution) of percent time habitat is suitable in each region versus X2, the interaction between X2 and region and season, as well as post-hoc analyses of which X2 trends were significant and which regions were significantly different from one another. df = Degrees of Freedom, Sum Sq = Sum of Squares, Mean Sq = Mean Square, SE = Standard Error.

Predictor	df	Chisq	Pr(>F)	
Region	3	15.3	0.0016	
X2	1	50.44	<.0001	
Season	1	1.33	0.248	
Region:X2	3	65.23	<.0001	
Residuals	111			
Trend Comparisons				
Region	X2 Trend	SE	lower.CL	upper.CL
Grizzly Bay	-0.304	0.0463	-0.395	-0.213
Suisun Bay	-0.237	0.0366	-0.309	-0.165
Suisun Marsh	-0.240	0.0411	-0.321	-0.159
Lower Sacramento River	0.0312	0.0272	-0.022	0.084
Regional Contrasts				
	Estimate	SE	z-ratio	P-value
Grizzly Bay - Suisun Bay	-0.067	0.058	-1.158	0.653
Grizzly Bay - Suisun Marsh	-0.064	0.061	-1.046	0.722
Grizzly Bay - Lower Sacramento River	-0.335	0.053	-6.294	<.0001
Suisun Bay - Suisun Marsh	0.003	0.054	0.060	0.999
Suisun Bay - Lower Sacramento River	-0.268	0.045	-5.949	<.0001
Suisun Marsh - Lower Sacramento River	-0.271	0.049	-5.513	<.0001

Figure 8. Percent of time water quality is within Delta smelt thresholds versus seasonal average X2 location by season and region. The top row represents the number of days where all three water quality parameters are suitable, the second row shows just time salinity is < 6 PSU, the third row shows time turbidity is > 12 NTU, and the final row shows time temperature is < 20°C. Points indicate the amount of time habitat was suitable in either summer (red) or fall (blue) for each year. A linear trend line +/- 1 SE is plotted through each dataset.

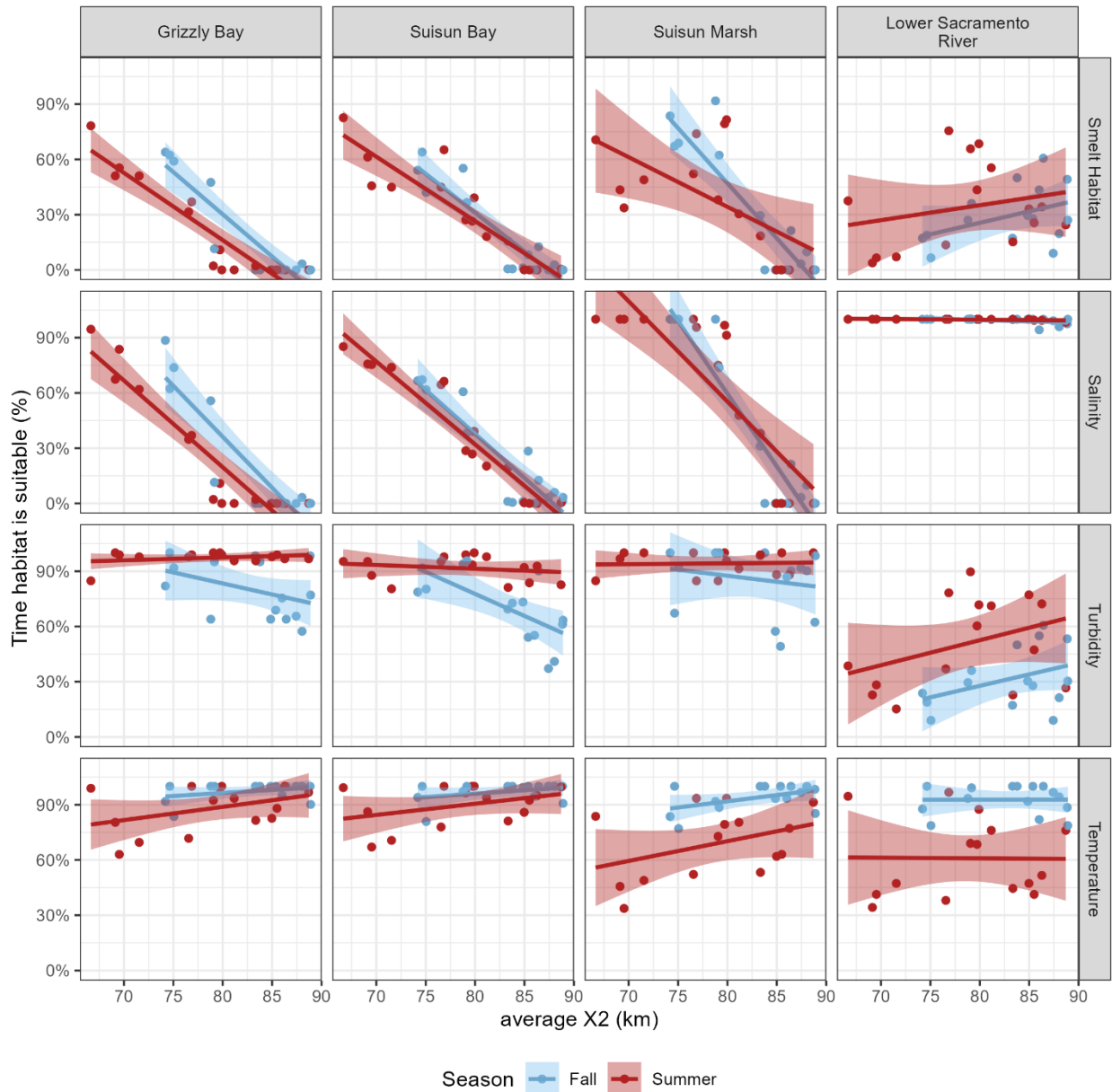
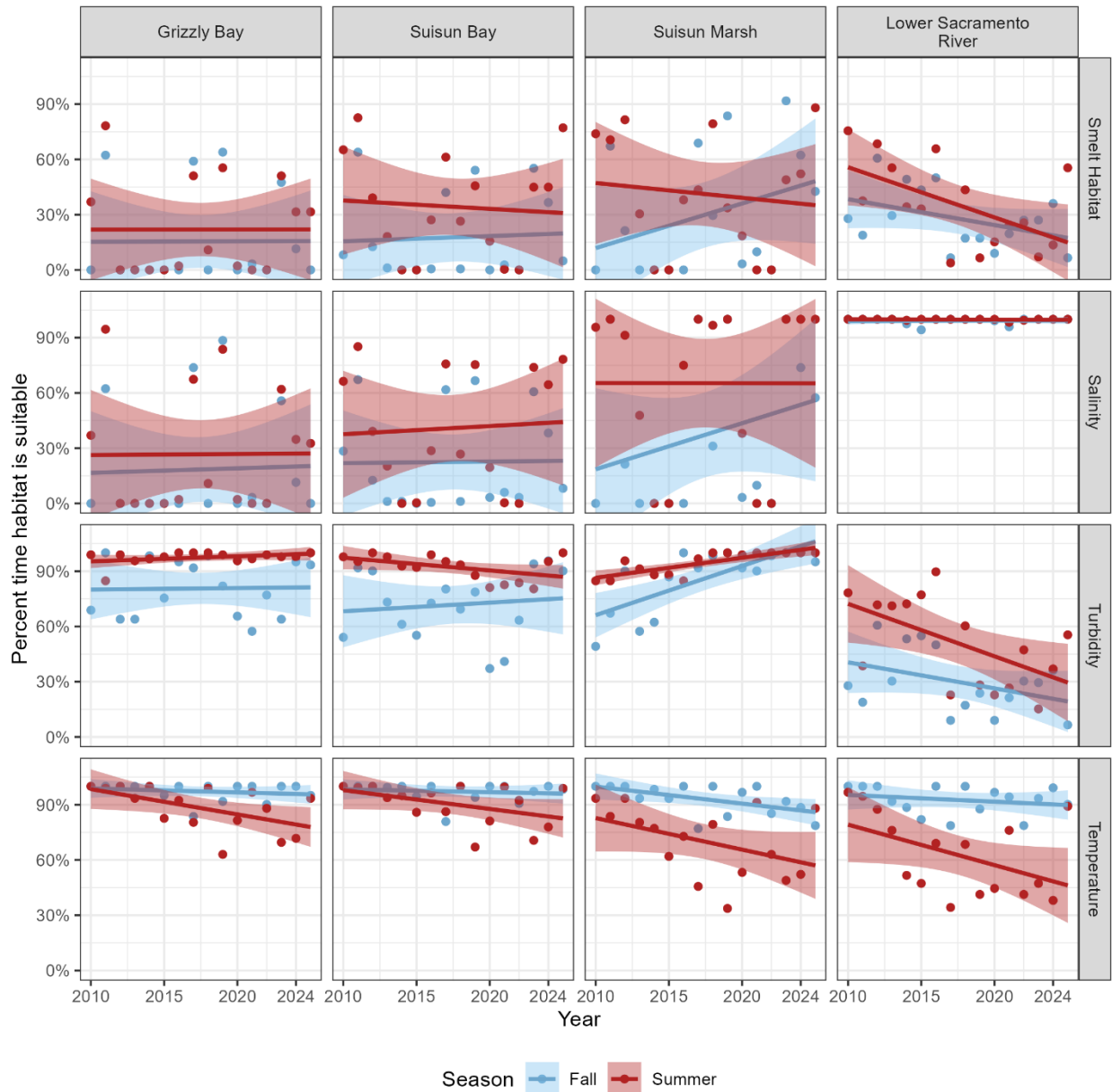


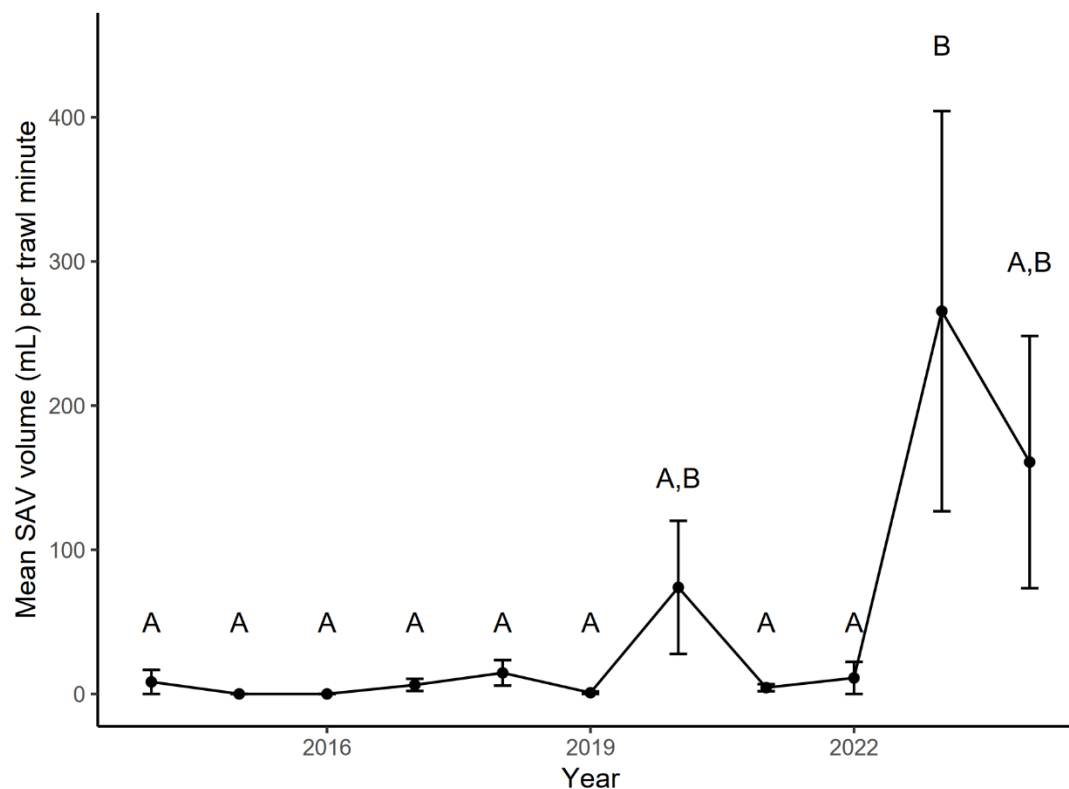
Figure 9. Percent of time water quality is within Delta smelt thresholds versus year by season and region. The top row represents the number of days where all three water quality parameters are suitable, the second row shows just time salinity is < 6 PSU, the third row shows time turbidity is > 12 NTU, and the final row shows time temperature is < 20°C. Points indicate the amount of time habitat was suitable in either summer (red) or fall (blue) for each year. A linear trend line +/- 1 SE is plotted through each dataset.



Aquatic Vegetation

The SAV capture rate in the otter trawls from the three stations in the eastern Montezuma Slough was low in most years (i.e., $< 15 \text{ mL min}^{-1}$) (Figure 10). Capture rates were relatively higher in the years 2020, 2023, and 2024, exhibiting means $5.1\times$, $18.1\times$, and $11.0\times$ higher, respectively, than that of 2018, the year with the next highest rate (Figure 10). However, these three recent years also exhibited high variation (Figure 10), with some samples containing no SAV and the rest exhibiting capture rates that spanned three orders of magnitude. Consequently, 2023 was the only year that was statistically significantly higher than the other years (but not different from 2020 or 2024).

Figure 10. Time series of submerged aquatic vegetation (SAV) bycatch in eastern Montezuma Slough based on three otter trawling stations of the University of California – Davis Suisun Marsh Fish Survey. Each point represents the mean of ~ 12 samples (3 stations \times 4 months). Error bars represent standard errors. Years that share letters are not statistically significantly different.



Habitat Area Modeling

Observed LSZ Area from 2011–2024

When examining the area of the LSZ over the course of each summer and fall from 2011–2024 (Figure 11, Figure 12), we see similar results to the continuous water quality analysis. Habitat area in Suisun Bay and Grizzly Bay is greatest in Wet and Above Normal water year types. When the SMSCG was operated in a Below Normal water year type (August of 2018), it did not result in habitat in Grizzly Bay (Figure 12). Habitat in Suisun Marsh was greatest in years with Wet and Above Normal years with both X2 and SMSCG operations, though increases in total available habitat area due to wetland restoration in 2019–2022 means that not all of the increased habitat in 2023 and 2024 was due to the X2 and SMSCG operations.

Figure 11. Analysis of LSZ area out of the total area of the region by day of year based on SCHISM modeling for historical conditions for 2011–2024 in Grizzly Bay (top plot), Suisun Bay (middle plot) and Suisun Marsh (bottom plot). Years plotted in shades of red were Critically Dry, shades of orange were Dry, shades of yellow were Below Normal, green were Above Normal, and blue were Wet.

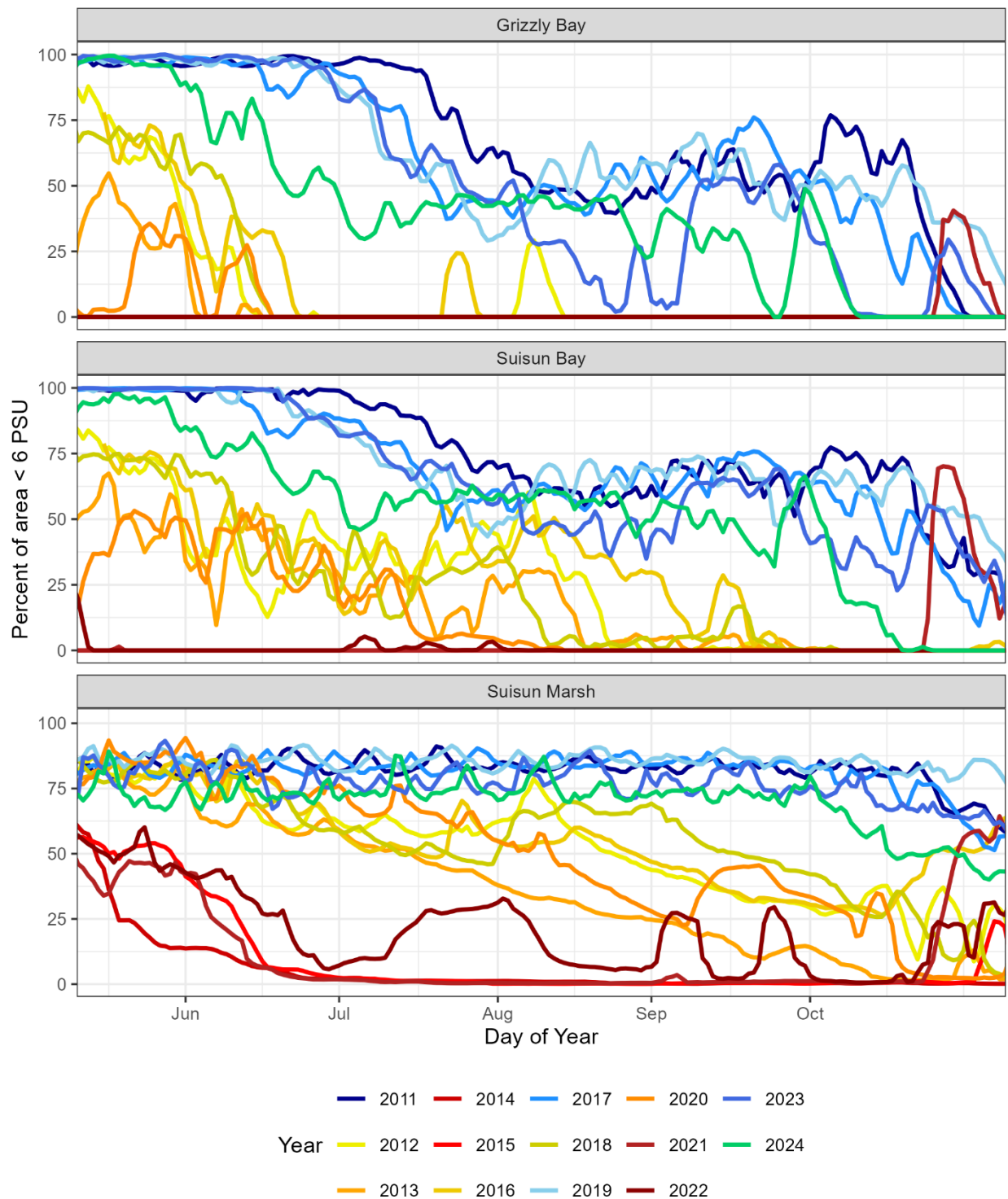
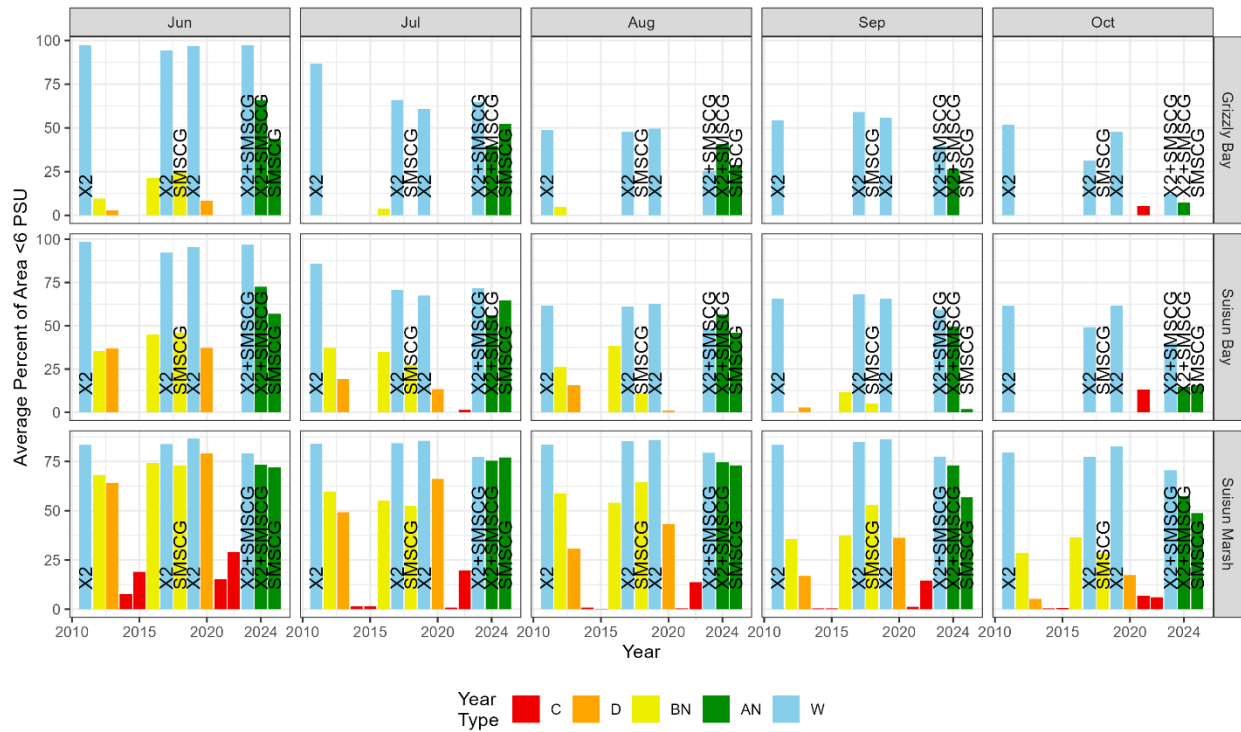


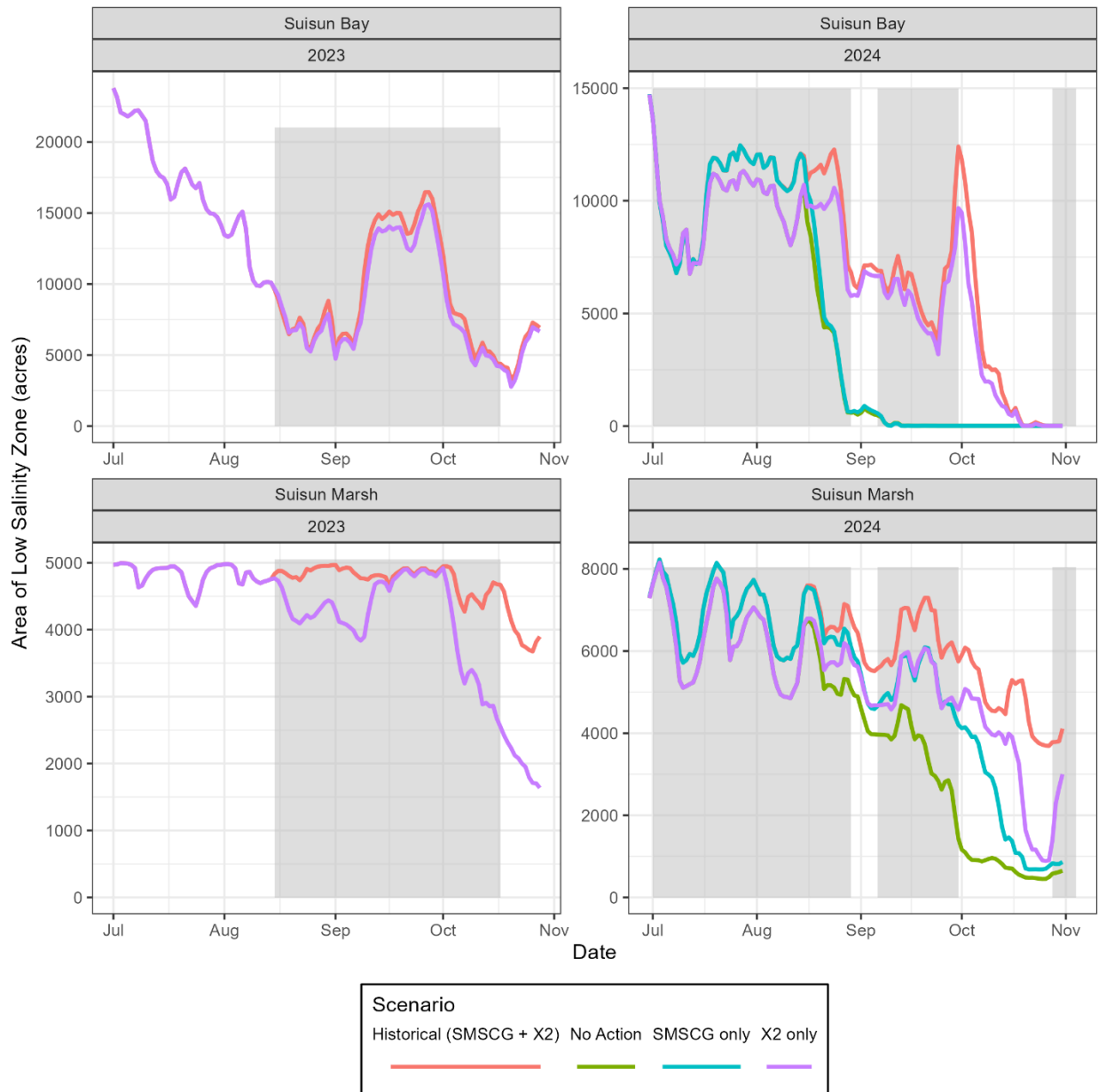
Figure 12. Monthly average area of the LSZ across years by region.



Analysis of 2023 and 2024 Actions

Looking at the actions in 2023 and 2024 (Figure 13), the historical scenario (SMSCG + X2) increased the habitat area versus the X2-only scenario more in 2024 than 2023. In 2023, there was a slight increase in area in Suisun Bay during the action, and an increase in area in Suisun Marsh in August and September, but no increase in area later in September and October because the X2 action freshened the entire Marsh below 6 PSU without any gate operation. In 2024, the SMSCG action increased LSZ area in Suisun Bay in the second half of July and August, but the operations in early July and September resulted in only a very small increase in area above the X2-only scenario. In Suisun Marsh, the SMSCG + X2 scenario added several hundred acres of habitat throughout the operational period compared to the X2-only scenario, unlike what was observed in 2023. The 2024 scenarios also included a “no-action” scenario without X2 or SMSCG operations and a scenario with only SMSCG operations and no X2 action. Both the SMSCG-only scenario and the Fall X2-only scenario had similar area of habitat in Suisun Marsh compared to the no-action scenario for September, though the X2 scenario had higher habitat in October.

Figure 13. Modeled area of the LSZ in Suisun Bay (top) and Suisun Marsh (bottom) in 2023 and 2024 for different operational scenarios. Note that the bathymetry of Suisun Marsh was updated in 2024 to reflect new wetland restoration, so maximum area is higher. Also, the SMSCG-only and no-action scenarios were only run in 2024.



Alternative Gate Timing

The analysis of alternative gate timing (Figure 14) showed that the increase in LSZ area differs in different water year types.

Results from the 2020 Dry Year Modeling Surrogate showed operation of the SMSCG increased the amount of LSZ area in Suisun Marsh from an average of 521 acres to over 2000 acres (Figure 14). Operating the SMSCG tidally for 60 days continuously created a somewhat lower average LSZ area than operating for 7-days on, 7-days open, because operations could be stretched later into the summer (Figure 14). LSZ area decreased slightly in Suisun Bay when the SMSCG were operated, going from 535 acres in the base case with no gate operation to 360–449 acres under the operational scenarios; no LSZ area was available in Grizzly Bay under any scenario (Figure 14).

Results from the 2016 Below Normal year modeling surrogate showed operation of the SMSCG increased the amount of LSZ area in Suisun Marsh from an average of 1550 acres to over 4000 acres (Figure 14). Operating SMSCG tidally for 60 days continuously created a somewhat lower average LSZ area than operating for 7-days tidal, 7-days open. Operations could be stretched later into the summer when operating discontinuously, but the continuous operation increased LSZ area in Grizzly Bay more than the discontinuous operation scenario (Figure 14). LSZ area in Suisun Bay also increased slightly more during the continuous operation than the discontinuous operation.

Results from the 2010 Above Normal water year modeling surrogate showed operation of the SMSCG increased the amount of LSZ area in Suisun Marsh from an average of 3612 acres with no SMSCG operation to over 4000 acres with SMSCG operation (Figure 14). Operating the SMSCG tidally for 60 days continuously created a somewhat lower average LSZ area than operating for 7-days tidal, 7-days open because SMSCG operations could be stretched later into the summer. There was more LSZ area created in Grizzly Bay in July and August with the continuous operation scenario, but greater area in Grizzly Bay in September during the 7-days tidal, 7-days open scenario. When compared to the drier years, the base case had more existing LSZ area, meaning there was a lower increase when the SMSCG were operated (average increase of 14–20% in Suisun Marsh LSZ area for Above Normal scenarios versus an increase of 96–133% for Below Normal years).

Results from the 2017 Wet Water Year Modeling Surrogate showed operation of the SMSCG starting July 1 increased the area of LSZ in Suisun Marsh only slightly versus the base case (only about a 1% increase, on average) (Figure 14). Operating SMSCG tidally starting on August 15 created a slightly greater increase in LSZ area in Suisun Marsh (~3% on average). Grizzly Bay saw a similar pattern of a slight increase in LSZ area in July and August under the July 1 scenario, with a slightly larger increase in area under the August 15 scenario, but these increases in area were relatively small when compared to increases in other water year types.

Figure 14. Low Salinity Zone area in Suisun Marsh, Suisun Bay, and Grizzly Bay for different SMSCG operational scenarios and different water year types.



Chlorophyll

Visually examining the chlorophyll data from Suisun Marsh over the past eight years since we started collecting the data, there appears to be a trend of declining chlorophyll immediately after gate operation started at some of the stations (Figure 15, see Figure 2 for station locations). At Collinsville (Station CSE, upstream from SMSCG), there was no consistent pattern, but at both National Steel (Station NSL, just downstream from SMSCG) and Belden's Landing (Station BDL, further downstream), there is a step decline in chlorophyll immediately after gate operation begins in most (but not all) years. Further downstream at Hunter Cut (Station HUN), there does not seem to be the same step-decrease, but this station is located on the intersection of two sloughs, so it is influenced by conditions in Suisun Slough as well as Montezuma Slough. Stations off Suisun Slough (Volanti, [VOL], and Goodyear [GOD]) do not seem to show consistent patterns with gate operations.

Using a lognormal generalized linear model, we found a significant reduction in chlorophyll post-SMSCG operations at National Steel (Figure 16, Table 7). Belden's Landing, which is located midway along Montezuma Slough, showed a decrease in chlorophyll after SMSCG operations began in most years, but the relationship was not statistically significant ($p= 0.10$), possibly due to the anomalous high chlorophyll spike that occurred after SMSCG operations in 2022. Variation was higher, and there was no significant trend in chlorophyll with gate operations at CSE or HUN. Diagnostic plots for this model are included in Appendix A (Figure 60). The model did not show an exact fit along the QQ plot, indicating residuals were not entirely normally distributed, and the data were slightly overdispersed, but this model provides a starting point for further exploration of chlorophyll dynamics during SMSCG operation.

Figure 15. Time series of chlorophyll fluorescence at one station in the lower Sacramento River (CSE) and several stations in Suisun Marsh during the summer and fall of each year (June–October). Gray boxes indicate time periods when the SMSCG were operating.



Figure 16. Effects plot of linear model of chlorophyll fluorescence from sondes before and after SMSCG operations from 2018–2025.

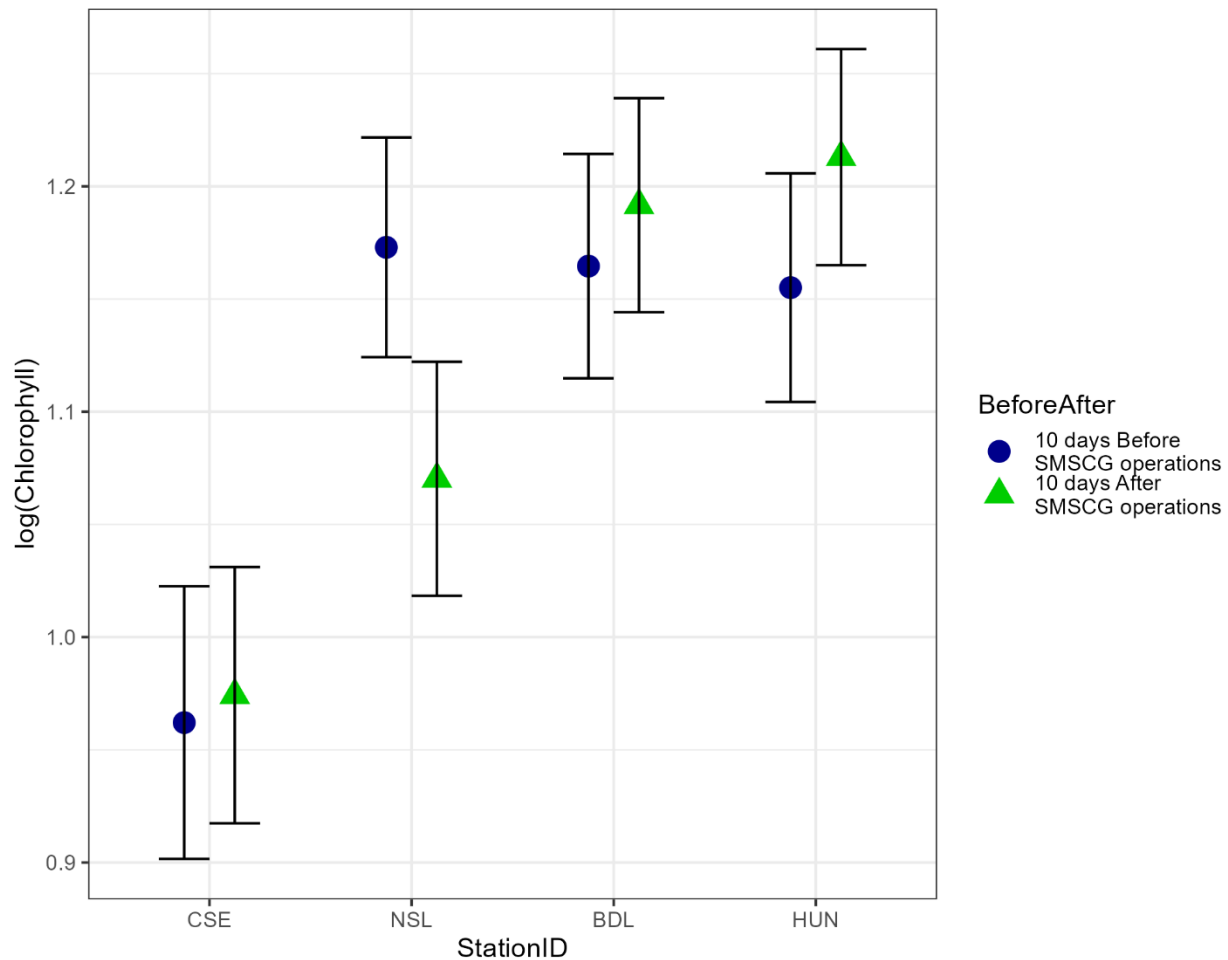


Table 7. Results of the fixed effects from the lognormal linear model of chlorophyll fluorescence during the ten days before and ten days after start of SMSCG operations. Variance on the random effect of year was 0.002885, +/- 0.0537.

Predictor	Estimate	SE	df	t value	Pr(> t)
(Intercept) Before, BDL	0.5327	0.0320	16.62	<0.0001	0.5327
Station - CSE	-0.2025	0.0294	-6.89	<0.0001	-0.2025
Station - HUN	-0.0096	0.0193	-0.50	0.620	-0.0096
Station - NSL	0.0083	0.0192	0.43	0.664	0.0083
After	0.0270	0.0166	1.63	0.104	0.0270
Lag Chlorophyll	0.1965	0.0038	51.23	<0.0001	0.1965
CSE: After	-0.0149	0.0344	-0.43	0.666	-0.0149
HUN: After	0.0309	0.0254	1.22	0.224	0.0309
NSL: After	-0.1297	0.0274	-4.73	<0.0001	-0.1297

Predictor	Estimate	SE	df	t value	Pr(> t)
Post-Hoc contrasts					
BDL: Before - After	-0.0270	0.0166		-1.68	0.104
CSE: Before - After	-0.0122	0.0300		-0.405	0.6851
HUN: Before - After	-0.0579	0.0196		-1.858	0.0635
NSL: Before - After	0.1027	0.0223		4.597	<0.0001

Discussion

Temperature, Turbidity, Salinity

All of the observations and models presented here support previous research showing that lower X2 provides greater area of the LSZ (Feyrer et al. 2011), as well as higher turbidity and lower temperature in the LSZ when compared to higher X2. Modeling also demonstrated increased habitat area during SMCSG operations in moderate water year types (Dry, Below Normal or Above Normal) but less increase in Wet water years. It was difficult to empirically show higher habitat area in years with SMCSG operations because two out of four of these years also had Fall X2 actions. It also is difficult to extract the impact of intentional Fall X2 actions from extremely wet conditions that may have kept the entire region fresh throughout the summer and fall.

Since Feyrer et al. (2007) first demonstrated that lower Fall X2 increases LSZ area in Suisun Bay and Suisun Marsh, LSZ area has been used as a surrogate for Delta smelt habitat availability (Murphy and Weiland 2019). Impact of water project operations on Delta smelt has been measured in terms of abiotic habitat area in the 2019/2020 and 2024 BiOps and ITP (USFWS 2019; CDFW 2020; CDFW 2024), though because of difficulties in predicting future temperatures and turbidities, these analyses focused on the area of the LSZ rather than an integrated assessment of turbidity, temperature, salinity, and food supply. We show that the observed area and number of days with appropriate temperature, turbidity, and salinity are generally higher during years with Fall X2 actions than years without Fall X2 actions (Figure 8, Figure 12). Because Fall X2 actions have occurred in every Wet year we analyzed, we have no empirical “no-action” data for comparison, but modeling of X2 versus a no-action alternative suggests the action provides a significant increase in habitat area over what would have happened without Fall X2 (Figure 13).

The effectiveness of the SMCSG action in lowering salinity in Suisun Marsh is clear, especially when it does not occur in conjunction with a Fall X2 action (Sommer et al. 2020). However, it was difficult to detect a change in the number of days of suitable habitat when SMCSG actions occur in conjunction with Fall X2, since most of Suisun Marsh would be suitable without gate operations (Figure 13, Figure 14).

The hydrodynamic models give a better demonstration of the effectiveness of the action – lowering salinity across the Marsh when it is above 6 PSU and adding some habitat in Grizzly Bay (Figure 13, Figure 14).

While SMSCG actions to date (2018, 2023, 2024, 2025) have been continuous operations or mostly continuous, modeling suggests that discontinuous operations – such as a week of tidal operations followed by a week when gates are held open – can extend the duration of LSZ habitat in Suisun Marsh. However, this is at the expense of less habitat being created in Grizzly Bay. Due to the lower temperatures in Grizzly Bay during the summer (Pien et al. 2025), it may be more beneficial to increase the duration of suitable habitat in Grizzly Bay during the summer than extend Suisun Marsh habitat into the fall when temperatures are already cooler. However, the ultimate effectiveness of a SMSCG action for increasing Delta smelt population viability will rely on smelt using the habitat, which is not a certainty in either scenario. In some years, a large proportion of the population remains year-round in freshwater (Hobbs, Lewis et al. 2019; Young et al., in review; Hobbs, Denney et al. 2019), and overall low population makes it difficult to estimate how many fish occupy Suisun Marsh.

The modeling across several example water years also demonstrated a greater increase in habitat area in drier years than wetter years, since more habitat was available in the base case in wetter years. This was also demonstrated in the comparison of actual gate operations in 2023 and 2024, with a greater increase in area with the 2024 action than the 2023 action. The difference between 2023 and 2024 is partially due to the X2 action only occurring in September in 2024, not September and October. The SMSCG action was also longer in 2024, totaling 86 days versus 63 days in 2023. However, the different underlying hydrology may explain more of the difference. 2023 was a Wet year, whereas 2024 was an Above Normal year, so salinity began declining earlier in the summer, allowing the SMSCG to have a greater impact on salinity across the summer.

Of the three abiotic habitat components we looked at, there was no single factor that was limiting in all regions and years. In the Sacramento River, turbidity was the most frequently limiting, followed by temperatures, while salinity was almost never limiting. The long-term decline in turbidity is most apparent in the Delta, with less of a decline downstream in Suisun Bay (Schoellhamer 2011; Hestir et al. 2016), so the Sacramento River is likely to continue its trend of poor habitat quality due to water clarity alone. Temperatures limited habitat availability in both Suisun Marsh and the Sacramento River regions more frequently than Suisun Bay or Grizzly Bay, which tended to be cooler. Temperatures have also been increasing across the system, though increases to date have been more significant in the fall than the summer (Bashevkin, Mahardja et al. 2022). While the SFHA was originally intended to maximize the area of the LSZ, the importance of the LSZ overlapping with the cooler water of Suisun Bay and Grizzly Bay is now being recognized.

Despite these analyses showing clear increases in Delta smelt habitat area, it is not well understood whether increased abiotic habitat area will result in a more robust population. For example, Feyrer et al. (2011) found a strong relationship between Fall X2 and an abiotic habitat, but a much weaker relationship between abiotic habitat and Delta smelt population indices. Similarly, Polansky et al. (2024) found a strong relationship between Delta smelt population growth and summer outflow (which corresponds to increased habitat area), but a much weaker relationship between population growth and fall outflow. We further explore the relationship between habitat and individual Delta smelt growth and health in the [Smelt Growth – Wild Fish](#) section.

Aquatic Vegetation

Over the 11 years that the UC Davis Suisun Marsh Fish Survey has quantified SAV bycatch in otter trawls, only the stations in eastern Montezuma Slough have shown more than trace amounts of SAV (Figure 5). This is the area of the Marsh we would anticipate the most abundant SAV, because it is in closest proximity to the Delta, meaning it is the freshest and the most exposed to SAV propagules from other heavily invaded areas. The three stations in eastern Montezuma Slough still showed relatively low levels of SAV in all but three years (2020, 2023, and 2024), and of these three years, only 2023 exhibited significantly higher levels compared to most (but not all) years. Based on this time series, it remains unclear how much freshening the Marsh contributes to changes in SAV abundance. Both 2023 and 2024 were wetter years, each with a combination of X2 and SMSCG actions occurring (Table 1), which is consistent with our hypothesis of higher SAV under fresher conditions. However, 2020 was a Dry year with neither of these management actions occurring during the summer (Table 1, Figure 7), so fresher conditions do not explain why this year exhibited the third highest mean SAV capture rate. Also, 2017 and 2019 were Wet years with X2 actions (Table 1), but these were not years with elevated SAV abundances. It may be that SAV abundance is driven by a complex mix of factors beyond simply how fresh the Marsh is during a given year. Also, it is important to recognize that this analysis is based on an ancillary data set from a fish monitoring survey, not a dedicated vegetation monitoring program. It is unknown how well the abundance of SAV fragments captured in this survey reflects abundances of SAV growing in the channels, but this is currently the best data set available for this analysis.

Chlorophyll

SMSCG operations tended to decrease chlorophyll concentrations in the region immediately downstream of the gates, but this effect was relatively localized and not consistent across all years (Figure 16). This effect was likely caused by the decrease in residence time during gate operations and the transport of lower productivity water from upstream (Collinsville, station CSE). Suisun Marsh is generally higher in chlorophyll concentration than Suisun Bay or the lower

Sacramento River (Sommer et al. 2020), most likely due to a combination of higher residence time, extensive wetlands, lower densities of invasive clams, and extensive shallows. When the gates operate, they decrease the residence time, flushing some of the phytoplankton out of Montezuma Slough. Residence time is considered one of the primary drivers of chlorophyll biomass in the estuary (Glibert et al. 2014; Hammock, Moose et al. 2019), so while operation of the SMSCG is thought to increase transport of *P. forbesi* and other zooplankton from upstream (see [Smelt Food](#) section), it may disrupt the conditions leading to high chlorophyll concentration in the Marsh. Furthermore, although abundance and biomass of *P. forbesi* is higher upstream, chlorophyll is often higher in the Marsh than the lower Sacramento River (Sommer et al. 2020), though the highest biomass is generally in the south or central Delta where residence times are even longer (Bosworth et al. 2024; Richardson et al. 2025).

The decline in chlorophyll was notable, but unlikely to significantly decrease the effectiveness of the SMSCG action for Delta smelt habitat. The effect was relatively localized, only impacting the eastern and middle of Montezuma Slough, not affecting chlorophyll on the western side of the Marsh. We do not have continuous chlorophyll data for many of the dead-end sloughs in Suisun Marsh, but many special studies indicate these areas have very high chlorophyll and zooplankton (Aha et al. 2021; Williamshen et al. 2021). With lower influence of the SMSCG on local hydrodynamics in dead-end sloughs such as Nurse Slough, Denverton Slough, and Suisun Slough, there are not likely to be major changes in chlorophyll in the areas with high chlorophyll during SMSCG operation.

While chlorophyll is often used as an indicator of overall ecosystem productivity, it is not a direct measure of primary productivity, which may have still been high despite low biomass. Areas with higher chlorophyll are correlated with higher Delta smelt body condition factor (Hammock et al. 2022); however, high chlorophyll is not required for Delta smelt habitat. The abundance of *P. forbesi*, their most important prey during the summer, is not directly correlated with chlorophyll (Hartman et al. 2025), and there is mixed evidence for chlorophyll increasing *P. forbesi* growth and reproductive rates (Gearty et al. 2021; Kimmerer, Ignoffo et al. 2018; Kimmerer et al. 2014). Therefore, lower chlorophyll may not have any negative effects on the prey resources for Delta smelt, especially if it is accompanied by a subsidy of juvenile and adult copepods from upstream (Hassrick et al. 2023; as shown by Kimmerer, Gross et al. 2018).

Conclusions

When assessing our hypotheses about the influence of SMSCG actions and Fall X2 actions, we found support for our main hypothesis that lower X2 in the summer and fall, and lower salinity in Belden's Landing will increase the extent and duration of suitable turbidity, temperature, and salinity habitat in Suisun Marsh, Suisun Bay, and Grizzly Bay. Breaking this into more specific hypotheses:

- *Hypothesis:* There will be more days of overlapping suitable salinity, temperature, and turbidity and a greater area of the LSZ in Suisun Bay during years with Fall X2 actions.
 - *Supported.*
 - Analysis of continuous sonde data showed years with X2 actions had more days of appropriate habitat than years without X2 actions.
 - There was also a significant linear relationship between X2 and number of days of suitable habitat in both summer and fall.
 - Modeling of habitat area demonstrated a greater area of the LSZ in Suisun Bay during Fall X2 actions.
- *Hypothesis:* There will be more days of overlapping suitable salinity, temperature, and turbidity in Suisun Marsh during years with Fall X2 actions or SMSCG actions.
 - *Partially Supported.*
 - Analysis of continuous sonde data showed years with X2 actions had more days of appropriate habitat than years without X2 actions.
 - There was also a significant linear relationship between X2 and suitable habitat in both summer and fall.
 - There was greater modeled LSZ area during SMSCG operations than modeled habitat area without an action, but this effect was more pronounced when conditions were more saline (drier water years).
- *Hypothesis:* SMSCG operations will cause a greater increase in LSZ area in Suisun Marsh in drier years, but LSZ area in Grizzly Bay will only increase in Above Normal or Below Normal years.
 - *Supported.*
 - Based on comparisons of the effectiveness of the action in 2023 and 2024, as well as modeling of hypothetical scenarios in different water year types, we found greater increases to habitat area in drier years, with Grizzly Bay habitat only increasing in moderate water year types.
 - Retrospective analysis of habitat area in 2018, which was a Below Normal year with SMSCG operation in August showed no LSZ habitat in Grizzly Bay during the action.
- *Hypothesis:* Multiple years with low X2 and lower salinity in Suisun Marsh will result in increased prevalence of submerged aquatic vegetation in Suisun Marsh and Suisun Bay.
 - *Not supported.*
 - While submerged vegetation increased, the increase was not clearly correlated with SMSCG operations or wetter conditions.
- *Hypothesis:* Operation of the SMSCG will decrease concentration of phytoplankton in Montezuma Slough.
 - *Partially supported.*

- There was a decline in chlorophyll concentration downstream of the SMSCG in Montezuma Slough after operation began in most, but not all, years.
- *Hypothesis:* Abiotic habitat improvements with lower X2 will be similar in summer and fall.
 - *Supported.*
 - Habitat availability as defined by water quality parameters responded similarly in summer and fall, though temperatures were less frequently limiting in fall.

Smelt Food

Introduction

The Delta Smelt SFHA was originally conceptualized as increasing total LSZ habitat area and optimizing the overlap of low salinity, low temperature, and high turbidity (Feyrer et al. 2007; Nobriga et al. 2008; Sommer et al. 2020). Early analyses (such as Feyrer et al. 2007 and Nobriga et al. 2008) did not take food supply in the LSZ into account. However, food limitation is considered one of the major causes of low survival during the summer and fall (Hammock et al. 2015). While the importance of food limitation, turbidity, or temperature as a limiting factor changes regionally and inter-annually, increased food supply in Suisun Bay and Suisun Marsh is particularly important for maximizing growth in these regions (Smith and Nobriga 2023).

Suisun Marsh and Suisun Bay tend to have lower zooplankton biomass than upstream regions, largely due to competition and predation by the invasive clam *Potamocorbula amurensis* (Kimmerer and Lougee 2015; Kimmerer, Gross et al. 2018). The existing zooplankton community is dominated by the small cyclopoid copepod *Limnoithona tetraspina* (Bouley and Kimmerer 2006), which is much smaller than the dominant taxa upstream and thought to be less nutritionally valuable for Delta smelt (Rose et al. 2013a). In the freshwater reaches of the Delta, the summer zooplankton community is dominated by the larger calanoid copepod *P. forbesi*, where it provides a key resource for Delta smelt, comprising 50–90% of their diet during June–November (Slater and Baxter 2014; Slater et al. 2019). While *P. forbesi* are generally more abundant in fresh water than the LSZ (Kayfetz and Kimmerer 2017), their abundance in the LSZ increases with increased flow (Kimmerer, Ignoffo et al. 2018). The reasons for this increase include physical transport of individuals with increased flow from the higher densities upstream (Kimmerer, Ignoffo et al. 2018; Hassrick et al. 2023) as well as decreasing salinity and associated reduction in predation from predatory copepods that prefer higher salinity (Kayfetz and Kimmerer 2017). Thus, actions such as Fall X2 and the SMSCG operations are now thought to benefit Delta smelt by increasing the abundance of this important prey item in downstream areas as well as increasing habitat area in Suisun Marsh and Suisun Bay.

P. forbesi is one of the most important zooplankton taxa for Delta smelt in the summer and fall, but it is certainly not the only taxa eaten during this time period, and other food items may also increase with increased flow. Overall zooplankton biomass decreases in the broader Suisun region during droughts (Hartman et al. 2024), though not all taxa respond the same way (Barros et al. 2024). The mysid shrimp, *Neomysis mercedis*, was historically important in Delta smelt diets and increased with higher flows, but its current abundance is very low, so it only provides a minor source of smelt food (Kimmerer 2002; SWRCB 2017; Avila and

Hartman 2020). The dominant mysid in today's estuary is *Hyperacanthomysis longirostris*, but this taxon does not have as clear of a relationship with flow (Barros et al. 2024). *Eurytemora carolleeae* was one of the dominant copepods in the estuary prior to introduction of *P. forbesi* and still provides an important contribution to Delta smelt diets in the spring (Slater et al. 2019), but it is rare in summer and does not show a relationship with summer or fall flows (Kimmerer 2002; SWRCB 2017). Some taxa, including the predatory copepods *Acartia sp.*, *Tortanus sp.*, and *Limnoithona tetraspina*, decrease with increased flow (Barros et al. 2024; Bollens et al. 2011; Ambler et al. 1985).

It is well established that increased flow and decreased salinity increase total zooplankton biomass (and biomass of *P. forbesi* in particular) in both Suisun Bay and Suisun Marsh (Lee et al. 2023; Kimmerer, Ignoffo et al. 2018), but there are some important differences between these two areas that may impact food supply for Delta smelt. Suisun Bay is mostly open water, with high densities of invasive clams, cooler water, and extensive shallow shoals (Bever et al. 2016; Pien et al. 2025; Zierdt Smith et al. 2023). Suisun Marsh, in contrast, has lower densities of clams (particularly in smaller sloughs and wetlands) (Wells et al., in review), higher temperatures, extensive dead-end channels, tidal wetlands, and dendritic sloughs (Moyle et al. 2014; Pien et al. 2025; Hammock, Hartman et al. 2019). Both phytoplankton and zooplankton densities tend to be higher in the Marsh than the Bay (Hartman et al. 2024). There is some evidence that Delta smelt that are caught near tidal wetlands have higher stomach fullness even when ambient zooplankton density is low, suggesting they may forage in wetland habitat (Hammock, Hartman et al. 2019). Therefore, interactions between food supply and physical habitat in these different regions may result in different benefits of actions targeting the two regions.

Hypotheses

Our main hypothesis (repeated from the introduction of this report) is that lower X2 in the summer and fall will increase the abundance of *P. forbesi* in Suisun Marsh, Suisun Bay, and Grizzly Bay. Lower salinity at Belden's Landing will increase the abundance of *P. forbesi* in Suisun Marsh. To further explore the importance of a *P. forbesi* subsidy to Suisun Marsh and Suisun Bay for Delta smelt in the summer and fall, we explored several ancillary hypotheses:

- *P. forbesi* is the most important organism in Delta smelt diets during the summer and fall.
- No other significant component of Delta smelt diets during the summer or fall has a significant relationship with Delta outflow.
- The influence of X2 on *Pseudodiaptomus* spp. abundance in the LSZ will be larger in summer than fall because abundance of this taxa peaks in June and July.

- Increases to *Pseudodiaptomus* spp. abundance in the LSZ will result in increased Delta smelt growth and survival.

Methods

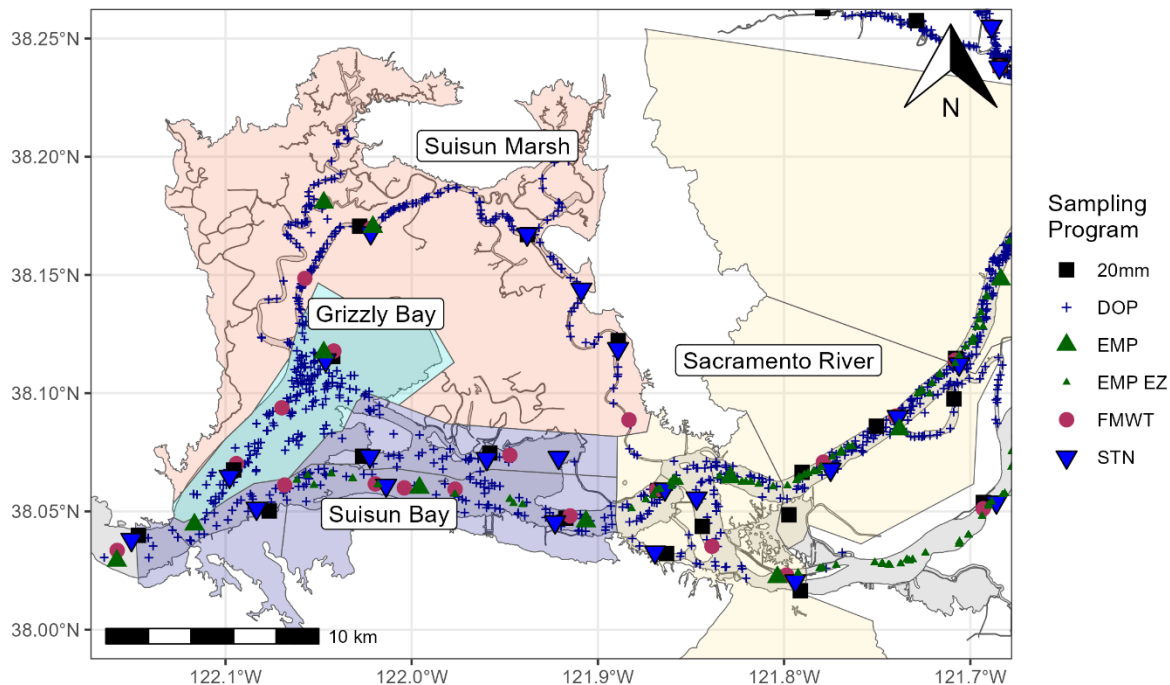
Data Access

We collated all zooplankton data collected by the CDFW Survey (20mm), CDFW Summer Townet Survey (STN), CDFW Fall Midwater Trawl Survey (FMWT) (Breining-Aday et al. 2025), DWR/CDFW Environmental Monitoring Program (EMP) Zooplankton Survey (Shaw 2025), and the Reclamation-led DOP (Schultz and Kalmbach 2023) in the Suisun Marsh, Suisun Bay, Confluence, and lower Sacramento River. We used data from 1995–2024 for flow-abundance relationships and generalized additive models. We used data from 2011–2024 for analyses of *Pseudodiaptomus* spp. changes with flow actions (sample locations shown in Figure 17). All these surveys use a 150 micron mesh net and sample once or twice per month. We integrated these surveys using methods developed by Bashevkin et al. (2022a), using the R package *zooper* (Bashevkin, Hartman et al. 2023a). This package standardizes the component datasets to have constant column names and units and combines the data so they have consistent levels of taxonomic resolution. For example, if one survey identifies juvenile “*Pseudodiaptomus forbesi*” separately from juvenile “*Pseudodiaptomus marinus*”, and another survey identifies all juveniles as “*Pseudodiaptomus* spp.”, the integrated dataset will combine all *Pseudodiaptomus* into “*Pseudodiaptomus* spp.” See Kayfetz et al. (2020) and Bashevkin, Hartman et al. (2022) for further details on the component datasets and data integration methods.

Flow-Abundance Relationships of Major Zooplankton Taxa

To explore which Delta smelt food resources are most positively impacted by flow actions, we first screened the major groups of zooplankton for flow-abundance relationships. We used taxonomic groups developed for the Delta Smelt Individual-Based Model by Smith and Nobriga (2023) and Rose et al. (2013a). We also analyzed mysid shrimp (chiefly *H. longirostris* in recent years), which were historically an important food source for Delta smelt, though they are rare today. We used mesozooplankton (150–160 micron mesh) data from EMP, FMWT, DOP, 20mm survey, and STN, and mysid data (500 micron mesh) from EMP, FMWT, and DOP. We integrated all data from 1995 to 2024, subset the data to just June–October, and plotted log-transformed abundance +1 per cubic meter versus log-transformed outflow. One was added to all values of abundance to allow log-transformation of data that included zeros. We then plotted generalized additive models, one for each region, through the data using the ‘*geom_smooth*’ function from the *ggplot2* package in R. These models were not analyzed in detail, just used as a visual aid to detect patterns in the data.

Figure 17. Zooplankton sampling stations. Large points are fixed stations sampled once or twice per month. Smaller points are randomly distributed (DOP) or correspond to particular salinities (EMP EZ stations).



Pseudodiaptomus spp. Abundance

To test our main hypothesis that lower X2 was related to more *Pseudodiaptomus* spp., we used two different analyses to explore the relationship between *Pseudodiaptomus* spp. abundance, salinity, and flow. We first used abundance of *Pseudodiaptomus* spp. as measured by IEP long-term monitoring surveys and special studies in Suisun Marsh and Suisun Bay, which we analyzed using a zero-inflated lognormal distribution of abundance per cubic meter versus monthly average X2, salinity at Belden's Landing, region of the estuary, and season (summer or fall). We also examined an alternative model with salinity bins instead of region and compared the two models using Bayesian information criterion (BIC). The second analysis examined the difference in predicted abundance of *Pseudodiaptomus* spp. from generalized additive models developed on data from 1995–2024, observed values from 2011–2024, and compared residuals net Delta outflow as calculated by Dayflow.

For these analyses, we filtered the integrated dataset described above to include only adults and copepodites (juveniles) of the genus *Pseudodiaptomus*. This includes both *P. forbesi* and *P. marinus*, but they were combined for analysis because juveniles were not identified to species in all surveys. Of the surveys that did specify the genus, *P. marinus* was less than 1% of the total catch, so any

differences in the two species' responses to flow are not likely to significantly change the model results.

Data for daily X2 value came from DWR's Dayflow Model (CDWR 2002). See details in "[Smelt Habitat](#)" methods.

To test change in abundance with different levels of X2, we constructed generalized linear models on the abundance per cubic meter of *Pseudodiaptomus spp.* adults and copepodites (combined). We used zero-inflated lognormal models of abundance per cubic meter, with month and year as random effects using the 'glmmTMB' function in the glmmTMB package in R (Brooks et al. 2025). We included an interaction with season (summer = June–Aug, fall = Sep–Oct) to test for differences in the effectiveness of flow actions with season. Data Source (EMP, 20mm, DOP, or FMWT), calendar year, and month of the year were included as random effects in all models, and the zero-inflation term was intercept-only. We chose the zero-inflated lognormal model because the data did not fit a gaussian distribution, and we only had density, not the raw count data that the density was built on, precluding use of a Poisson or negative binomial distribution. There were only 65 zeros out of the > 4000 data points in the dataset, so the zero-inflation component did not substantially add to the explanatory power of the model but was necessary to fit a lognormal model given the presence of any zeros. The model was followed by post-hoc tests for differences in the slope of the abundance-X2 relationship by region using the 'emtrends' function from the emmeans package (Lenth et al. 2024). All models were examined to make sure they met the assumptions of normality of residuals and equal variance. Diagnostic plots are included in Appendix A.

- One model had X2 and region, with the interaction of X2, region, and season as predictors.
 - Abundance \sim X2 * Region * Season + (1 | Month) + (1 | Year) + (1|Data Source)
- The second model replaced "Region" with "Salinity Zone".
 - Abundance \sim X2 * Salinity Zone * Season + (1 | Month) + (1 | Year) + (1|Data Source)
- To test for relative effect of X2 actions when compared to SMSCG actions, we modeled zooplankton abundance in Suisun Marsh versus salinity at Belden's Landing and compared the model output to a model with X2 as a predictor using AIC and BIC.
 - Abundance \sim X2 * Season + (1 | Month) + (1 | Year) + (1|Data Source)
 - Abundance \sim Salinity * Season + (1 | Month) + (1 | Year) + (1|Data Source)

Salinity zones were defined as "Fresh, 0–0.5 PSU", "Low Salinity Zone 0.5–6 PSU", and "Brackish >6 PSU". These zones were chosen based on known salinity preferences of Delta smelt and habitat zones for zooplankton in the estuary. We

used salinity zone instead of geographic region because increases in zooplankton abundance in a particular geographic region may not translate to increases in the LSZ (where most juvenile Delta smelt are found). We chose to use salinity zones instead of a continuous metric of salinity because of the hypothesized importance of the LSZ for Delta smelt, but we had no hypothesis about the importance of salinity within this zone. This analysis was designed to test whether *Pseudodiaptomus* spp. was merely changing its distribution instead of changing in absolute abundance within its preferred salinity range.

To assess whether existing salinity-abundance models accurately predict zooplankton abundance during X2 or SMSCG actions, we used a generalized additive model (GAM) process developed by Samuel Bashevkin (State Water Resources Control Board) for the 2022 DCG SDM process and later adapted for the Collaborative Science and Adaptive Management Program (CSAMP) Delta Smelt Structured Decision-Making (SDM) process (CSAMP Delta Smelt Technical Working Group et al. 2024). We adapted this analysis for our project by using all zooplankton data from EMP, 20mm, STN, FMWT, and DOP from 1995–2024. We used the 'gam' function in the 'mgcv' package in R (Pedersen et al. 2019) to develop three models for log-transformed biomass of *Pseudodiaptomus* spp. juveniles and adults in each region.

The first model was the same as the one developed by Bashevkin (2024) and used the tensor product smooth of surface salinity and day of year, using $k=5$ and cubic splines with shrinkage. A smooth of year (as a factor) was also included as a random effect, using the following formula:

$$\log(\text{Biomass}+1) \sim \text{te}(\text{Salinity}, \text{DayofYear}, k=c(5,5), \text{bs}=c(\text{"cs"}, \text{"cs"})) + s(\text{Year}, \text{bs}=\text{"re"}) + s(\text{Station}, \text{bs} = \text{"re"})$$

The second model used the tensor product smooth of log-transformed daily mean net Delta outflow and day of year using $k=5$ and cubic splines with shrinkage. A smooth of year (as a factor) was also included as a random effect, using the following formula:

$$\log(\text{Biomass}+1) \sim \text{te}(\log(\text{Outflow}), \text{DayofYear}, k=c(5,5), \text{bs}=c(\text{"cs"}, \text{"cs"})) + s(\text{Year}, \text{bs}=\text{"re"}) + s(\text{Station}, \text{bs} = \text{"re"})$$

The third model used both the smooths of outflow and salinity, but we were concerned that these terms would be too highly correlated and cause concurvity issues in the final model, so we examined the model for concurvity before choosing our final model:

$$\log(\text{Biomass}+1) \sim \text{te}(\log(\text{Outflow}), \text{DayofYear}, k=c(5,5), \text{bs}=c(\text{"cs"}, \text{"cs"})) + \text{te}(\text{Salinity}, \text{DayofYear}, k=c(5,5), \text{bs}=c(\text{"cs"}, \text{"cs"})) + s(\text{Year}, \text{bs}=\text{"re"}) + s(\text{Station}, \text{bs} = \text{"re"})$$

We checked each model for goodness of fit and concurvity using ‘gam.check’ and ‘concurvity’ functions from the mgcv package and ranked the models using BIC to determine which model was most appropriate for use with the data.

We then used the best model to predict the biomass of *Pseudodiaptomus* spp. in each region for 2011–2024 and calculated the residuals to see whether the model accurately predicted biomass during flow actions.

Relative Importance of Each Taxon in the Diet

Delta smelt diet data came from the CDFW Diet and Condition Study (S. Slater, unpublished data), which has been collecting information on Delta smelt diets since 2005. These fish were collected by numerous long-term monitoring studies conducted under the auspices of the Interagency Ecological Program, including 20mm, FMWT, STN, and EDSM (EDSM; 2017–2024 only). These surveys each use different sampling methods targeting different taxa and life stages of fish (see individual survey metadata for details). All Delta smelt collected by these surveys were preserved in liquid nitrogen and transferred to the University of California, Davis. Thawed fish were dissected, and the gastrointestinal tract was preserved in 95% ethanol and transferred to CDFW’s Diet Study laboratory for analysis (Stockton, CA). In the laboratory, stomach contents were identified under a microscope to the lowest practical taxonomic level and counted. When possible, lengths of intact organisms were measured to the nearest mm.

We used two methods to analyze Delta smelt stomach contents and relate smelt diet to environmental conditions (water surface temperature, salinity, turbidity), fish body size (fork length, FL) and season (Winter [Dec–Feb], Spring [Mar–May], summer [Jul–Aug], fall [Sep–Nov]); note that temperature, FL, and season are not independent of one another; however, each is graphically analyzed separately below. We first calculated the index of relative importance (IRI) (Pinkas et al. 1970; Martin et al. 1996). We then used a graphical method introduced by Costello (1990) and modified by Amundsen et al. (1996) to add a more nuanced analysis of the variation in DS prey importance across environmental and FL gradients and by season.

IRI is calculated as:

$$IRI = (A_i + B_i)F_i$$

Where A_i is the numerical percent abundance and B_i is the percentage by biomass of prey taxon i across all fish stomachs dissected, and F_i is the frequency of occurrence of prey taxon, i.e., the proportion of fish stomachs in which prey taxon i was found. Prey biomasses were estimated using average weights (for microzooplankton) and length-weight regression coefficients (for macrozooplankton) compiled by Burdi et al. (2021) and Kayfetz et al. (2020).

Amundsen et al. (1996) calculated percent abundance, P_i , of a prey item among fish stomachs in a sample by dividing the total biomass of prey taxon i , S_i , by the total biomass of all prey found in only those fish in which prey taxon ii was found, S_{t_i} . They allowed “abundance” to mean either numerical abundance or biomass; however, we used biomass (carbon weight, μg). Prey-specific abundance is thus:

$$P_i = \left(\sum S_i \div \sum S_{t_i} \right) \left(\sum S_i \div \sum S_{t_i} \right) \times 100$$

In the graphical analysis, a prey taxon appears as a single point in $F_i - P_i$ space, where F_i is as above. While a number of important ecological inferences may be drawn from the points’ relative locations on the graph (see Amundsen et al. 1996, Figure 3), the present analysis is primarily concerned with the anti-diagonal: prey on the lower left are unimportant to the Delta smelt diet, while prey on the upper right are highly important.

The Delta smelt collected for diet analysis were caught across temperature, salinity and turbidity gradients and at different times of year, and they varied in fork length; these data were recorded at the time of catch. A large number of Delta smelt is required for a reliable IRI calculation or to generate a single point in the diet analysis graph. Thus, to determine how a given DS prey taxon’s importance to the Delta smelt diet varied across environmental and fork length gradients, we divided each of these continuous variables into 20 quantiles, each quantile containing ~ 75 individual Delta smelt. We divided catch dates into seasons and each diet analysis calculation was applied within each quantile or season. IRI for each taxon was standardized within each quantile by dividing its value by the highest IRI in that quantile. We attempted to replicate this method with time-lagged X2 as the predictor, however X2 did not vary sufficiently during the relevant surveys to offer any informative insights.

The calculation of IRI, F_i and P_i for each individual prey taxon included all taxa consumed by Delta smelt. However, we only calculated these metrics for the eight individual or grouped prey taxa and life stages that were consistently abundant in the Delta smelt stomach contents. These were all copepods: *Acanthocyclops* spp.; adult *Eurytemora* spp.; juvenile *Eurytemora* spp.; adult *Limnoithona* spp.; grouped “other” adult calanoids (which included mostly *Sinocalanus* spp. at lower salinities); grouped “other” juvenile calanoids; adult *Pseudodiaptomus* spp.; and juvenile *Pseudodiaptomus* spp.

Bioenergetic Model of Prey Saturation Point

To see whether the change in *Pseudodiaptomus* spp. seen during a SFHA would affect Delta smelt growth, we used the Delta Smelt Bioenergetic Model (Smith and

Nobriga 2023). This model was originally developed by Rose et al. (2013a) as part of an individual-based life cycle model and expanded upon by Smith and Nobriga (2023) to provide an index of habitat suitability based on relative growth rate potential.

The bioenergetics model is a modified Wisconsin fish bioenergetics model with an associated multi-species functional response equation that dynamically varies prey choice based on empirical zooplankton densities. The model is an energy-balance equation with the following form: growth rates = consumption rates – (respiration rates + egestion rates + excretion rates + specific dynamic action). We used the updated temperature constraints developed by Smith and Nobriga (2023), which lowered the threshold for when the consumption rate declines to 0.98 from 23 to 21.6°C. The model also extended the Wisconsin Model to include additional foraging constraints based on turbidity and day length. Foraging increased as turbidity increased from the minimum turbidity (5 NTU) to the optimal turbidity range of 35–80 NTU (as per Smith and Nobriga 2023) based on studies by Hasenbein et al. (2016) demonstrating increased foraging with higher turbidities. Day length was also added as a foraging constraint because Delta smelt are thought to forage only during daylight hours (Smith and Nobriga 2023). We used the same 11 prey categories that were used by Smith and Nobriga (2023) for juvenile Delta smelt - *Pseudodiaptomus* spp. adults, *Pseudodiaptomus* spp. copepodids, *Eurytemora carolleeae* adults, *Eurytemora carolleeae* copepodids, *Limnoithona* spp., other calanoid copepodids, other calanoid copepod adults, *Daphnia* spp., other Cladocera, other cyclopoid copepods and “other.” Further details of the DSM Bioenergetics Model can be found in Rose et al. (2013) and Smith and Nobriga (2023).

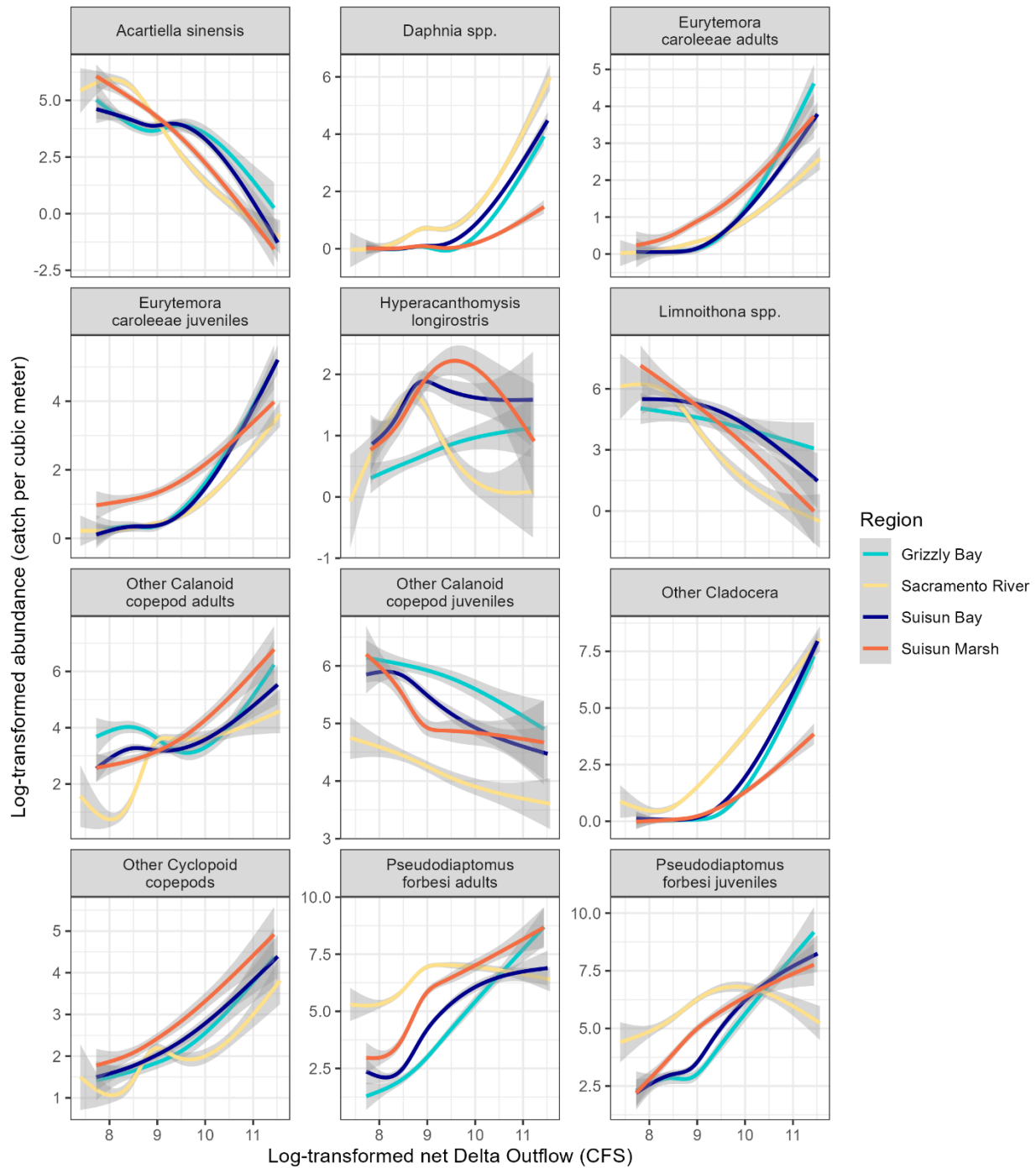
To test the potential effect of increasing abundance of *Pseudodiaptomus* spp. on Delta smelt growth in Suisun Bay, we calculated the average zooplankton abundance (by taxon), temperature, and turbidity in Suisun Bay for each day of the summer and fall for 2011–2024. We then changed the abundance of *Pseudodiaptomus* spp. juveniles and adults per day by -90%, -50%, +50%, 100%, 400%, 1000%, and 2000%. Abundance of all other taxa were not changed, since *Pseudodiaptomus* spp. is the most abundant taxon that is likely to be impacted by flow actions. We ran the bioenergetic model with these inputs from June 1 to Oct 31 to see the point at which increasing *Pseudodiaptomus* spp. no longer resulted in an increase in growth rate. We started each run assuming Delta smelt began as juveniles at a length of 23 mm. We used the size-dependent mortality term from Rose et al. (2013b) to estimate the proportional survival over the entire time period based on the lengths predicted from the model for each scenario. We did not include starvation-induced mortality because no scenarios resulted in fish losing weight.

Results

Flow-Abundance Relationships of Zooplankton Taxa

When visualizing the June–October flow-abundance relationships for the major groups of zooplankton included in the Delta Smelt Individual-Based Model (Rose et al. 2013a; Smith and Nobriga 2023), we see that *Daphnia*, other Cladocera, and *Eurytemora* (adults and juveniles) all have a consistent positive relationship with outflow in all the regions tested (Figure 18). *Pseudodiaptomus* spp. has a consistent positive relationship in the downstream regions of Grizzly Bay, Suisun Bay, and Suisun Marsh, but peaks at middle values of outflow in the Sacramento River region (Figure 18). *Acartiella*, *Limnoithona* spp., other juvenile calanoids, and other cyclopoids all have a negative relationship with flow (Figure 18). Of the taxa with a positive flow-abundance relationship, *Pseudodiaptomus* spp. is by far the most abundant, so that is the taxa we focus on in the rest of this report.

Figure 18. Plots of GAMs showing the relationship between log-transformed summer and fall abundance per cubic meter of major zooplankton groups and log-transformed net Delta outflow for each region. These models were not analyzed in detail and are presented here as a visual aid to identify which taxa to focus on in this report.



Pseudodiaptomus spp. Abundance

Figure 19. Log-transformed mean biomass per cubic meter of *Pseudodiaptomus* spp. (adults and juveniles) by year and season, color coded by water year type.

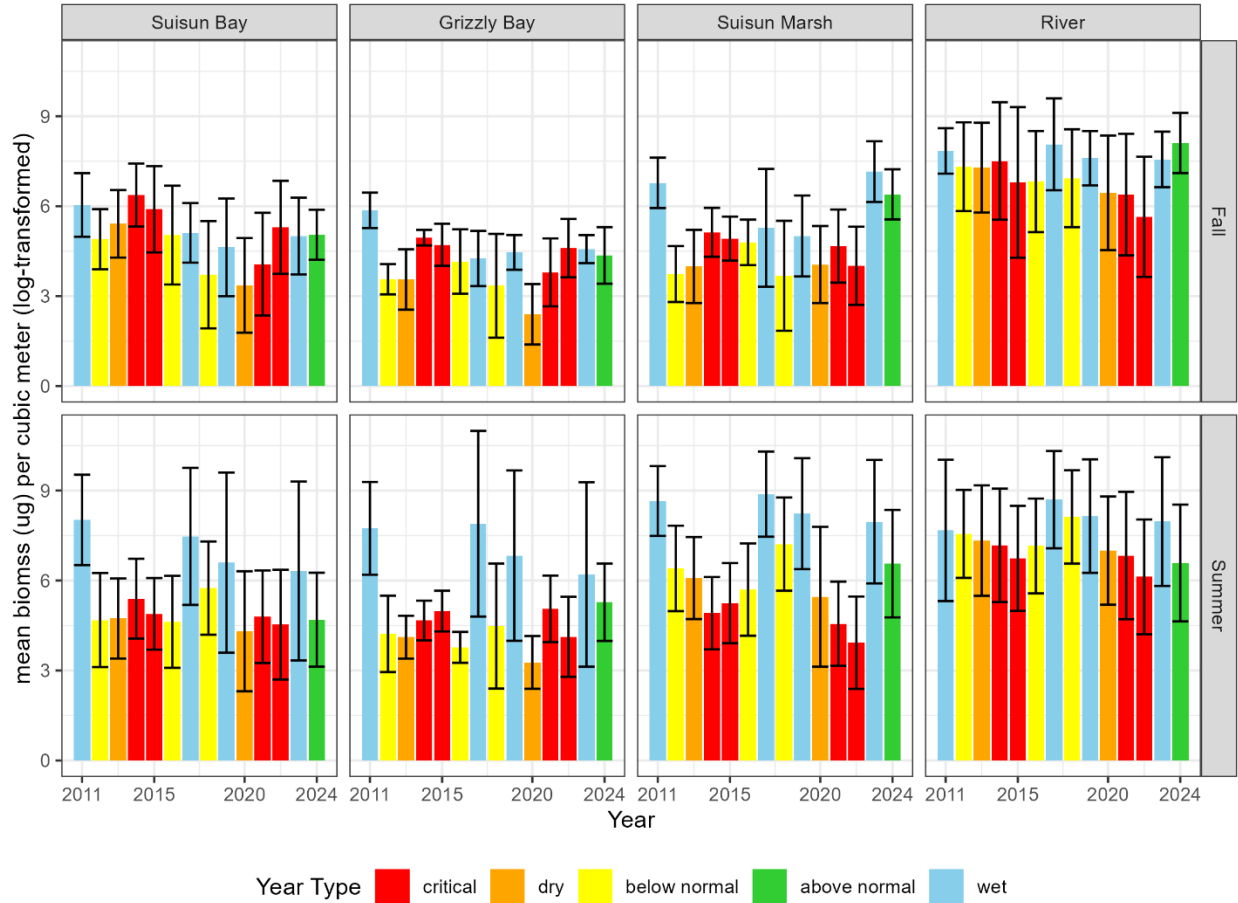
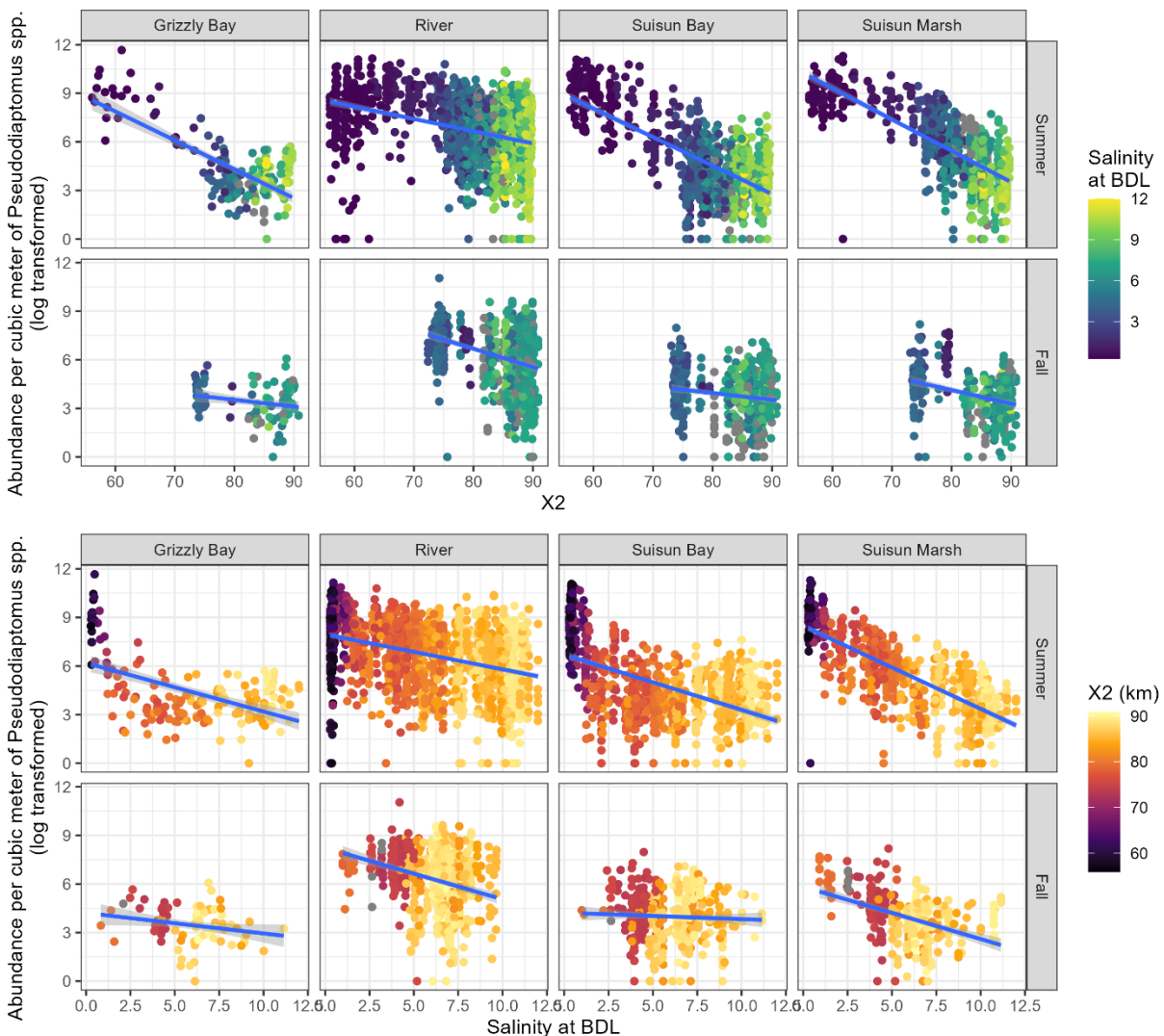


Figure 20. Plot of log-transformed *Pseudodiaptomus* spp. abundance per cubic meter versus X2 (top panels) and salinity at Belden's Landing (bottom panels) by season. Salinity at Belden's Landing is highly correlated with X2, so points are colored by the salinity at BDL in the plot of the X2 relationship and colored by X2 in the plot of the salinity relationship. Lines show the slope of a simple linear regression of abundance versus X2 or salinity, which is further explored in the linear model presented in Table 8.



Comparing biomass of *Pseudodiaptomus* spp. by year, we found that biomass is generally higher in Wet and Above Normal summers in Suisun Bay, Grizzly Bay, and Suisun Marsh (2011, 2017, 2019, 2023, 2024). This effect is less clear in the Sacramento River and also less apparent in fall than in summer (Figure 19).

When modeling *Pseudodiaptomus* spp. abundance versus X2 with region and season as interaction terms, we saw there was a strong negative correlation between X2 and abundance (Figure 20, Table 8). This correlation was most strongly negative in Grizzly Bay in the summer (7.1% increase in abundance per km decrease in X2, $p < 0.05$), less negative in Suisun Bay and Suisun Marsh (6.7% and 6.0% increase in abundance per km decrease in X2). However, there was no significant difference in trends between these three regions (post-hoc $p > 0.05$). The Sacramento River did have a significantly lower trend, which was not significantly different from zero, and there was no trend in the River region (0.7% decrease in abundance per km decrease in X2, $p > 0.05$) (Figure 20, Table 8). The effect of X2 during fall was much lower than the effect of X2 during summer (less than 1% change in any region, not statistically different from zero, $p > 0.05$). Diagnostic plots for this model show some variation from 1:1 in the QQ plot, indicating residuals were not completely normally distributed (Appendix A, Figure 61), but it is within an acceptable range given the high variance inherent in zooplankton data.

Table 8. Results of zero-inflated lognormal model of *Pseudodiaptomus* spp. catch per unit volume versus X2, region, season, and their interactions. Diagnostic plots are available in Appendix A, Figure 61.

Predictor	Estimate	SE	z value	Pr(> z)
(Intercept - Fall, Grizzly Bay)	6.184	1.539	4.019	0.0001
X2	0.003	0.019	0.186	0.8525
Region - Sacramento River	4.825	1.514	3.187	0.0014
Region - Suisun Bay	-0.155	1.607	-0.097	0.9230
Region - Suisun Marsh	1.576	1.630	0.967	0.3337
Season - Summer	6.616	1.591	4.159	<0.0001
X2:Sacramento River	-0.042	0.018	-2.288	0.0221
X2:Suisun Bay	0.004	0.019	0.208	0.8354
X2:Suisun Marsh	-0.015	0.020	-0.757	0.4492
X2:Summer	-0.077	0.019	-4.008	0.0001
Sacramento River:Summer	-9.083	1.618	-5.614	<0.0001
Suisun Bay:Summer	-0.060	1.715	-0.035	0.9723
Suisun Marsh:Summer	-1.906	1.728	-1.103	0.2701
X2:Sacramento River:Summer	0.108	0.020	5.473	<0.0001
X2:Suisun Bay:Summer	-0.0004	0.021	-0.017	0.9867
X2:Suisun Marsh:Summer	0.027	0.021	1.268	0.2048
Zero-Inflation Intercept	-4.290	0.116	-36.897	<0.0001
Post-hoc Result				
Contrast - Difference in X2 Effect	Estimate	SE	z value	Pr(> z)
Fall: Grizzly Bay - Sacramento River	0.0419	0.0183	2.288	0.1007

Predictor	Estimate	SE	z value	Pr(> z)
Fall: Grizzly Bay - Suisun Bay	-0.0040	0.0194	-0.208	0.9968
Fall: Grizzly Bay - Suisun Marsh	0.0149	0.0197	0.757	0.8738
Fall: Sacramento River - Suisun Bay	-0.0460	0.0091	-5.042	<0.0001
Fall: Sacramento River - Suisun Marsh	-0.0271	0.0095	-2.848	0.0228
Fall: Suisun Bay - Suisun Marsh	0.0189	0.0116	1.633	0.3602
Summer: Grizzly Bay - Sacramento River	-0.0663	0.0075	-8.902	<0.0001
Summer: Grizzly Bay - Suisun Bay	-0.0037	0.0078	-0.470	0.9656
Summer: Grizzly Bay - Suisun Marsh	-0.0118	0.0076	-1.556	0.4040
Summer: Sacramento River - Suisun Bay	0.0626	0.0035	17.914	<0.0001
Summer: Sacramento River - Suisun Marsh	0.0545	0.0029	19.037	<0.0001
Summer: Suisun Bay - Suisun Marsh	-0.0081	0.0038	-2.137	0.1414

When using salinity zone instead of region, there was still a significant negative relationship between *Pseudodiaptomus* spp. abundance and X2 in the summer. The fresh region (<0.5 PSU) and the brackish region (>6 PSU) had the weakest X2 relationships (less than 1% change in abundance per 1 km change in X2), and they were not significantly different from each other (post-hoc p-values <0.05). The LSZ (0.5–6 PSU) had a much stronger negative relationship, with a 4.4% increase in abundance per km change in X2 (Table 9, Figure 21). During the fall, both the fresh regions and low salinity zones had a slightly positive relationship with X2 (1.7% and 1.9% increase in abundance for 1 km change in X2). Diagnostic plots for this model also show some variation from 1:1 in the QQ plot, indicating residuals were not completely normally distributed (Appendix A, Figure 62).

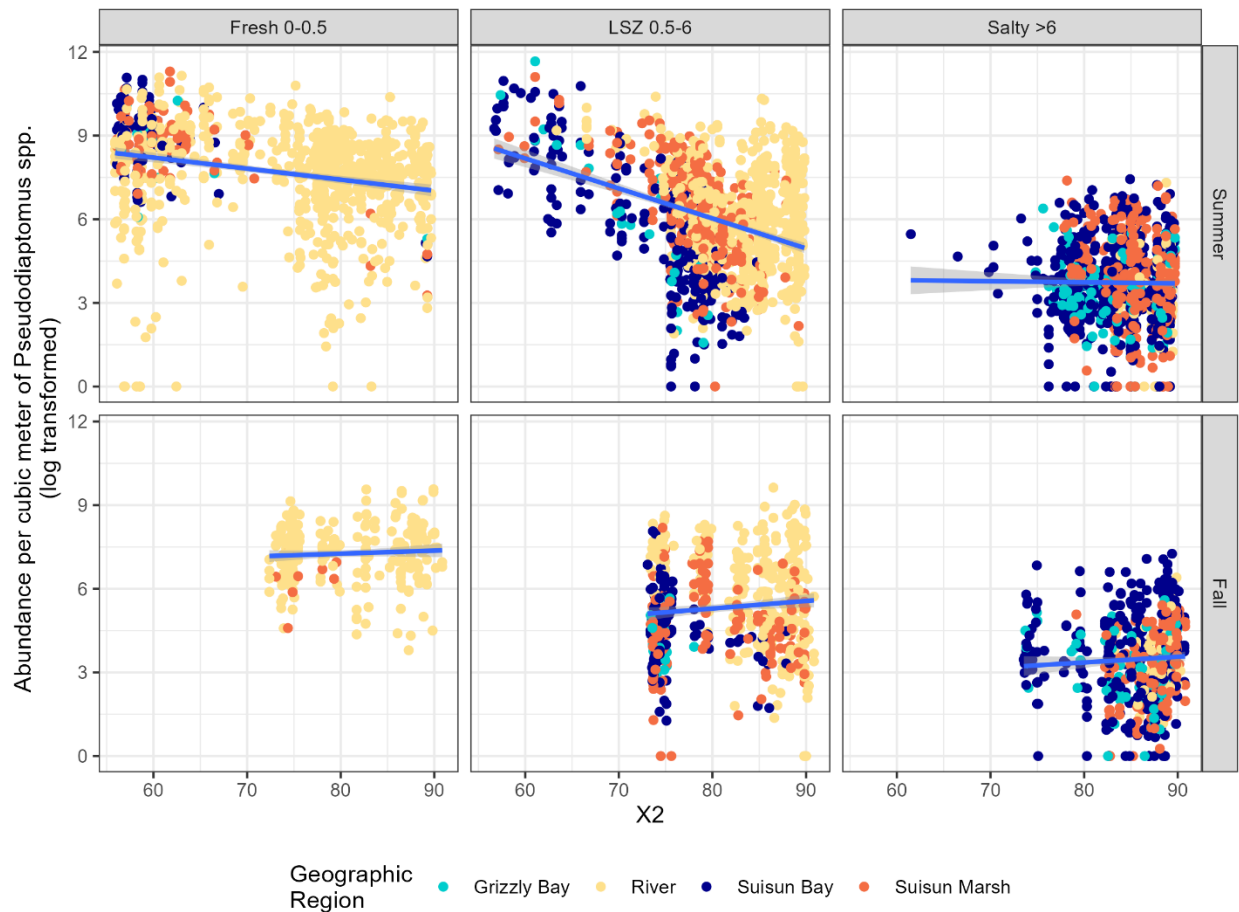
Comparing the model of *Pseudodiaptomus* spp. by region versus by salinity zone showed that the model using salinity zone provided a better fit than the model using region (BIC of 69806 versus 82226), demonstrating that salinity provides more predictive power than geographic area for assessing abundance of *Pseudodiaptomus* spp.

Table 9. Results of a hurdle lognormal model of *Pseudodiaptomus* spp. catch versus X2, salinity zone, season, and their interactions. Diagnostic plots are included in Appendix A.

Predictor	Estimate	SE	z value	Pr(> z)
(Intercept - Fresh, Summer)	8.500	0.295	28.831	<0.0001
X2	-0.002	0.003	-0.724	0.4688
Salinity Zone - LSZ 0.5–6	2.811	0.312	9.003	<0.0001
Salinity Zone - Salty >6	-2.383	0.793	-3.007	0.0026
Season - Fall	-1.746	0.627	-2.783	0.0054
X2:LSZ 0.5–6	-0.043	0.004	-10.669	<0.0001
X2:Salty >6	0.009	0.009	0.927	0.3538

Predictor	Estimate	SE	z value	Pr(> z)
X2:Fall	0.022	0.007	2.937	0.0033
LSZ 0.5-6:Fall	-3.725	0.800	-4.657	<0.0001
Salty >6:Fall	0.607	1.386	0.438	0.6615
X2:LSZ 0.5-6:Fall	0.041	0.010	4.111	<0.0001
X2:Salty >6:Fall	-0.011	0.016	-0.663	0.5076
Zero-Inflation Intercept	-4.243	0.123	-34.485	<0.0001
Post-Hoc Contrasts				
Contrast	Estimate	SE	z value	Pr(> z)
Summer: Fresh 0-0.5 - LSZ 0.5-6)	0.0429	0.0040	10.669	<0.0001
Summer: Fresh 0-0.5 - Salty >6	-0.0088	0.0095	-0.927	0.6231
Summer: LSZ 0.5-6 - Salty >6	-0.0516	0.0098	-5.263	<0.0001
Fall: Fresh 0-0.5 - LSZ 0.5-6	0.0021	0.0091	0.230	0.9712
Fall: Fresh 0-0.5 - Salty >6	0.0021	0.0137	0.153	0.9871
Fall: LSZ 0.5-6 - Salty >6	0.00001	0.0133	0.001	1.0000

Figure 21. Plot of *Pseudodiaptomus* spp. abundance per cubic meter versus X2 by salinity zone and season for each sampling event during the summer and fall of 2011–2024. Lines show the slope of a simple linear regression of abundance versus X2 or salinity, which is further explored in the linear model presented in Table 9.



When looking specifically at Suisun Marsh, the model using X2 fit better than the model using salinity at Belden’s Landing (BIC of 15249 versus 15374), and the effect of X2 was stronger in summer than in fall (Table 10). This matches the model run on the entire dataset.

Table 10. Model comparison table for predictions of *Pseudodiaptomus* spp. abundance in Suisun Marsh. X2 was found to be a stronger predictor than local salinity for predicting *Pseudodiaptomus* spp. abundance.

Model	K	AIC	BIC	Log Likelihood
X2*Season	9	15204	15249	-7593
Salinity*Season	9	15329	15374	-7655

The biomass-salinity GAMs that were fit on data from 1995–2024 had reasonably good fit, with 69–75% of deviance explained (depending on region) (Figure 22, Table 11). The residuals from observed data in 2011–2024 were regressed against log-transformed Delta outflow (Figure 23, Table 12), and we see that the GAM models slightly underpredict biomass during high-flow years, and the Delta outflow accounts for approximately 8% of the residual variation (based on the adjusted R²). Therefore, we can expect more *Pseudodiaptomus* spp. during high flows even at the same salinity.

Given the reduced predictive capacity of these models at higher outflow, it would be logical to assume adding outflow to the model would improve it. However, the set of models that replaced salinity with Delta outflow explained a lower percent of the variance and were not ranked as high with BIC in any of the regions (Table 13). The model with salinity alone was ranked lower (via BIC) than salinity + outflow or outflow alone in all regions but Suisun Marsh (Table 13). However, concavity between salinity and flow was 1.00 in the worst case and over 0.5 in the observed case for all four regions (Table 14), so including them both in the same model could be problematic. Therefore, we used salinity alone for all additional analyses in this report.

Table 11. Results of generalized additive models of *Pseudodiaptomus* spp. biomass from 1995–2024 by the tensor product smooth (te) of salinity and day of year, with smooths (s) of Year and Station as additional predictors. Adjusted R-squared for Grizzly Bay model was 0.76, R-squared for Suisun Marsh model was 0.83, R-squared for Suisun Bay model was 0.78, and R-squared for the Sacramento River model was 0.59. edf = estimated degrees of freedom, res.df = residual degrees of freedom. Diagnostic plots are included in Appendix A (Figure 63–Figure 66).

Region	Coefficient Type	Predictor	Estimate	edf	res.df	F or t-value	p-value
Sacramento River	Parametric	intercept	7.71			102.5	<0.0001
Sacramento River	Smooth	te(Salinity, DOY)		17.39	24	431.7	<0.0001
Sacramento River	Smooth	s(Year)		25.42	29	10.58	<0.0001
Suisun Marsh	Parametric	intercept	6.32			45.3	<0.0001
Suisun Marsh	Smooth	te(Salinity, DOY)		17.42	24	1675	<0.0001
Suisun Marsh	Smooth	s(Year)		26.81	29	10.03	<0.0001
Suisun Bay	Parametric	intercept	5.33			63.55	<0.0001
Suisun Bay	Smooth	te(Salinity, DOY)		19.02	24	870.3	<0.0001
Suisun Bay	Smooth	s(Year)		25.2	29	6.711	<0.0001
Grizzly Bay	Parametric	intercept	4.44			16.69	<0.0001
Grizzly Bay	Smooth	te(Salinity, DOY)		16.29	24	192.5	<0.0001
Grizzly Bay	Smooth	s(Year)		24.22	29	5.35	<0.0001

Figure 22. Results of GAM model of *Pseudodiaptomus* spp. abundance versus salinity for each region, parameterized on data from 1995–2024. Points represent the monthly average biomass data from 2011–2024, color coded by water year type, with the black line representing predicted *Pseudodiaptomus* spp. abundance on the fifteenth day of each month based on the GAM of biomass versus salinity and day of year. Colored points are the monthly average *Pseudodiaptomus* spp. biomass for 2011–2024, color coded by water year type.

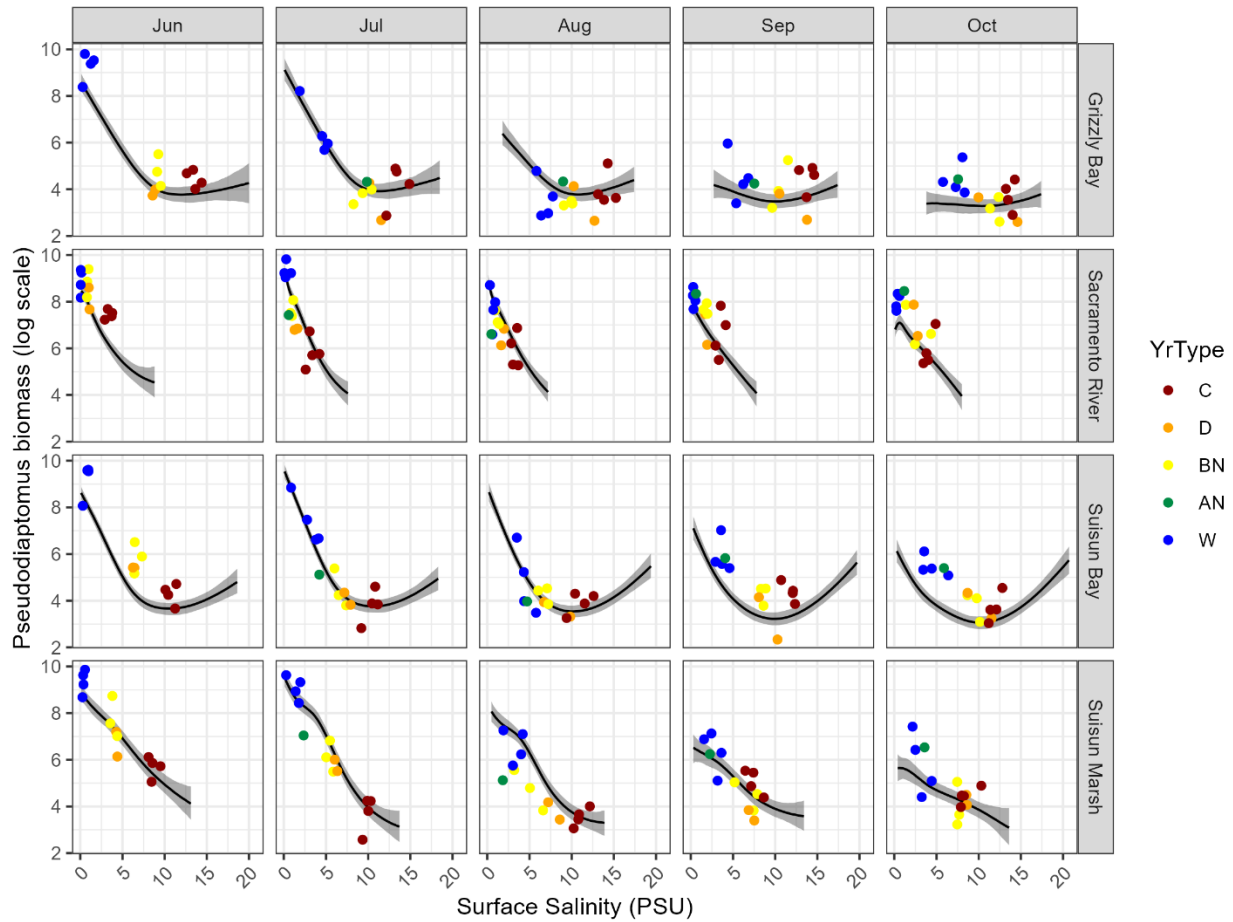


Figure 23. Residuals of predicted *Pseudodiaptomus* spp. abundance via GAMs listed above and mean monthly abundance from June–October, 2011–2024 versus log-transformed net Delta outflow. Values below the dotted line indicate actual values were lower than modeled abundance, and values over the line indicate actual values were higher than modeled abundance.

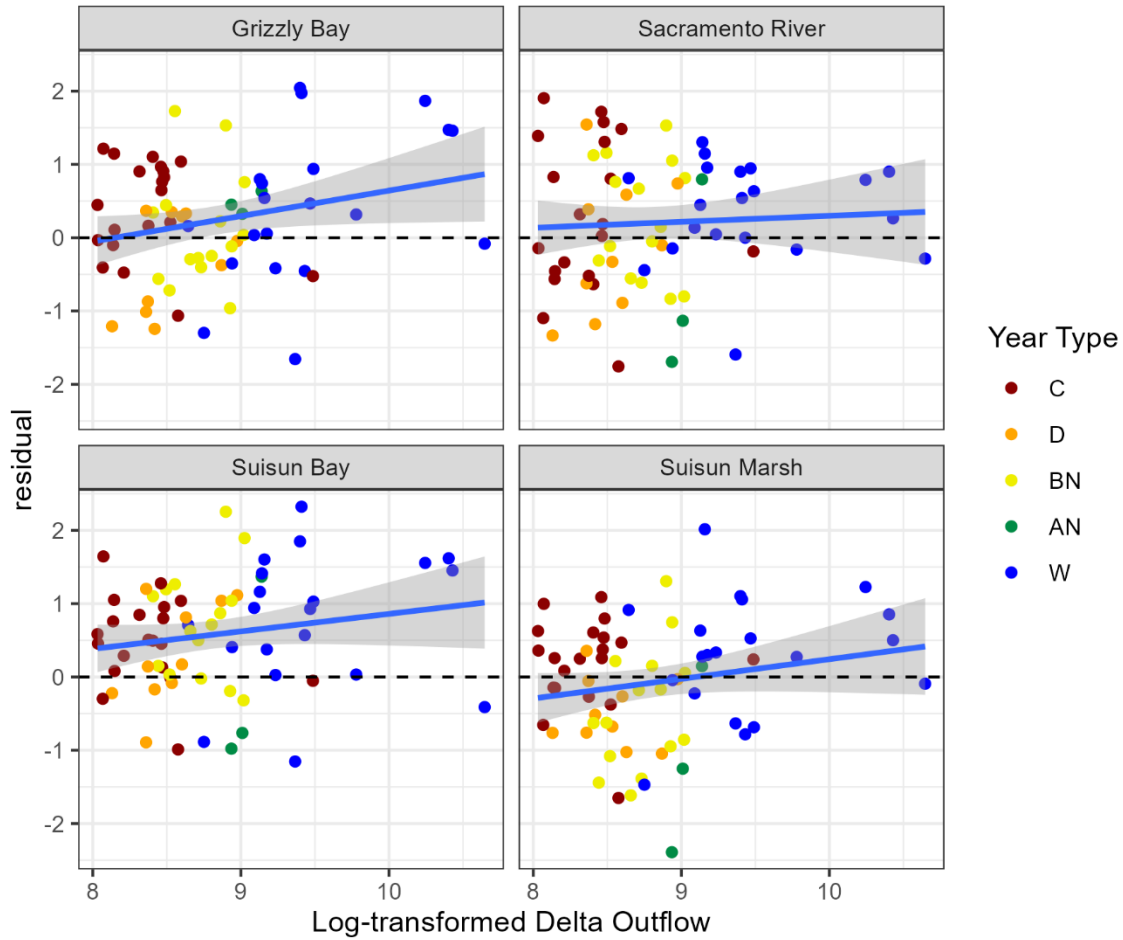


Table 12. Results of a linear model of the residuals of *Pseudodiaptomus* spp. abundance as predicted by the GAM on data from 2011–2024 versus log-transformed net Delta outflow by region. Adjusted R2 was 0.077.

Predictor	Estimate	SE	t value	Pr(> t)
Intercept – Grizzly Bay	-2.832	1.540	-1.839	0.067
log(Outflow)	0.347	0.174	1.996	0.047 *
Sacramento River	2.313	2.177	1.062	0.289
Suisun Bay	1.304	2.177	0.599	0.550
Suisun Marsh	0.393	2.177	0.180	0.857
log(Outflow)*Sacramento River	-0.266	0.246	-1.079	0.281
log(Outflow)*Suisun Bay	-0.210	0.399	-0.527	0.5990
log(Outflow)*Suisun Marsh	-0.532	0.399	-1.334	0.1845

Table 13. Ranks of three different models of *Pseudodiaptomus* spp. abundance in each region (Sacramento River, Grizzly Bay, Suisun Bay, and Suisun Marsh) with BIC and percent deviance explained. The model ranked best using BIC is highlighted in bold text. In the case of Grizzly Bay, two models were within BIC of one from each other, meaning the two models are essentially equal.

Region	Type	BIC	Deviance Explained
Grizzly Bay	Null	3371	0.549
Grizzly Bay	Salinity	3076	0.701
Grizzly Bay	Outflow	3129	0.686
Grizzly Bay	Salinity + Outflow	3075	0.722
Suisun Marsh	Null	5186	0.660
Suisun Marsh	Salinity	4772	0.762
Suisun Marsh	Outflow	5116	0.694
Suisun Marsh	Salinity + Outflow	4776	0.773
Suisun Bay	Null	7822	0.504
Suisun Bay	Salinity	6688	0.732
Suisun Bay	Outflow	7700	0.554
Suisun Bay	Salinity + Outflow	6666	0.744
Sacramento River	Null	8813	0.355
Sacramento River	Salinity	7957	0.561
Sacramento River	Outflow	8720	0.402
Sacramento River	Salinity + Outflow	7922	0.582

Table 14. Concurvity of GAM models ranked in Table 13, with the worst, observed, and estimated values for each parameter.

Region	Model	Parameter	Worst	Observed	Estimate
Grizzly Bay	Flow	Salinity:DOY	0.810	0.294	0.175
Grizzly Bay	Flow	Year	1.000	0.477	0.186
Grizzly Bay	Null	DOY	0.165	0.124	0.070
Grizzly Bay	Null	Year	1.000	0.050	0.066
Grizzly Bay	Salinity	Salinity:DOY	0.810	0.294	0.175
Grizzly Bay	Salinity	Year	1.000	0.477	0.186
Grizzly Bay	Salinity+flow	log(OUT):DOY	1.000	0.778	0.673
Grizzly Bay	Salinity+flow	Salinity:DOY	1.000	0.758	0.563
Grizzly Bay	Salinity+flow	Year	1.000	0.437	0.246
Sacramento River	Flow	log(OUT):DOY	0.800	0.085	0.212
Sacramento River	Flow	Year	1.000	0.607	0.157
Sacramento River	Null	DOY	0.060	0.056	0.036
Sacramento River	Null	Year	1.000	0.064	0.047
Sacramento River	Salinity	Salinity:DOY	0.521	0.268	0.085
Sacramento River	Salinity	Year	1.000	0.161	0.088
Sacramento River	Salinity+flow	log(OUT):DOY	1.000	0.743	0.561
Sacramento River	Salinity+flow	Salinity:DOY	1.000	0.507	0.286
Sacramento River	Salinity+flow	Year	1.000	0.377	0.164
Suisun Bay	Flow	log(OUT):DOY	0.798	0.202	0.208
Suisun Bay	Flow	Year	1.000	0.655	0.160
Suisun Bay	Null	DOY	0.104	0.066	0.043
Suisun Bay	Null	Year	1.000	0.006	0.047
Suisun Bay	Salinity	Salinity:DOY	0.599	0.382	0.091
Suisun Bay	Salinity	Year	1.000	0.235	0.094
Suisun Bay	Salinity+flow	log(OUT):DOY	1.000	0.670	0.588
Suisun Bay	Salinity+flow	Salinity:DOY	1.000	0.600	0.352
Suisun Bay	Salinity+flow	Year	1.000	0.335	0.165
Suisun Marsh	Flow	log(OUT):DOY	0.802	0.105	0.204
Suisun Marsh	Flow	Year	1.000	0.680	0.183
Suisun Marsh	Null	DOY	0.088	0.084	0.044
Suisun Marsh	Null	Year	1.000	0.092	0.059
Suisun Marsh	Salinity	Salinity:DOY	0.762	0.396	0.156
Suisun Marsh	Salinity	Year	1.000	0.455	0.153
Suisun Marsh	Salinity+flow	log(OUT):DOY	1.000	0.615	0.638
Suisun Marsh	Salinity+flow	Salinity:DOY	1.000	0.758	0.507
Suisun Marsh	Salinity+flow	Year	1.000	0.596	0.227

Relative Importance of Each Taxon in the Diet

When we plotted both the IRI and feeding strategy plots of major zooplankton groups by salinity, we saw that the most important prey taxa at low salinities (< 2 PSU) were *Pseudodiaptomus* spp. adults and other calanoid adults (which were chiefly *Sinocalanus* spp.). At higher salinities, *Acanthocyclops* spp. and *Eurytemora carolleeae* became more important prey items, though *Pseudodiaptomus* spp. continued to be consumed as well. *Limnoithona* spp. adults were also important prey taxa across salinities (Figure 24, Figure 25).

When we looked at IRI and feeding strategy plots by season, we found that *Acanthocyclops* spp. and *E. carolleeae* (adults and juveniles) were most important in the winter (when Delta smelt are adults) (Figure 24, Figure 25). *Pseudodiaptomus* spp. and *Limnoithona* were most important in the summer and fall (when Delta smelt are juveniles).

Additional IRI and feeding strategy plots, binned by turbidity, temperature, and Delta smelt fork length are available in Appendix A.

Figure 24. Normalized index of relative importance (Pinkas et al. 1971) of eight zooplankton taxonomic and/or life stage categories enumerated in Delta smelt gut content samples. Normalized IRI is plotted against mean values of 20 quantiles of salinity (top plot) and by season (bottom plot). Normalized IRI is calculated as $IRI/\max(IRI)$ within each quantile or season. Each abiotic quantile represents 75–76 individual DS. Seasons (Winter, Spring, Summer, Fall) represent 414, 253, 541 and 295 individual DS, respectively

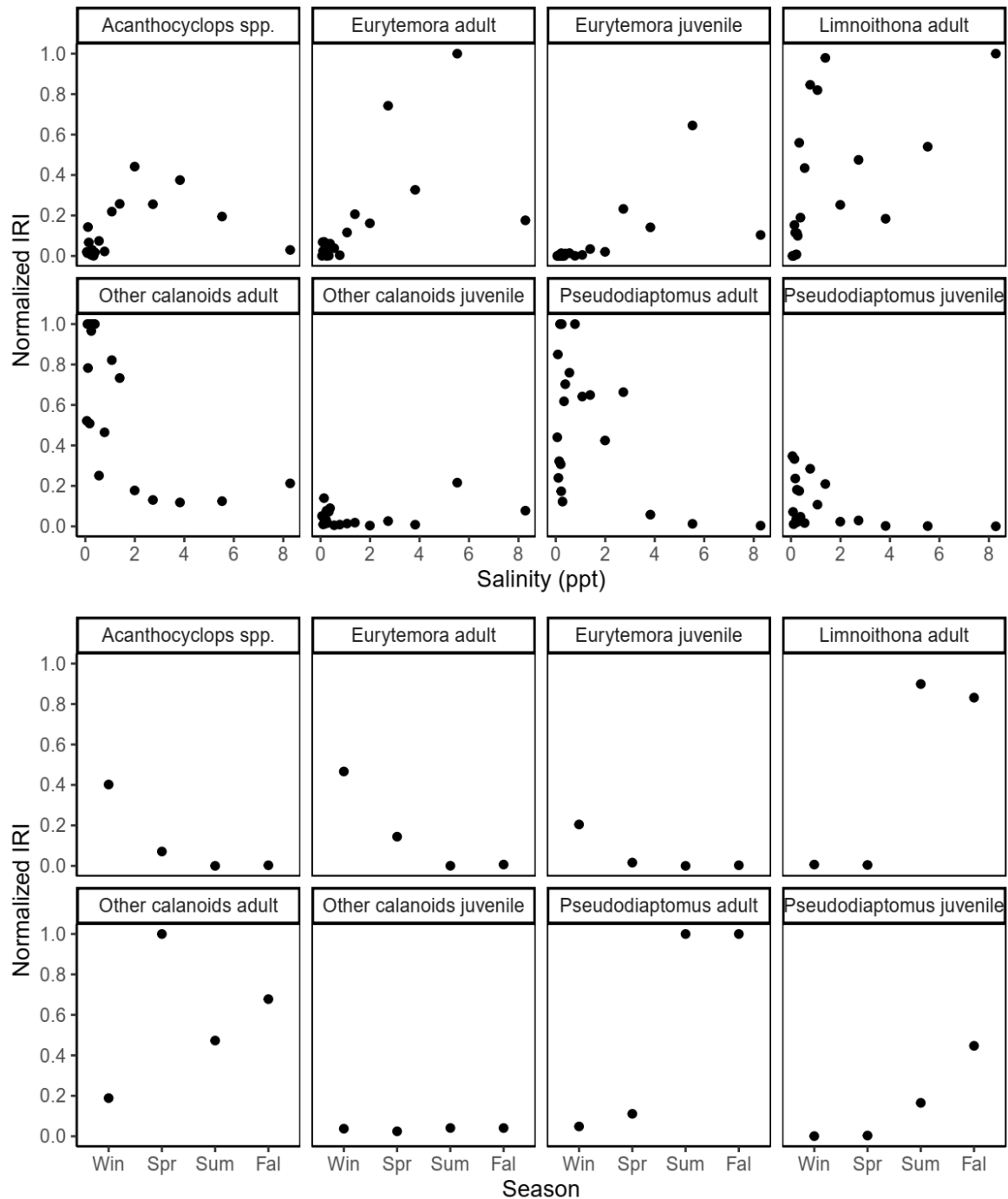
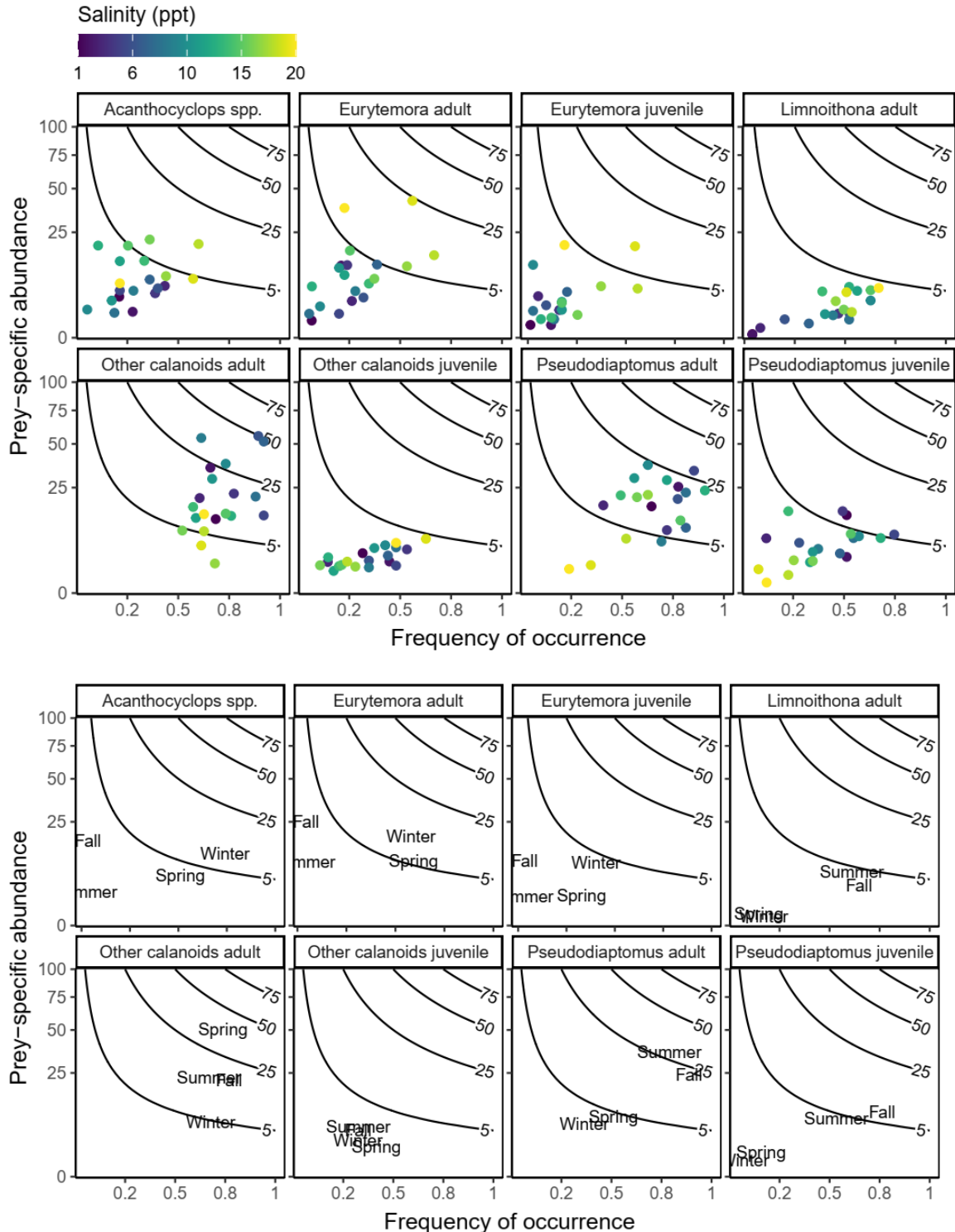


Figure 25. Feeding strategy plots (Amundson et al. 1996). Each point represents an abiotic quantile (N = 20) or season (N = 4), as in the IRI plots in Figure 26. In each panel, the x-axis is the proportion of DS individuals that consumed the indicated prey item within the corresponding quantile or season; the y-axis is the percentage of total biomass (carbon weight, μg) represented by the indicated prey item across all DS that ate at least one of that prey item by quantile or season.



Bioenergetic Model

When running the bioenergetic model with increased densities of *Pseudodiaptomus* spp. copepodites and adults, we found that Delta smelt continued to increase in growth with increasing densities of *Pseudodiaptomus* spp. until the average density over the entire season surpassed 20 mg/m³ (Figure 26), over ten times the average density seen in Suisun Bay during the highest year in this analysis (geometric mean density of *Pseudodiaptomus* spp. in Suisun Bay ranged from 0.045 mg/m³ in 2020 to 1.687 mg/m³ in 2011) (Figure 27). Therefore, any increase in *Pseudodiaptomus* spp. should result in increased potential Delta smelt growth, though the maximum growth observed will be dependent on water temperature (Figure 26). For example, a 50% increase in *Pseudodiaptomus* spp. across the entire summer could result in a 0.1 g increase in final smelt weight, which translates to approximately a 0.3% increase in survival probability (Figure 27).

Figure 26. Predicted increase in weight for Delta smelt in Suisun Bay from June 1 to October 31 versus average biomass of *Pseudodiaptomus* spp. copepodites and adults (combined) for different temperature scenarios. Turbidity was constant across all scenarios, and salinity was assumed to be within Delta smelt habitat range for the entire time period. Note that the average biomass used in the scenarios was artificially increased above what is normally seen in the data.

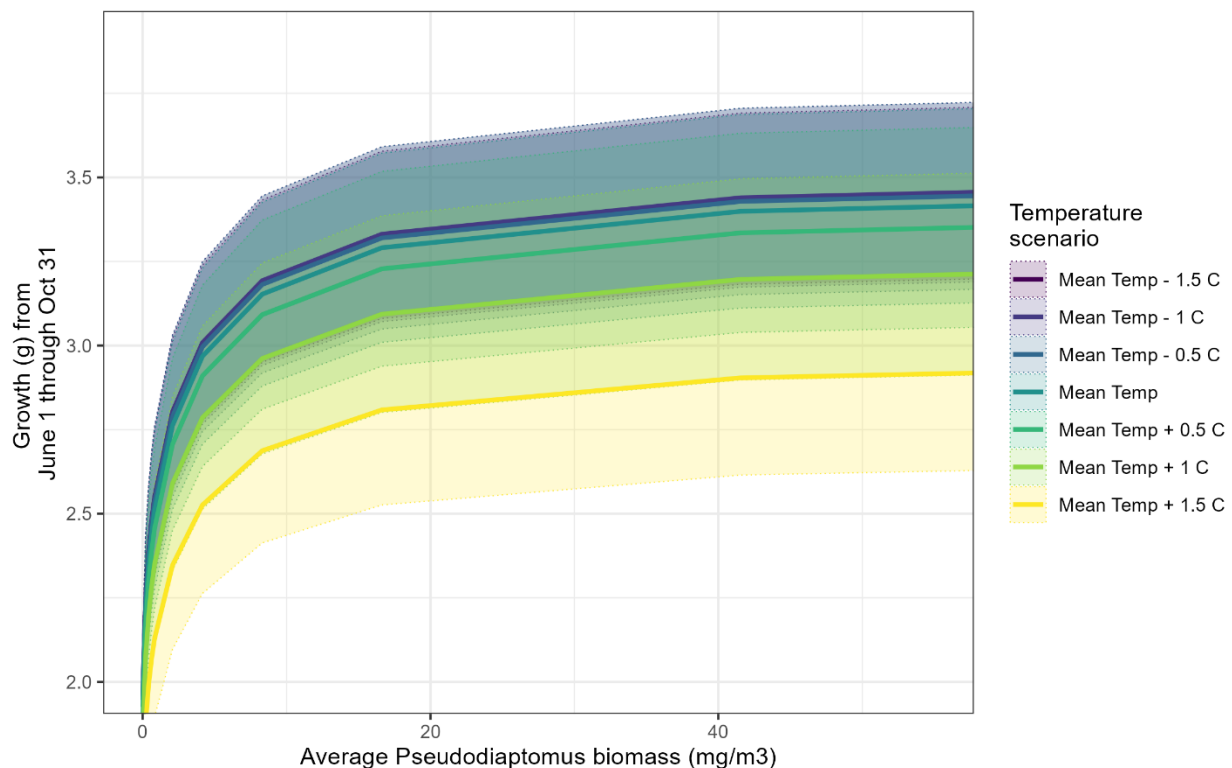
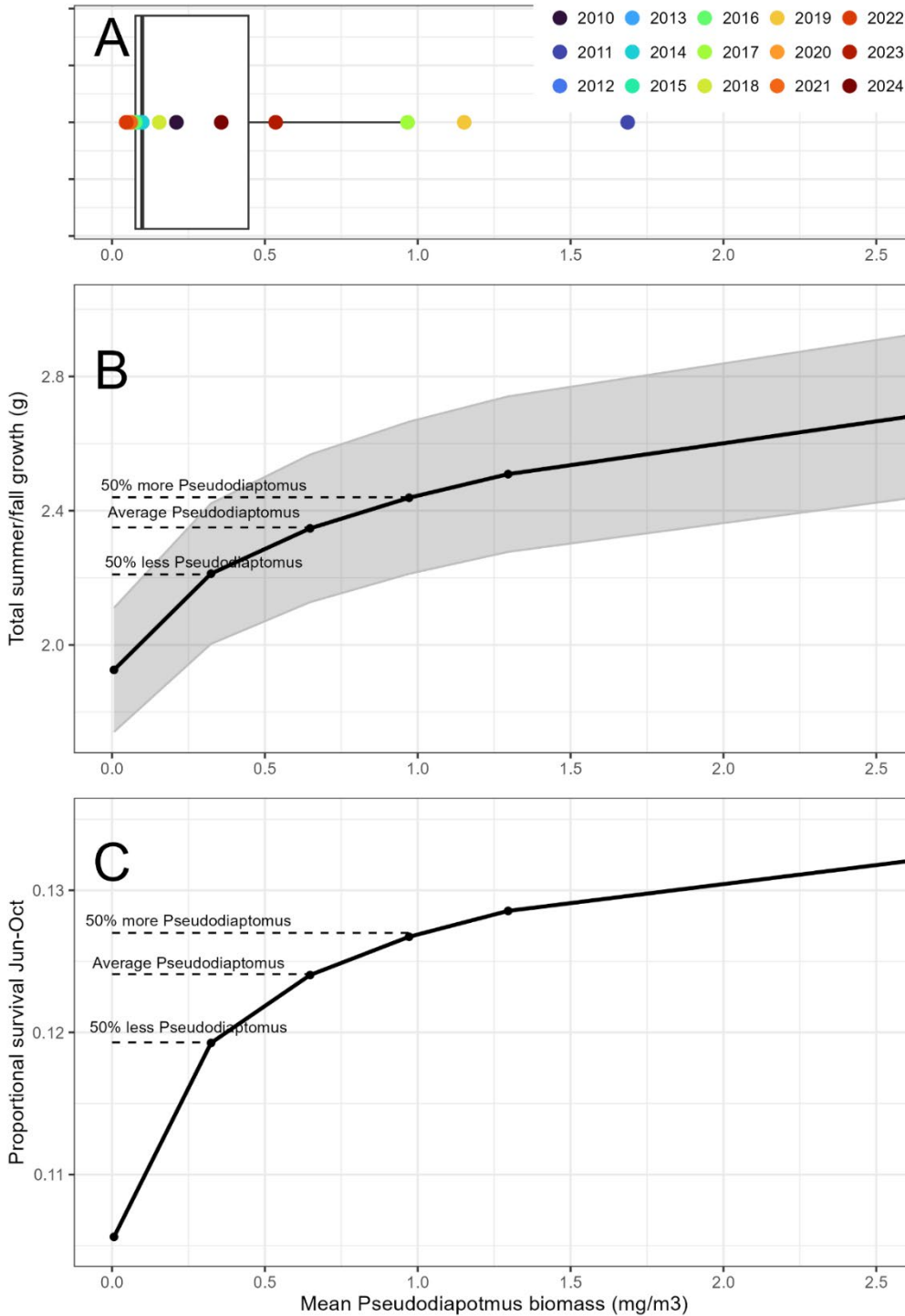


Figure 27. A) Box plot showing distribution of mean density of *Pseudodiaptomus* spp. juveniles and adults for June–October of 2010–2024. B) Total growth of Delta smelt in Suisun Bay versus average *Pseudodiaptomus* spp. biomass. C) Change in survival with change in growth rate. Turbidity and temperature were set to the average value for that date across 2011–2024, and it was assumed that salinity would remain <6 PSU over the course of the simulation.



Discussion

Our analyses demonstrate that higher flow and lower salinity during both the summer and the fall increase the abundance of important Delta smelt food (specifically *Pseudodiaptomus* spp.) in the LSZ (0.5–6 PSU) generally, and in Suisun Bay, Suisun Marsh, and Grizzly Bay specifically. Both the total abundance of *Pseudodiaptomus* spp. and the increase in *Pseudodiaptomus* spp. with lowered salinity are greater in summer than fall due to the seasonal peak in the population of this important prey item. It is also important to note that while densities of *Pseudodiaptomus* spp. increase in downstream areas with higher flow, the highest densities remain in the upstream (Sacramento River) region even at the highest flows, meaning food is likely to be more limiting in downstream areas regardless of outflow.

What Do Smelt Eat Anyway?

Analysis of Delta smelt diets collected between 2011–2024 demonstrate that the most important food sources for juvenile Delta smelt in the LSZ are *Pseudodiaptomus* spp., *Limnoithona tetraspina*, and *Eurytemora carolleeae* (Figure 24, Figure 25). We could not directly test for changes to diets with different values of X2 or Delta outflow because the great majority of the samples were taken when X2 was high and Delta outflow was very low. Plots give the misleading impression that certain prey items are only consumed at high X2 or low outflow because of the X2/outflow distributions. However, we did describe differences in diets due to salinity, season, and life stage that have implications for different X2/outflow results.

Pseudodiaptomus spp. was especially important for juvenile Delta smelt at the lower salinities (<3 PSU), with *Limnoithona* increasing in importance as salinity increased (Figure 24, Figure 25). This finding fits well with previous research highlighting the dominance of *Pseudodiaptomus* spp. in the zooplankton communities of freshwater and lower salinity regions during June and July (Merz et al. 2016) (so Delta smelt are eating what's there), with increasing dominance of *L. tetraspina* as salinity increases (Bouley and Kimmerer 2006). While *L. tetraspina* is much smaller than *Pseudodiaptomus* spp. adults and is hypothesized to be less energy-dense (Rose et al. 2013a), it has become an increasingly common component of Delta smelt diets due to its ubiquity in the water column, though it appears to be selected against (Slater and Baxter 2014). *E. carolleeae* also increases in importance with salinity (Figure 24, Figure 25), which is surprising since this taxa is generally considered to be higher in abundance in freshwater and peaks in late winter or early spring, when salinity in the estuary is generally low (Merz et al. 2016).

We also found high importance of *Acanthocyclops* spp. in Delta smelt diets, especially for larger individuals at higher salinities during the winter. This taxon has not been a focus of Delta smelt diet studies in the past, but it was present in 800 out of 4317 Delta smelt processed by CDFW's Diet and Condition Study (21% of the fish with food in their stomachs) (Bashevkin, Burdi et al. 2023), and it is common in diets of Longfin smelt and Pacific herring (Jungbluth et al. 2021). It is thought to have higher nutritional content than *L. tetraspina* (Kratina and Winder 2015). While it obtains peak abundances in April or May in fresh and very low salinity water (<0.13 PSU), it has an earlier peak in January or February in the LSZ (Bashevkin, Burdi et al. 2023), coinciding with the time and salinity it is most important for Delta smelt.

Mysids have historically been an item of importance in pelagic fish diets (Knutson Jr. and Orsi 1983; Orsi and Knutson Jr. 1979), however abundance of all mysids have been in decline over the past 40 years (Orsi and Mecum 1996; Barros 2021). Additionally, the community has shifted from dominance of *N. mercedis* to *H. longirostris*, a smaller taxon with higher thermal and salinity tolerances (Avila and Hartman 2020). Even when mysids are locally abundant, they make up a relatively small proportion of the Delta smelt diet in summer and fall due to the relatively small size of fish at this age and the relatively large size of the mysids (Slater and Baxter 2014; Slater et al. 2019).

Flow-Abundance Relationships

Of the taxa most important to Delta smelt diets, the strongest flow-abundance relationship was found for *Pseudodiaptomus* spp. (Figure 18). This is not surprising since multiple previous authors have described a relationship between *P. forbesi* abundance in the LSZ and either net Delta outflow or X2 (Lee et al. 2023; Kimmerer, Ignoffo et al. 2018). *E. carollleeae* also demonstrated a positive flow-abundance relationship (Figure 18), as also documented by Kimmerer (2002). However, they were present in much lower abundance than *Pseudodiaptomus* spp. and did not comprise an important part of diets during the summer (Figure 24). Other taxa with a positive flow-abundance relationship included Cladocera, which are rarely eaten by juvenile Delta smelt, probably due to their larger size and their rare occurrence in the LSZ (Slater et al. 2019) and copepod nauplii, which are also rarely eaten by juvenile Delta smelt due to their small size (Slater et al. 2019).

Some taxa exhibited negative flow-abundance relationships, most likely due to higher salinity niches. *Acartiella sinensis*, other cyclopoids (chiefly *Acanthocyclops* spp.) and *Limnoithona* spp. all decreased in abundance with increasing outflow. The predation of *Acartia* spp. on *Pseudodiaptomus* spp. is thought to be a major factor limiting *P. forbesi* to fresher water, so while Delta smelt will occasionally eat these predatory copepods (Slater et al. 2019; Slater and Baxter 2014), the extra link in the food chain reduces trophic efficiency (Hartman et al. 2025). As mentioned above, *Limnoithona* spp. are also potential prey for Delta smelt, but their small size

and likely low nutrient density make them a less efficient source of calories (Rose et al. 2013a). Therefore, the benefits of increased *Pseudodiaptomus* spp. with higher flows and lower salinities will outweigh the costs of decreased *Limnoithona* spp. and other predatory copepods.

While the native mysid *Neomysis mercedis* historically increased with lower X2 in summer (Kimmerer 2002), it is now quite rare in the Delta, and the most common mysid (*Hyperacanthomysis longirostris*) peaks at mid-salinities, without a consistent flow-abundance relationship (Figure 18) (Avila and Hartman 2020).

Therefore, with *Pseudodiaptomus* spp. being both the most important diet item in the summer and the taxon with one of the strongest flow-abundance relationships, we focused the rest of our analyses on this genus.

Impact of X2 and SMSCG on *Pseudodiaptomus* spp.

Our linear model of *Pseudodiaptomus* spp. abundance versus X2 by season shows that decreasing X2 does increase *Pseudodiaptomus* spp. in the LSZ in both seasons, but variance remains quite high, and the effect of X2 in summer is much stronger than in fall (Figure 20). Many other water quality and biological factors influence abundance of *Pseudodiaptomus* spp., including vertical migration (Kimmerer et al. 2002), predation (Kayfetz and Kimmerer 2017; Kimmerer and Lougee 2015), water quality (Barros et al. 2024), and food supply (Owens et al. 2019; Holmes and Kimmerer 2022). Hydrodynamic modeling paired with growth rate and reproductive estimates indicate that most of the increase in *Pseudodiaptomus* spp. in the Suisun region is due to transport from upstream areas rather than in-situ production (Kimmerer, Ignoffo et al. 2018). While we did not model transport of zooplankton explicitly, we did see that the X2-abundance relationship was much lower or nonsignificant in upstream and freshwater areas and that overall abundance was much higher upstream than downstream (Figure 20, Figure 21). We also saw that GAMs based on salinity slightly underestimated abundance at higher Delta outflows (Figure 23). The slightly hump-shaped relationship seen in the Sacramento River region in the exploratory GAMs (Figure 18) indicates that *Pseudodiaptomus* spp. may be transported completely out of the region at very high flows. The upstream regions could have acted as a reservoir of high population abundance with downstream increases due to transport from upstream, as shown by Hassrick et al. (2023) and Kimmerer, Gross et al. (2018).

While transport of zooplankton from upstream may explain a good deal of the increase in zooplankton in Suisun Marsh and Suisun Bay, the fact that the increase remains significant when using salinity bin instead of geographic region indicates that either flow is increasing zooplankton density faster than it is decreasing salt, or that changes in absolute abundance are contributing to the observed patterns.

Within Suisun Marsh, the linear model showed that salinity at Belden's Landing – which is driven by both Delta outflow and SMSCG operation – was not as good a predictor of *Pseudodiaptomus* spp. abundance as X2 (Table 10). However, the GAM selection process found that the model using salinity as a predictor performed better than the model using outflow and was preferred over the model using both salinity and outflow in the Marsh (Table 13). The highly correlated nature of salinity and flow makes it difficult to determine the mechanism for this relationship. Lowered salinity could be allowing *Pseudodiaptomus* spp. to escape from predation (Kayfetz and Kimmerer 2017), or the increased flow could be physically transporting organisms from areas of higher abundance upstream (Kimmerer, Ignoffo et al. 2018). The SMSCG may be acting to transport higher densities of *Pseudodiaptomus* spp. into Suisun Marsh than would be expected by increased Delta outflow alone. However, due to the high correlation between X2 and salinity in the Marsh, we were not able to differentiate how much of the effect was caused by the SMSCG operations and how much caused by Delta outflow. In the future, particle tracking models may be able to further explore this relationship.

Benefits to Delta Smelt

Whether increasing zooplankton transport to downstream areas results in benefits to Delta smelt will depend on whether smelt are food limited in these areas and whether the increase in transport is enough to allow for a “meaningful” increase in growth (where “meaningful” is highly subjective and dependent on management goals). Both bioenergetics modeling and histopathology have demonstrated that Delta smelt are frequently nutritional stressed (i.e. food limited) in the estuary, with Suisun Bay being an area with the lowest observed stomach fullness (Hammock et al. 2015) and where increased food has the highest potential to increase growth rates (Hammock et al. 2015; Smith and Nobriga 2023).

Our analysis found that observed *Pseudodiaptomus* spp. biomass was well below the point at which food would become saturating, so any increase in zooplankton should relate to an increase in Delta smelt growth if temperature and turbidity are not limiting (Figure 26). McCormick et al. (2025) and Hammock et al. (2022) both found that increased zooplankton biomass increased Delta smelt hepatosomatic index, a measure of fish health and energy stores. Fichman (2022) also found that increased food increased Delta smelt growth rates in a laboratory setting. While the bioenergetic model only provides a relative measure of potential growth rate, using it in combination with studies that demonstrate the benefits of increased food supports the hypothesis that increased zooplankton will increase growth rates.

Increased zooplankton will increase growth, but whether or not this increase provides a “meaningful” impact on the Delta smelt population trajectory depends on the goals of the management action. Increased individual growth during the summer and fall should result in increased survival (Rose et al. 2013b) and increased reproduction the following spring (Damon et al. 2016). Increased

reproduction should increase population growth (Polansky et al. 2024). However, the growth and survival range predicted by the bioenergetic model across the observed zooplankton densities over the past 14 years were relatively modest, with the length-dependent survival model predicting less than a 1% change in proportional survival over the course of June–October (Figure 27). Furthermore, many other factors besides individual summer and fall growth rates contribute to the population growth rates (spring food supply, spring temperatures, winter turbidity, etc.) (Polansky et al. 2024). To increase the growth of an average Delta smelt by 0.1 g (approximately 5% of the average weight gain over the summer–fall period, and an increase in survival of approximately 0.3%), *Pseudodiaptomus* spp. juvenile and adult abundance in Suisun Bay would need to increase by 50% across the entire time period (Figure 27). Other taxa also contribute to Delta smelt food supply, but *Pseudodiaptomus* spp. are by far the most common taxa in smelt diets in the summer (Figure 24). The next most important taxon, *Limnoithona* spp., has a more complicated relationship between flow and abundance (Figure 18), so changes to its availability with flow actions will require further analysis. Further analyses are also needed to explore what action taken during only part of the time period or in other regions of the estuary would do to Delta smelt food supply and potential increases to growth rates.

Other factors, particularly temperature, may limit the ability to see increases in growth. For example, increases in *Pseudodiaptomus* spp. in the LSZ during the summer or fall of 2017 and 2019 were not significantly correlated with increases in Delta smelt growth or survival (Lee et al. 2023), and high temperatures may have been a driving factor (FLOAT-MAST 2021). Furthermore, while bioenergetic models can predict potential growth rates, many factors not included in the model can impact realized growth rates. For example, Hammock et al. (2017) found that Delta smelt in brackish water (>0.55 PSU) had higher stomach fullness per zooplankton than those caught in fresher water despite the lower abundance of many of their zooplankton prey. It is not clear exactly what mechanism underlies this trend, but higher turbidity in downstream (higher salinity) regions may increase foraging efficiency (Smith and Nobriga 2023), and higher areas of tidal wetlands in the downstream region may provide off-channel foraging opportunities not included in the zooplankton dataset (Hammock, Hartman et al. 2019). Fish caught in Suisun Marsh also tend to have lower lesion loads than those caught in Suisun Bay or the Delta (Hammock et al. 2015), indicating lower levels of contaminants.

Conclusions

Taken together, these analyses provide support for our main hypothesis that lower X2 in the summer and fall, and lower salinity in Belden’s Landing, will increase the abundance of *P. forbesi* in Suisun Marsh, Suisun Bay, and Grizzly Bay. There was a strong negative relationship between *Pseudodiaptomus* spp. abundance and X2 across the entire Suisun region, and a strong negative relationship between abundance and salinity at Belden’s Landing within Suisun Marsh. The relationship

between X2 and abundance was much weaker in the Sacramento River region, though biomass was almost always higher in the River than downstream. Breaking this into more specific hypotheses we found:

- *Hypothesis: P. forbesi* is the most important organism in Delta smelt diets during the summer and fall.
 - *Supported.*
 - *Pseudodiaptomus* spp. had one of the highest indices of relative importance for Delta smelt juveniles during the summer and fall in both freshwater and the LSZ.
 - Similar results were found by Slater and Baxter (2014) and Slater et al. (2019).
- *Hypothesis:* No other significant component of Delta smelt diets during the summer or fall has a significant positive relationship with Delta outflow.
 - *Supported.*
 - The only other taxa with strong positive relationships with Delta outflow are uncommon in summer and fall (*Eurytemora carolleeae*) or are uncommon in Delta smelt diets (*Daphnia* and other Cladocera).
 - Similar results were found by Lee et al. (2023) and Kimmerer (2002).
- *Hypothesis:* The influence of X2 on *Pseudodiaptomus* spp. abundance in the LSZ will be larger in summer than fall because abundance of this taxa peaks in June and July.
 - *Supported.*
 - Linear models of *Pseudodiaptomus* spp. biomass showed a stronger relationship between abundance and X2 in summer than fall.
- *Hypothesis:* Increases to *Pseudodiaptomus* spp. abundance in the LSZ will result in increased Delta smelt growth and survival.
 - *Supported.*
 - Bioenergetic models indicate Delta smelt food supply is not saturating, so any increase in *Pseudodiaptomus* spp. biomass will increase smelt growth, with a 50% increase from the average *Pseudodiaptomus* spp. abundance causing an estimated 0.1 g increase in growth over the course of the summer and fall.
 - Increased food has also been correlated to increased hepatosomatic index in the wild (McCormick et al. 2025) and increased somatic growth in the laboratory (Fichman 2022).

Smelt Growth—Wild Fish

Introduction

The ultimate objective of the SFHA is to mitigate for impacts of the SWP and CVP by benefitting Delta smelt food supply and habitat, thereby increasing individual growth, individual survival, and population growth of Delta smelt in years where actions are taken. However, the population of Delta smelt has been so low over the past fifteen years that it is very difficult to make conclusions about the effect of the actions on Delta smelt in the wild.

The original analyses leading to the Fall X2 standards (Feyrer et al. 2007; Nobriga et al. 2008; Feyrer et al. 2011) used abundance indices from the FMWT and STN to measure population growth and regress abundance versus a habitat index that was tied to the LSZ (indexed by X2). We cannot extend these analyses to more recent years because catch of Delta smelt dropped below the detection limit in both surveys, but we can make use of a number of new datasets not available to previous researchers.

Starting in 2011, there was increased value put on each individual fish caught by all long-term monitoring surveys and increased focus on habitat conditions. The CDFW Diet and Condition Study began in 2005 and has evaluated the stomach contents of most Delta smelt caught between 2011 and 2024 (methods described in Slater and Baxter 2014; Hammock et al. 2022; Slater et al. 2019). Researchers at the University of California, Davis, began studying Delta smelt otoliths to determine growth rates and migratory patterns (Lewis et al. 2021; Hobbs, Lewis et al. 2019), histopathology to determine contaminant exposure (Teh et al. 2020; Hammock et al. 2015), and other indicators of overall health and condition including liver weight, glycogen, and RNA:DNA ratio (Hammock et al. 2022; Ramírez-Duarte et al. 2019). These studies on wild-caught Delta smelt were reinforced by targeted experiments on cultured Delta smelt, allowing a greater understanding of physiological tolerances and bioenergetics (Hammock et al. 2020; Dhayalan et al. 2024; Hasenbein et al. 2013; Hasenbein et al. 2016).

The EDSM Program, established in 2016 to improve and standardize detection of Delta smelt, is now the only survey regularly catching Delta smelt in the estuary. This survey provides weekly, regional abundance estimates, but even their catch has been so low that the abundance estimates have huge variance associated with them. Furthermore, we can only compare abundance estimates between 2016 and the present because EDSM uses a different study design, leading to CPUE that is not equivalent to that of the former CDFW surveys. This makes it difficult to draw comparisons between current and past Delta smelt abundance. However, the EDSM program was accompanied by the DOP led by Reclamation (Schultz 2019). This was an intensive effort to monitor environmental conditions, with randomized sampling

of zooplankton and phytoplankton alongside EDSM, and every Delta smelt caught was processed for histopathology, otolith analysis, diet, growth rates, and other health metrics (Lee et al. 2023; Hassrick et al. 2023; Teh et al. 2020), which led to many publications (e.g. Hammock et al. 2020; Teh et al. 2019).

Further enhancing and complicating potential analyses, an experimental release program began in 2021, with a full population supplementation program in 2024 to bolster the Delta smelt population with cultured fish. While these releases have substantially increased catch relative to before they started, the release of cultured fish every winter limits our ability to detect inter-annual responses to flow actions.

Although catch of Delta smelt has been in severe decline, tools to analyze the potential impacts of our actions on smelt without catching them have improved. Several different models have been applied to Delta smelt based on historical data. Most notably, the Delta Smelt Life Cycle Model demonstrated that summer outflow was a better predictor of individual survival and population growth rate than fall outflow (Polansky et al. 2024), and a bioenergetic model demonstrated that high temperatures, low food supply, and low turbidity may all limit Delta smelt growth and survival rates during the summer and fall in different years and regions of their range (Smith and Nobriga 2023). An individual-based model of Delta smelt population growth has also been used to evaluate how environmental variability and management actions may impact smelt population growth and survival (Rose et al. 2013a; Rose et al. 2013b; CSAMP Delta Smelt Technical Working Group et al. 2024).

Given the difficulties in accurate population estimates and new developments in life cycle modeling, we have taken several different approaches to assess the efficacy of SFHAs from 2011–2024.

1. We also used bioenergetic modeling to estimate the maximum potential growth rate of individual Delta smelt during this time period based on the observed temperatures, turbidity, and zooplankton abundance. While this model may not provide precise observations of Delta smelt growth, it can provide an index of suitability for growth during the summer–fall time period.
2. We compared bioenergetic models of growth rates to observed growth rates derived from wild fish otoliths as well as the overall body condition of fish caught during this time period.
3. We use data on liver weights (an indicator of overall health and condition) to test for correlations between health and X2 during the summer and fall (see [Smelt Health](#) section).
4. We used data from three years of enclosure experiments to see how fish respond to different habitat conditions (see [Smelt Enclosure](#) section).

Hypotheses

This section focuses on two of the hypotheses listed in the introduction of this report:

- Years with Lower X2 in the summer and fall, and lower salinity at Belden’s Landing will have higher Delta smelt growth, health, and condition during the summer and fall.
- The influence of X2 and salinity in Suisun Marsh on Delta smelt growth will be greater in summer than in fall.

Methods

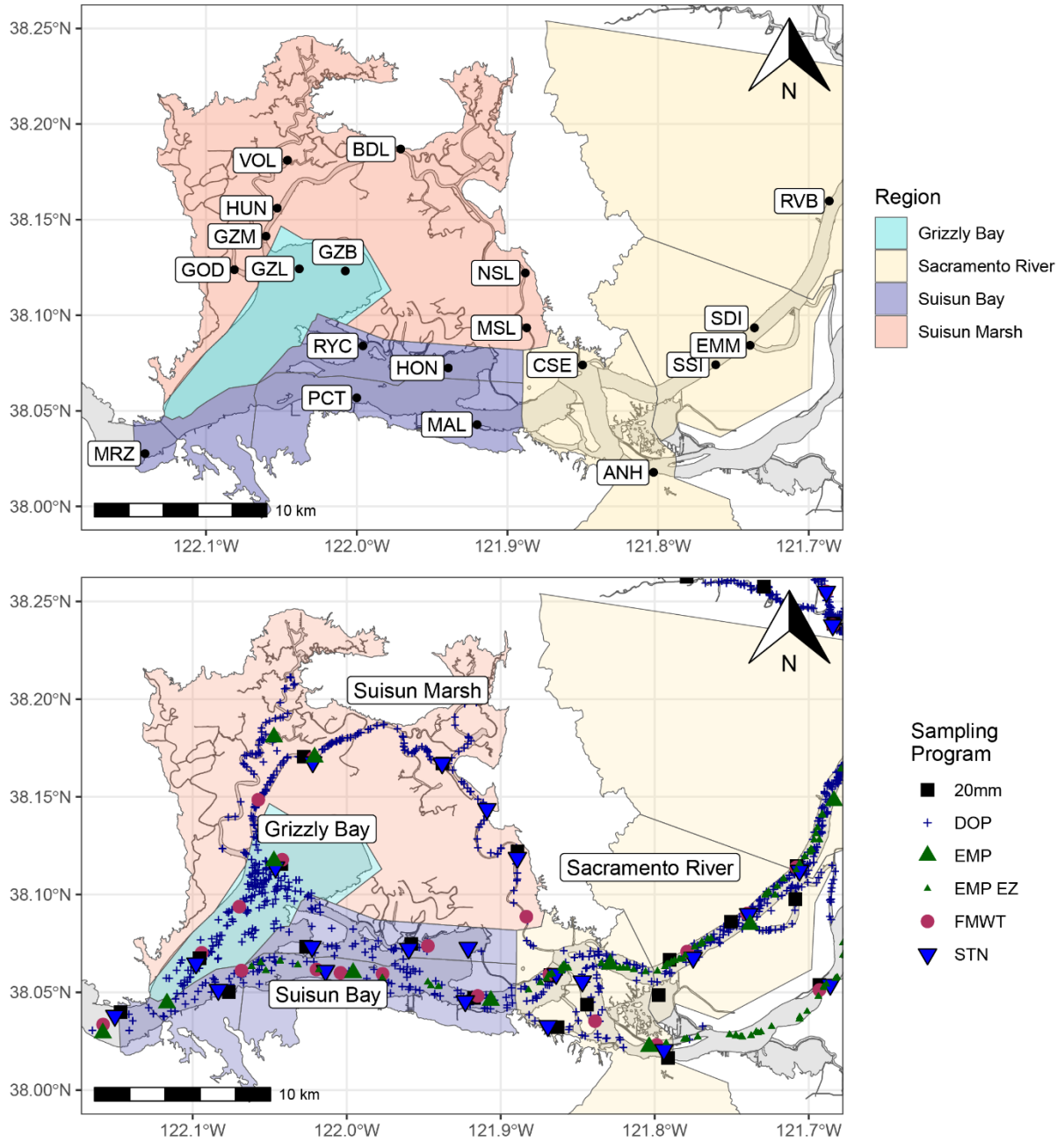
Bioenergetic Modeling of Potential Growth

To test the relative habitat suitability of summer and fall conditions with and without flow actions, we used a bioenergetic modeling approach similar to Smith and Nobriga (2023). This model was originally developed by Rose et al. (2013a) as part of an individual-based life cycle model and expanded upon by Smith and Nobriga (2023) to provide an index of habitat suitability based on relative growth rate potential.

The bioenergetic model used in this report is described in brief in the [Smelt Food](#) section and described in detail in Rose et al. (2013) and Smith and Nobriga (2023).

Input data were average observed temperature, salinity, turbidity, and zooplankton values collected by IEP’s long-term monitoring surveys in the regions developed by Rose et al. (2013) thought to be most directly impacted by the SFHA (Figure 28).

Figure 28. Regions of the estuary developed for the Rose et al. individual-based model with locations of continuous sondes (top) and zooplankton samples (bottom)



Where possible, we used continuous sondes for temperature, salinity, and turbidity (stations shown in Figure 28). Data were collected by DWR’s Continuous Environmental Monitoring Program and/or Suisun Marsh Program, US Geological Survey (USGS), or Reclamation and underwent quality review before analysis (see description of continuous stations in the [Smelt Habitat](#) section). Outliers and values outside normal range for each parameter were removed.

Only two sondes in the area had turbidity values from before 2015 (RVB and MAL). For regions without turbidity measurements in earlier years, we used the average monthly turbidity from all point samples taken by IEP’s boat-based monitoring surveys, accessed through the `discretewq` package in R (Bashevkin, Perry et al. 2023). Using discrete measurements may miss short-term extreme events but should provide a sense of long-term patterns.

Zooplankton data came from mesozooplankton trawls conducted by IEP surveys throughout the area, including STN, EMP, FMWT, 20mm, and DOP, using 150 or 160 micron mesh nets and integrated using the `zooper` package (Bashevkin, Hartman et al. 2023b). These data provide good estimates for the most important components of Delta smelt diets, including calanoid copepods and Cladocera, but do not quantitatively sample smaller organisms, such as *L. tetraspina*, which may be important components of smelt food when they are abundant (Slater et al. 2019). However, EMP is the only program that samples smaller zooplankton and does not have the spatial and temporal balance of the other programs (Bashevkin, Hartman et al. 2022), so it was not included to avoid spatial biases in our analysis. The zooplankton taxa were grouped into 12 categories as used by Smith and Nobriga (2023), and we calculated regional monthly averages for each group for 2010–2024.

We used the observed temperature, turbidity, and zooplankton data to calculate the average predicted increase in Delta smelt growth from June 1 through October 31 for each year in each region. We assumed all fish started out with a fork length of 23mm in each year (the mean total length for Delta smelt post larvae observed in the 2016–2020 EDSM catch, per Smith and Nobriga, 2023) to test the difference in habitat conditions during the summer and fall without taking pre-existing conditions into account. We then performed a sensitivity analysis by using observed data for one of the factors (temperature, turbidity, or zooplankton), while holding the other factors constant. We used the size-dependent mortality term from Rose et al. (2013b) to estimate the proportional survival over the entire time period based on the lengths predicted from the model for each scenario. We did not include starvation-induced mortality because no scenarios resulted in fish losing weight.

The bioenergetic model does not include a salinity term, so to calculate a single value for the potential growth rate of Delta smelt in the regions where they are most likely to occur, we calculated the daily mass-specific growth rate in each region, removed all subregions where salinity was > 6 PSU, and calculated the mean potential growth in the remaining regions. This assumes there was no movement between regions, which is unrealistic but simplifies the analysis.

To assess the impact of changes in both Summer and Fall X2 on growth rate, we re-ran the bioenergetics model on only June and July (for summer growth) and only September and October (for fall growth). In these scenarios we assumed all fish started at 23 mm in length. This is unrealistic for the fall scenarios, but it allows a more direct comparison of the potential benefit of flow actions during the fall time. We then ran a linear regression on change in weight versus the seasonal average X2 with an interaction of X2 and season.

Comparing Growth Rate Metrics

To provide context for the bioenergetic and liver weight results, we compared the potential growth rates as measured using bioenergetics to observed Delta smelt condition and growth rates. Condition factor came from a 10-year dataset of Delta smelt bioassays (Hammock et al. 2022; Hammock, Hartman et al. 2019), which used fish captured by EDSM, SKT, STN, and FMWT within the upper San Francisco Estuary from 2011–2021. These fish were sent to UC Davis (laboratory of Dr. Swee Teh and Dr. Burce Hammock), where they were measured for length, weight, liver weight, and glycogen level (this same dataset is used for the Delta smelt health analysis). A subset of these data included growth rates derived from otolith analysis (Lewis et al. 2021). We visually compared the 14-day, age-corrected growth rate (mm fork length per day, log-transformed, as calculated by Lewis et al. (2021) for Delta smelt caught in the focal area in summer and fall by water year type. We then regressed the adjusted growth rate against the X2 value on the day the fish were captured using a linear mixed-effects model with X2, season (summer versus fall), water temperature, and the interaction of X2 and season as predictor terms, with year as a random effect. Predictor terms were scaled and centered before running the model. We also visually compared the condition factor, adjusted growth rate, and modeled growth rate of Delta smelt caught in the focal area (Suisun Marsh, Suisun Bay, Grizzly Bay, and the lower Sacramento River) in summer and fall by water year type.

Results

Otolith Analysis

Analysis of age-corrected, 14-day growth rates for Delta smelt caught in summer and fall showed much higher growth in 2011 and 2012 than 2013–2019, with no clear correlation with water year type (Figure 29). However, the linear mixed-effect model showed a significant negative relationship between growth and X2 during the summer and a slight positive effect in the fall after temperature was taken into account (Figure 30, Table 15).

Figure 29. Box plot showing log-transformed, age-corrected, 14-day growth rate for Delta smelt caught in summer and fall in Suisun Bay, Suisun Marsh, and the lower Sacramento River. Number of fish included in the sample is in the box above the x-axis. No smelt were analyzed from 2016.

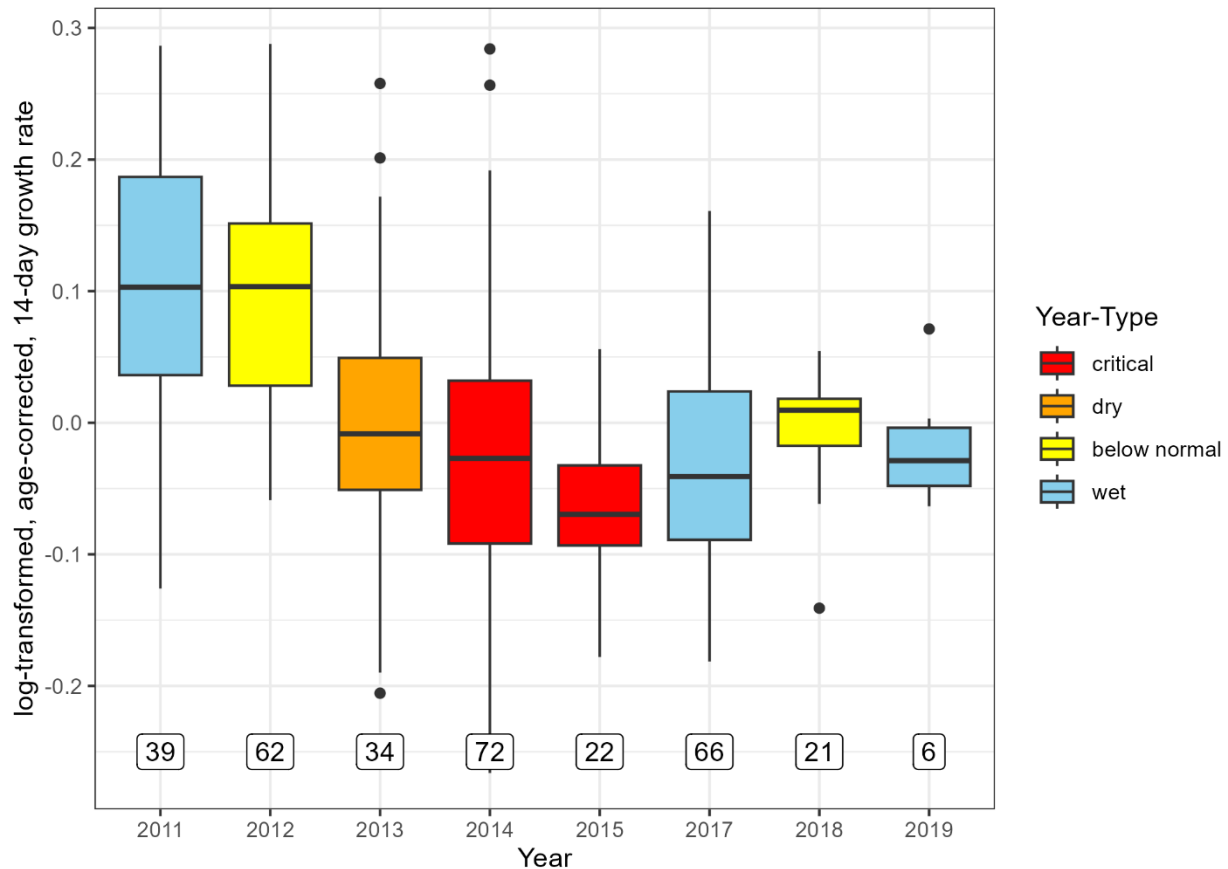


Figure 30. Partial residual plots showing the effect of water temperature and X2 on individual Delta smelt growth rates from otolith data.

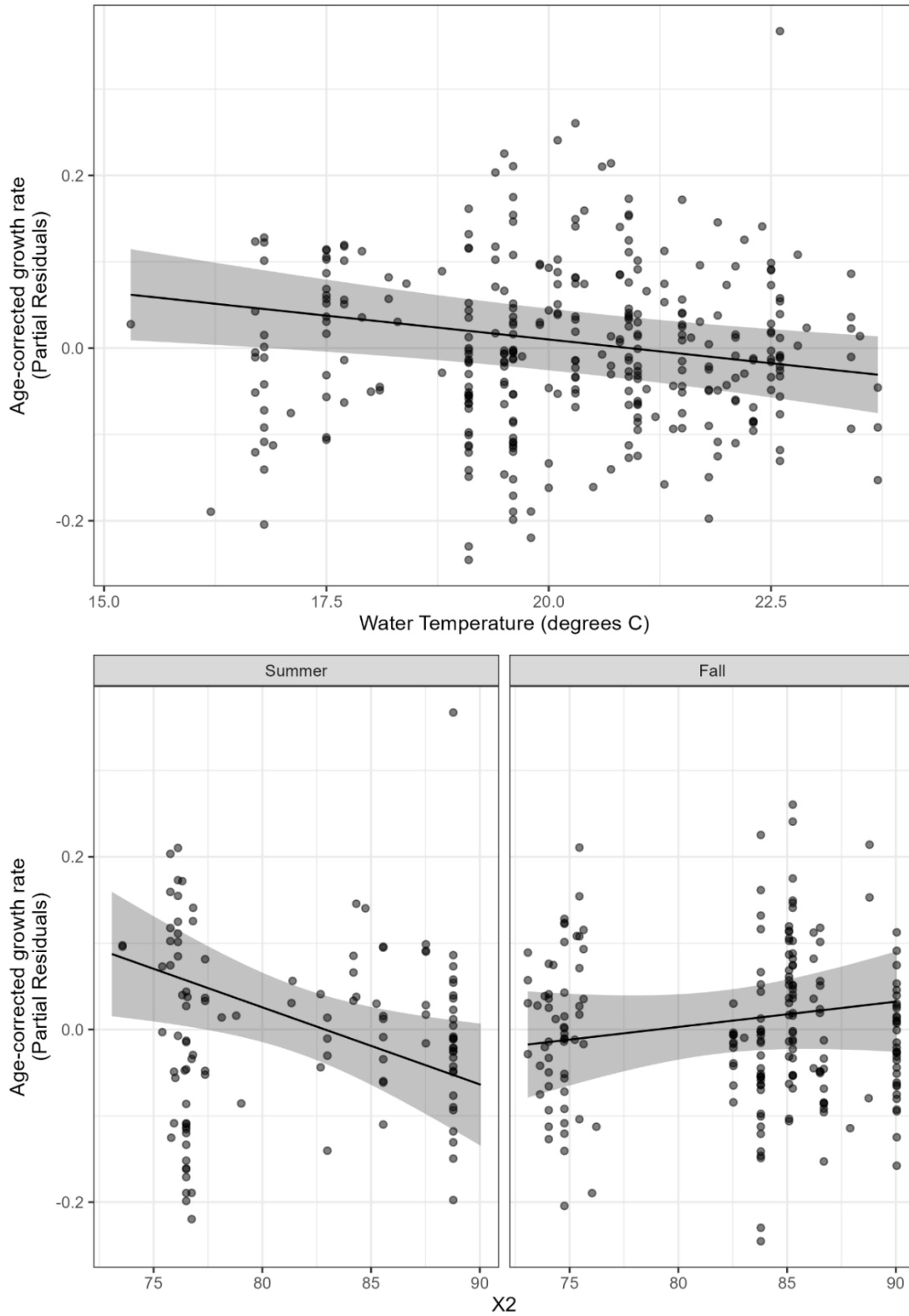


Table 15. Model coefficients for a linear mixed model of age-corrected, 14-day growth rate versus X2, season, and water temperature.

Predictor	Estimate	SE	df	t-value	Pr(> t)
(Intercept - summer)	-0.0007	0.0196	9.0	-0.04	0.9727
X2	-0.0468	0.0189	14.9	-2.48	0.0258
Season (fall)	0.0082	0.0119	316.3	0.69	0.4887
Temperature	-0.0199	0.0072	316.4	-2.78	0.0058
X2:Season	0.0621	0.0100	242.1	6.21	<0.0001

Bioenergetic Modeling

Running the bioenergetic model on the observed temperature, turbidity, and zooplankton from 2011–2024 found that the highest growth rates occurred in 2011 in Grizzly Bay, Suisun Bay, and Suisun Marsh, though growth in the Sacramento River region was slightly higher in 2016 than 2011 (Figure 31). Comparing regions, there were differences in which region had the highest growth, with Grizzly Bay being highest in 2011, 2015, 2018, 2020, 2021, and 2022, the River being highest in 2012 and 2016, Suisun Bay being highest in 2017, 2019, and 2023, and Suisun Marsh being highest in 2014.

Looking at average potential Delta smelt growth in subregions that were less than 6 PSU (Figure 32), 2011 experienced the highest growth by far, followed by 2018 and 2017. The lowest growth was experienced in 2022 (a very Dry summer) with the drought years of 2015 and 2020 being the next lowest. Comparing these results to data from otoliths and condition factors collected over the same time period, 2011 was consistently the highest in all three metrics (Figure 33). There were no clear patterns between condition factor, otolith-based growth rate, and bioenergetic growth for years besides 2011. There were correlations between bioenergetics-based growth rates and the mean annual otolith-based growth rate as well as between the bioenergetics-based growth rate and the mean annual condition factor, though they did not quite make the $p < 0.05$ threshold for statistical significance ($P = 0.06$ and $P = 0.07$) (Figure 34). There was a significant relationship between mean annual condition factor and mean annual otolith-based growth rate, but this was chiefly driven by the outlier of 2011 ($P = 0.003$) (Figure 34).

When zooplankton and turbidity were held constant and only temperature and salinity varied between years (Figure 32b), growth was higher in this simulation than when zooplankton and turbidity varied for all years, with highest growth in 2012, followed by 2018 and 2011, and the lowest growth in 2024. When temperature and zooplankton were held constant and only salinity and turbidity changed between years (Figure 32c), growth was highest in 2016, followed by 2017 and 2018, and the lowest growth in 2021, 2020, and 2015, all of which were Dry or Critically Dry years. When temperature and turbidity were held constant and only zooplankton and salinity were allowed to change, growth was slightly higher than

the “observed” scenario but lower than the scenarios where differences were due to turbidity or temperature. The highest growth was in 2011, followed by 2014 and 2017, with the lowest growth in 2022. Together, these analyses indicate that zooplankton was usually the most limiting factor for Delta smelt growth, and the high growth in 2011 was caused by a combination of high zooplankton and lower temperatures.

When we calculated growth rates separately for summer (June–July) and fall (September–October), we found that potential growth rates in summer were consistently higher than in fall, though the difference between years was more pronounced in summer (Figure 35). There was also a significant effect of average X2 in summer but not in fall (Figure 36, Table 16).

Figure 31. Results from bioenergetic model of potential Delta smelt growth from June 1 through October 31 in each of the major regions of the estuary by year. Years plotted in shades of red represent Critically Dry years. Shades of orange represent Dry years. Shades of yellow represent Below Normal years, shades of green represent Above Normal years, and shades of blue represent Wet years. See Table 1 for more information on water year types.

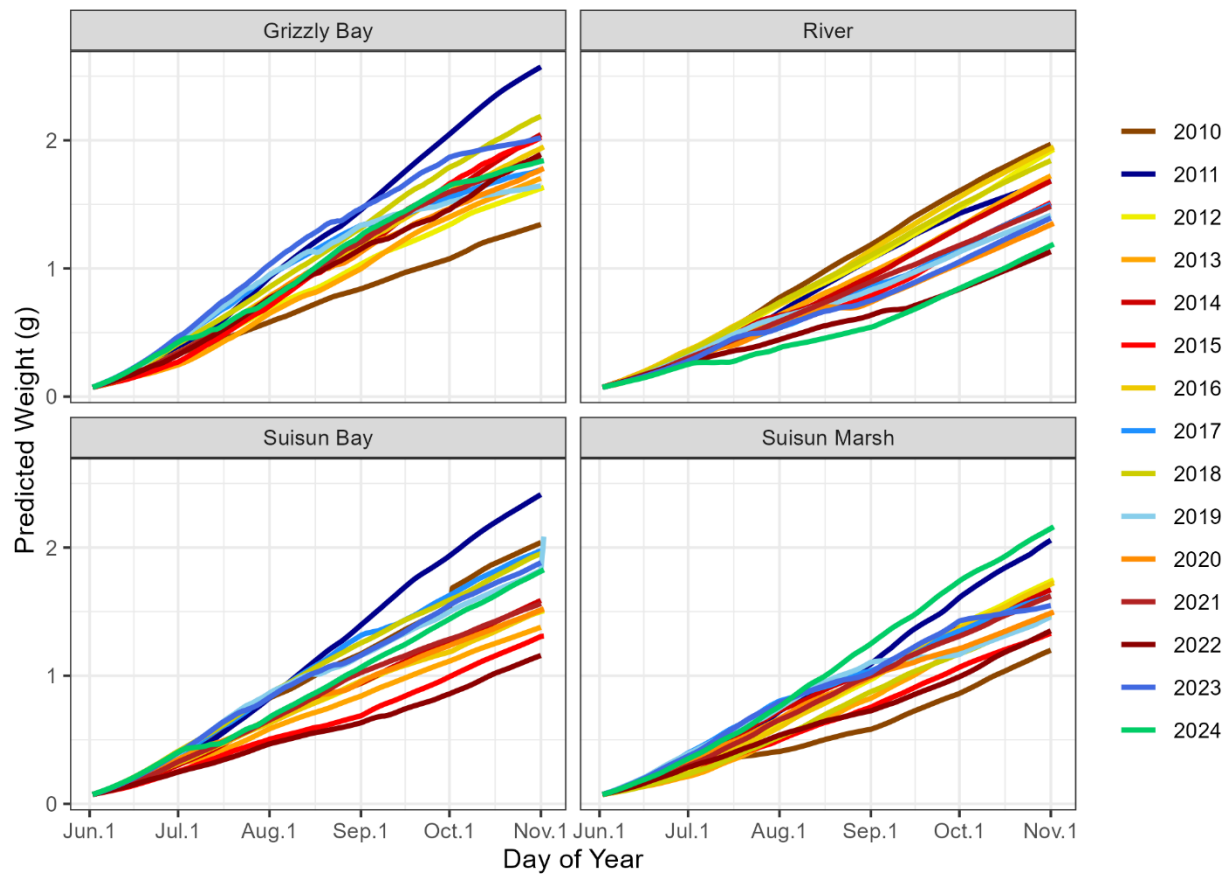


Figure 32. Predicted growth rate of Delta smelt in regions where salinity is less than 6 PSU. A) Scenario with observed changes in temperature, turbidity, zooplankton, and salinity between years. B) Scenario with observed changes in temperature and salinity between years, with turbidity and zooplankton held constant. C) Scenario with observed changes in turbidity and salinity with temperature and zooplankton held constant. D) Scenario with observed changes in zooplankton and salinity with temperature and turbidity held constant. Years plotted in shades of red represent Critically Dry years. Shades of orange represent Dry years. Shades of yellow represent Below Normal years, shades of green represent Above Normal years, and shades of blue represent Wet years. See Table 1 for more information on water year types.

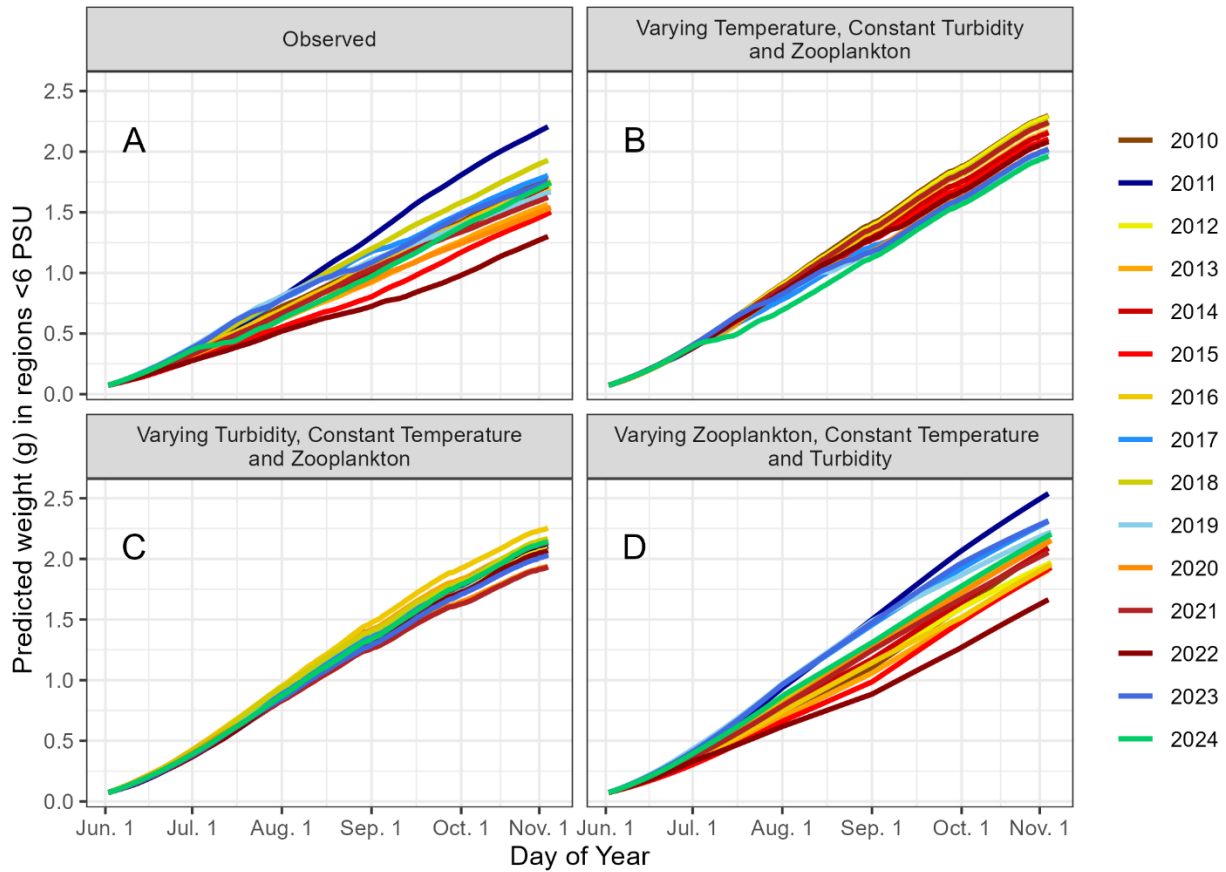


Figure 33. Plot comparing three different measures of Delta smelt conditions. The top set of panels show the predicted growth from summer (June–July) and the bottom set of panels show fall (September–October) in regions with less than 6 PSU salinity by year. The second panels show the condition factor of fish collected in summer (June–August) and fall (September–October) in Suisun Bay, Suisun Marsh, and the lower Sacramento River (Data from Bruce Hammock). The third panels show the size-corrected mass-specific growth rate anomaly from the 14-day period immediately prior to capture derived from otolith analysis in the same regions and time period. (Data courtesy of Dr. Levi Lewis, UC Davis, 2025).

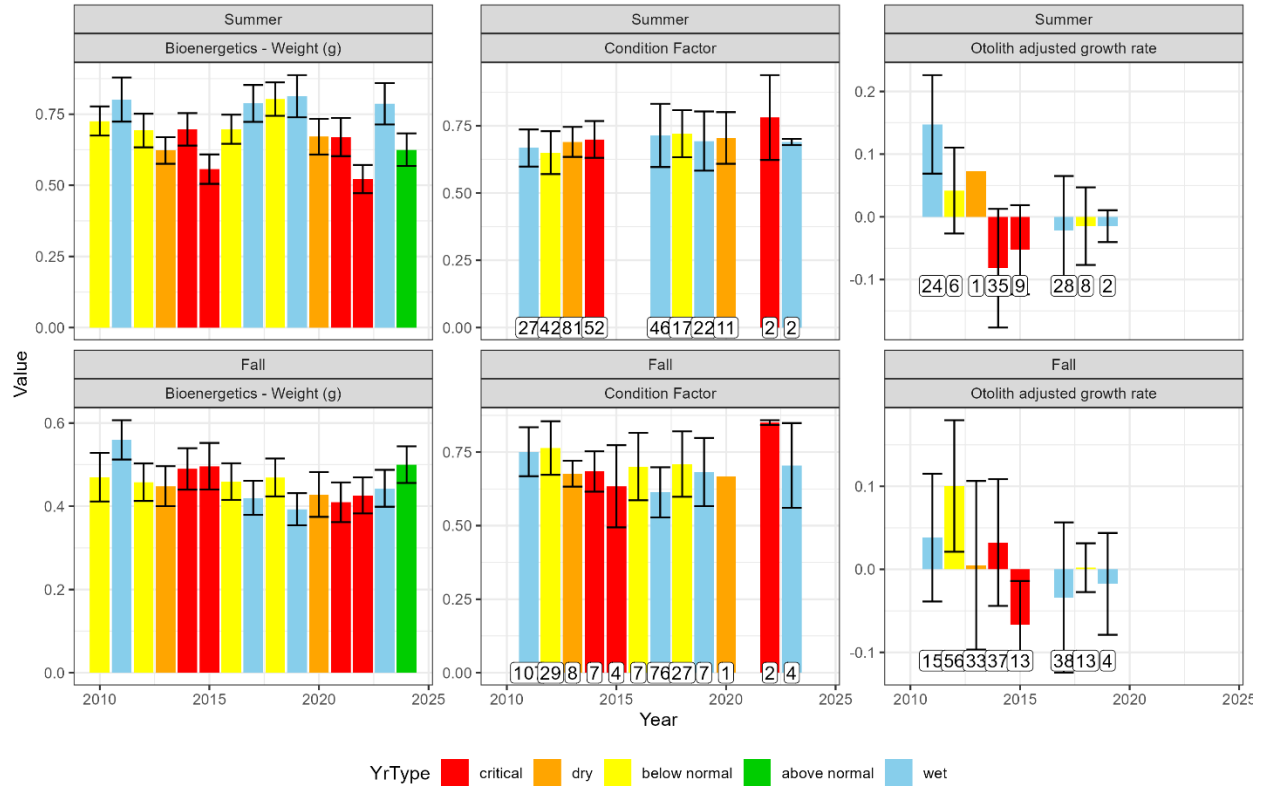


Figure 34. Correlations between bioenergetic model growth rates, condition factor, and otolith-based growth rates.

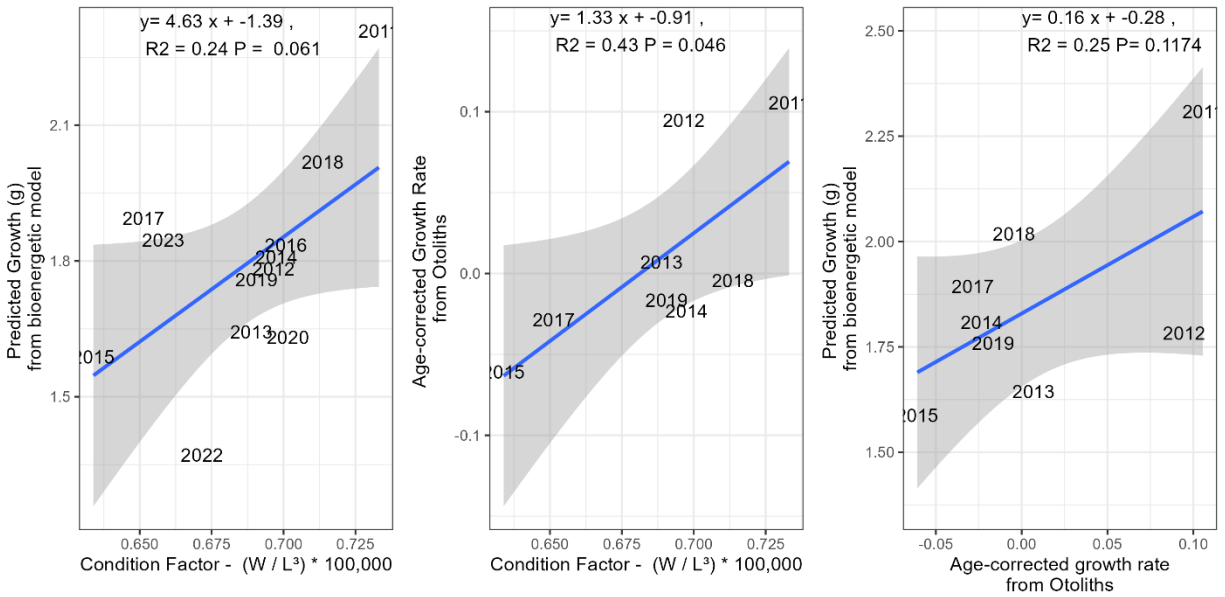


Figure 35. Predicted weight of Delta smelt in each year in summer versus fall in regions where salinity was less than 6 PSU using observed temperature, turbidity, salinity, and zooplankton (top panel), then holding temperature, turbidity, or zooplankton constant. Years plotted in shades of red represent Critically Dry years. Shades of orange represent Dry years. Shades of yellow represent Below Normal years, shades of green represent Above Normal years, and shades of blue represent Wet years. See Table 1 for more information on water year types.

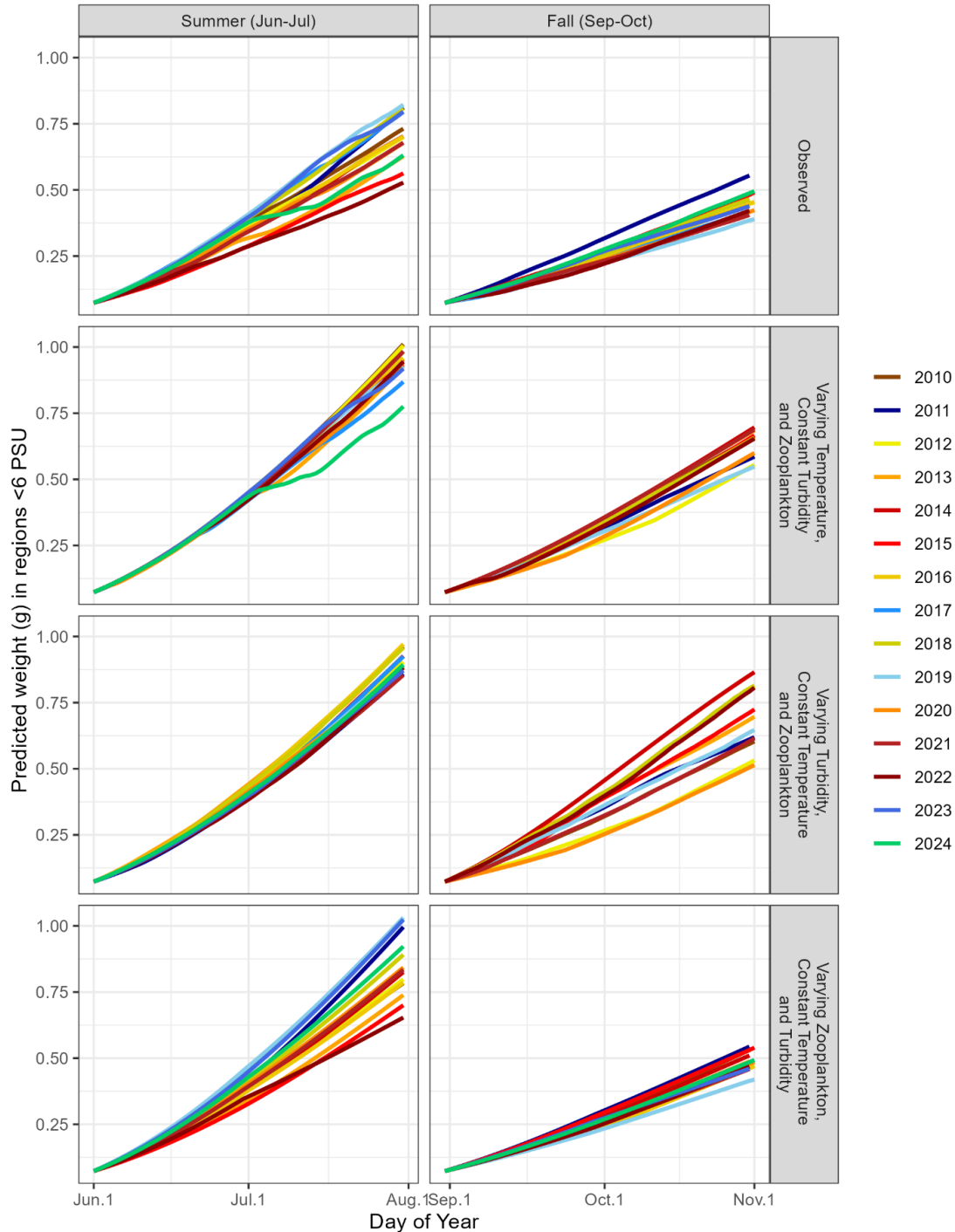


Figure 36. Linear regression of predicted change in weight of Delta smelt in each season versus the mean seasonal X2 location in regions that were less than 6 PSU.

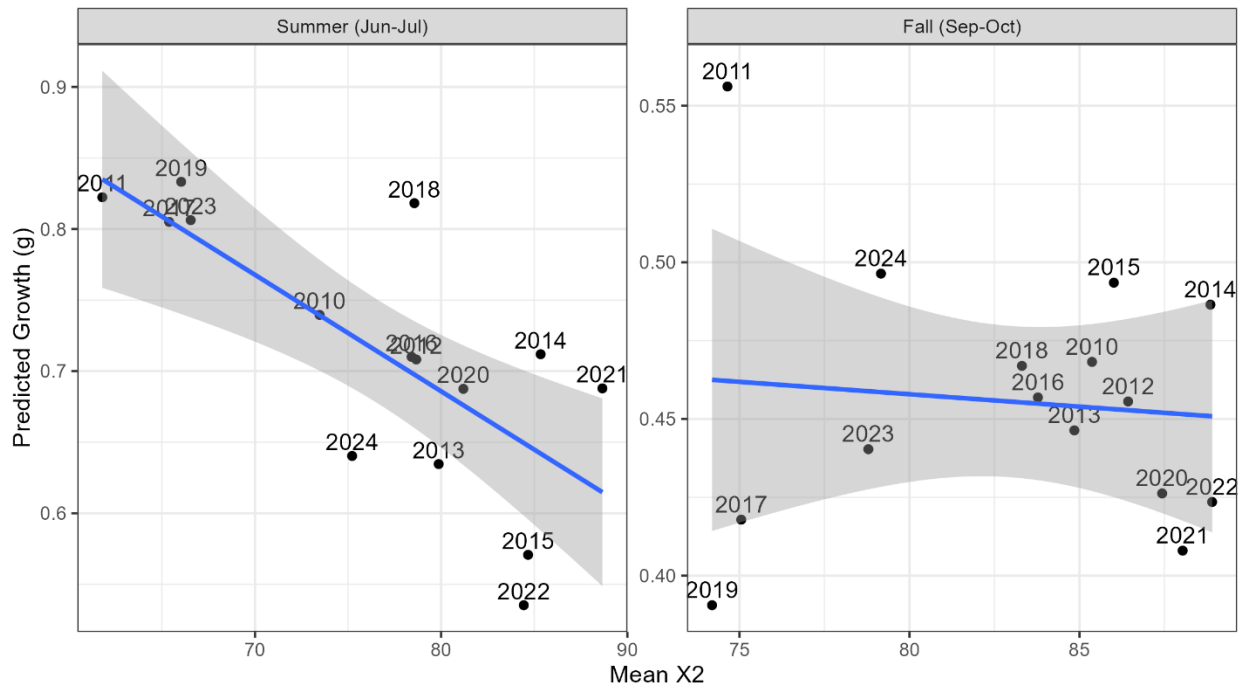


Figure 37. Proportion of the Delta smelt population surviving from June 1 through October 31 for each scenario based on a size-based mortality function, color coded by water year type.

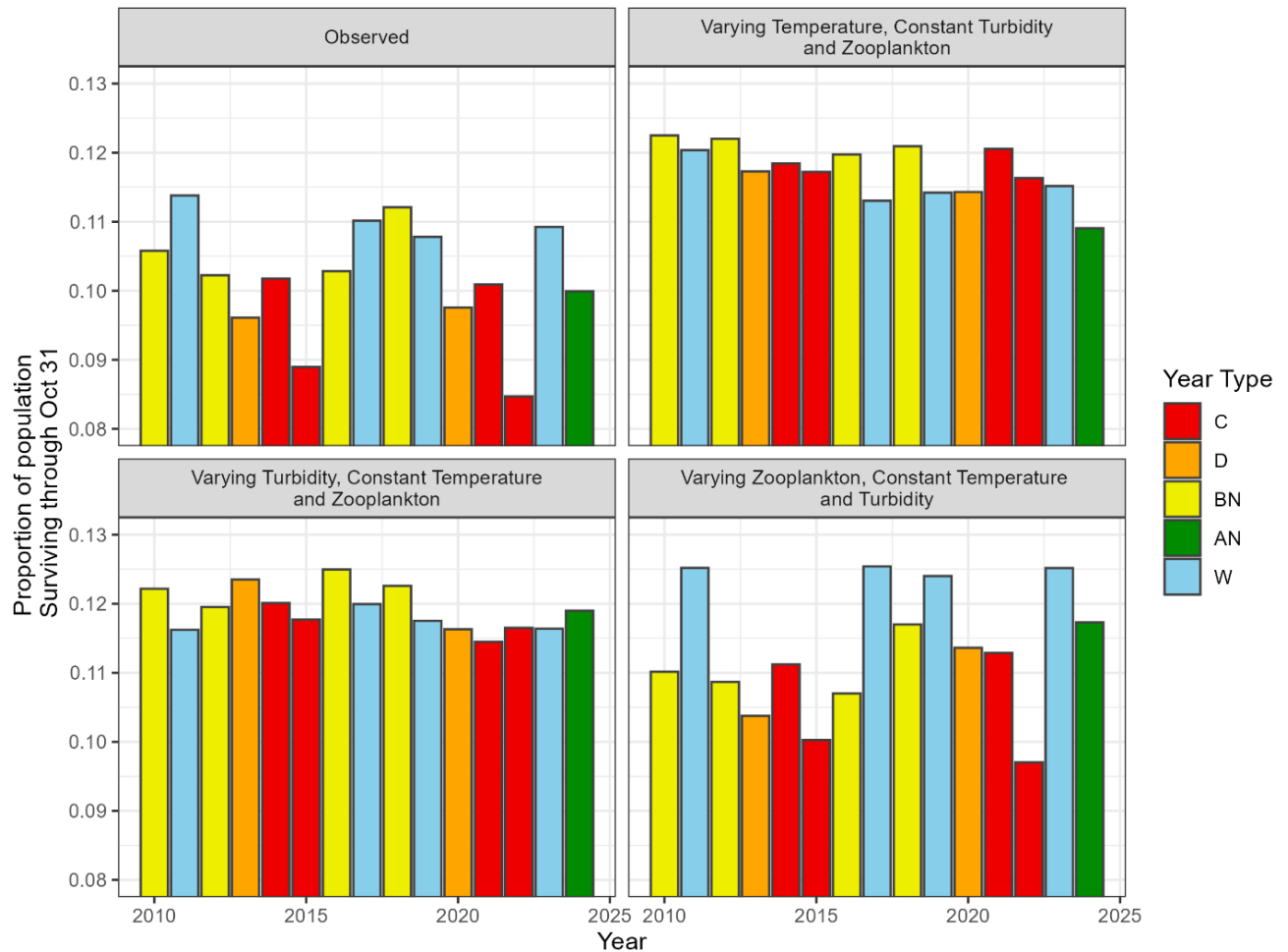


Table 16. Results of a linear regression of predicted Delta smelt growth versus X2, season, and the interaction of X2 and season. Adjusted R-squared 0.860, F-statistic 56.2 on 3 and 24 df, $p < 0.0001$.

Predictor	Estimate	SE	t-value	Pr(> t)
(Intercept: Summer)	1.331	0.137	9.667	<0.0001
Season:Fall	-0.803	0.271	-2.95	0.0065
X2	-0.0081	0.0018	-4.54	0.0001
Fall*X2	0.0074	0.0033	2.21	0.0363

Discussion

The low abundance of Delta smelt during the focal period (2011–2024) makes any statements about the effectiveness of SFHA difficult, but some correlations can be drawn between habitat conditions and smelt growth rates. The clearest conclusion we found was that 2011 was a particularly good year for Delta smelt, due to the high food supply, lower temperatures, and higher turbidity throughout the LSZ. Conditions in other Wet years with Fall X2 actions (2017, 2019, 2023, 2024) either did not provide the same habitat benefits, occurred when the population was already too low to detect benefits, or both. In general, more of the analyses show benefits of higher flows in summer when compared to fall.

Good Years and Bad Years

When looking over the past 15 years, the highest observed growth rates (where otolith data are available), highest juvenile Delta smelt condition factor in the LSZ, highest predicted growth rates over the summer and fall using bioenergetics, and highest population indices all occurred in 2011. The otolith data, in particular, showed much higher growth and survival in 2011 than any other year (Figure 29, Figure 37), though residual variation in growth rate among years is quite high, even when temperature and X2 values are taken into account (Figure 30). The otolith data does come with some caveats. In particular the low sample size in more recent years and uneven sample size across temperatures, values of X2, and times of year may introduce biases into the analysis that were not fully accounted for in our model. However, there was relatively high sample size in 2011 ($n = 39$), so we feel more confident about the high growth rates during this year than the results from 2019 ($n=6$). Furthermore, similar trends in potential growth rates were observed using the bioenergetic model.

Previous analyses identified cooler temperatures in 2011 (compared to 2017 or 2006) for high Delta smelt population growth in that year (FLOAT-MAST 2021). However, the bioenergetic modeling conducted in this report suggested that high food supply in the LSZ was equally as important as low temperatures, especially in the fall, since higher or lower zooplankton biomass produced a larger change in growth and higher survival than changing temperatures (Figure 32, Figure 35). Density of *Pseudodiaptomus* spp. was particularly high in 2011, with densities in Suisun Marsh, Suisun Bay, and Grizzly Bay higher than in the Sacramento River during June (Figure 19) and higher than average throughout the entire summer (Figure 19). While *Pseudodiaptomus* spp. abundance was also quite high in 2023 and 2024, high temperatures in both those years resulted in lower growth rates than would have been expected from high food availability, with the heat wave experienced in July of 2024 being particularly stressful (Figure 35). In contrast, summer temperatures in 2012 were relatively cool, resulting in one of the highest predicted growth rates when temperature was the only varying factor across years

(Figure 35). However, 2012 had relatively low *Pseudodiaptomus* spp. biomass (Figure 19), and had one of the lowest growth rates when zooplankton was the only factor varying across years (Figure 35).

Analysis of available habitat showed that 2011 had more days of appropriate salinity, temperature, and turbidity in Suisun Bay and Grizzly Bay than any other year analyzed here, as well as consistently high area of the LSZ (Figure 7, Figure 11). Cooler temperatures allowed the benefits of high *Pseudodiaptomus* spp. abundance to stretch further since Delta smelt require less food to grow in cooler temperatures. The subsequent actions all had warmer than normal summer and fall periods, with more days above 22°C (Figure 7). Therefore, the combination of high food, low temperatures, and high turbidity in the LSZ was unique to 2011 out of all the years analyzed. Because extensive monitoring of many of these metrics only began after 2011 (or even more recently in the case of expanded zooplankton surveys and Delta smelt health metrics), we do not know whether conditions like 2011 occurred more frequently and resulted in higher smelt growth rates prior to the population decline in the early 2000s. But the long-term declines in turbidity (Schoellhamer 2011; Stern et al. 2020), increases in water temperature (Bashevkin, Mahardja et al. 2022; Mahardja et al. 2025), and shifts in zooplankton populations (Bashevkin, Burdi et al. 2023; Merz et al. 2016) may mean that “good years” like 2011 will be increasingly hard to come by in the future. It may also mean that the effectiveness of high freshwater flow in providing benefits to Delta smelt may decrease as the climate warms and turbidity further declines, so ensuring as much flow as possible during the rare cool summers may become more important if smelt are going to survive the following warm and/or Dry years.

Summer Versus Fall

The Fall X2 action was predicated on the finding that CVP and SWP operations were implicated in decreasing the area of suitable habitat in fall (Feyrer et al. 2007), but the same decrease in habitat across years was not present in the summer (Nobriga et al. 2008). However, this early work did not conclusively tie habitat availability to individual Delta smelt growth or smelt population growth. More recent life cycle modeling has determined summer outflow to be more important than fall outflow in predicting Delta smelt population growth (Polansky et al. 2024), and our analyses support this conclusion.

Food supply is often limiting the growth of Delta smelt across the estuary, and high temperatures can exacerbate the impacts of food limitation because metabolic demands are higher at higher temperatures. While there was no clear trend toward lower age-adjusted growth rates in fall when compared to summer (Figure 33), bioenergetic simulations suggest growth rates will be lower in fall for fish of the same body size (Figure 31). The lower predicted growth in fall versus summer, despite more appropriate temperatures, may have been caused by lower abundance of zooplankton, particularly *Pseudodiaptomus* spp., in the fall.

Pseudodiaptomus spp. densities are often an order of magnitude lower in fall and are often an order of magnitude lower in the downstream regions of Suisun Bay and Suisun Marsh than in the lower Sacramento River (see [Smelt Food](#) section). During the summer, high flows transport enough copepods into Suisun Bay and Suisun Marsh to generate relatively high growth, but in the fall there may not be enough *Pseudodiaptomus* spp. in the upstream regions to result in a subsidy that would cause Suisun habitat to become preferable to upstream habitat, especially when temperatures upstream are no longer at stressful levels.

The otolith data further supports the role of temperature in driving the relationship between X2 and growth rate. Growth rates were lower at higher temperatures (Figure 30), which was also demonstrated by Lewis et al. (2021), and there was a significant correlation between lower growth rates and higher X2 in summer but not in fall (Figure 36). This may have been caused by the availability of lower temperature habitat in Suisun Bay in the summer of wetter years when other areas were too hot, whereas fall temperatures tend to be lower across the estuary (Pien et al. 2025).

Other information on fish health, including liver and gill lesions, was not analyzed in this report but could provide further insight into potential impacts of flow on Delta smelt. In particular, Teh et al. (2020) found that liver lesions were most prevalent in Cache Slough and Suisun Bay and least prevalent in Suisun Marsh and the Confluence. Surprisingly, they also found lesions to be relatively high in 2011 and relatively low in 2017, contrary to the other health and condition metrics in our analysis, which indicated 2011 was better than 2017. Teh et al. (2020) did not find any significant relationship between outflow or X2 and prevalence of liver lesions, but Stillway et al. (2024) found lower lesions in the Dry year of 2018 than the Wet years of 2017 and 2019. Many studies have found increased contaminants during high flows (Werner et al. 2010), most likely due to increased runoff from agricultural land during storms. Therefore, increased contaminants during high-flow periods may partially offset the habitat and food supply benefits of a summer or fall flow action.

Conclusions

- *Hypothesis:* Years with lower X2 in the summer and fall, and lower salinity at Belden’s Landing will have higher Delta smelt growth, health, and condition during the summer and fall.
 - *Supported*, with greater support for summer than for fall.
 - Lower X2 was also associated with higher growth rates based on otoliths in summer, but not in fall.
- *Hypothesis:* Years with lower X2 in the summer and fall, and lower salinity in Belden’s Landing, will increase the percentage of the population surviving to the end of the fall.

- *Partially supported.*
- Bioenergetic modeling of Delta smelt growth indicates that smelt would be expected to grow larger and have higher survival during the summer when X2 is low, but this relationship does not carry through to the fall.
- *Hypothesis:* The influence of X2 and salinity in Suisun Marsh on Delta smelt growth and survival will be greater in summer than in fall.
 - *Supported.*
 - Both bioenergetic modeling and otolith growth rate analysis showed that wetter summers supported higher growth, but wetter falls did not necessarily show increased growth.

All the analyses in this section support the Polansky et al. (2024) model, showing improved health and higher growth rates with increased flow in summer, but weaker or no impact of flow in fall. Therefore, when resources are limited, managers can prioritize management actions that move X2 downstream in the summer; this activates higher-quality habitat and provides temperature refuges to benefit the Delta smelt population, particularly for the larger, faster growing individuals who in turn have a disproportionate contribution to the reproductive success of the species.

Smelt Health—Wild Fish

Introduction

The SFHA augments freshwater outflow to move the 2-ppt isohaline (X2) downstream. This is hypothesized to provide Delta smelt with more and higher-quality habitats, as the low salinity zone moves into areas like Suisun Marsh and Suisun Bay (Feyrer et al. 2011; Brown et al. 2014), increasing foraging opportunities and limiting nutritional stress (Hammock et al. 2015; Hammock, Hartman et al. 2019). However, recent life cycle models suggest that the summer period may be a more significant bottleneck for the population than the fall (Smith et al. 2021; Polansky et al. 2024). This creates an important knowledge gap that is especially significant as natural resources available to benefit the species are limited.

To better understand this gap, this study leverages a ten-year dataset of individual Delta smelt bioassays to investigate environmental conditions associated with fish health across the summer and fall. Although previous studies have utilized this same dataset (McCormick et al. 2025; Hammock et al. 2022), this study introduces additional data streams by integrating environmental data from high-frequency data sondes across the SFE, uses a machine learning approach to explore running averages and lags, and explicitly models the allometric relationship between liver weight and body size by treating total weight as a covariate to isolate environmental effects on physiological condition. The primary objective is to better understand if environmental conditions in the summer or fall are more strongly correlated with improved Delta smelt health; the findings from this study can help managers better understand which period to allocate limited resources to best support the species.

Hypotheses

- Lower X2 in the summer and fall will be correlated with higher Delta smelt health during the summer and fall.
- The influence of X2 on Delta smelt health will be greater in summer than in fall.

Methods

Data Access

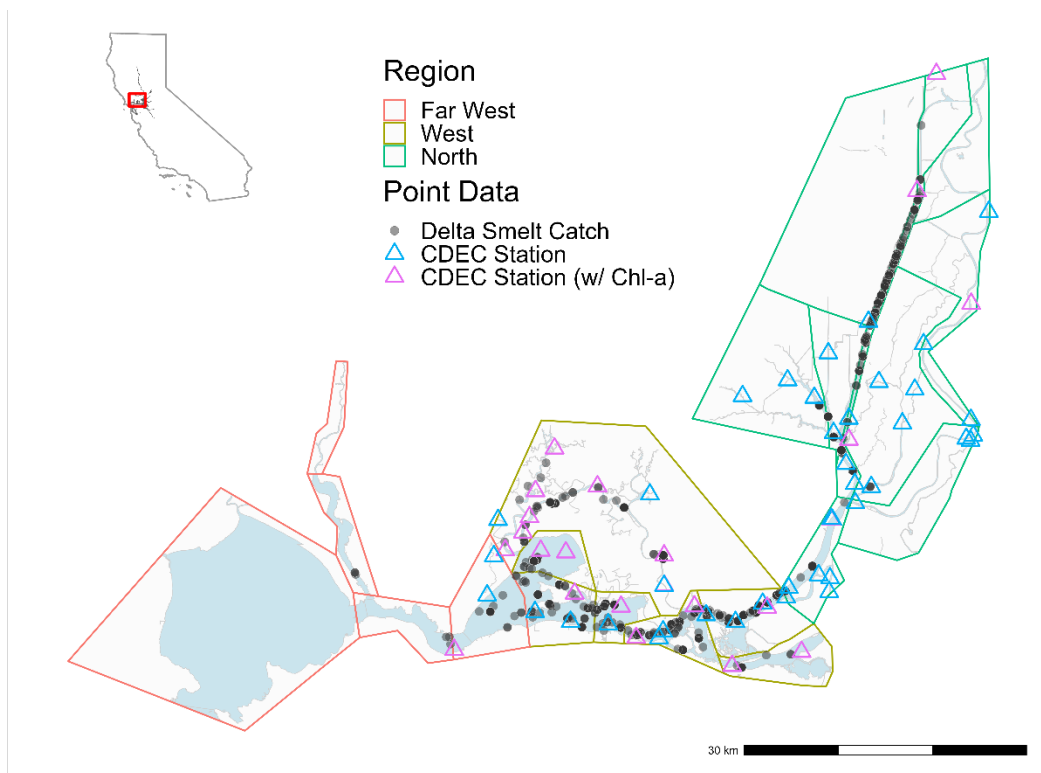
Delta Smelt Health and Survey Data

Delta smelt captured across four fish surveys—EDSM, SKT, STN, and FMWT—within the upper San Francisco Estuary from 2011–2021 (Figure 39) were sent to UC Davis for bioassays to develop a dataset of fish morphometric, nutritional status,

and health data. Various metrics were recorded, including fish length, weight, liver weight, and glycogen level (estimated histologically), and calculated, such as condition factor (CF) and hepatosomatic index (HSI). Environmental data at the time of capture were either provided with the health data or obtained directly from the original survey and merged with the health data. EDSM data were downloaded from the Environmental Data Initiative data repository (USFWS et al. 2025) and the SKT, STN, and FMWT data from CDFW’s FTP website ([filelib.wildlife.ca.gov - /Public/](https://filelib.wildlife.ca.gov/-/Public/)).

Not all fish data were kept. Following Hammock et al. (2021), all females from January to May were removed to avoid conflating reproductive investment with somatic growth. Additionally, two specific individuals were removed: one with an identified liver tumor (fish ID 1380) that would bias its health metric, and the single fish caught in 2021, which would cause instability in estimating the cohort-year random effect. The final dataset contained 1,704 Delta smelt records.

Figure 38. Delta smelt catch ($n = 1,704$) across the San Francisco Bay Delta Estuary used in the dataset. All fish were caught across three EDSM (Enhanced Delta Smelt Monitoring Program) regions (17 subregions), represented by colored polygons. Environmental monitoring CDEC stations are distributed throughout the area. Each unique CDEC station is shown by a colored triangle; blue triangles represent a CDEC station (each with multiple sensors), while purple triangles represent a station with a chlorophyll-a sensor, the least common sensor in the dataset (to showcase spatial coverage).



High-Frequency CDEC Environmental Data

In addition to the environmental data recorded by the surveys at the time of sampling, data from surrounding high-frequency water sondes from the California Data Exchange Center (CDEC - <https://cdec.water.ca.gov/>) network were added. Water temperature (sensor numbers 25, 146), turbidity (27, 221), specific conductivity (100, 102, 294), dissolved oxygen (61, 201, 202), and chlorophyll (28) data were downloaded from all CDEC stations within the study region (Figure 39), as defined by the subregions of the EDSM (available from the `deltamapr` package) (Bashevkin 2021). Turbidity data measured in NTU (27) and FNU (221) were pooled to maximize spatiotemporal resolution of the analysis, as they are considered numerically equivalent in water that is not strongly colored (Alexander et al. 2022). In total, data from 127, 127, 91, 65, and 50 CDEC gages were downloaded for water temperature, specific conductivity, turbidity, dissolved oxygen, and chlorophyll, respectively. When available, data from 2011-05-24 to 2021-08-21 (91 days before and 1 day after the span of the health dataset to accommodate subsequent running average and lag calculations) were downloaded at every gage; when not available, as much data as possible within the specified date range were downloaded. The highest frequency data available were prioritized for download, i.e., 15-minutes, hourly, then daily data.

All raw CDEC data were subjected to a robust outlier detection process in R (version 4.5.1) (R Core Team 2025) to correct for sensor malfunctions and misreadings. Water temperature and specific conductivity data were automatically removed as outlying if values met one of two conditions: 1) if values were beyond the expected range, i.e., $>45^{\circ}\text{C}$ for water temperature and $50,000\ \mu\text{Siemens/cm}$ for specific conductivity, or 2) if two or more outlier flags created from a suite of statistical tests were present. Outlier flags were assigned if a value was beyond a constant scaling factor (k) times its median absolute deviation using the `mad()` function in the “stats” package (version 4.5.1) (R Core Team 2025) from the median value of the distribution. Outlier flags were calculated using four methods: 1) the remainder component of a multi-seasonal time-series decomposition using the `mstl()` function from the “forecast” package (version 8.24.0) (Hyndman et al. 2025) with seasonal periods defined as daily, weekly, and quarterly, $k = 6$; 2) the daily median value, $k = 3$; 3) the difference between daily values 1, 2, and 3 days apart, $k = 6$; and 4) the number of consecutive repeating daily values, $k = 9$. This automated flagging system was followed by a visual inspection of the time-series data to remove remaining likely outliers, e.g., periods of obvious sensor malfunctions or implausible values in the context of surrounding values. Due to the lack of strong seasonality, data for turbidity, dissolved oxygen, and chlorophyll were subjected only to a visual inspection for outliers. Specifically, turbidity values greater than 700 NTU/FNU or less than 0 NTU/FNU, oxygen values greater than 18 mg/L or less than 0 mg/L, chlorophyll values less than 0 $\mu\text{g/L}$, and additional values were removed after visual determination per gage.

Cleaned sensor data were then aggregated spatially and temporally. First, high-frequency data were averaged to the daily time-step for each station. Second, data for stations within each EDSM subregion were averaged together to create a complete daily time series at the subregional level. For days at this subregional level without data, missing values were imputed using the values from all other subregions within the same, larger EDSM region on each given day. Finally, running daily averages (3-, 7-, 14-, and 30-day) and lags (0-, 3-, 7-, 14-, and 30-day) were calculated from this completed daily subregion-level dataset, resulting in 206 unique variables. All running averages were strictly right-aligned to ensure that no data from after the time of capture was included in the predictor calculations. This created a robust dataset with predictors that may better capture cumulative and delayed effects of environmental conditions on fish physiology, i.e., liver size. Indeed, laboratory studies have shown that the ratio of liver weight to body weight significantly reduces beginning at four days after starvation, as hepatic energy stores are rapidly mobilized (Hammock et al. 2020).

Dayflow Data

Daily average hydrology data were retrieved from Dayflow and related to the fish health data, specifically: Sacramento River flow at Freeport (SAC, cfs), San Joaquin River flow at Vernalis (SJR, cfs), net Delta outflow (OUT, cfs), and the position of the 2-ppt isohaline as measured from the Golden Gate Bridge (X2, km) (CDWR 2002).

Statistical Analysis

Analytical Overview

The analysis consists of four distinct, interlocking parts. First, we established a health metric with viable linear correlations to environmental conditions, using a mixed-effect framework to account for natural variations across years and regions. Second, multiple time-lags and running averages were tested across all environmental predictors to more accurately represent the delayed biological response to changing environmental conditions, resulting in 206 potential predictors. Due to the quantity and the highly correlated nature of these predictors, a least absolute shrinkage and selection operator (LASSO) model was used to maximize model fit and remove redundant predictor variables by shrinking their coefficients to zero. Third, with the pool of potential predictors now limited to a reasonable number, two-way interactions of the remaining predictors were tested using a stepwise linear mixed model. And finally, overall model fit was evaluated on a holdout dataset (unseen data before refitting the final model to all available data for interpretation). All analyses were executed using R (version 3.5.1) (R Core Team 2025).

Response Variable Definition

An initial exploration rejected using CF, HSI, and glycogen level as response variables representing proxies for Delta smelt health, due to a lack of strong correlation to environmental conditions (CF and HSI, Pearson's correlation) or the presence of too many missing data points (glycogen level). Raw liver weight similarly did not produce strong correlations to environmental conditions; however, the residuals of the allometric relationship between liver weight and body weight did produce stronger correlations to the environmental predictors. As such, the final modeling framework treats liver weight as the response variable and explicitly includes total weight as a covariate, in addition to potential environmental predictors. This accounts for allometry similar to HSI, liver weight standardized by total weight, which has historically been used as a proxy for fish nutritional health (Hammock et al. 2020; Hammock et al. 2022), but with two distinct advantages. First, this approach does not assume an isometric (1:1) relationship between liver weight and total weight to enable comparisons between individuals (Packard and Boardman 1988) and accounts for allometric growth common in teleost fishes (Killen et al. 2006; Post and Lee 1996). Second, this framework allows for the inclusion of interaction terms of body size with other predictors, such as water temperature, to increase potential model fit.

Several transformations were explored to linearize this allometric relationship, i.e., square root, log-log, log-square root, and Box-Cox. Although the Box-Cox transformation produced the highest Pearson's correlation linear model ($R^2 = 0.783$), the log-log transformation was chosen due to a similar model performance ($R^2 = 0.771$), its theoretical appropriateness for modeling allometric relationships (Clarke and Johnston 1999), and greater ease of interpretation.

Mixed-Effect Structure

To this base allometric model, several random-effect structures were explored, specifically, year, cohort year (calculated as June 1 being Day 1), and EDSM subregions. A mixed-effect framework is required as Delta smelt are an annual species (Moyle et al. 2016) and catches within the same year and region are not independent (Gelman and Hill 2007). We compared models with different random-effect structures using BIC, which supported using cohort year and EDSM subregions as random effects in the subsequent models.

We considered various fixed-effect predictor variables besides the allometric relationship to total weight to correlate environmental conditions and time of year with liver weight; these potential predictors were water temperature, turbidity, salinity, dissolved oxygen, chlorophyll, and day of the spawning year (June 1 as Day 1, cohort day). Various data transformations were explored, i.e., square root, log, and Box-Cox, for each predictor to better linearize their relationship to the response variable and to minimize the influence of extreme values.

The correlation between environmental predictors and body weight to liver weight was explored using two distinct but connected modeling steps: a LASSO model for variable selection and a linear mixed-effect model of the selected predictors. A LASSO model is a machine learning model that minimizes the sum of the squared residuals (maximizing model fit) and a penalty value based on the sum of the absolute values of the model coefficients, making it capable of shrinking predictor coefficients to zero to effectively perform automated variable selection (Tibshirani 2018). Variable selection allows the model to become more interpretable and potentially fit better (Kuhn 2008; Hastie et al. 2009). The linear mixed-effect model was chosen to account for the hierarchical structure of the data and to explore interactions between the chosen predictors (from the LASSO).

Variable Selection Using LASSO Regularization

Data were divided into an 80/20 data split, i.e., 80% reserved for model training and 20% held out for final model evaluation, using the `initial_split` function in the `rsample` package (version 1.3.1) (Frick et al. 2025). A stratified k-fold approach was used to train the LASSO model using cross-validation, a process that iteratively trains and validates the model on different assortments (folds) of the training data (Arlot and Celisse 2010).

Two specific techniques were used to better account for the hierarchical structure of the data and mimic the random-effect component of a mixed-effect model during the training of the LASSO model: 1) the cohort-year and subregion variables were converted into dummy variables, assigning each value as a binary predictor in the model; and 2) the total weight (representing the allometric relationship), cohort year, and subregion variables were treated as unpenalized predictors (`penalty.factor = 0`) to be present in every model iteration. All remaining potential predictors were scaled by centering to a mean of zero and standardizing to a standard deviation of 1. To prevent sampling bias (caused by varying fish catches across samples), the means and standard deviations were calculated from unique tows rather than individual fish records.

The LASSO model was trained using the `cv.glmnet` function from the `glmnet` package (version 4.1-10) (Friedman et al. 2010) with `alpha` set to 1. The training used a 5-fold cross-validation stratified on cohort year to achieve consistent proportions of cohort years across all folds, mirroring those in the full training data. A stratified k-fold strategy was used due to the differing numbers of samples across each cohort year and to prioritize returning a stable set of predictors. The training was evaluated on mean-squared error (MSE). The final model was determined at `lambda` within 1 standard error of the `lambda` value that resulted in the minimum MSE to maximize model fit while preserving parsimony and guarding against overfitting (`lambda.1se`).

Given the large number of potential fixed-effect predictors (206), two variable selection pathways were used to train the LASSO model. One process allowed all potential predictors to be selected for, while the other limited potential predictors to a list curated by expert opinions (10) from members of the DCG Science and Monitoring Working Group (Table 16). The results from this dual pathway were compared to allow for a more robust investigation of finding highly significant predictors, i.e., predictors chosen in both pathways.

For each pathway, one hundred instances of the LASSO model using unique starting seeds were trained. One hundred instances served to account for starting seed effect (where in the data the model begins training) and to enable an assessment of the stability of variable selection. Specifically, selected predictors across all instances were tallied to calculate a selection frequency. A comparison of the most frequently selected predictors from both selection pathways showed that five predictors were consistently selected for. Specifically, four predictors were selected by both pathways: total weight, turbidity, chlorophyll, and X2; the remaining predictor was water temperature, of which the pathway with access to all predictors chose the daily water temperature while the expert-solicited pathway, which did not have this variant as a choice, chose the 7-day running average water temperature (0 lag). Due to the similarities between the two pathways, predictors from the pathway with access to all predictors were chosen moving forward: total weight log (total_weight_log), water temperature (temperatureWater), 3-day running average turbidity 14 days prior (turbidityAvg3Lag14), log chlorophyll, and the 30-day running average X2 from 14 days prior (X2Avg30Lag14).

Table 17. Comparison of final predictors selected using LASSO between the expert-solicited vs. unconstrained pathways. “Expert Reasoning” describes the biological justification for including specific temporal structures. The expert-solicited pathway selected only from the listed predictors, while all predictors (206) were available for selection in the unconstrained pathway. Selection probability is the ratio of selection across the 100 models (i.e., 1.0 means the predictor was selected across all runs).

Variable	Units	Temporal Structure	Expert Reasoning	Selection Probability (Expert)	Selection Probability (Unconstrained)
Biometric: Total Weight (log)	g	Allometry		1.00	1.00
Hydrology: Isohaline Position (X2)	km	30-day Avg, 14-day Lag	Generalized habitat conditions	0.06	0.09
Water Quality: Chlorophyll (log)	µg/L	Instantaneous	Feeding conditions	0.07	0.09
Water Quality: Chlorophyll (log)	µg/L	14-day Avg, 7-day Lag	Feeding conditions	0.01	
Water Quality: Dissolved Oxygen	mg/L	3-day Avg, 3-day Lag			0.01
Water Quality: Dissolved Oxygen	mg/L	7-day Avg, 3-day Lag	Immediate stress exposure	0.01	
Water Quality: Dissolved Oxygen	mg/L	14-day Avg, 30-day Lag			0.04
Water Quality: Dissolved Oxygen	mg/L	30-day Avg, 30-day Lag			0.01
Water Quality: Turbidity	FNU/NTU	3-day Avg, 14-day Lag	Feeding conditions, potential fish movement	0.07	0.10
Water Quality: Turbidity	FNU/NTU	7-day Avg, 30-day Lag			0.01
Water Quality: Temperature	°C	Instantaneous			0.11
Water Quality: Temperature	°C	3-day Avg, 0-day Lag			0.05
Water Quality: Temperature	°C	7-day Avg, 0-day Lag	Fish movement	0.09	

Final Model Selection and Construction

Candidate predictors selected by the LASSO models were next subjected to a stepwise, forward and backward, selection process to arrive at a final mixed-effect linear model using the `lmer` function in the `lme4` package (version 1.1-37) (Bates et al. 2015). This selection step is discrete from the LASSO model in serving two purposes: 1) to further simplify the model to increase interpretability of the model; and 2) to test two-way interaction terms from a more limited pool of potential fixed effects.

Ideally, the forward and backward selection using the same pool of fixed-effect predictors converges to the same model; however, due to the instability associated with stepwise selection (Hastie et al. 2009), this was rarely the case, and we chose the selection with the higher evaluation metric. All stepwise, nested models were trained exclusively on the training data. Nested models were compared using a likelihood ratio test (Chi-squared test, `anova` function; version 4.5.1) (R Core Team 2025), with a p-value < 0.05 considered as a significant improvement. The BIC was also assessed with a difference greater than two providing strong support. All predictors of the trained model were assessed for significance using a Type-III ANOVA, i.e., assessing the unique contribution of a predictor with all other terms present, using the `Anova` function from the `performance` package (version 0.15.0) (Lüdtke et al. 2021). Multicollinearity was tested by calculating the Variance Inflation Factor (VIF) of all predictors. The final linear mixed-effect model was trained using Restricted Maximum Likelihood (REML).

Model Evaluation and Interpretation

The predictive performance of the final model was evaluated on the held-out testing dataset by calculating its marginal and conditional R^2 (Lüdtke et al. 2021) The final model was then retrained on the full dataset to produce final parameter estimates used for model interpretation and visualization of marginal effects.

Marginal effects of each fixed-effect predictor were analyzed using the `effects` R package (version 4.2-4) (Fox and Weisberg 2019). Specifically, the `Effect` function was used to calculate the marginal effect of a predictor on the response (liver weight) using the `'xlevels'` arguments. For predictors without interactions, this was done across 100 equidistant values; for predictors involved in an interaction, 100 equidistant values of the primary predictor were explored across 5 quantile values (0.05, 0.25, 0.5, 0.75, 0.95) of the secondary predictor. All predictor values were back-transformed (from their mean and standard deviation) and limited to the historical range observed in the dataset, e.g., water temperature was limited to a range of 7.1 to 24.76°C, to avoid extrapolation.

For any predictor involved in multiple two-way interactions, a systematic threshold analysis was used to better understand the complex relationship. A prediction grid was generated using 200 equidistant values across the observed ranges of each conditional covariate. The coordinates in this grid represent a range of potential scenarios, for each, a threshold value of the focal predictor was identified that would achieve a predicted response significantly higher than a reference baseline value. The baseline was defined as the focal predictor value associated with the poorest predicted response, e.g., the maximum observed value if the focal predictor was a stressor. A significant difference was defined as the lower 95% confidence limit of the scenario in question exceeding the upper 95% confidence interval of the baseline reference, i.e., non-overlapping confidence intervals.

Results

The final dataset contained 1,704 Delta smelt and 206 candidate predictors across 11 cohort years (2010–2020) and 17 EDSM subregions.

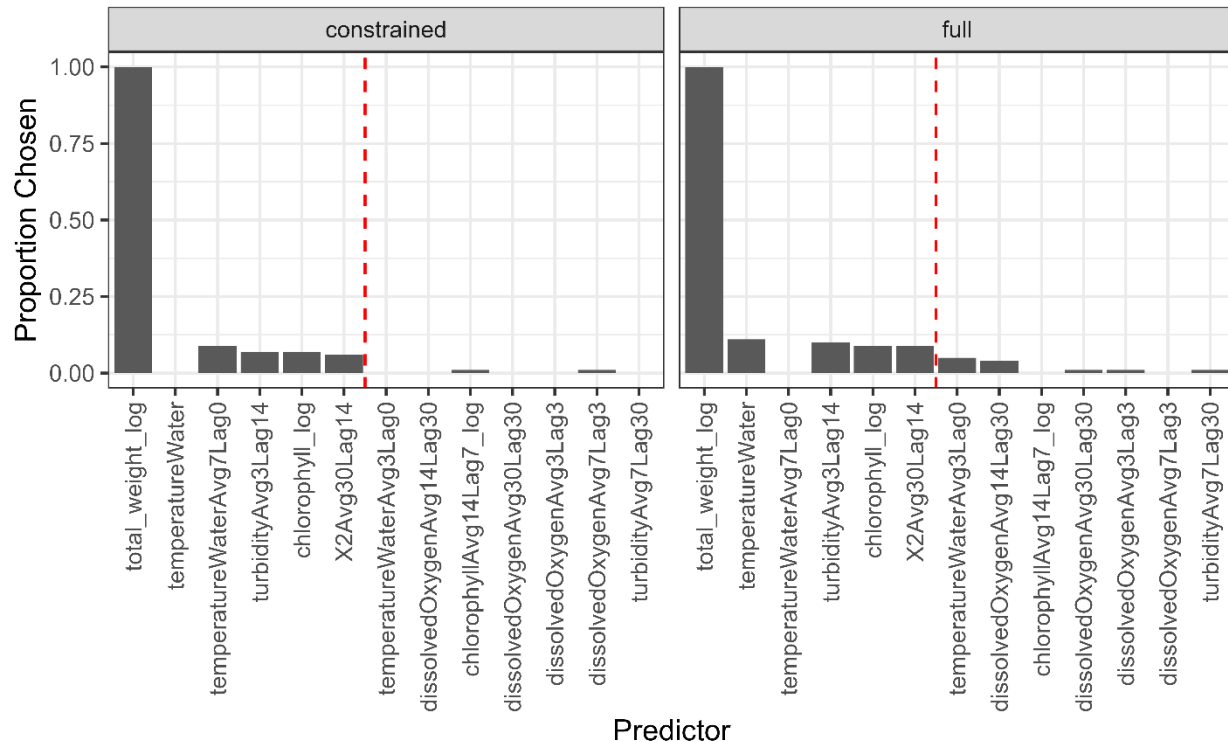
Allometric Relationship and Base Model

Modeling began with a baseline mixed-effect model describing the allometric relationship between log-transformed liver weight and log-transformed total weight across cohort years and EDSM subregions (the random effects). When evaluated on the held-out test data, this base model achieved a marginal R^2 (variance explained by the fixed effects) of 0.741 and a conditional R^2 (variance explained by fixed and random effects) of 0.7667.

Variable Selection and Final Model

A variable selection process using LASSO regularization produced four additional predictors for inclusion to the base allometry model. These were the most frequently chosen predictors across 100 iterations of the LASSO model with access to all (206) predictors; specifically, water temperature, the 3-day running average turbidity lagged 14 days, log-transformed chlorophyll level, and the running 30-day average X2 lagged 14 days were chosen in 9–11% of model runs, compared to just 5% or lower for all other predictors (Figure 39).

Figure 39. Variable selection frequency across 100 LASSO models for the constrained and full selection pathways (facets), ordered from the most to the least often selected across both pathways. The red line indicates the top candidate predictors used in subsequent model selection steps.



A backward selection of these predictors and log-transformed total weight, all two-way interactions, and the random effects of cohort year and subregion produced a final model:

$$\text{Liver weight (log)} \sim \text{Total weight (log)} + \text{X2Avg30Lag14} + \text{temperatureWater} + \text{turbidityAvg3Lag14} + \text{Total weight (log):X2Avg30Lag14} + \text{X2Avg30Lag14:temperatureWater} + (1 \mid \text{cohortYear}) + (1 \mid \text{SubRegion})$$

On the held-out test data, this final model achieved a nuanced improvement over the base allometry model, with a slightly lower marginal R^2 of 0.731 and a higher conditional R^2 of 0.777. This suggests that the environmental predictors explain more variance in the data, but only after accounting for year and subregion effects. This is intuitive, as environmental conditions likely cause deviations from the allometric relationship only during non-normal conditions. The random effects of cohort year and subregion accounted for 17.6% and 4.6% of the variance that was not explained by the fixed effects. A comparison of model fit on the training data using BIC strongly supported the inclusion of the environmental predictors, BIC = 890.13 vs 942.64, a difference of 52.51, justifying the added model complexity for the additional variance explained.

Further assessment of the predictors in the final model was supported by a Type-III ANOVA (`anova()`, argument type = "III"), which assesses the unique contribution of each main effect and interaction term when all other terms are present. The final model's fixed-effect parameter estimates, calculated using Restricted Maximum Likelihood (REML) on scaled predictors, show strong, non-zero effects for all retained environmental variables and their interactions (Table 18). Finally, a check for multicollinearity among all fixed-effect predictors showed low correlation with all VIF scores less than 2.2, well below the common threshold for concern ($VIF < 5$) (Lüdecke et al. 2021).

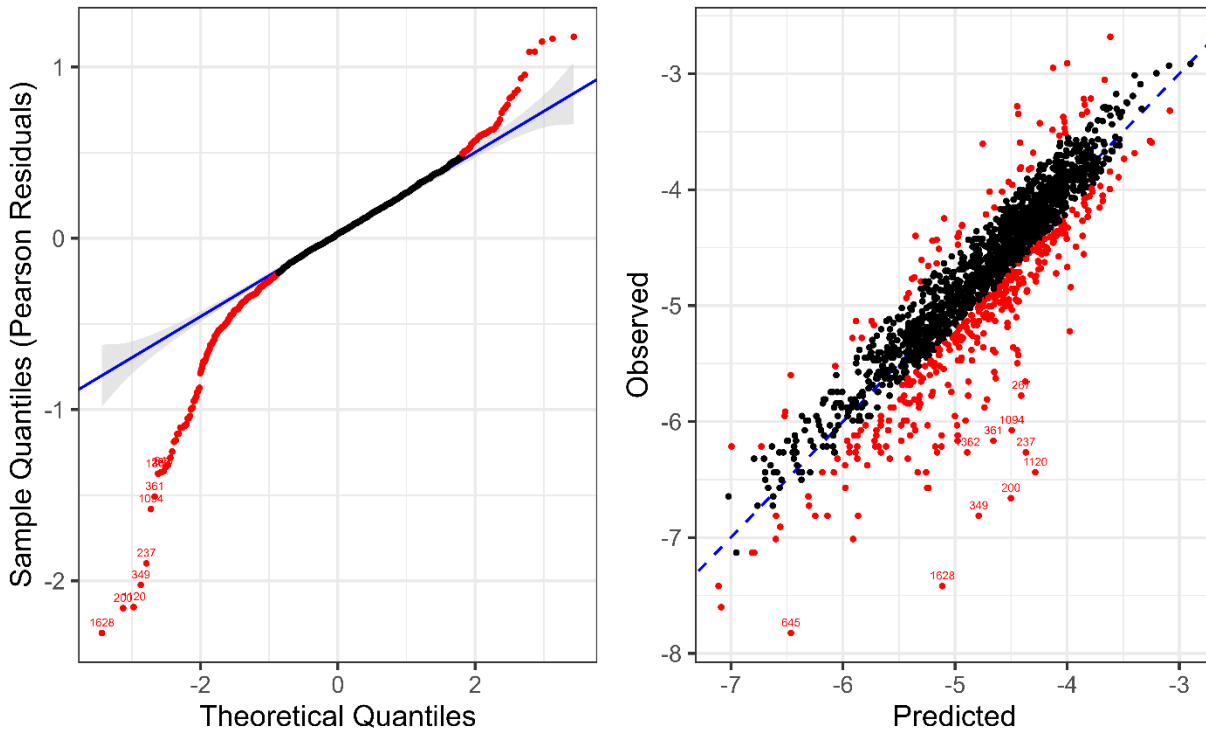
Table 18. Fixed-effect parameter estimates (β), standard error (SE), and t-value for the final linear mixed-effect model, fitted using Restricted Maximum Likelihood (REML). Predictors were scaled and centered. The model includes random intercepts for subregion ($\sigma^2 = 0.006$) and Cohort Year ($\sigma^2 = 0.024$).

Fixed Effect	Variable Code	Estimate (β)	Standard Error	t-value
Total Weight (log)	total_weight_log	0.738	0.012	59.244
Turbidity	turbidityAvg3Lag14	0.043	0.012	3.707
Water Temperature	temperatureWater	0.090	0.013	6.819
Isohaline Position (X2)	X2Avg30Lag14	-0.043	0.013	-3.328
Total Weight (log) \times X2	total_weight_log:X2Avg30Lag14	-0.059	0.015	-4.054
X2 \times Water Temperature	X2Avg30Lag14:temperatureWater	-0.086	0.016	-5.493

Model Limitation

A Q-Q plot of the model residuals showed non-normality with heavy tails (Figure 40, left panel). Plotting the observed vs. predicted showed that the majority and most extreme individuals are those with much smaller liver weights than would be expected based on their total weight, a breakdown of the main allometric relationship, far greater than what can be explained by the included environmental predictors (Figure 40, right panel). Despite these heavy tails, the large sample size ($n = 1704$) ensures that the parameter estimates and their confidence intervals remain statistically robust due to the Central Limit Theorem (Lumley et al., 2002) to allow inference of the mean population-level trends. However, the heavier lower tail exerts a downward pull on the regression estimates, which may slightly underestimate the liver weight of the typical fish (median, those not at the biological extremes), and prediction intervals will fail to accurately capture the true probability of encountering fish with these severe liver weights.

Figure 40. Left, a Quantile-quantile (Q-Q) plot of the Pearson residuals of the final model. Black circles represent residual values within the 95% confidence envelope, while red circles represent values beyond. Right, an observed vs predicted value plot. A 1:1 line is shown as a dashed blue line. Red circles correspond to those beyond the confidence envelope shown in the left Q-Q plot. The ten most extreme values are labeled with their row indices.



Model Interpretation

The marginal effect of each predictor and their interactions were explored to better understand the potential implications of the model. All predictors were back-transformed (from their scaled, centered, and standardized values) to aid interpretation. Turbidity did not interact with other fixed-effect predictors and indicates that larger liver weights are associated with more turbid conditions (Figure 41). The position of X2 interacts with total weight of the fish; specifically, larger liver weight is associated with lower X2 (farther downstream) but mostly for larger individuals (greater total weight) (Figure 42). Although there is a potential confounding with ripe females (vitellogenesis), this is unlikely as all females from January–May were removed at the onset of the analysis and the number of unsexed individuals is likely small compared to the overall sample size. At the average water temperature (15.5°C), this interaction is most pronounced at very low X2 levels, i.e., a steepening slope between predicted liver weight and total weight as X2 decreases with the greatest increase observed at the 5% quantile (60.15 km) (Figure 42). The position of X2 also interacts with water temperature, where larger

liver weight is expected when X2 is low at higher water temperatures (Figure 43) for the average-sized fish (1.4 g). Taken altogether, the model supports three general conditions that contribute to larger liver weight beyond the base allometry: 1) more turbid conditions, 2) the combination of low X2 and larger sized fish, and 3) the combination of low X2 and higher water temperature. This indicates that the benefits of higher outflow (which leads to lower X2) are most pronounced when water temperature is high, especially for larger fish.

Figure 41. The marginal effect of turbidity (the 3-day average turbidity from 14 days before capture) on predicted liver weight. A rug plot indicates the distribution of the turbidity data.

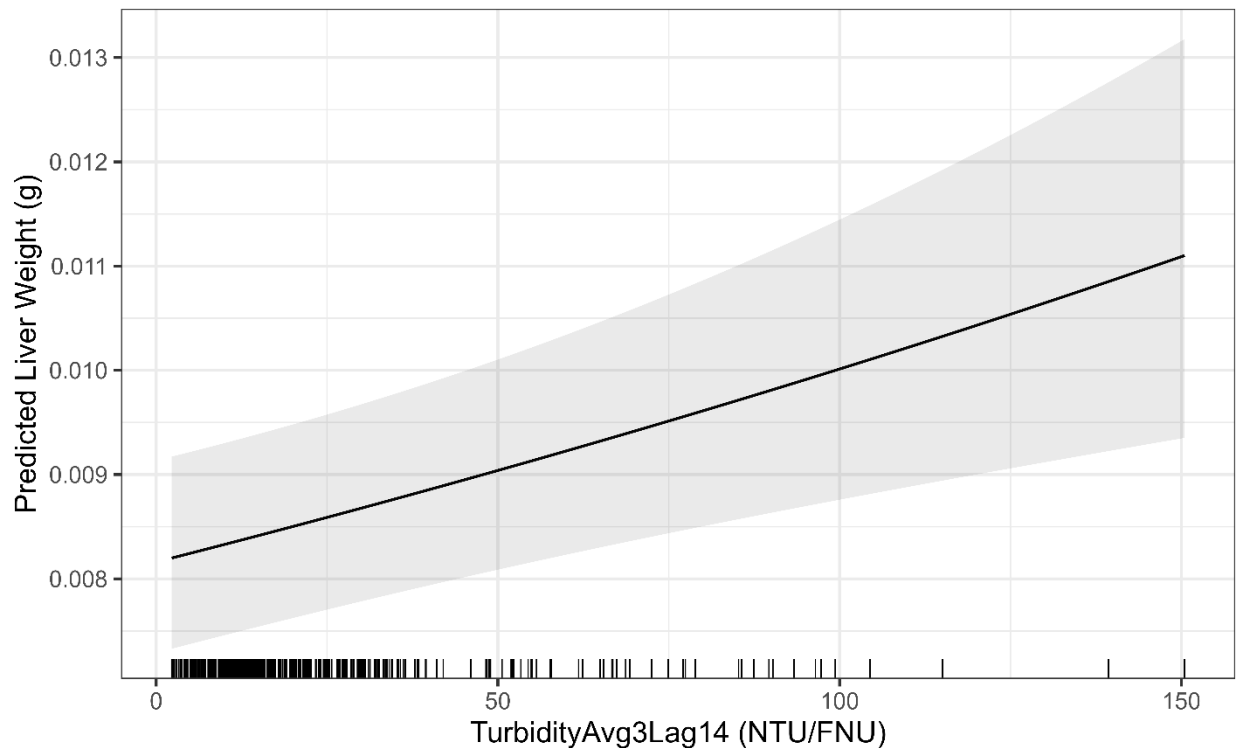


Figure 42. The marginal effect of X2 (the 30-day average X2 from 14 days before capture) on predicted liver weight conditional on total weight. Lines represent predictions at the 5th, 25th, 50th, 75th, and 95th percentiles of observed X2. The rug plot indicates the marginal distribution of the total weight. A convex hull of the joint observed total weight and X2 data space limits the predictions to avoid extrapolation beyond sampled conditions; therefore, weights visible in the rug plot may not have a corresponding prediction if their associated X2 value falls outside of the hull at the chosen quantiles.

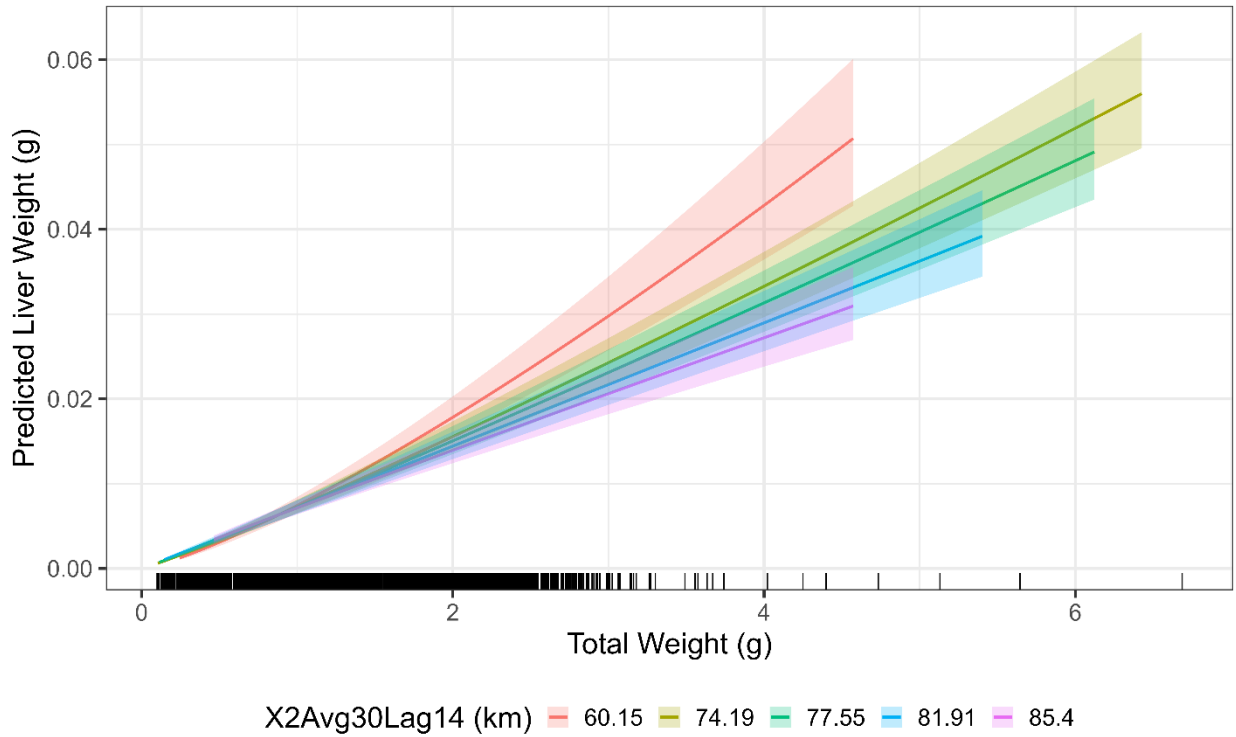
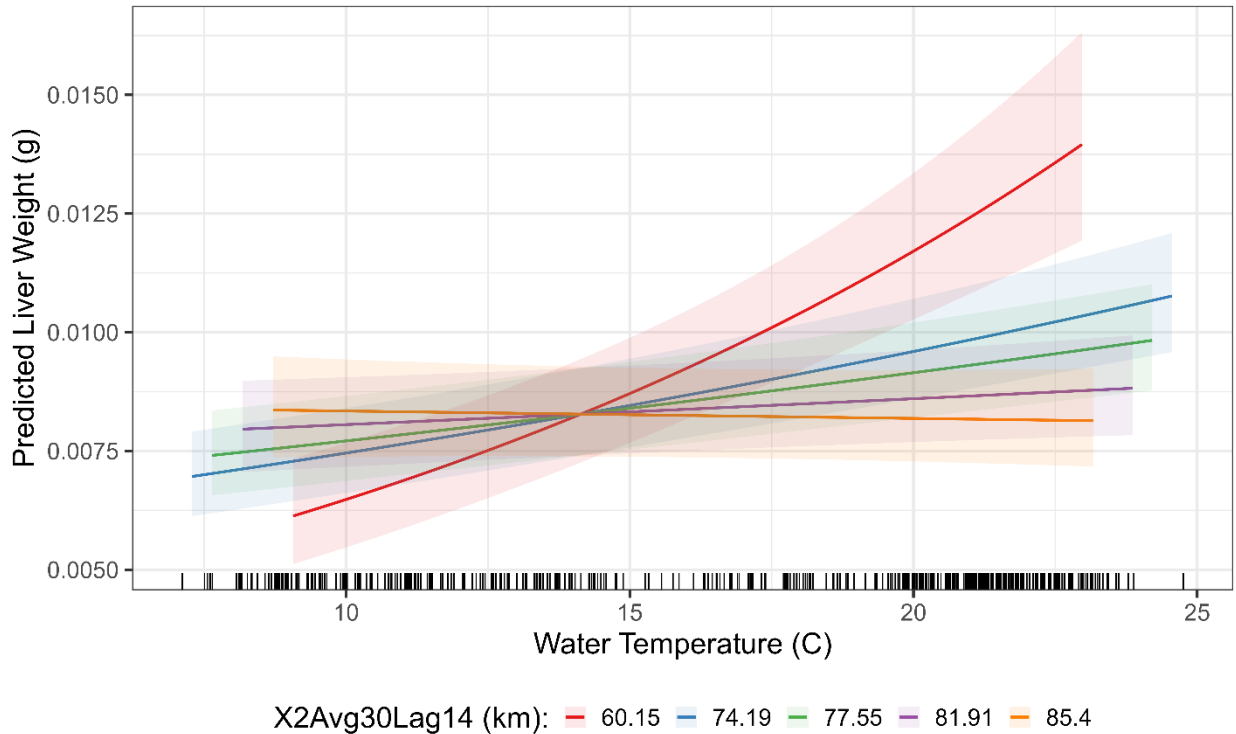


Figure 43. The marginal effect plot of X2 (the 30-day average X2 from 14 days before capture) on predicted liver weight conditional on water temperature. A rug plot indicates the distribution of the water temperature data. Lines represent predictions at the 5th, 25th, 50th, 75th, and 95th percentiles of observed X2. The rug plot indicates the marginal distribution of water temperature. A convex hull of the joint observed water temperature and X2 data space limits the predictions to avoid extrapolation beyond sampled conditions; therefore, water temperatures visible in the rug plot may not have a corresponding prediction if their associated X2 value falls outside of the hull at the chosen quantiles.

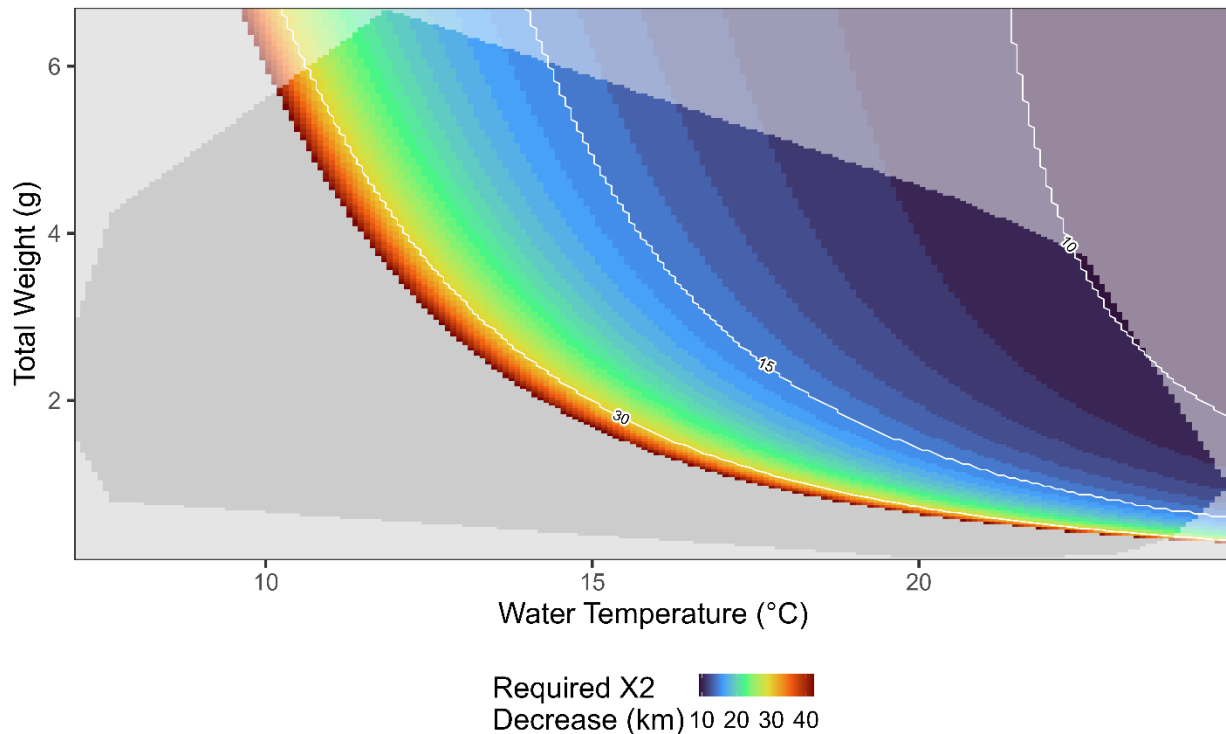


To further explore these interactions with X2, predicted liver weight was simulated across the range of water temperatures and total weights, while holding water turbidity at its average (Figure 44). The simulation identifies the maximum X2 threshold required to achieve a predicted liver weight significantly higher than a baseline X2 condition (X2 = 89.3 km, the highest observed value). A significant increase was defined as the lower 95% confidence limit exceeding the upper 95% confidence interval of the baseline (non-overlapping confidence intervals).

The results suggest that a significant increase in liver weight is most easily achieved when total weight and water temperatures are high; in these scenarios, benefits are detectable at higher X2 thresholds (e.g., 77–80 km). Conversely, for smaller fish in cooler water temperature, the reduction in X2 is likely to be larger (< 60 km) before a significant increase in predicted liver weight is detectable. The minimum and maximum X2 thresholds associated with a significant increase are 46.9 and 80.2 km, respectively. Scenarios that do not yield statistically different

increases occur when water temperature decreases below 9.6°C or the fish is smaller than 0.27 g (fish with fork lengths less than 23–36 mm in the dataset) (Figure 44).

Figure 44. Modeled interaction between water temperature, body size, and the predicted change in X2 necessary to see a significant increase in liver weight. The heatmap shows the decrease in X2 (km) required to achieve a significantly higher predicted liver weight than a baseline worst-case scenario (X2 = 89 km). Significance is defined as the first instance where the lower 95% confidence interval of the prediction exceeds the upper 95% confidence interval of the baseline scenario (non-overlapping intervals). Darker blue regions represent scenarios where significance is more quickly achieved (higher X2), while green, yellow, and red areas represent scenarios where a greater reduction in X2 is required. Gray regions represent scenarios where manipulation of X2 does not yield significant differences over baseline (overlapping intervals). A convex hull of the joint observed water temperature and total weight data space (not transparent colors) limits the predictions to avoid extrapolation beyond sampled conditions. Larger fish in warmer water temperatures show the fastest response to decreasing X2.



Discussion

The liver, an energy-storing organ, is expected to grow allometrically with body size and provides an indicator of an individual's short-term (4–5 days) energetic budget (Hammock et al. 2020). Deviations from this baseline relationship can serve as a proxy for physiological condition, reflecting how recent environmental drivers may influence the organism's health and survival prospects. This report leverages this logic to reveal that the condition of Delta smelt is significantly influenced by a complex interplay of various habitat and environmental factors. Specifically, model results reveal liver weight is largest when turbidity is high and when X2 is low, conditional on water temperature being high and especially pronounced for the larger fish in the population.

Nutritionally Healthier Fish in More Turbid Water

Model results predict larger liver weight in more turbid water (Figure 41). This relationship applies to Delta smelt across all lengths, as water turbidity does not interact with other model predictors. This finding is in line with previous studies that show increased feeding and decreased stress with higher turbidity. Laboratory experiments have shown that larval Delta smelt feed more successfully in murkier water, with the hypothesized mechanism being improved prey-detection contrast (Hasenbein et al. 2013). Evasion of predators is another hypothesized benefit of more turbid water, and one that extends beyond the larval stage (Hasenbein et al. 2016; Pasparakis et al. 2023; Ferrari et al. 2014). This is likely a product of visual predators being less able to detect prey items (Delta smelt) and the perceived reduction in predation risk by the prey, resulting in increased foraging opportunity, time, and success (Higham et al. 2015).

At the ecosystem scale in the SFE, turbidity spikes locally at the interface of salty and fresh water where hydrological forces mix sediment and food items, generally corresponding to the location of X2 (Kimmerer 2004). Delta smelt are commonly caught in the LSZ bracketing X2 (Merz et al. 2011; Sommer and Mejia 2013), highlighting the likely benefits of turbidity for the species. When the LSZ is centered over Suisun Bay and Suisun Marsh in the summer and fall, high winds over the shallow shoals of Grizzly Bay will also increase turbidity in the region (Bever et al. 2018). However, other metrics are also at play, and Hendrix et al. (2023) found that local salinity was more important than X2 location in determining Delta smelt occupancy.

Finally, during the winter and spring, high outflow events cause the transport of sediment downstream, resulting in higher turbidity during these events. Delta smelt have been documented to move with these flow events, using tidal action to facilitate upstream movement (Bennett and Burau 2015) and to take advantage of decreased predation risk associated with faster water flows and more turbid conditions (Sommer et al. 2011). Previous life cycle models have also suggested

that higher water turbidity is beneficial across all Delta smelt life stages (Smith et al. 2021; Polansky et al. 2024).

Nutritionally Healthier Fish in Low X2 When Water Temperature is High

Larger liver weights correlate to lower X2 but are strongly conditional on water temperature. For the average-sized fish across our study (total weight = 1.4 g) in the average water turbidity (19.57), predicted liver weight increases as X2 decreases and becomes especially significant when water temperature is high (Figure 43).

Lower X2 allows greater access to higher-quality downstream habitats that can offset the increased metabolic cost associated with higher water temperature. As X2 decreases below 74 km, the influx of freshwater creates low salinity habitat in Suisun Marsh and Suisun and Grizzly Bays (Feyrer et al. 2011; Brown et al. 2014). These areas contain an abundance of shallow habitat that Delta smelt prefer (Hobbs et al. 2006; Kimmerer et al. 2013) and are structurally more complex (Brown et al. 2014; Bever et al. 2016) and cooler than upstream regions (Wagner et al. 2011; Huntsman et al. 2024), providing both indirect and direct access to temperature refugia for the species. These areas also benefit from a subsidy of zooplankton from upstream regions as a function of flow (Kimmerer, Ignoffo et al. 2018; Kimmerer, Gross et al. 2018) at a rate that outpaces the grazing pressure from overbite clams (*Potamocorbula amurensis*) (Kimmerer and Thompson 2014), increasing the potential food supply for the species. Indeed, Delta smelt historically caught in Suisun Marsh exhibit higher stomach fullness and condition factor than in other regions throughout the Delta (Hammock et al. 2015; Hammock et al. 2022); and Suisun Marsh, Suisun Bay, and Grizzly Bay are historically areas with the highest Delta smelt catches (Bever et al. 2016), though Suisun Bay fish have lower stomach fullness than Suisun Marsh (Hammock et al. 2015; Hammock et al. 2022).

The conditional nature of these benefits with higher water temperatures likely reflects the thermal tolerance limits of the species. In the wild, Delta smelt are caught between 7°C and 25°C (Sommer and Mejia 2013), with most individuals caught under 20°C (Bennett 2005). Laboratory studies have shown that wild Delta smelt can tolerate water temperature up to 25°C but begin to exhibit signs of physiological stress, changes in gene expression, and changes in behavior as low as 20°C (Jeffries et al. 2016; Davis et al. 2019) and experience acute mortality beyond 25°C (Swanson et al. 2000; Komoroske et al. 2014). Additionally, absolute resting metabolic rate, i.e., the energy required simply for maintenance, increases dramatically with increasing water temperature in fish (Clarke and Johnston 1999). Therefore, below a critical threshold, such as 20°C, the marginal effect of decreasing X2 is less significant as Delta smelt are not exposed to conditions that are physiologically stressful. Above this threshold, predicted liver weight becomes more sensitive to decreasing X2 (Figure 43, Figure 44) as energetic demand

increases rapidly and individuals are forced to decrease their metabolic demand (by seeking temperature refuges) and/or increase their energy budget (increased feeding). However, it is unclear if an increase in energy storage can sufficiently offset the physiological costs for Delta smelt in warmer conditions (Jeffries et al. 2016; Davis et al. 2019).

Nutritionally Healthier Fish in Low X2 Are More Important for Larger Individuals

Figure 42 Model results show a size-dependent effect of X2 on predicted liver weight. At the average water temperature (15.5°C) and turbidity, liver weight is predicted to increase as X2 decreases, especially pronounced for larger individuals (Figure 41). This conditional relationship is likely due to larger individuals being physically and physiologically better equipped to exploit greater feeding conditions associated with the activation of higher-quality habitats in lower X2 conditions.

The lack of significant differences in liver weights at the smallest sizes regardless of X2 (Figure 43) may be, in part, explained by the physiological constraints and evolutionary trade-offs of early development. During the larval stage, fish exhibit high mass-specific metabolic rates driven by respiratory surface area constraints and the demands of rapid organogenesis (Post and Lee 1996). This may result in a period where small fish must allocate almost all of their energy intake to immediate maintenance and structural development, leaving little surplus for energy storage in the liver, even under favorable environmental conditions (Post and Lee 1996). As fish transition out of this stage to become juveniles, around 25 mm for Delta smelt (Bennett 2005), specific traits of the individuals become critical in determining individual mortality and success, such as size and somatic growth rate (Sogard 1997). Size becomes increasingly important from this stage on as fish are gape-limited, capable of feeding only on items that can physically fit in their mouths and outgrowing the gape limits of their predators (Sogard 1997; Bennett 2005).

This developmental progression of increasing foraging ability is coupled with increases in overall metabolic activities. As fish get larger, their absolute resting metabolic rate increases substantially (Clarke and Johnston 1999; Sogard 1997; Hammock et al. 2017), requiring more energy to be dedicated to maintenance; however, this is coupled with increased metabolic efficiency (Post and Lee 1996) as larger individuals have larger overall energy reserves available (Killen et al. 2006) to dedicate to maintenance. Larger fish are also more capable predators, possessing larger gapes (Sogard 1997; Bennet 2005) and being more efficient and capable swimmers (Schmidt-Nielsen 1972; Post and Lee 1996; Swanson et al. 1998; Killen et al. 2006). These characteristics all favor larger individuals in the population when habitat conditions are improved, such as from low X2 conditions allowing access to higher-quality habitats through lowered salinity and increasing food transport to the low salinity zone. Larger individuals can not only better exploit these conditions but can also dedicate more resources to somatic growth. This

creates a positive feedback loop: larger individuals can more effectively exploit favorable habitat conditions to grow even larger, which in turn further increases their efficiency at exploiting those resources. Larger individuals may also contribute more to the population than smaller individuals (Rose et al. 2013a; Damon et al. 2016), so benefits of increased habitat to the individual may lead to population-level benefits.

Nutritionally Healthiest Fish in Low X2 When Temperature is High for the Largest Individuals

The simultaneous interactions of X2 with total weight and water temperature reveal that lower X2 (higher outflow) provides the greatest discernable benefits to the largest individuals experiencing the hottest conditions (Figure 44). This cumulative relationship likely reflects a supply-and-demand process revolving around minimizing metabolic costs, maximizing foraging capabilities, and fueling high metabolic rates.

On the demand side, Delta smelt incur higher metabolic costs when either water temperature or body size increases. Specifically, absolute resting metabolic cost increases in either condition, and signs of physiological stress, which may be inferred from changes in gene expression, appear as low as 20°C (Jeffries et al. 2016). Below this threshold, however, somatic growth is expected to increase with water temperature in ectothermic fishes, up to a maximum growth rate (Lewis et al. 2021). Therefore, the largest individuals in the warmest water operate closer to the species' upper physiological limits, but they are also capable of rapid somatic growth under favorable habitat conditions.

On the supply side, low X2 conditions are associated with more favorable habitat conditions for the species. Specifically, higher outflow activates higher-quality downstream habitats for Delta smelt, increasing access to temperature refugia and zooplankton subsidies. Large individuals may be the best equipped to exploit these conditions, possessing larger gapes, more efficient swimming capacity, and potentially higher aerobic scope to dedicate to somatic growth.

These insights, therefore, showcase a convergence of conditions that predict the largest liver weights: large fish in warm water possess the highest potential for growth, but this can only be realized under favorable habitat conditions (e.g., low X2) that minimize metabolic costs and provide sufficient energy resources to support high energy expenditure associated with rapid growth. Figure 46 highlights this dynamic, as large fish in warm water are highly sensitive to X2 manipulations, requiring less drastic decreases in X2 to show significant improvement in nutritional health (liver weight) compared to small fish.

However, using liver weight as the sole proxy for habitat benefits requires a critical caveat regarding ontogeny. As previously discussed, small fish prioritize allocating

energy intake to somatic growth, to outgrow gape-limited predators, rather than increasing energy reserves. As such, small fish may benefit from more moderate reductions in X2 than what is depicted in Figure 44, which represents environmental conditions correlated to a significant increase in liver weight, a potential secondary objective during the earliest life stages.

Limitations and Future Efforts

While the model successfully explains a significant portion of liver weight variance, there remain limitations. The non-normal distribution of the residuals, specifically the heavy lower tail driven mainly by individuals with smaller-than-expected liver weights given their body weight, indicates a breakdown of the allometric relationship beyond the scope of the environmental predictors specified in the model. This may be due to our predictor variables being defined on the subregional scale, making them more appropriate for describing overall habitat quality for the typical fish rather than localized conditions, acute stressors, or individual fish health that might drive severe liver depletion. Additionally, while larger liver weight is typically an indicator of nutritional status, other factors can cause enlarged livers, including contaminants, tumors, or fat deposits (Hinton et al. 2008). These unexplained variances may be remedied by adding additional, more localized predictors, such as disease, parasite loads, contaminant exposure, or alternative specifications of the included predictors, such as the use of zooplankton counts as a more direct measure of food abundance.

Another limitation of the model is the assumption of monotonic relationships for environmental predictors like temperature and X2. Bioenergetic principles dictate that Delta smelt health must eventually decline at their upper thermal tolerance, just as the physical area of suitable low salinity habitat does not consistently increase as X2 moves further downstream (Kimmerer et al. 2013). However, our dataset is constrained to conditions where Delta smelt were successfully captured and naturally reflects the environmental realities of the typical fish within its occupied range. Indeed, our linear approximations fit the bulk of the observed data well, and poorly-predicted individuals are scattered broadly across the prediction range rather than being tightly clumped. Therefore, model interpretations should be limited to describing environmental conditions for the typical fish and should not be extrapolated beyond historical ranges and to more localized (i.e., below subregional level) scales. Finally, the model is entirely correlational, and although mechanisms are hypothesized here, targeted experimental studies will be needed to establish causation.

Conclusions

- *Hypothesis:* Lower X2 in the summer and fall will be correlated with higher Delta smelt health during the summer and fall.
 - *Partially supported with health defined as predicted liver weight.*
 - Lower X2 is correlated to higher predicted liver weight but is highly conditional on water temperature and fish size, most beneficial when water temperature is high and for larger individuals.
- *Hypothesis:* The influence of X2 on Delta smelt health will be greater in summer than in fall.
 - *Partially supported.*
 - The effect of X2 was greater at higher temperatures, which are generally seen in the summer, though high temperatures in fall may have the same results.

Smelt Growth and Survival—Enclosures

Introduction

In response to Delta smelt declines, a conservation hatchery maintaining a genetically managed refuge population of Delta smelt was created in 2008 (the UC Davis Fish Conservation and Culture Laboratory or “FCCL”), and a fall outflow action (known as Fall X2) was included as a requirement in Biological Opinions (BiOps) for the long-term operations of the CVP and SWP (USFWS 2008).

In 2019 and 2020, Project permits were updated to include both a Fall X2 action and operations of the Suisun Marsh Salinity Control Gates (SMSCG). Both the SMSCG and Fall X2 actions are aimed at expanding low salinity available for Delta smelt. The long-standing hypotheses behind summer–fall actions are that expanding the area of low salinity zone habitat (< 6 PSU) allows access to habitat with higher turbidity, food, and potentially cooler temperatures, all of which will support Delta smelt growth, survival, and recruitment (Sommer et al. 2020; FLOAT-MAST 2021). During recent actions, positive habitat outcomes such as expansion of lower salinity habitat and increased zooplankton abundance have been observed; however, detections of Delta smelt have been limited, making it challenging to evaluate the efficacy of summer–fall actions.

When species detections are rare, it becomes tremendously challenging to understand if and how managed actions provide meaningful benefits (Diefenderfer et al. 2021). Many of the actions currently managed for Delta smelt are based on knowledge and models of the historical population. However, recent evidence suggests that the wild Delta smelt population is no longer self-sustaining, and it is highly likely that all detections in recent years have at least partial hatchery ancestry (USFWS 2025). In an attempt to better inform Delta smelt responses to changes in habitat conditions, DWR began testing the use of Delta smelt enclosures in 2018. Enclosures in the natural environment are a tool used by fisheries managers and scientists to better understand species responses to wild conditions while still maintaining enough control to allow performance to be measured. Use of enclosures as a bioassay of fish responses has been used with other species of concern including rearing conditions for juvenile Chinook salmon in Suisun Marsh (Aha et al. 2021) and juvenile Coho salmon in the Shasta River basin (Lusardi et al. 2020), as well as endangered suckers and boneytail in the rivers and lakes of Utah (Belk et al. 2008; Christopherson et al. 2004).

DWR’s Delta smelt enclosure program was specifically designed to test responses and survival of cultured Delta smelt outside of the hatchery environment, and exposed fish to different habitat conditions across seasons and locations in the estuary. Three enclosure studies have been conducted during the summer–fall period, each holding cultured fish at the same sites near Belden’s Landing in Suisun

Marsh and near Rio Vista in the lower Sacramento River. These studies were conducted in 2019, 2023, and 2024 and assessed survival, fish health and diet, and localized environmental conditions. Detailed descriptions of enclosure design and each individual study can be found in the public dataset (Tempel et al. 2025) and in study-specific manuscripts (Baerwald et al. 2023; Davis et al. 2024; Tempel et al., in review). Enclosures allow for Delta smelt to experience a semi-wild environment, including ambient water quality conditions and access to wild food, without having to avoid predation.

Although enclosure studies in 2019, 2023 and 2024 tested various study questions, all were similarly focused on quantifying Delta smelt responses with relatively consistent sites in summer and fall periods using similar performance metrics. Enclosure studies in 2023 and 2024 were not intended to directly test efficacy of the summer–fall management actions but rather inform how Delta smelt survive and respond physiologically to a different set of habitat conditions in Suisun Marsh and the lower Sacramento River. Lower salinity habitat in Suisun Marsh is an objective of summer–fall actions to expand the area of better habitat for Delta smelt aligning fresher water with higher turbidity, food availability, and potentially cooler water temperatures westward.

Hypotheses

Our overall hypothesis is that lower salinity at Belden’s Landing will mean Delta smelt in Suisun Marsh will have higher smelt growth, health, and condition in the summer and fall when compared to Delta smelt in the Sacramento River. We have broken this hypothesis down into several sub-hypotheses:

- Suisun Marsh will have higher turbidity, cooler temperatures, and higher prey availability when compared to the Sacramento River.
- Delta smelt in enclosures at Belden’s Landing will have higher survival than smelt in enclosures at Rio Vista.
- Delta smelt in enclosures at Belden’s Landing will have higher condition factor, liver glycogen, and critical thermal maximum (indicators of health) than smelt at Rio Vista.
- Differences in health and survival will be driven by differences in water temperature, turbidity, prey availability, and water velocity.
- Enclosures will provide a realistic setting in which to test differences in habitat suitability for Delta smelt.

To test these hypotheses, we used data from the 2019, 2023, and 2024 enclosure studies that were consistent in methodologies and sites and analyzed the effect of year and site to help interpret potential Delta smelt responses to management actions. However, caution is warranted in interpreting outcomes due to differences

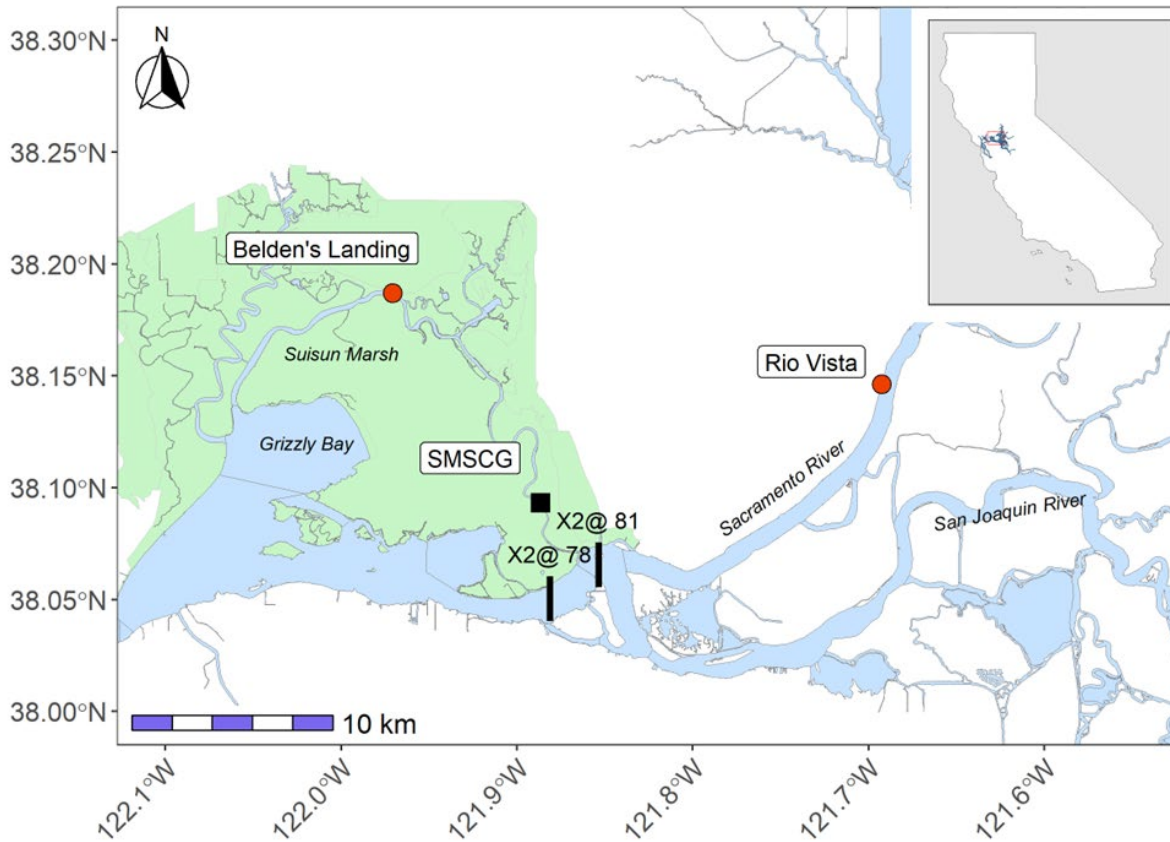
between study timing and water years and potential enclosure effects that likely affected Delta smelt behavior.

Methods

Enclosure Deployments

We combined data from Delta smelt enclosure experiments conducted in 2019 (Davis et al. 2024), 2023 (Tempel et al., in review), and 2024 (presented here). Each of these deployment years included slightly different study questions, hypotheses, and methodologies; however, the relatively consistent timing and deployment sites allowed us to test hypotheses about Delta smelt habitat in summer and fall. Deployments in each of the three years occurred at Belden's Landing in Suisun Marsh and Rio Vista on the Lower Sacramento River (Figure 45), each with respective controls held in a hatchery environment at the UC Davis FCCL.

Figure 45. Map of enclosure locations (red points) at Belden's Landing in Suisun Marsh and Rio Vista in the Lower Sacramento River. The location of the Suisun Marsh Salinity Control Gates (SMSCG) and examples of Fall X2 targets (in kilometers) are shown. Image reproduced from Tempel et al. (in review).



In Suisun Marsh, Delta smelt were held in Montezuma Slough, just upstream of the Belden’s Landing boat launch (Figure 45). This site was within the area where salinity is lowered during a SMSCG action, and in 2023 and 2024 Delta smelt were in the enclosures during the action period (Table 19). In the Sacramento River, Delta smelt were held near the city of Rio Vista (Figure 45). This site was outside of the area where salinity is lowered during a SMSCG action and was selected to provide a good reference comparison. Fish were held at these sites for four- (2019 and 2024) or six- (2023) week periods. During the 2024 study, we experienced repeated failure of the anchoring system in Montezuma Slough, causing the enclosures to unexpectedly drift and tangle. Survival remained high following the study; however, this may have had an unaccounted for effect on the 2024 results presented below.

Table 19. Delta smelt enclosures deployments during applicable summer–fall management periods. Summer–fall actions include operations of the Suisun Marsh Salinity Control Gates (SMSCG) and Fall X2 (the position of the 2PSU isohaline in km). BDL is Belden’s Landing in Suisun Marsh, RVB is Rio Vista Bridge on the Sacramento River, and FCCL is the Fish Conservation and Culture Laboratory control fish. DPH is estimated days post hatch.

Year	2019	2023	2024
Water Year Type	Wet	Wet	Above Normal
Summer–Fall Action: SMSCG	No operations	Aug. 15–Oct 17	July 1–Aug. 30, Sep. 6–Sep. 30
Summer–Fall Action: X2 (km)	Average 74.6 (Sep.) and 73.8 (Oct.)	Average 79 (Sep.) and 80.6 (Oct.)	Average 80.5 (Sep.) and >81 (Oct.)
Enclosure: Deployment Period	BDL: Oct. 9–Nov. 7, RVB: Oct. 9–Nov. 6 FCCL: Oct. 8–Nov. 5	BDL: Aug. 30–Oct. 10 RVB: Aug. 31–Oct. 11 FCCL: Aug. 31–Oct. 10	BDL: Aug. 27–Sep. 25 RVB: Aug. 28–Sep. 26 FCCL: Aug. 27–Sep. 26
Enclosure: Smelt Age (DPH)	264–291	216	~200
Enclosure: n-cages (n-fish/cage)	BDL: 3 (60) RVB: 3 (60) FCCL: 1 (90)	BDL: 4 (70) RVB: 4 (70) FCCL: 1 (24)	BDL: 4 (70) RVB: 4 (70) FCCL: 1 (70)

Habitat Conditions

Water quality was assessed using data collected from nearby continuous sondes (Table 20). CDEC station RVB was selected to characterize Rio Vista water quality, which is located approximately 1.7 km upstream of the enclosure installation site, and CDEC station BDL was selected to characterize the Belden’s Landing enclosure location, which is located approximately 100 m upstream of the enclosure site. We used hourly collection data to calculate daily average, minimum, and maximum

values for water temperature, salinity, and turbidity from August to December of each deployment year (2019, 2023, and 2024).

Table 20. Continuous water quality station information.

Station Name	Station Metadata	Latitude	Longitude
Sacramento River at Rio Vista Bridge (RVB)	https://cdec.water.ca.gov/dynamics/staMeta?station_id=RVB	38.159737°	-121.686355°
Belden’s Landing (BDL)	https://cdec.water.ca.gov/dynamics/staMeta?station_id=BDL	38.186900°	-121.970800°

Zooplankton samples were also collected to assess Delta smelt food availability. In 2019, zooplankton samples were collected once or twice per week using a SEA-GEAR conical 0.5×2 m plankton net with 53- μ m mesh and towed subsurface for two minutes, within 15 m of the enclosures. Samples were preserved with 5% formalin and dyed with Rose Bengal and sent to BSA Environmental Services, Inc. (Beachwood, Ohio) for enumeration and identification of mesozooplankton and microzooplankton. In 2023 and 2024, samples were collected once per week from both inside and outside the enclosures to ensure that zooplankton samples collected outside the enclosures were adequately characterizing food availability inside the enclosures. Zooplankton samples were obtained by filtering ten gallons of water through a 60 μ m mesh using Geopump Easy-Load II peristaltic pumps with a combined flow rate of approximately 2 gal/min (the maximum pump velocity). To do so, three Geopumps were set up in parallel and connected to a total of five 3/8-inch internal diameter intake hoses. Pump intake hoses were set at 0.15, 0.36, 0.57, 0.79, and 1 meter below the water’s surface, being careful to ensure no intakes were in direct contact with the surface of the enclosures. Samples were preserved in 10% formalin, dyed with Rose Bengal, and transported to ICF International, Inc. (Richmond, CA) for processing. All invertebrate samples were enumerated and identified to the lowest practicable level of taxonomic resolution.

We compared samples taken within or immediately next to the enclosures to samples collected by the EMP and FMWT nearby. We used stations from within Suisun Marsh (FMWT samples from stations 606, 609, and 611 with EMP samples from station NZ032) to compare to Belden’s Landing and samples from the lower Sacramento River (FMWT stations 706, 707, 708, 709, 711 and EMP stations NZ068 and D22) to compare to Rio Vista. These samples were collected by a 10-minute stepped-oblique tow using 150-micron mesh net, and were processed by the CDFW, Stockton laboratory. Due to the larger mesh size, these programs are more effective at sampling large, mobile copepods (such as *Pseudodiaptomus* spp.) and less effective at sampling small rotifers, copepod nauplii, and small copepods such as *Limnoithona* spp. All invertebrate samples were enumerated and identified to the lowest practicable level of taxonomic resolution.

The species identifications were then aggregated to larger taxonomic groups to match those used in the bioenergetics model (Smith and Nobriga 2023) (see “Wild Smelt Growth” section), with the addition of amphipods and insects, both of which were present in the biofouling community on the side of the enclosures.

Communities were visually compared across time and between stations to assess potential Delta smelt food resources.

Delta Smelt Responses

Survival and Condition

We evaluated the effects of different habitats on enclosed Delta smelt by quantifying physiological performance metrics across biological scales (e.g., whole-fish responses, organ, and cellular processes). Estimated *Percent Survival* of Delta smelt was calculated from each site, as the number of smelt recovered from each replicate enclosure following the 4- or 6-week deployment. We also used *Fulton’s Condition Factor (CF)* and *Critical Thermal Maximum (CTmax)* as indices of whole-fish level responses. CF is a proxy for growth and can also be used as general index of nutritional condition. CF is calculated as the cubed proportion of weight to length:

$$CF = 100 \times \left(\frac{W}{L^3} \right)$$

CTmax is an acute measure of upper temperature tolerance, near lethal limits, with the hypothesis that if fish are in better condition they would be able to withstand more thermal stress. Methods for measuring CTmax of Delta smelt in the field are described in Davis et al. (2024). At the organ and cellular level, we evaluated Delta smelt livers to calculate hepatosomatic index (HSI) and the concentration of *glycogen*, providing insight into general nutritional status and potential metabolic stress. HSI, an energy reserve proxy, was calculated as the proportion of liver weight to body weight:

$$HSI = \left(\frac{\text{Liver Weight (mg)}}{\text{Fish Weight (mg)}} \right) \times 100$$

Liver glycogen concentration, another proxy for food limitation and a biochemical measure of metabolic responses, was quantified in 2023 and 2024 using a colorimetric spectrophotometry assay described in Dhayalan et al. (2024) and Tempel et al. (in review). Glycogen concentrations were quantified as μg of glycogen per mg of liver tissue. Glycogen data was not included from 2019 deployments given different analytical methods (Davis et al. 2024).

To determine the effect of site and year on Delta smelt physiological responses, we used a series of models that best fit the datasets. We used linear mixed-effect regression models (the `lmer` function from the `lme4` package) (Bates et al. 2015) to quantify the effect of site and year and their interactions on CF, HSI, and liver glycogen (log-transformed) parameters. We used a binomial mixed-effect regression model (the `glmer` function from `lme4`) to quantify the effect of site (RV, FCCL, or BDL) and year on survival (the number of fish surviving at the end of the experiment out of the number starting the experiment). Due to low replication in number of cages per experiment, we could not include the interaction of site and year on survival. For each mixed-effect model, enclosure replicate was included as a random effect in the model. We used a linear model to test the effects of site (BDL, RV) and year on CTmax. We removed the FCCL site in the CTmax analysis given there were no measures in 2019, and we also removed values < 23°C as outliers not likely to be true measures based on variability documented in previous studies. For all linear models, we conducted Tukey post-hoc contrasts using estimated marginal means (`emmeans` function) (Lenth 2025).

Diets

Stomachs of 5–8 fish per enclosure were dissected and sent to the Wetland Ecosystem Team laboratory (Seattle, Washington) for diet analysis. The total contents of each stomach were weighed when possible, and all prey items were identified and enumerated to the lowest taxonomic level practicable. We compared the relative abundance of each taxon in the diets at each location, emphasizing taxa considered to be most important in Delta smelt diets (particularly *Pseudodiaptomus* spp., *Limnoithona* spp., *Acanthocyclops* spp., and *Eurytemora carolleeae* - see [Smelt Food section](#)). We compared the diets between sites and years using a permutational multivariate analysis of variance (PERMANOVA) and visually compared communities using stacked bar plots.

Bioenergetic Growth Modeling

The enclosures provided an opportunity to see how cultured fish performed when deployed in containment in a microhabitat within the region. However, it is uncertain how wild or free-swimming fish in the same area would respond to the same conditions. Therefore, we used the Delta Smelt Bioenergetic Model developed by Rose et al. (2013a) and improved upon by Smith and Nobriga (2023) to estimate growth rates of Delta smelt under the same temperature, turbidity, and food supply circumstances as those seen in the enclosure studies (see [Smelt Growth](#) section for more details on modeling).

Continuous temperature and turbidity came from nearby continuous monitoring stations listed above. A comparison of discrete data taken within the cages and the data from these nearby stations found them to be substantially similar, so we used the continuous data to allow daily growth rate estimates. Zooplankton were only

collected at the enclosures once every one to two weeks, so we used the average biomass of zooplankton over the entire two-week period. To better differentiate between potential enclosure effects and overall environmental differences, we ran the model a second time with zooplankton collected by FMWT, STN, and EMP in surrounding channels (see [Smelt Food](#) section for details on zooplankton collection).

To see whether higher water velocities at the enclosure site at BDL were driving the differences between modeled growth rates and actual growth rates, we added an additional term to the model describing the additional respiration required for increased swimming speed. This term, per Hewett and Johnson (1987), is:

$$\text{Activity} = \exp(\text{RTO} * (\text{ACT} * (\text{Wt}^{\text{RK4}}) * \exp(\text{BACT} * \text{Temp})))$$

Wt = mass of fish in grams

RTO = coefficient for swimming speed dependence of metabolism

RK4 = mass dependence coefficient for swimming speed

ACT = intercept (cm/sec for a 1-gram fish at 0°C) of the relationship for swimming speed versus mass

BACT = water temperature dependence coefficient of swimming speed

Temp = water temperature

We did not have RTO, ACT, RK4, or BACT values for Delta smelt, or any related taxa, so set RK1 to 0.0196 and ACT to 1 as per Whitlege and Hayward (1997) and used the mean values for all taxa that had values for RK4 (0.16) and BACT (0.103) Fish Bioenergetics 4.0 Model (Deslauriers et al. 2017). We then varied the relative swimming speed from 1 (same speed at both sites) to 2 (twice as much swimming at BDL). Because the swimming speed model is not parameterized with values for Delta smelt, and we do not have precise water velocities for the entire deployment periods, this should be treated only as a thought exercise for how current speed may affect growth rates.

Results

Habitat Conditions

Water quality data at nearby continuous sondes showed that Belden's Landing tended to have higher temperatures, salinities, and turbidities compared to Rio Vista (Figure 46). During the 2023 and 2024 deployments, stress-inducing temperatures (>22°C) for Delta smelt were observed more frequently at Belden's Landing than at Rio Vista. Salinities remained within the Delta smelt's preferred range (<6 PSU) at both locations during the 2023 and 2024 deployments but

slightly exceeded that range at Belden's Landing during the 2019 deployment. Turbidities higher than 12 FNU (preferred by Delta smelt) were consistently observed at Belden's Landing during the deployment periods and unfavorable, clear conditions were consistently observed at Rio Vista.

Zooplankton biomass densities were similar between the two sites and across years (Figure 47), but Belden's Landing was dominated by the cyclopoid copepod *Limnoithona* spp. and Rio Vista was dominated by *Pseudodiaptomus* spp. in 2019, amphipods and *Pseudodiaptomus* spp. in 2023, and a mix of rotifers, amphipods, and other zooplankton in 2024 (Figure 47). Samples from adjacent open-water habitat showed near total dominance of *Pseudodiaptomus* spp. at Rio Vista in all three years, and relatively more *Acartiella* spp. and cyclopoids than Rio Vista (Figure 48). These samples had much lower biomass of *Limnoithona* spp. than those samples collected near the cages, but this was most likely due to the larger mesh used rather than difference in zooplankton communities.

Figure 46. Daily average (black) and daily range (colored) of water temperature (°C), salinity (PSU), and turbidity (FNU) across sites and years before and after summer–fall actions. Turbidity values >100 are not shown here. Delta smelt deployment periods are highlighted in gray. Dotted lines indicate thresholds of Delta smelt preferred habitat (temperature <22°C, salinity <6 PSU, turbidity >12 FNU).

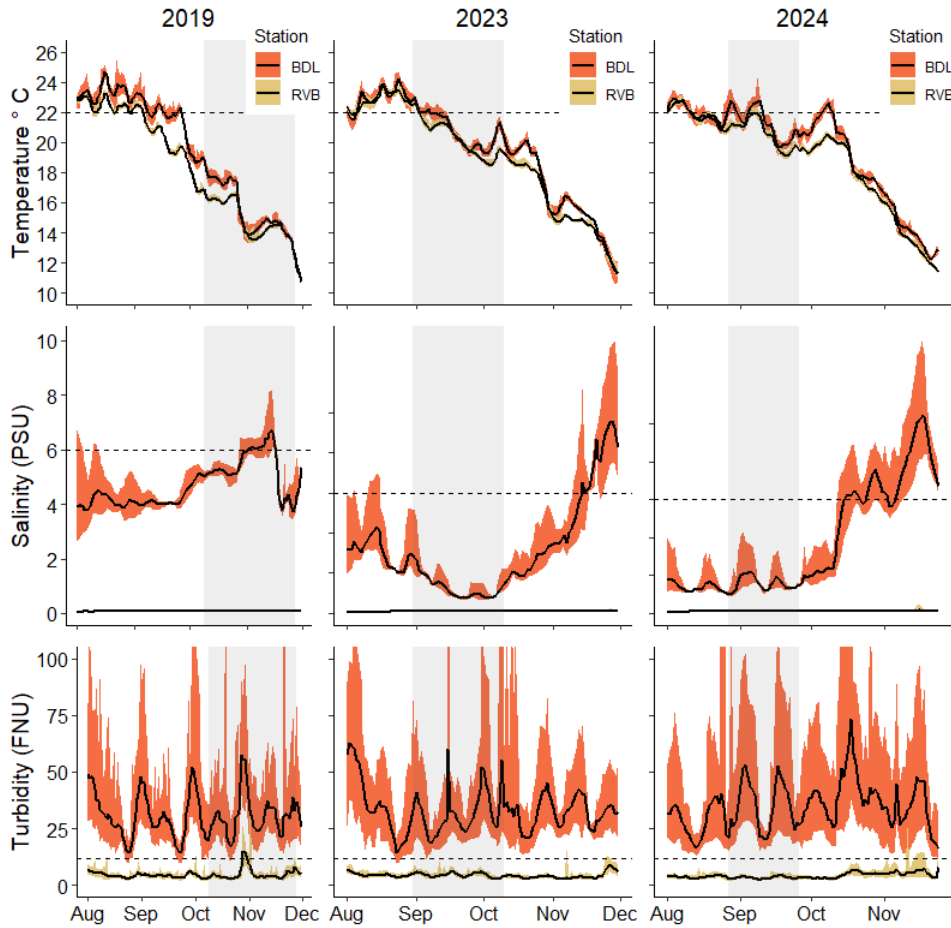


Figure 47. Time series plot of zooplankton density in individuals per cubic meter (top) and mg per cubic meter (bottom) collected inside or just outside the enclosures in each year. Sampling occurred once per week in 2019, once every two weeks in 2023 and 2024. Data from 2019 was collected by towing nets outside the enclosures, while data from 2023 and 2024 was collected from pumps inside and directly outside the enclosures.

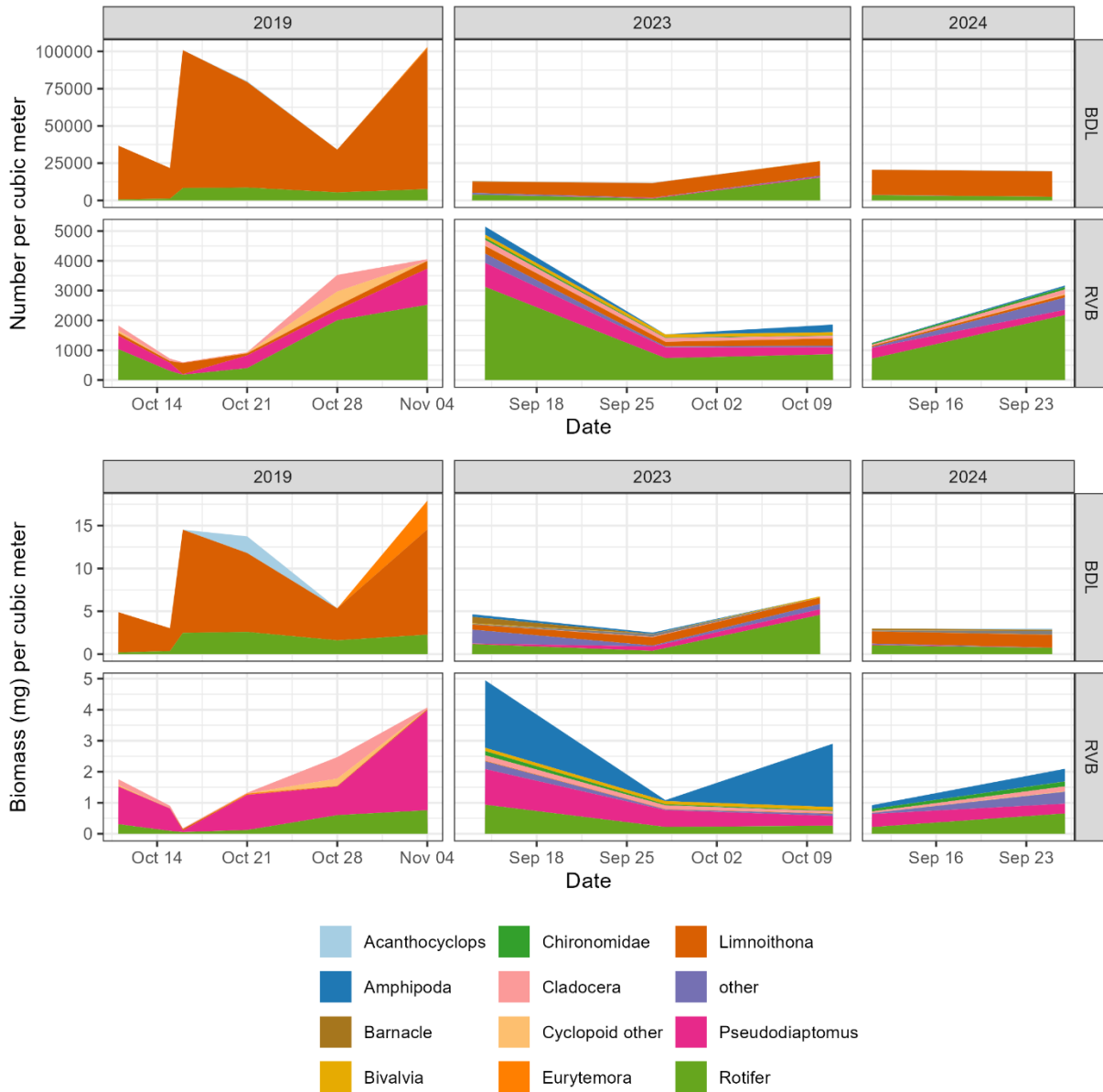
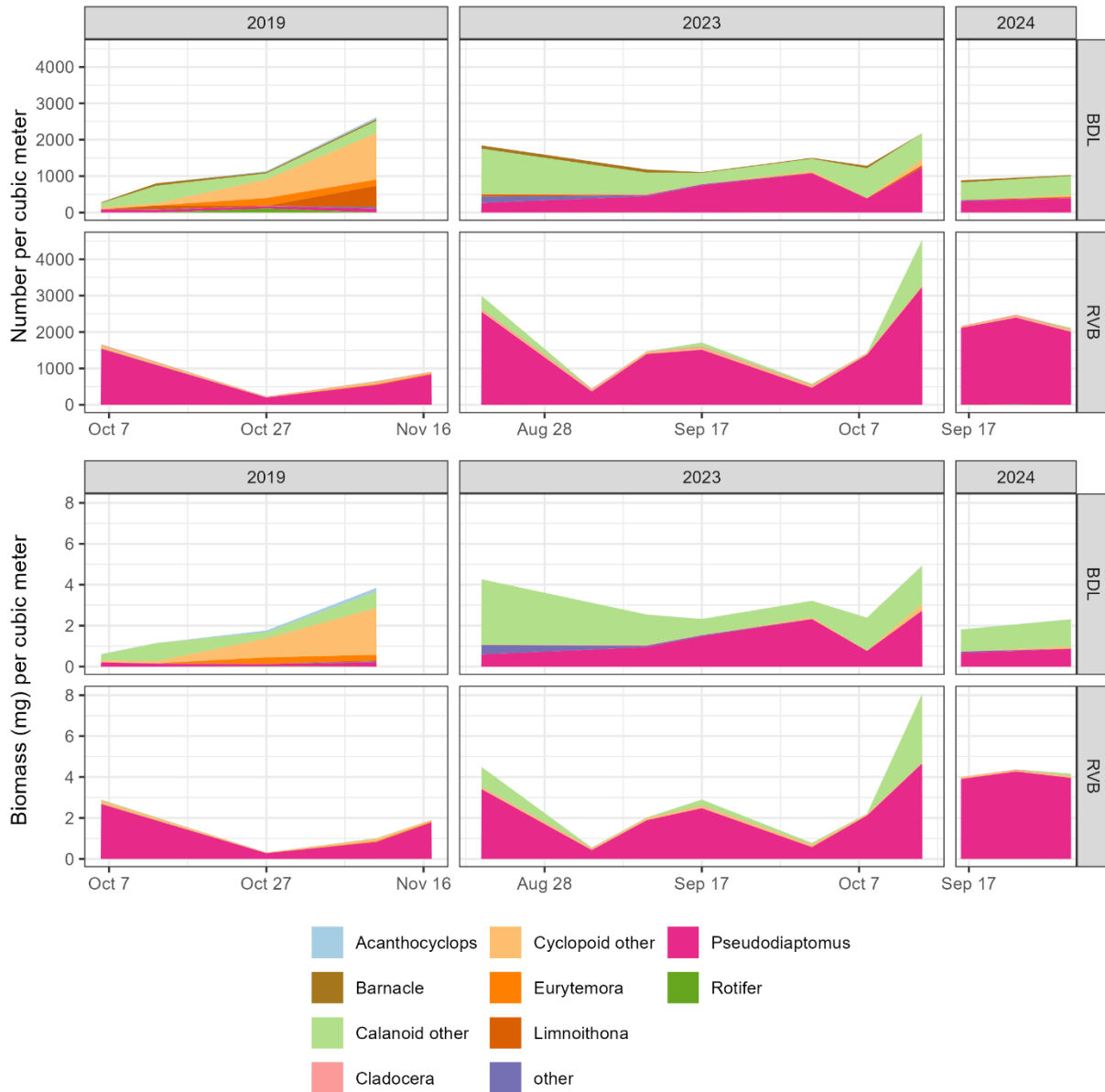


Figure 48. Time series plot of zooplankton density in individuals per cubic meter (top) and mg per cubic meter (bottom) collected by the FMWT Survey in surrounding channels during the enclosure studies.



Survival and Condition

The average size of sub-adult Delta smelt in the analysis was (mean ± STD) 5.9 ± 0.8 cm fork length and 1.43 ± 0.63 g in weight (Figure 49). Delta smelt in 2019 were on average ~1 cm and ~0.5 g larger than smelt in 2023 and 2024 before fish were transferred to field enclosures or control tanks (Table 21). Delta smelt survival following 4- to 6-weeks in enclosures was $77.9\% \pm 0.18$ (STD) (Figure 50a). Survival was significantly higher at FCCL than at the field enclosures (Table 22),

and significantly higher in 2019 than in the other two years (Table 22). Survival was lowest at BDL (range 55–64%) in 2023 and 2024 compared to RV (81–85%) and FCCL (80–98%), while survival in 2019 was more similar (88–99%) across sites (Table 24).

Condition factor of Delta smelt yielded similar results to survival with 2023 and 2024 fish having lower CF at BDL compared to RV ($P < 0.001$) (Table 23) but similar CF between the sites in 2019 (Figure 50b). Site had the strongest effect on liver responses (Table 22), with enclosed Delta smelt at BDL or RV having lower HSI and liver glycogen concentrations compared to the control fish at FCCL (Table 23, Figure 50c,d). In 2023 and 2024, HSI was similar at BDL and RV, in contrast to liver glycogen that was lowest at BDL compared to RV in both years (Table 23, Figure 50c,d).

CTmax of Delta smelt was dependent on site and year with a significant interaction ($p = 0.001$) (Table 22). In 2019 and 2024, CTmax was similar at BDL and RV ($p > 0.05$), but in 2023 RV was 1.2°C higher than BDL ($p = 0.005$) (Table 23). Within sites, CTmax of fish at RV was higher in summer of 2023 and 2024 compared to fall of 2019, which differed from fish at BDL where 2024 CTmax was higher than 2019 and 2023. Model outcomes indicate there was no main effect of site, however, pairwise comparisons indicate marginal differences between RV and BDL, and we attribute this as the model was not fitting the results well.

Figure 49. Scatter plot of Delta smelt size before and after deployment in 2019, 2023, and 2024. FCCL represents reference fish, RV is Rio Vista, and BDL is Belden’s Landing.

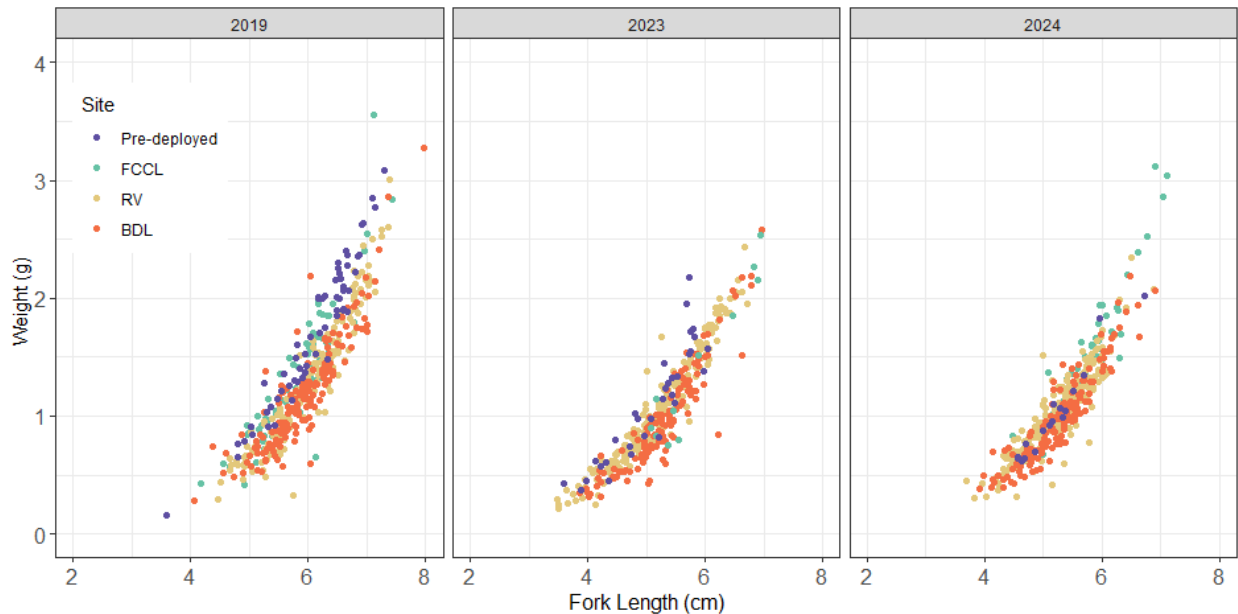


Table 21. Average fork length (cm) and weight (g) of Delta smelt before deployment and after deployment across years and sites. Std = Standard Deviation.

Year	Site	Length (cm) ± Std	Weight (g) ± Std
2019	Pre-deployed	6.09 ± 0.70	1.72 ± 0.61
2019	FCCL	5.84 ± 0.60	1.37 ± 0.54
2019	RV	6.03 ± 0.66	1.33 ± 0.53
2019	BDL	5.88 ± 0.60	1.17 ± 0.46
2023	Pre-deployed	5.08 ± 0.67	1.11 ± 0.48
2023	FCCL	5.91 ± 0.75	1.43 ± 0.67
2023	RV	5.18 ± 0.74	1.07 ± 0.49
2023	BDL	5.25 ± 0.63	0.96 ± 0.43
2024	Pre-deployed	5.20 ± 0.56	1.04 ± 0.40
2024	FCCL	5.78 ± 0.61	1.55 ± 0.55
2024	RV	5.22 ± 0.54	1.03 ± 0.34
2024	BDL	5.24 ± 0.57	0.98 ± 0.37

Figure 50. Delta smelt survival (top left), condition factor (top right), hepatosomatic index (bottom left), and liver glycogen (bottom right) after enclosure deployments in 2019, 2023, and 2024. FCCL represents reference fish, RV is Rio Vista, and BDL is Belden’s Landing. No glycogen was collected in 2019.

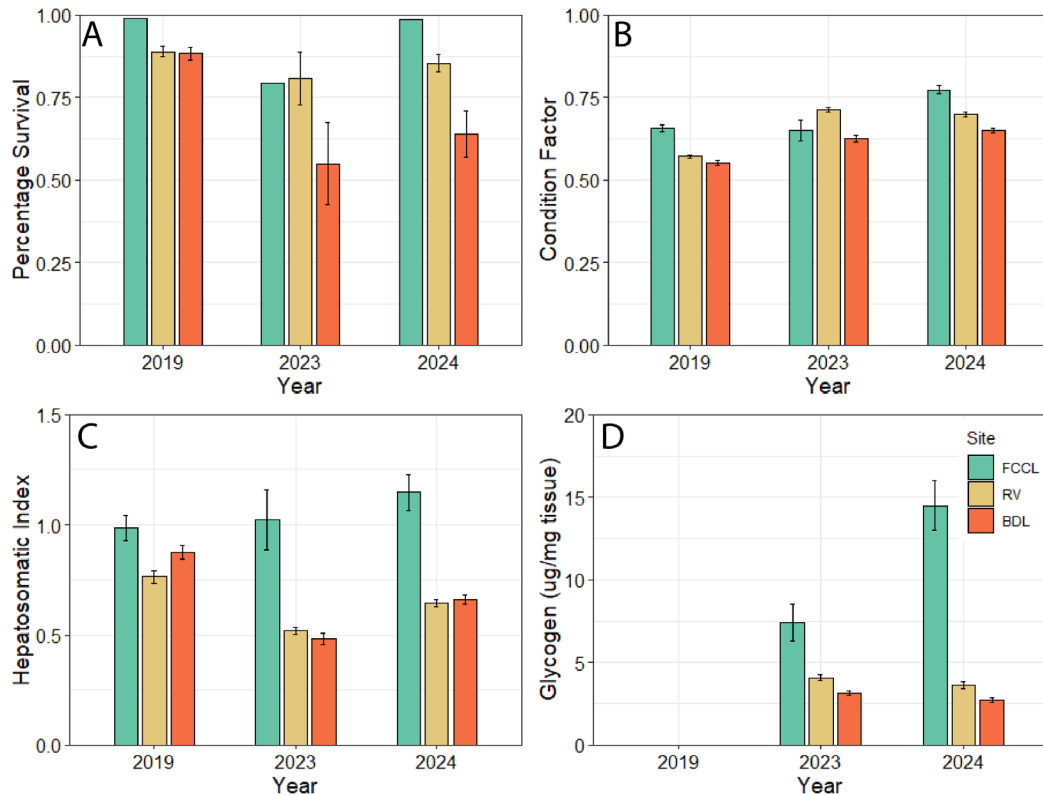


Figure 51. CTmax of Delta smelt across years and sites. FCCL represents reference fish at the Fish Conservation and Culture Facility, RV is Rio Vista, and BDL is Belden’s Landing. No CTmax tests were run for FCCL fish in 2019.

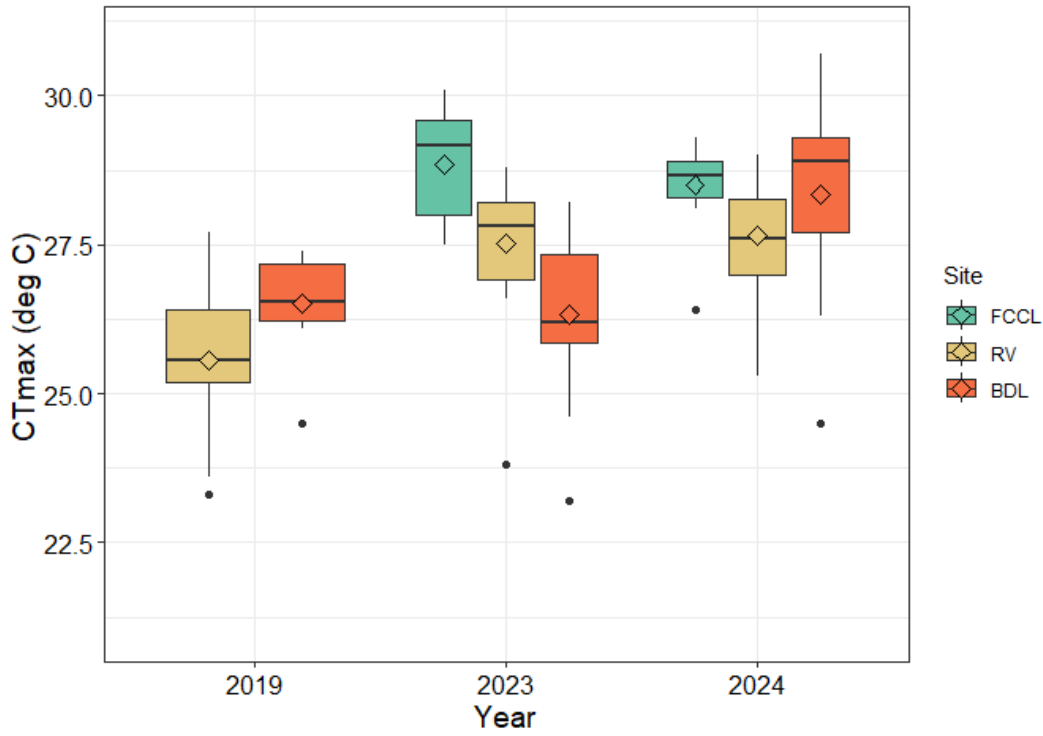


Table 22. Model outcomes for Delta smelt responses to site and year. Chi-squared (X^2) is presented for GLMER and LMER models, whereas F-statistic is presented for LM. Degrees of freedom is noted as df.

Response Variable	Predictor	Sum Sq	df	X^2	F	P-value
Survival	Site	-	2	17.0001	-	0.0002
Survival	Year	-	2	20.000	-	<0.0001
CF	Site	-	2	42.294	-	<0.0001
CF	Year	-	2	56.750	-	<0.0001
CF	Site*Year	-	4	27.754	-	<0.0001
HSI	Site	-	2	91.089	-	<0.0001
HSI	Year	-	2	43.361	-	<0.0001
HSI	Site*Year	-	4	20.248	-	<0.001
Glycogen	Site	-	2	167.3616	-	<0.0001
Glycogen	Year	-	1	6.8071	-	0.00907
Glycogen	Site*Year	-	2	13.3822	-	0.00124
CTmax	Site	0.007	1	-	0.0045	0.946637
CTmax	Year	50.861	2	-	17.0676	<0.0001
CTmax	Site*Year	21.268	2	-	7.1369	0.001372

Table 23. Estimated marginal means (emmeans) post-hoc comparisons between sites within each year. FCCL represents reference fish at the Fish Conservation and Culture Facility, RV is Rio Vista, and BDL is Belden’s Landing.

Metric (Year)	Contrast	Estimate	SE	df	T or z-ratio	P-value
Survival (All)	FCCL-RV	1.926	0.657	Inf	2.934	0.0094
Survival (All)	FCCL-BDL	2.458	0.628	Inf	3.917	0.0003
Survival (All)	RV-BDL	0.532	0.295	Inf	1.803	0.1684
CF (2019)	FCCL-RV	0.0856	0.0216	17.2	3.967	0.0027
CF (2019)	FCCL-BDL	0.1052	0.0215	17.1	4.881	0.0004
CF (2019)	RV-BDL	0.0196	0.0103	1154.5	1.904	0.1380
CF (2023)	FCCL-RV	-0.0717	0.0303	1136.2	-2.363	0.0480
CF (2023)	FCCL-BDL	0.0157	0.0347	145.7	0.452	0.8936
CF (2023)	RV-BDL	0.0874	0.0191	17.1	4.575	0.0007
CF (2024)	FCCL-RV	0.0755	0.0284	14.6	2.660	0.0450
CF (2024)	FCCL-BDL	0.1242	0.0287	15.3	4.325	0.0016
CF (2024)	RV-BDL	0.0486	0.0183	15.8	2.654	0.0437
HSI (2019)	FCCL-RV	0.2288	0.0723	37.1	3.164	0.0085
HSI (2019)	FCCL-BDL	0.1145	0.0723	37.1	1.583	0.2655
HSI (2019)	RV-BDL	-0.1143	0.0452	511.9	-2.531	0.0313
HSI (2023)	FCCL-RV	0.5002	0.0748	428.1	6.683	<.0001
HSI (2023)	FCCL-BDL	0.5410	0.0839	79	6.445	<.0001
HSI (2023)	RV-BDL	0.0408	0.0486	15.3	0.839	0.6850
HSI (2024)	FCCL-RV	0.5021	0.0742	14.1	6.769	<.0001
HSI (2024)	FCCL-BDL	0.4889	0.0741	14.1	6.597	<.0001
HSI (2024)	RV-BDL	-0.0132	0.0467	13.8	-0.283	0.9571
Glycogen (2023)	FCCL-RV	0.560	0.1790	139.4	3.129	0.0060
Glycogen (2023)	FCCL-BDL	0.811	0.1830	50.4	4.425	0.0002
Glycogen (2023)	RV-BDL	0.251	0.0844	12.2	2.968	0.0290
Glycogen (2024)	FCCL-RV	1.301	0.1260	10.9	10.305	<.0001
Glycogen (2024)	FCCL-BDL	1.580	0.1260	11.1	12.495	<.0001
Glycogen (2024)	RV-BDL	0.279	0.0802	10.9	3.479	0.0133
CTmax (2019)	RV-BDL	-0.960	0.546	84	-1.759	0.0823
CTmax (2023)	RV-BDL	1.195	0.413	84	2.896	0.0048
CTmax (2024)	RV-BDL	-0.691	0.431	84	-1.673	0.0980

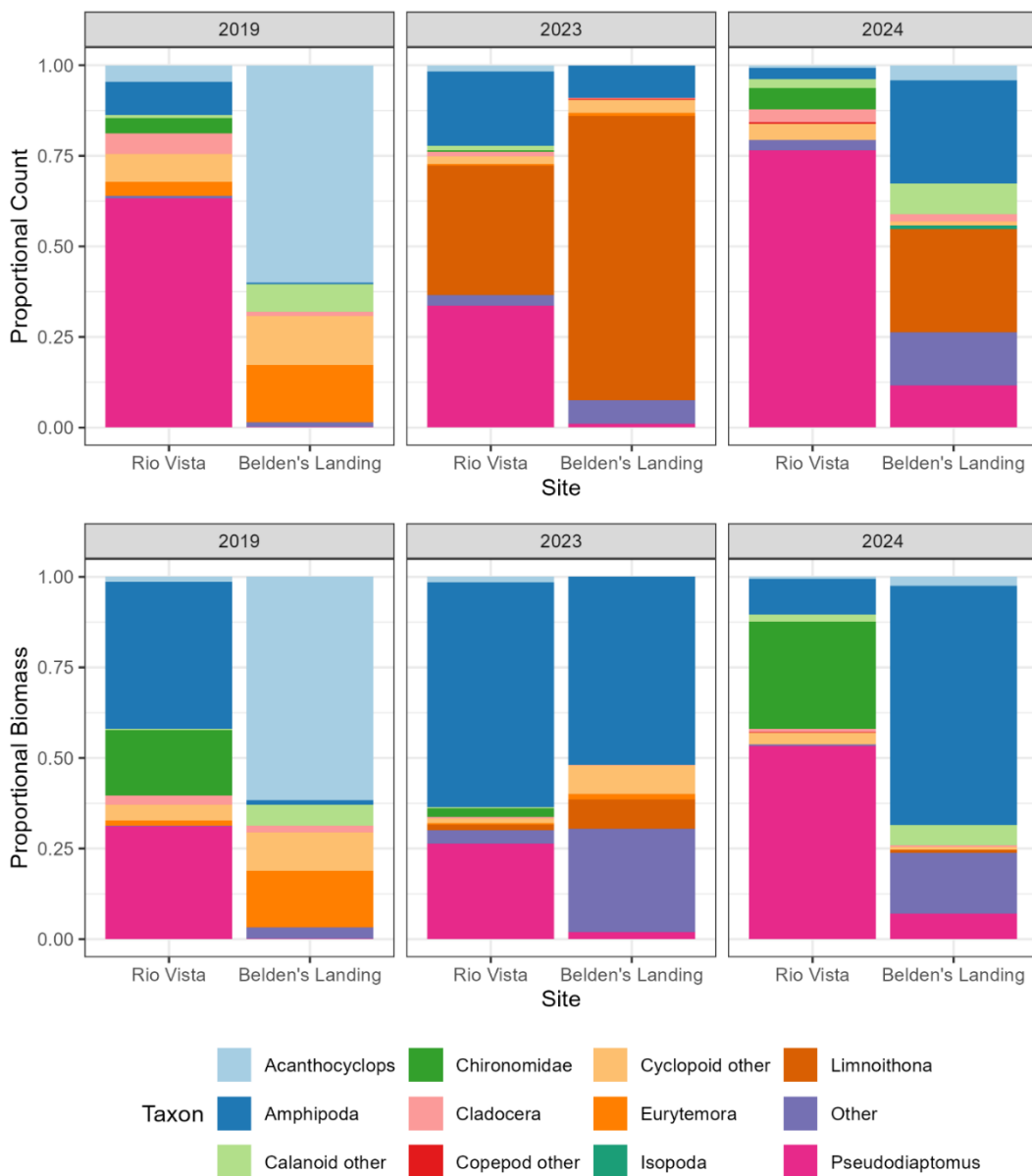
Table 24. Estimated marginal means (emmeans) post-hoc comparisons by years within each site. FCCL represents reference fish at the Fish Conservation and Culture Facility, RV is Rio Vista, and BDL is Belden’s Landing.

Metric (Site)	Contrast	Estimate	SE	df	T-ratio	P-value
Survival (All)	2019–2023	1.483	0.4	Inf	3.711	0.0006
Survival (All)	2019–2024	1.048	0.4	Inf	2.620	0.0239
Survival (All)	2023–2024	-0.434	0.14	Inf	-3.094	0.0056
CF (RV)	2019–2023	-0.1401	0.0194	14.5	-7.238	<.0001
CF (RV)	2019–2024	-0.1262	0.0193	14.2	-6.556	<.0001
CF (RV)	2023–2024	0.0139	0.0179	14.5	0.773	0.7247
CF (BDL)	2019–2023	-0.0723	0.0203	16.3	-3.560	0.0068
CF (BDL)	2019–2024	-0.0971	0.0197	15.4	-4.936	0.0005
CF (BDL)	2023–2024	-0.0249	0.0195	18.4	-1.277	0.4253
CF (FCCL)	2019–2023	0.0172	0.0354	130.2	0.486	0.8783
CF (FCCL)	2019–2024	-0.1161	0.0300	16.1	-3.869	0.0036
CF (FCCL)	2023–2024	-0.1333	0.0406	55.6	-3.283	0.0050
HSI (RV)	2019–2023	0.2425	0.0546	19.1	4.443	0.0008
HSI (RV)	2019–2024	0.1180	0.0545	18.9	2.164	0.1037
HSI (RV)	2023–2024	-0.1246	0.0469	14.1	-2.659	0.0462
HSI (BDL)	2019–2023	0.3976	0.0560	20.1	7.100	<.0001
HSI (BDL)	2019–2024	0.2191	0.0544	18.8	4.025	0.0020
HSI (BDL)	2023–2024	-0.1786	0.0484	15.1	-3.688	0.0058
HSI (FCCL)	2019–2023	-0.0288	0.0956	91.1	-0.302	0.9511
HSI (FCCL)	2019–2024	-0.1554	0.0881	22.5	-1.763	0.2046
HSI (FCCL)	2023–2024	-0.1265	0.1010	38.2	-1.253	0.4300
Glycogen (RV)	2023–2024	0.188	0.0799	10.7	2.358	0.0385
Glycogen (BDL)	2023–2024	0.217	0.0848	12.4	2.557	0.0246
Glycogen (FCCL)	2023–2024	-0.552	0.2060	31.4	-2.682	0.0116
CTmax (RV)	2019–2023	-1.958	0.486	84	-4.024	0.004
CTmax (RV)	2019–2024	-2.084	0.481	84	-4.330	0.001
CTmax (RV)	2023–2024	-0.127	0.413	84	-0.307	0.9494
CTmax (BDL)	2019–2023	0.198	0.481	84	0.411	0.9113
CTmax (BDL)	2019–2024	-1.815	0.486	84	-3.732	0.0010
CTmax (BDL)	2023–2024	-2.013	0.413	84	-4.876	<.0001

Diets

There were significant differences in the diets of fish in the enclosures between sites, with less difference between years (Figure 52) (PERMANOVA $F = 16.6$, $P = 0.001$, $R^2 = 0.287$). Diets at Rio Vista were dominated by *Pseudodiaptomus* spp. in all years, though *Limnoithona* spp. made a significant contribution to diet in 2023. Diets in Suisun Marsh showed more variation year to year, with *Acanthocyclops* spp. and *Eurytemora* dominating the diets in 2019, *Limnoithona* spp. dominating in 2023, and amphipods and *Limnoithona* spp. dominating in 2024.

Figure 52. Relative contribution by number (top) and by biomass (bottom) of each invertebrate taxonomic group in diets of Delta smelt in enclosures.



Bioenergetics

When parameterized with the starting weights of fish going into each experiment, the water quality from nearby continuous sondes, and zooplankton samples collected inside or immediately outside the enclosures, we found that the bioenergetic model predicted higher growth at Belden's Landing than Rio Vista in all three years, opposite from what was seen with empirical measurements (Figure 53). To estimate growth rates of fish not restricted to enclosures, we also modeled growth using zooplankton density estimates from nearby FMWT and EMP zooplankton sampling stations (Figure 54). These results show similar trends to the enclosure zooplankton data, with BDL having higher predicted growth than RV, though growth rates were similar between sites in 2019.

Increasing the swimming speed for fish at BDL decreased the growth rates (Figure 55), though because the coefficients of the model were not calibrated for Delta smelt, the results should be viewed in a relative rather than absolute context. When fish at both sites had the same activity rates, fish at BDL grew faster, but as activity at BDL increased relative to Rio Vista (as would be expected given higher velocities at BDL and the inability of enclosure fish to seek refuge from high velocities), growth rates were more similar. If activity at BDL increased by 75–80%, Rio Vista had higher growth rates. While we do not have data on swimming rates, clod cards (blocks of plaster of Paris used to measure relative water flow) deployed in 2023 lost weight 50% faster inside and outside of the enclosures at BDL than RV (Figure 56), indicating water velocities were significantly higher and likely forced Delta smelt in the enclosures to swim at a higher rate to avoid impingement.

Figure 53. Predicted growth curves for Delta smelt in each enclosure experiment based on temperature, turbidity, and zooplankton values collected during the experiments.

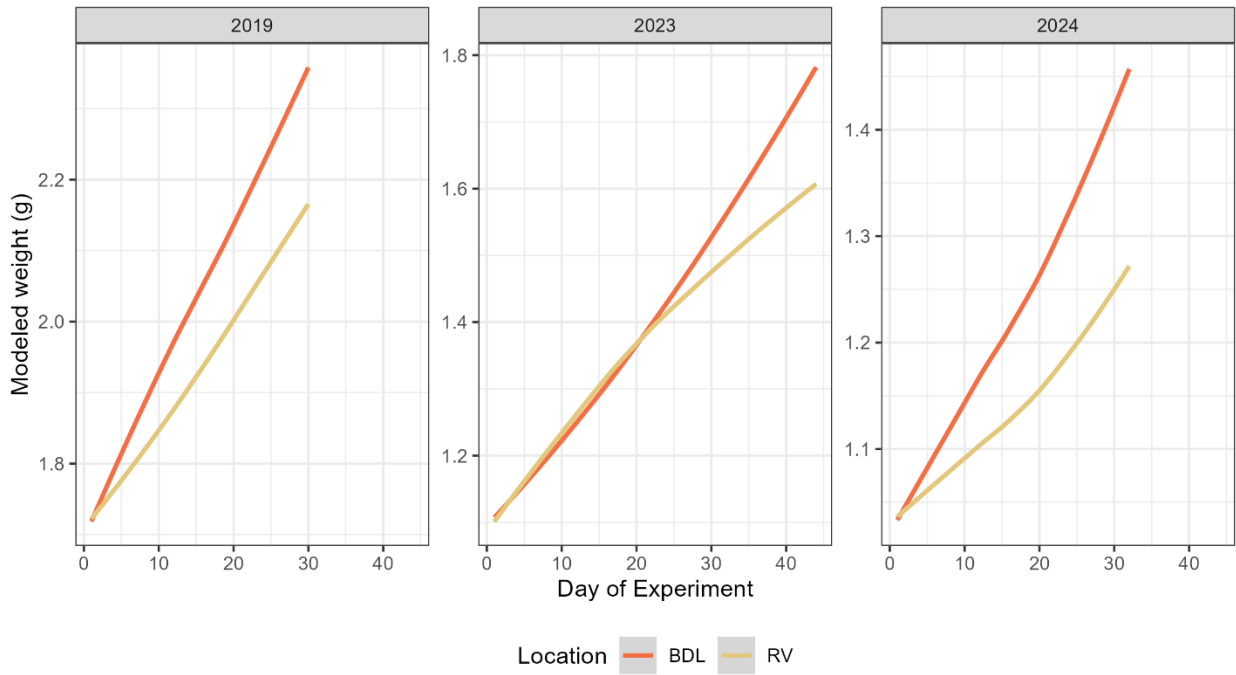


Figure 54. Predicted growth curves for Delta smelt in each location based on zooplankton collected at nearby FMWT stations and temperature and turbidity based on nearby sondes.

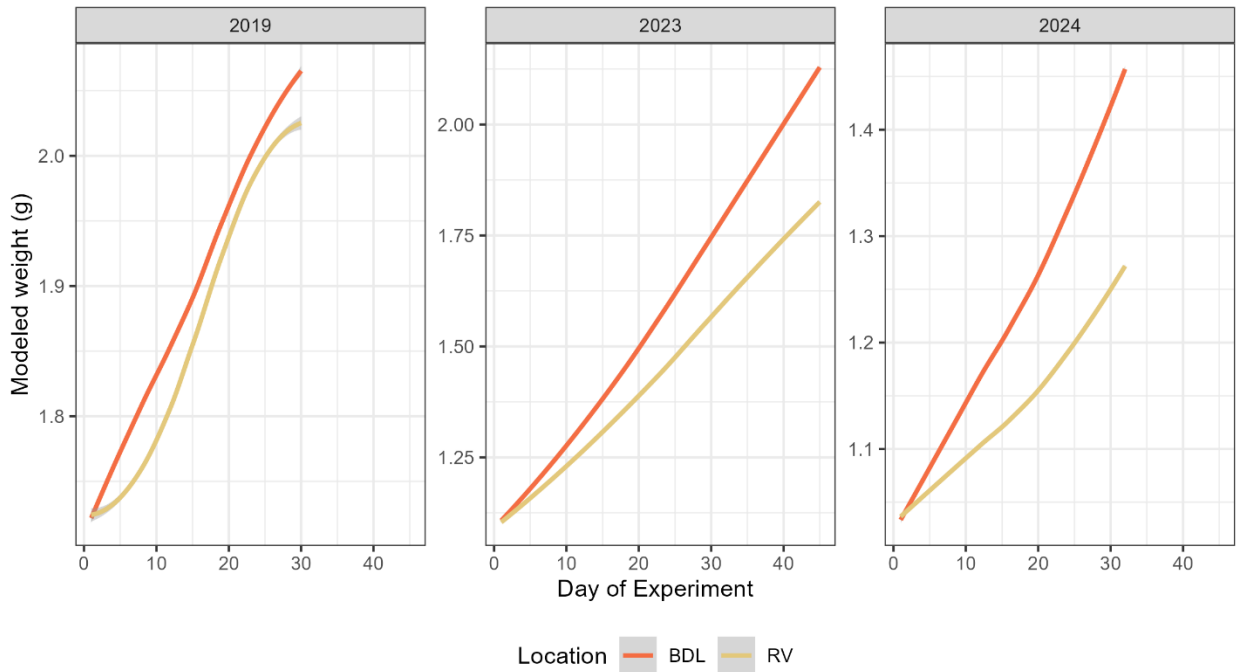


Figure 55. Modeled growth at BDL under different activity levels, as would be caused by swimming against different current strengths. Relative activity level of 1 represents equal swimming at RV and BDL, whereas 2 is twice as much activity. Dotted line is growth rate at RV.

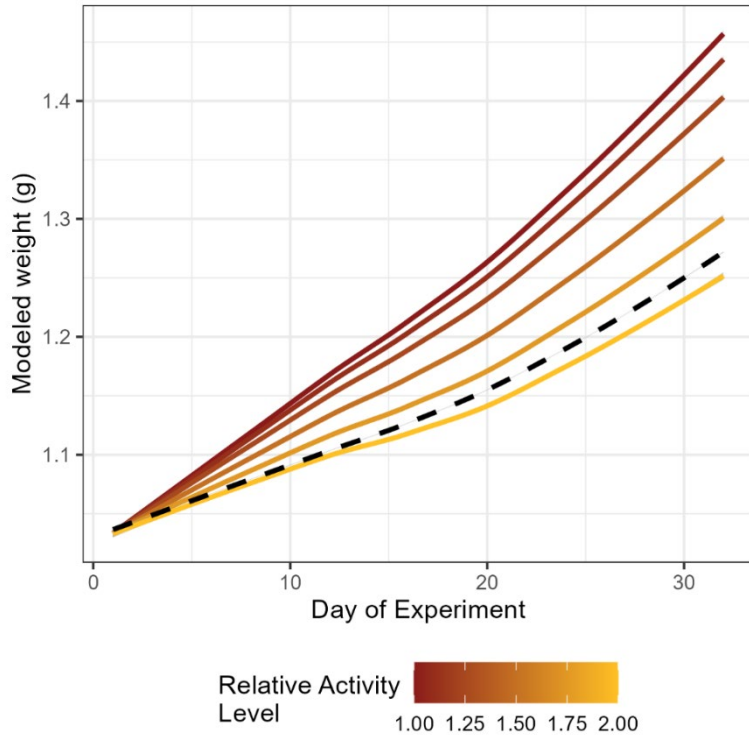
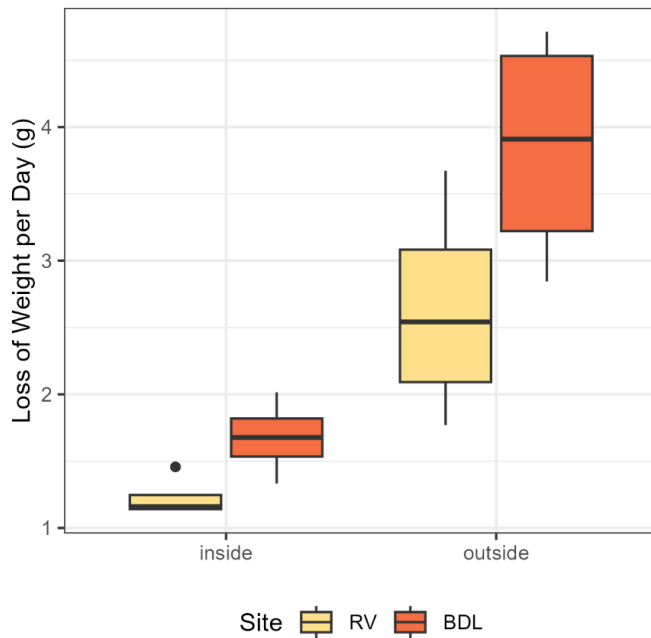


Figure 56. Loss of weight from clod cards deployed at Rio Vista and Belden's Landing for one week during the 2023 enclosure experiment.



Discussion

We hypothesized that beneficial habitat conditions (higher turbidity, possibly lower temperatures) in Suisun Marsh would result in improved Delta smelt growth and survival when compared to Rio Vista. Our results were mostly counter to this hypothesis, leading us to conclude either that our hypothesis was incorrect or that the enclosures did not provide a realistic evaluation of broader habitat conditions.

Differences in Space and Time

Delta smelt in enclosures responded differently to the 2019 late-fall deployment than the 2023 and 2024 summer deployments. The 2019 deployment was characterized by cooler temperatures ($<20^{\circ}\text{C}$), whereas the 2023 and 2024 deployments both occurred earlier in years when water temperatures were warmer ($18^{\circ}\text{C} - 25^{\circ}\text{C}$). During the 2019 deployment, we saw similar survival and condition factor at Belden's Landing and Rio Vista (Figure 50). In addition, we saw higher hepatosomatic index (indicating higher energy reserves) and a (nonsignificant) trend toward higher CTmax in the Belden's Landing fish compared to Rio Vista (Figure 51). These results indicate habitat was similar between sites or better at Belden's Landing during the 2019 deployment. In contrast, during the 2023 and 2024 deployments we saw an opposite trend, where fish held at Rio Vista showed higher survival, condition factor, and liver glycogen compared to fish held at Belden's Landing (Figure 50), indicating that the Marsh may have been a less-favorable location during those years. This difference may have been driven by the higher temperatures during the early fall deployments of 2023 and 2024 (Figure 46). Several prior studies have found that Delta smelt experience stress in water temperatures over 20°C , as indicated by changes in gene expression above 22°C (Komoroske et al. 2015; Komoroske et al. 2021), lower growth rates in wild Delta smelt in water above 20°C (Lewis et al. 2021), behavioral changes and increased energy demand at 21°C (Davis et al. 2019), and reduced consumption rates at 21.6°C (Smith and Nobriga 2023). While Suisun Marsh was higher in temperature than Rio Vista in all three deployments, temperatures in 2019 stayed below 22°C at both sites and may not have differentially impacted Delta smelt growth rates, whereas Suisun Marsh temperatures during the 2023 and 2024 deployments may have had a more pronounced effect. It should be noted that, while Rio Vista was warmer during the three years analyzed here, this pattern is not consistent across years, with some summers having warmer temperatures at Rio Vista than Suisun Marsh (e.g. 2022, see Reclamation and DWR 2023). Ambient water temperatures should be an important consideration when implementing habitat improvements for Delta smelt.

Salinity was consistently higher in Suisun Marsh than Rio Vista. However, many studies demonstrate Delta smelt are somewhat physiologically insensitive to a range of salinities (Komoroske et al. 2014; Kammerer 2016; Hammock et al. 2017;

Davis et al. 2019). A couple studies have detected changes at cellular and/or molecular levels in response to increased salinity (>10 PSU), but Delta smelt have the capacity to buffer and/or acclimate physiologically, such that effects at the whole-fish level are limited or not observed with similar survival, condition, metabolism, and tolerances. Delta smelt do appear to show preference for fresher water (<6 PSU or even <2 PSU) in field surveys (Feyrer et al. 2007; Sommer and Mejia 2013; Bennett 2005) and some laboratory studies (Hung et al. 2022), but smelt that migrate for rearing in the LSZ (0.5-6 PSU) tend to have higher growth rates than those that stay in freshwater year-round (Lewis et al. 2021). Therefore, our results showing higher growth and survival at Rio Vista are unlikely to be caused by differences in salinity.

Diets were also significantly different between years and sites. At Rio Vista, *Pseudodiaptomus* spp. dominated the diets in all three years (Figure 52) and were one of the most common organisms in the ambient zooplankton community (Figure 48). *Pseudodiaptomus* spp. has long been recognized as one of the most important diet items for Delta smelt in summer and fall (Slater et al. 2019; Slater and Baxter 2014) and is generally much higher in abundance upstream at Rio Vista than downstream at Suisun Marsh (see [Smelt Food](#) section). Suisun Marsh diets varied more from year to year, with the cyclopoid copepod *Acanthocyclops* spp. and the calanoid copepod *E. carolleeae* dominating in 2019 and *Limnoithona* spp. and amphipods dominating in 2023 and 2024 (Figure 52). Greater *Pseudodiaptomus* spp. availability may have been one of the important driving factors behind the higher condition factor at Rio Vista, because it is considered one of the most important and nutritious sources of Delta smelt food (Slater et al. 2019; Rose et al. 2013a). In contrast, *Limnoithona* spp. is believed to have lower nutritional value (Rose et al. 2013a; Kratina and Winder 2015), and it is significantly smaller (Bouley and Kimmerer 2006), so Delta smelt must expend more energy foraging for the same number of calories.

While diets appeared to be lower quality in Suisun Marsh, the bioenergetic model indicated that the difference in zooplankton availability (with more, high-value *Pseudodiaptomus* spp. in Rio Vista) was not important enough to result in lower growth in Suisun Marsh (Figure 53). This pattern held whether we used zooplankton data collected nearby or inside the cages (Figure 47) or the open-water zooplankton collected by the long-term monitoring programs (Figure 48), indicating food should not have been limiting their growth rates. It may have been that the higher turbidity and lower temperatures compensated for the reduced nutritional value of the zooplankton. Alternatively, the enclosures could have changed the feeding environment, resulting in different foraging patterns than those included in the model.

The fish used in 2019 were also older and slightly larger than those used in 2023 and 2024 and may have been more robust to stressful conditions. Larger fish require more food per individual than smaller fish but generally have lower

metabolic requirements per gram (Clarke and Johnston 1999) and are able to take advantage of larger prey items (such as *Acanthocyclops* spp. and amphipods) that may be too large for smaller individuals.

Enclosure Effects

The enclosures were designed to provide a low-stress environment that maximizes Delta smelt survival in a semi-natural setting, but the experience of a fish in an enclosure is not identical to the experience of a free-swimming fish, limiting the generalizability of our results. Fish in an enclosure cannot search for thermal refugia, avoid high flows, or forage for food in microhabitats where food may be more abundant. Some of the hypotheses for the benefits of Suisun Marsh as Delta smelt habitat rely on fish taking advantage of hydrologic heterogeneity (Bever et al. 2016), foraging in or near wetland areas (Hammock, Hartman et al. 2019), and finding thermal refugia caused by cooling of water on wetland planes at night (Enright et al. 2013). None of these benefits are available to the fish inside enclosures.

When we applied the bioenergetic model to the observed temperature, turbidity, and food supply observed at both sites, we found that conditions in Suisun Marsh should have resulted in higher growth rates than Rio Vista (Figure 53). When fish condition data showed the opposite trend, it was evidence that the enclosures may have introduced new factors not included in the model, or that the model was not parameterized accurately.

In particular, variations in water velocity between sites may have impacted our results, because Delta smelt in enclosures could not move to their preferred low-velocity habitat. The Belden's Landing site is located in an area that is subjected to high flows, while the Rio Vista site experiences comparatively lower flow rates, as evidenced by the clod card data (Figure 56). While velocities inside the enclosures were significantly lower than outside the enclosures, they were still higher at Belden's Landing than Rio Vista, meaning that fish had to expend greater energy reserves to maintain their position within the enclosure. Greater energy expenditure combined with slightly higher temperatures and lower densities of their preferred food (*Pseudodiaptomus* spp.) may have caused the difference in growth and survival between sites. This theory is supported by the bioenergetic modelling results, whereby increasing swimming speeds at Belden's Landing resulted in lowered predicted growth rates (Figure 55). Bever et al. (2016) found that Delta smelt were significantly less common at FMWT stations with higher current speeds, though it is uncertain whether that relationship was due to avoidance of high current speed by Delta smelt, the association of high current speed with deep channel habitat, or lower gear efficiency in higher current speeds.

In all three years the cages were subject to biofouling – thick growth of algae and associated invertebrates (Tempel et al., in review) – which may have increased the

proportion of the diet that came from amphipods and insects associated with biofouling communities (Figure 52). Historically, juvenile Delta smelt caught in the wild consume mostly copepods with very few insects or amphipods (Slater and Baxter 2014; Slater et al. 2019), though the frequency of insects and amphipods in their diet increases when Delta smelt are associated with tidal wetland habitat (Whitley and Bollens 2014). Zooplankton samples collected inside the cages included a larger number of amphipods and insects than samples collected in open-water nearby (compare data from the enclosures in Figure 47 versus the FMWT data in Figure 48), which were likely knocked loose from the biofouling community. This novel food landscape further confounds our ability to apply our results to wild-swimming fish.

Additionally, because the enclosures were installed in a single location within each geographic region, our results are not necessarily reflective of the region as a whole, given the wide variability in microhabitats across the Suisun Marsh and the lower Sacramento River regions. The enclosures themselves had a geographic footprint of about 25 cubic meters at each field site. This allows for a very small snapshot of Delta smelt response, given the vastness of the geographic regions that summer–fall actions are intended to affect. While our study design may provide insight into Delta smelt responses to general habitat differences, it is very possible that our results may have been drastically different had different installation sites been selected in either or both locations. Enclosures have proven to be a useful tool to measure fish responses to specific conditions but are likely not appropriate for broad geographic generalizations given the high variability of environment in the estuary and the sensitive nature of the species.

Conclusions

Overall, the results of our enclosure studies did not support the hypothesis that lowering salinity in Suisun Marsh would increase Delta smelt growth and survival by giving them access to better habitat in Suisun Marsh. Delta smelt in enclosures in the Sacramento River, which we hypothesized to be poor habitat, had higher growth and survival than smelt in enclosures in Suisun Marsh. However, walking through our sub-hypotheses highlights that there are caveats to this conclusion, and the enclosure study results should not be used to make broader statements about the effectiveness of the SMSCG action.

- *Hypothesis:* Suisun Marsh will have higher turbidity, cooler temperatures, and high prey availability when compared to the Sacramento River.
 - *Partially supported.*
 - Suisun Marsh had consistently higher turbidity than Rio Vista. However, temperatures were higher in Suisun Marsh and prey availability was lower.
- *Hypothesis:* Delta smelt in enclosures at Belden’s Landing will have higher survival than Delta smelt in enclosures at Rio Vista.

- *Not supported.*
- Enclosures in Suisun Marsh had the same or lower survival rates as Rio Vista, although failure of anchors in 2024 may have contributed to this trend.
- *Hypothesis:* Delta smelt in enclosures at Belden’s Landing will have higher condition factor, liver glycogen, and critical thermal maximum (indicators of health) than smelt at Rio Vista.
 - *Not supported.*
 - Health results were mixed, with Rio Vista tending to have higher values.
 - CtMax was not statistically different or higher at Rio Vista (depending on year).
 - Condition factor was not significantly different or higher at Rio Vista.
 - Liver glycogen was significantly higher at Rio Vista.
- *Hypothesis:* Differences in health and survival will be driven by differences in water temperature, turbidity, prey availability, and water velocity.
 - *Partially supported.*
 - Bioenergetic modeling based on temperature, turbidity, and zooplankton abundance suggested that growth should have been higher at Belden’s Landing than Rio Vista.
 - Higher velocity at Belden’s Landing could have accounted for the discrepancy between the model and results, but additional model verification is needed to understand how Delta smelt respond to higher flows.
- *Hypothesis:* Enclosures provide a realistic setting in which to test differences in habitat suitability for Delta smelt.
 - *Not supported.*
 - Enclosures limit the fish’s ability to forage at will or seek refuge from heat and high velocity.
 - Biofouling and amphipod accumulation on the cages may have caused the diets of enclosed fish to be much different from wild fish historically caught in similar areas.

Synthesis

Low catch of Delta smelt since 2011 stymies our ability to explicitly test our overall hypothesis about the benefit of summer–fall habitat to Delta smelt population growth using contemporary information. We can use historical information to test many of our hypotheses, but changes to the system, including changes to water project operations, new invasive species, climate change, and the increasing role of cultured Delta smelt in the population may limit the applicability of our results in the future. However, in this report we draw together multiple lines of evidence to identify which time periods and drivers are most likely important in contributing to Delta smelt growth and survival (Table 25).

All the abiotic habitat analyses reinforce previous research that lower X2 in summer or fall increases the area and duration of suitable Delta smelt habitat (Feyrer et al. 2007; Nobriga et al. 2008; Feyrer et al. 2011). There was no significant difference in the habitat benefit of lower X2 in summer versus fall (Figure 8). However, the decline in appropriate temperatures for Delta smelt during the summer over the period of 2011–2024 may be contributing to lower benefits to Delta smelt in recent Wet years (2023, 2019, 2017) when compared to 2011 (Figure 9). Operation of the SMSCG also increased area of Delta smelt habitat in Suisun Marsh, but not as much as lowering X2 did (Figure 13) and caused a decrease in chlorophyll in the regions of Suisun Marsh just downstream of the SMSCG (Figure 16). While we demonstrated patterns between flow and habitat as determined by water quality, aquatic vegetation can be high in the eastern side of the Marsh in some years, so it may interfere with Delta smelt adequately using the habitat (Ferrari et al. 2014; Rasmussen et al. 2020). We did not see a correlation between higher flows or gate operations and vegetation, but vegetation appears to be increasing over time (Figure 10), with the implication that habitat quality is decreasing.

These results add a few more years of data to the wealth of existing analyses demonstrating the increase of Delta smelt abiotic habitat with increased flow and add evidence to the idea that the timing of increased flow is an important factor in predicting effectiveness of any flow action. However, in order to assess the effectiveness of the summer/fall managed flow actions, we must demonstrate that habitat area is the limiting factor in determining Delta smelt survival and population growth in both summer and fall, or that flow actions provide more direct benefits to smelt growth and survival.

The next line of evidence follows the increase in Delta smelt food supply with outflow in summer or fall. Food availability is an important part of habitat suitability, though it has not been included in many previous analyses of habitat for Delta smelt (e. g. Feyrer et al. 2011; Sommer and Mejia 2013). High densities of zooplankton prey increase Delta smelt health (Hammock et al. 2022; Hammock et al. 2015), increase smelt growth rates (Fichman 2022), and smelt occur more

frequently in areas with higher copepod abundance (Tillotson et al. 2025), so zooplankton abundance is an important component of any habitat analysis. We found that *P. forbesi* is one of the most important parts of the Delta smelt diet in the summer, though *Limnoithona tetraspina* becomes more important as salinity increases (Figure 24, Figure 25). Lower X2 (due to increased Delta outflow) and lower salinity at Belden's Landing (due to SMSCG operations or Delta outflow) correlated with increased abundance of *Pseudodiaptomus* spp. in Suisun Bay and Suisun Marsh (Figure 20). Although abundance was always lower than upstream in the Sacramento River, the flow/abundance relationship supports the hypothesis that flow transports more *Pseudodiaptomus* spp. into Suisun Bay/Marsh (as shown by Kimmerer et al. 2018). Furthermore, abundance of *Pseudodiaptomus* spp. is higher in the summer than in the fall, so the subsidies caused by the flow actions are also higher in summer when compared to fall. Therefore, the actions provide more benefits in summer than fall, and downstream abundance rarely equals upstream abundance even during the highest flow years.

Our analyses demonstrate that zooplankton may be imported from upstream into Suisun Bay/Suisun Marsh, but this pattern has been seen before. Many studies have empirically demonstrated or modeled increased abundance of *Pseudodiaptomus* spp. with increased flow (Hassrick et al. 2023; Lee et al. 2023; Kimmerer, Gross et al. 2018; Kimmerer, Ignoffo et al. 2018). However, our analysis took an integrated approach to analyze Delta smelt diet data in combination with an integrated dataset of zooplankton samples. We not only demonstrated that *Pseudodiaptomus* spp. was one of the most important diet items but also showed the increase in *Pseudodiaptomus* spp. availability using two different model frameworks (GLM and GAM) and showed that *Pseudodiaptomus* spp. abundance is generally well below the saturation point for Delta smelt (Figure 26). This suggests that increases in *Pseudodiaptomus* spp. could improve the growth and subsequent survival of Delta smelt.

While zooplankton analyses add one more piece to the puzzle, they still do not conclusively show that Delta smelt survival and population growth rates improve during years with low X2 or SMSCG operations. The sparse data we have collected on individual growth and health from 2011–2019 demonstrated that Delta smelt have increased liver weight when X2 is low and temperatures are high, but liver weights are not correlated with X2 at lower temperatures (Figure 43). We also found that individual growth rates (as measured by otolith analyses) were highest in 2011, which was a relatively cool summer with low X2, and there was a significant negative effect of higher X2 on growth rates in summer, but not in fall (Figure 30).

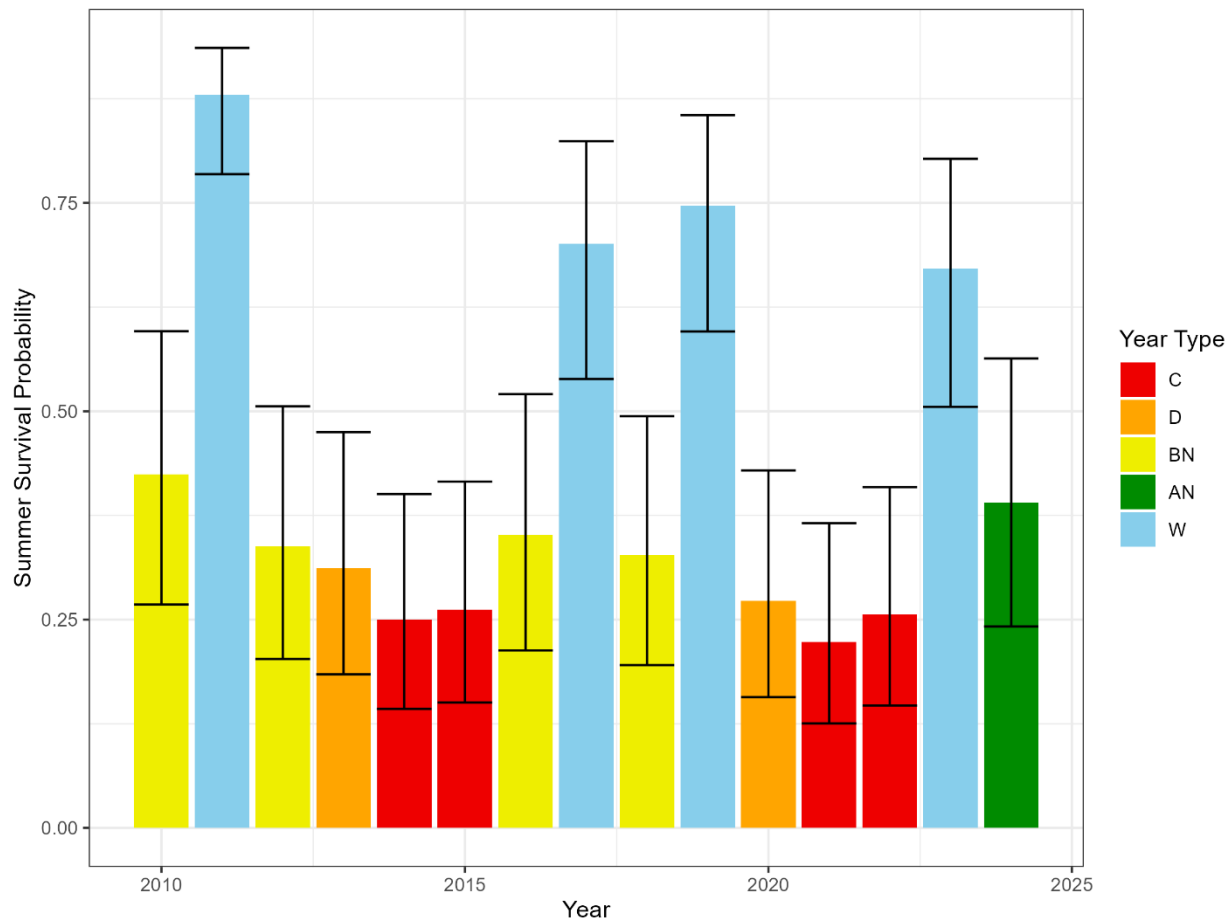
Modeling the effect of observed temperature, turbidity, and zooplankton on Delta smelt, we also found that conditions in 2011 were particularly conducive to rapid smelt growth, but none of the other years examined had conditions as conducive to growth as 2011 (Figure 32). There is a highly significant effect of X2 on modeled

potential summer growth rates, but not for fall growth rates (Figure 36) similar to the empirical evidence from otoliths. The significant effect of Summer X2 on growth supports findings by Smith and Nobriga (2023) documenting a decline in habitat availability over the course of the summer as temperatures increased and copepod densities decreased. By fall, *Pseudodiaptomus* spp. densities (and subsidies) had decreased, and temperatures in upstream regions had decreased, meaning that availability of habitat in cooler downstream regions had less effect on growth rates.

The Delta smelt enclosure studies, which were designed to test the hypothesis that habitat was better in Suisun than in the Sacramento River during a flow action, gave us opposite results from what we expected. Delta smelt grew more slowly and had lower survival and health metrics in Suisun Marsh (Figure 50), but bioenergetic modeling indicated growth should have been higher in Suisun Marsh (Figure 53). This result may have been caused by differences in velocity between the two sites and enclosure effects rather than differences in broader habitat metrics such as salinity, turbidity, food supply, or temperature, on which we based our hypothesis. However, the refuting of our hypothesis in the enclosure study does call into question our overarching hypothesis assigning higher habitat quality to Suisun Marsh than Rio Vista. In the end, we cannot draw wide-scale conclusions based on these results due to experimental differences between years, uncertainties caused by potential enclosure effects, and lack of wild-caught fish for comparison.

To scale our individual Delta smelt results up to the population level, we rely primarily on previous work by Polansky et al. (2024) and the CSAMP Delta Smelt SDM report (2024). Polansky et al. (2024) found a strong trend between summer outflow and population growth rates, with a much weaker relationship in fall. Using the Polansky et al. model and observed Delta outflow from 2010–2024 (from Dayflow), we can calculate the percentage of the population expected to survive the summer (June–August) (Figure 57). From this analysis we see that only Wet water years are likely to have resulted in greater than 50% survival over the summer. Delta outflow was the only parameter that contributed to predicted summer survival in the model, and the model does not provide a mechanism for how outflow increases survival. Increases in habitat quality and food availability are typically correlated with increased outflow (as discussed earlier in this report), but there is some variability in these relationships, and interactions between food availability and temperature may result in summer survival that is outside the predictions from the life cycle model. For example, high temperatures in 2017 and 2024 may have resulted in lower survival than would be predicted based on outflow.

Figure 57. Delta smelt summer survival probabilities based on the Polansky et al. (2024) Delta Smelt Life Cycle Model and observed values for average June–August Net Delta Outflow.



The emphasis on summer outflow instead of fall outflow also aligns with the outcomes of the CSAMP Delta Smelt SDM, which used three different smelt life cycle models (IBMR, LCME, and Limiting Factors models) to assess a range of alternative management actions and found that Summer X2 had higher benefits than Fall X2 across all three models (CSAMP Delta Smelt Technical Working Group et al. 2024). Mahardja et al. (2026) also used the IBMR to assess the relative benefits of summer and Fall X2 actions and found that summer actions had equal or greater benefits than Fall X2 actions in almost all cases.

Conclusions

We found support for some, but not all, of the hypotheses surrounding the role of summer–fall habitat in Delta smelt ecology. In general, our work supports the results from Polansky et al. (2024) and Smith and Nobriga (2023), which identifies summer, rather than fall, as the most sensitive time period for high flows to correlate to Delta smelt population growth.

- *Hypothesis:* Lower X2 in the summer and fall, and lower salinity in Belden’s Landing, will increase the extent and duration of high turbidity, low temperature, and low salinity habitat in Suisun Marsh, Suisun Bay, and Grizzly Bay.
 - *Supported.*
 - We found equal support for increased habitat in both summer and fall, though high temperatures limited habitat availability in summer.
 - Increases to habitat in Grizzly Bay were most pronounced when SMSCG operations were combined with Fall X2 actions.
- *Hypothesis:* Lower X2 in the summer and fall, and lower salinity in Belden’s Landing, will increase the abundance of *Pseudodiaptomus* spp. in Suisun Marsh, Suisun Bay, and Grizzly Bay.
 - *Supported.*
 - Lower X2 and lower salinity in Suisun Marsh were both correlated with increased *Pseudodiaptomus* spp. biomass.
 - There was a stronger relationship between X2 and *Pseudodiaptomus* spp. in summer than in fall.
- *Hypothesis:* Years with lower X2 in the summer and fall, and lower salinity at Belden’s Landing will have higher Delta smelt growth, health, and condition in the summer and fall.
 - *Supported for summer, but mixed results for fall.*
 - There is significant variation in effectiveness between years we analyzed, with 2011 showing better results than 2017, 2019, 2023, or 2024 due to the cooler temperatures and higher *Pseudodiaptomus* spp. biomass.
- *Hypothesis:* Years with lower X2 in the summer and fall, and lower salinity in Belden’s Landing, will increase the percentage of the population surviving at the end of the season.
 - *Supported for summer, but not for fall.*
 - The most recent work using the Delta Smelt Individual-Based Model and the Life Cycle Model show a stronger effect of summer outflow than fall outflow in predicting Delta smelt survival.
- *Hypothesis:* The influence of X2 and salinity in Suisun Marsh on Delta smelt habitat, food, growth, and survival will be greater in summer than in fall.
 - *Partially supported.*
 - Lower X2 increased habitat availability equally in summer and fall, but the influence of X2 on Delta smelt food, growth rates, and survival was stronger in summer than fall.

Table 25. Summary of all analyses in this report.

Hypothesis	Metric	Analysis	Prediction	Results	Support?
Smelt Habitat	#of days of good habitat	Linear models from continuous sondes	Higher in Suisun	Increase in Suisun, mostly driven by salinity	Yes, though more for X2 than SMSCG
Smelt Habitat	Area of good habitat	SCHISM habitat area models	Higher in Suisun	Increased area in Suisun Bay and Suisun Marsh with flow actions. Increases in Grizzly Bay when SMSCG and Fall X2 are combined	Yes
Smelt Habitat	Abundance of aquatic weeds	Frequency of occurrence in fish trawls	Higher in Suisun	No correlation between flow actions and abundance of weeds	No
Smelt Food	Abundance of <i>Pseudodiaptomus</i> spp.	Linear regression	Lower in Suisun with X2 or salinity at BDL	Both salinity and X2 significantly decrease abundance	Yes, though higher in summer than fall
Smelt Food	Importance of <i>Pseudodiaptomus</i> spp. in Delta smelt diets	Admunsen plots and IRI	Higher in Suisun	<i>Pseudodiaptomus</i> spp. is the most important diet item in freshwater in the summer, <i>Limnoithona</i> spp. as things get saltier	Yes
Individual Growth: Wild Fish	Liver weights	Mixed models of liver weight versus body weight, X2, and temperature	Higher	Interaction between X2 and temperature shows that liver weight increases with lower X2 at higher temperatures (summer) and for larger individuals	Supports benefit of low X2 in summer, not in fall
Individual Growth: Wild Fish	Individual smelt growth	Bioenergetic modeling	Higher	Model shows 2011 is clearly the best year, less clear patterns in other years, but X2 is a better predictor of growth in summer than fall	Supports benefit of X2 in summer, not in fall

Hypothesis	Metric	Analysis	Prediction	Results	Support?
Individual Growth: Wild Fish	Individual smelt growth	Otolith data	Higher	Growth was correlated with low X2 in summer, not in fall	Supports benefit of X2 in summer, not in fall
Individual Growth: Caged Fish	Survival	Non-parametric rank test (Kruskal)	Higher in Suisun	Lower in Suisun	No
Individual Growth: Caged Fish	Condition factor	Linear mixed-effect regression	Higher in Suisun	Lower in Suisun	No
Individual Growth: Caged Fish	Hepatosomatic index	Linear mixed-effect regression	Higher in Suisun	No consistent trend	No
Individual Growth: Caged Fish	Liver glycogen	Linear mixed-effect regression	Higher in Suisun	Lower in Suisun	No
Individual Growth: Caged Fish	Thermal tolerance	Linear model	Higher in Suisun	No consistent trend	No
Individual Growth: Caged Fish	Diets	Visual comparison	More high-value items in Suisun	More <i>Pseudodiaptomus</i> spp. in the River, less in Suisun	No
Individual Growth: Caged Fish	Growth	Bioenergetics	Higher in Suisun	Higher in Suisun	Yes, but unclear why this is different from empirical data
Smelt Population Growth and Survival	Smelt population growth	LCME results from Polansky et al	Higher the following year	Higher flow in summer had very strong relationship with summer survival and probability of $\lambda > 1$; Fall outflow did not have a significant relationship and was not included in the final model	Supports benefits of flow in summer, less in fall
Smelt Population Growth and Survival	Smelt population growth	CAMT SDM results	Higher the following year	Summer X2 had more benefits than Fall X2	Supports benefits of flow in summer, less in fall

References

- Aha NM, Moyle PB, Fanguie NA, Rypel AL, and Durand JR. 2021. "Managed Wetlands Can Benefit Juvenile Chinook Salmon in a Tidal Marsh." *Estuaries and Coasts* Volume 44: Pages 1440–1453. [Article.] Viewed online at: <https://doi.org/10.1007/s12237-020-00880-4>. Accessed: April 18, 2024.
- Ambler JW, Cloern JE, and Hutchinson A. 1985. "Seasonal Cycles of Zooplankton from San Francisco Bay." In: Cloern JE, Nichols FH, editors. *Temporal Dynamics of an Estuary: San Francisco Bay*. Springer Dordrecht. Viewed online at: <https://doi.org/10.1007/978-94-009-5528-8>.
- Amundsen P-A, Gabler H-M, and Staldvik FJ. 1996. "A New Approach to Graphical Analysis of Feeding Strategy from Stomach Contents Data—Modification of the Costello (1990) Method." *Journal of Fish Biology* Volume 48 (Issue 4): Pages 607–614. [Article.] Viewed online at: <https://doi.org/10.1111/j.1095-8649.1996.tb01455.x>.
- Arlot S, and Celisse A. 2010. "A Survey of Cross-validation Procedures for Model Selection." *Statistics Surveys* Volume 4: Pages 40–79, 40. [Article.] Viewed online at: <https://doi.org/10.1214/09-SS054>.
- Ateljevich E, Nam K, Liu L, Saha S, Wang R, and Zhang Y. 2015. "Bay-Delta SCHISM Model Developments and Applications." In: *Methodology for Flow and Salinity Estimates in the Sacramento-San Joaquin Delta and Suisun Marsh. 36th Annual Progress Report*. California Department of Water Resources. [Report].
- Ateljevich E, Nam K, Zhang Y, Wang R, and Shu Q. 2014. "Bay Delta Calibration Overview." In: *Methodology for Flow and Salinity Estimates in the Sacramento-San Joaquin Delta and Suisun Marsh. 35th Annual Progress Report*. California Department of Water Resources.
- Avila M, and Hartman R. 2020. "San Francisco Estuary Mysid Abundance in the Fall, and the Potential for Competitive Advantage of *Hyperacanthomysis longirostris* over *Neomysis mercedis*." *California Fish and Wildlife* Volume 106 (Issue 1): Pages 19–38. [Article.] Viewed online at: <https://nrm.dfg.ca.gov/FileHandler.ashx?DocumentID=175915>. Accessed: Feb. 28, 2023.

- Baerwald M, Kwan N, Pien C, Auringer G, Carson E, Cocherell D, Ellison L, Fangué N, Finger A, Gille D, Hudson H, Hung T-C, Sommer T, Stevenson T, and Schreier B. 2023. "Captive-reared Delta Smelt (*Hypomesus transpacificus*) Exhibit High Survival in Natural Conditions Using In Situ Enclosures." Plos ONE Volume 18. [Article.] Viewed online at: <https://doi.org/10.1371/journal.pone.0286027>. Accessed: Mar. 3, 2026.
- Barros A. 2021. "Zooplankton Trends in the Upper SFE, 1974-2018." IEP Newsletter Volume 40 (Issue 1): Pages 5–14. [Article.] Viewed online at: <https://cadwr.app.box.com/v/InteragencyEcologicalProgram/file/860495889310>. Accessed: Sep. 20, 2023.
- Barros A, Hartman R, Bashevkin S, and Burdi C. 2024. "Years of Drought and Salt; Decreasing Flows Determine the Distribution of Zooplankton Resources in the Estuary." San Francisco Estuary and Watershed Science Volume 22 (Issue 1). [Article.] Viewed online at: <https://doi.org/10.15447/sfews.2024v22iss1art3>. Accessed: Mar. 29, 2024.
- Bashevkin SM. 2021. "deltamapr: Spatial Data for the Bay-Delta." [R Package.] Viewed online at: <https://github.com/InteragencyEcologicalProgram/deltamapr>. Accessed: Feb. 6, 2023.
- Bashevkin SM, Burdi CE, Hartman R, and Barros A. 2023. "Long-term Trends in Seasonality and Abundance of Three Key Zooplankters in the Upper San Francisco Estuary." San Francisco Estuary and Watershed Science Volume 21 (Issue 3). [Article.] Viewed online at: <https://doi.org/10.15447/sfews.2023v21iss3art1>. Accessed: Mar. 3, 2026.
- Bashevkin SM, Hartman R, Thomas M, Barros A, Burdi C, Hennessy A, Tempel T, Kayfetz K, Alstad K, and Pien C. 2023a. "zooper v.2.5.0." Interagency Ecological Program. [Article.] Viewed online at: <https://github.com/InteragencyEcologicalProgram/zooper>. Accessed: Mar. 7, 2025.
- Bashevkin SM, Hartman R, Thomas M, Barros A, Burdi CE, Hennessy A, Tempel T, and Kayfetz K. 2022. "Five Decades (1972–2020) of Zooplankton Monitoring in the Upper San Francisco Estuary." Plos ONE Volume 17 (Issue 3). [Article.] Viewed online at: <https://doi.org/10.1371/journal.pone.0265402>. Accessed: May. 17, 2022.

- Bashevkin SM, Hartman R, Thomas M, Barros A, Burdi CE, Hennessy A, Tempel T, Kayfetz K, Alstad K, and Pien C. 2023b. "Interagency Ecological Program: Zooplankton Abundance in the Upper San Francisco Estuary from 1972-2021, An Integration of 7 Long-term Monitoring Programs. Version 4." Environmental Data Initiative. [Article.] Viewed online at: <https://doi.org/10.6073/pasta/8b646dfbeb625e308212a39f1e46f69b>. Accessed: Sep. 18, 2023.
- Bashevkin SM, Mahardja B, and Brown LR. 2022. "Warming in the Upper San Francisco Estuary: Patterns of Water Temperature Change from 5 Decades of Data." *Limnology & Oceanography* Volume 67 (Issue 5): Pages 1065–1080. [Article.] Viewed online at: <https://doi.org/10.1002/lno.12057>. Accessed: Jan. 3, 2023.
- Bashevkin SM, Perry SE, Stumpner EB, and Hartman R. 2023. "Six Decades (1959-2022) of Water Quality in the Upper San Francisco Estuary: An Integrated Database of 16 Discrete Monitoring Surveys in the Sacramento San Joaquin Delta, Suisun Bay, Suisun Marsh, and San Francisco Bay. Version 7." Environmental Data Initiative. [Article.] Viewed online at: <https://doi.org/10.6073/pasta/8dbd29c8c22f3295bbc5d3819fb51d00>. Accessed: Sep. 7, 2023.
- Bates D, Bolker B, and Walker S. 2015. "Fitting Linear Mixed-Effects Models Using lme4." *Journal of Statistical Software* Volume 67 (Issue 1). [Article.] Viewed online at: <https://doi.org/10.18637/jss.v067.i01>. Accessed: Mar. 3, 2026
- Belk MC, Benson LJ, Rasmussen J, and Peck SL. 2008. "Hatchery-induced Morphological Variation in an Endangered Fish: A Challenge for Hatchery-based Recovery Efforts." *Canadian Journal of Fisheries and Aquatic Sciences* Volume 65 (Issue 3): Pages 401–408. [Article.] Viewed online at: <https://doi.org/10.1139/f07-176>. Accessed: Mar. 3, 2026.
- Bennett WA. 2005. "Critical Assessment of the Delta Smelt Population of the San Francisco Estuary, California." *San Francisco Estuary and Watershed Science* Volume 3 (Issue 2): Article 1. [Article.] Viewed online at: <https://doi.org/10.15447/sfew.s.2005v3iss2art1>. Accessed: Jan. 3, 2023.
- Bennett WA, and Burau JR. 2015. "Riders on the Storm: Selective Tidal Movements Facilitate the Spawning Migration of Threatened Delta Smelt in the San Francisco Estuary." *Estuaries and Coasts* Volume 38 (Issue 3): Pages 826–835. [Article.] Viewed online at: <https://doi.org/10.1007/s12237-014-9877-3>. Accessed: Jan. 6, 2023.

- Bever AJ, MacWilliams ML, and Fullerton DK. 2018. "Influence of an Observed Decadal Decline in Wind Speed on Turbidity in the San Francisco Estuary." *Estuaries and Coasts* Volume 41 (Issue 7): Pages 1943–1967. [Article.] Viewed online at: <https://doi.org/10.1007/s12237-018-0403-x>. Accessed: Feb. 23, 2023.
- Bever AJ, MacWilliams ML, Herbold B, Brown LR, and Feyrer FV. 2016. "Linking Hydrodynamic Complexity to Delta Smelt (*Hypomesus transpacificus*) Distribution in the San Francisco Estuary, USA." *San Francisco Estuary and Watershed Science* Volume 14 (Issue 1). [Article.] Viewed online at: <https://doi.org/10.15447/sfews.2016v14iss1art3>. Accessed: Jan. 4, 2023.
- Bollens SM, Breckenridge JK, Vanden Hooff RC, and Cordell JR. 2011. "Mesozooplankton of the Lower San Francisco Estuary: Spatio-temporal Patterns, ENSO Effects and the Prevalence of Non-indigenous Species." *Journal of Plankton Research* Volume 33 (Issue 9): Pages 1358–1377. [Article.] Viewed online at: <https://doi.org/10.1093/plankt/fbr034>. Accessed: July 30, 2021.
- Borgnis E, and Boyer KE. 2015. "Salinity Tolerance and Competition Drive Distributions of Native and Invasive Submerged Aquatic Vegetation in the Upper San Francisco Estuary." *Estuaries and Coasts* Volume 39 (Issue 3): Pages 1–11. [Article.] Viewed online at: <https://doi.org/10.1007/s12237-015-0033-5>. Accessed: Jun. 22, 2023.
- Bosworth DH, Bashevkin SM, Bouma-Gregson K, Hartman R, and Stumpner EB. 2024. "The Anatomy of a Drought in the Upper San Francisco Estuary: Water Quality and Lower-Trophic Responses to Multi-year Droughts Over a Long-term Record (1975-2021)." *San Francisco Estuary and Watershed Science* Volume 22 (Issue 1). [Article.] Viewed online at: <https://doi.org/10.15447/sfews.2024v22iss1art1>. Accessed: Mar. 29, 2024.
- Bouley P, and Kimmerer WJ. 2006. "Ecology of a Highly Abundant, Introduced Cyclopoid Copepod in a Temperate Estuary." *Marine Ecology Progress Series* Volume 324: Pages 219–228. [Article.] Viewed online at: <https://doi.org/10.3354/meps324219>. Accessed: Feb. 28, 2023.
- Boyer K, Borgnis E, Miller J, Moderan J, and Patten M. 2013. "Habitat Values of Native SAV (*Stukenia spp.*) in the Low Salinity Zone of San Francisco Estuary, Final Project Report." Delta Stewardship Council. [Report].

- Boyer K, and Sutula M. 2015. "Factors Controlling Submersed and Floating Macrophytes in the Sacramento-San Joaquin Delta." Southern California Coastal Water Research Project. Technical Report 870. [Report.] Viewed online at:
https://ftp.sccwrp.org/pub/download/DOCUMENTS/TechnicalReports/870_FactorsControllingSubmersedAndFloatingMacrophytesInSac-SanJoaquinDelta.pdf. Accessed: Jun. 27, 2023.
- Breining-Aday SM, Slater SB, and Burdi CE. 2025. "Interagency Ecological Program: Zooplankton and Water Quality Data in the San Francisco Estuary Collected by the Summer Townet and Fall Midwater Trawl Monitoring Programs. Version 4." Environmental Data Initiative. [Article.] Viewed online at:
<https://doi.org/10.6073/pasta/daa4034cc132770e37e3f0051227cd3c>. Accessed: Mar. 6, 2025.
- Brooks M, Bolker B, Kristensen K, Magnusson A, McGillicuddy M, Skaug H, Nielsen A, Berg C, Bentham Kv, Maechler M, and Sadat N. 2025. Package 'glmmTMB': Generalized Linear Mixed Models using Template Model Builder. Version 1.1.13. [R Package.] Viewed online at:
<https://doi.org/10.6073/pasta/daa4034cc132770e37e3f0051227cd3c>. Accessed: Mar. 6, 2025.
- Brown LR, Baxter R, Castillo G, Conrad L, Culberson S, Erickson G, Feyrer F, Fong S, Gehrts K, Grimaldo L, Herbold B, Kirsch J, Mueller-Solger A, Slater S, Sommer T, Souza K, and Van Nieuwenhuysen E. 2014. "Synthesis of Studies in the Fall Low Salinity Zone of the San Francisco Estuary, September-December 2011." U.S. Department of the Interior, U.S. Geological Survey. 136. [Report.] Viewed online at: <http://dx.doi.org/10.3133/sir20145041>. Accessed: Mar. 6, 2026.
- Brown LR, Bennett WA, Wagner RW, Morgan-King T, Knowles N, Feyrer F, Schoellhamer DH, Stacey MT, and Dettinger M. 2013. "Implications for Future Survival of Delta Smelt From Four Climate Change Scenarios for the Sacramento-San Joaquin Delta, California." Estuaries and Coasts Volume 36: Page 754. [Article.] Viewed online at: <https://doi.org/10.1007/s12237-013-9585-4>. Accessed: Mar. 6, 2026.
- Burdi CE, Slater SB, Bippus TL, and Jimenez JA. 2021. "Mysid and Amphipod Length-Weight Relationships in the San Francisco Estuary." IEP Newsletter Volume 40 (Issue 1): Pages 15–25. [Article.] Viewed online at:
<https://cadwr.app.box.com/v/InteragencyEcologicalProgram/file/8604958893>. Accessed: Mar. 11, 2024.

- California Department of Fish and Wildlife (CDFW). 2020. "Incidental Take Permit for Long-Term Operation of the State Water Project in the Sacramento-San Joaquin Delta (2081-2019-066-00)." California Department of Fish and Wildlife to the California Department of Water Resources. 144. [Report.] Viewed online at: <https://water.ca.gov/-/media/DWR-Website/Web-Pages/Programs/State-Water-Project/Files/ITP-for-Long-Term-SWP-Operations.pdf>. Accessed: Feb. 6, 2023.
- California Department of Fish and Wildlife (CDFW). 2024. "Incidental Take Permit for Long-Term Operation of the State Water Project in the Sacramento-San Joaquin Delta (2081-2023-054-00)." California Department of Fish and Wildlife to the California Department of Water Resources. 122. [Report.] Viewed online at: https://water.ca.gov/-/media/DWR-Website/Web-Pages/News/Files/PDF--2081-2023-054-00-SWP-ITP_Final_20241104.pdf. Accessed: Dec. 30, 2025.
- California Department of Water Resources (CDWR). 2002. "Dayflow: And Estimate of Daily Average Delta Outflow. Dayflow Documentation 1997 Through Present." 25. [Report.] Viewed online at: <https://data.cnra.ca.gov/dataset/dayflow/resource/776b90ca-673e-4b56-8cf3-ec26792708c3>. Accessed: Jan. 4, 2023.
- California Department of Water Resources (CDWR). 2023. "Delta Smelt Summer-Fall Habitat Action 2023 Action Plan." 34 pp. [Report].
- California Natural Resources Agency. 2016. "Delta Smelt Resiliency Strategy." California Natural Resources Agency. 13 pp. [Report.] Viewed online at: <https://resources.ca.gov/CNRALegacyFiles/docs/Delta-Smelt-Resiliency-Strategy-FINAL070816.pdf>. Accessed: Mar. 3, 2026.
- Christman MA, Khanna S, Drexler JZ, and Young MJ. 2023. "Ecology and Ecosystem Effects of Submerged and Floating Aquatic Vegetation in the Sacramento-San Joaquin Delta." San Francisco Estuary and Watershed Science Volume 20 (Issue 4). [Article.] Viewed online at: <http://dx.doi.org/10.15447/sfews.2023v20iss4art3>. Accessed: Apr. 18, 2024.
- Christopherson KD, Birchell GJ, and Modde T. 2004. "Larval Razorback Sucker and Bonytail Survival and Growth in the Presence of Nonnative Fish in the Stirrup Floodplain." Final Report to the Upper Colorado River Endangered Fish Recovery Program, Denver, Colorado. Utah Division of Wildlife Resources, Publication:05-04. [Article.] Viewed online at: <https://coloradoriverrecovery.org/uc/wp-content/uploads/sites/2/2022/02/TechnicalReport-HAB-Christopherson-2004.pdf>. Accessed: Mar. 6, 2026.

- Clarke A, and Johnston NM. 1999. "Scaling of Metabolic Rate with Body Mass and Temperature in Teleost Fish." *Journal of Animal Ecology* Volume 68 (Issue 5): Pages 893–905. [Article.] Viewed online at: <https://doi.org/10.1046/j.1365-2656.1999.00337.x>. Accessed: Mar. 5, 2026.
- Conrad JL, Bibian AJ, Weinersmith KL, De Carion D, Young MJ, Crain P, Hestir EL, Santos MJ, and Sih A. 2016. "Novel Species Interactions in a Highly Modified Estuary: Association of Largemouth Bass with Brazilian Waterweed *Egeria densa*." *Transactions American Fisheries Society* Volume 145: Pages 249–263. [Article.] Viewed online at: <https://doi.org/10.1080/00028487.2015.1114521>. Accessed: Jan. 3, 2023.
- Costello M. 1990. "Predator Feeding Strategy and Prey Importance: A New Graphical Analysis." *Journal of Fish Biology* Volume 36 (Issue 2): Pages 261–263. [Article.] Viewed online at: <https://doi.org/10.1111/j.1095-8649.1990.tb05601.x>. Accessed: Mar. 3, 2026.
- CSAMP Delta Smelt Technical Working Group, Rudd S, and Crawford B. 2024. "CSAMP Delta Smelt Structured Decision Making – Round 1 Evaluation Report. Final Draft." Collaborative Science and Adaptive Management Program (CSAMP). 219 pp. [Report].
- Damon LJ, Slater SB, Baxter RD, and Fujimura RW. 2016. "Fecundity and Reproductive Potential of Wild Female Delta Smelt in the Upper San Francisco Estuary, California." *California Fish and Game* Volume 102 (Issue 4): Pages 188–210. [Article.] Viewed online at: <https://nrm.dfg.ca.gov/FileHandler.ashx?DocumentID=141865>. Accessed: Mar. 3, 2026.
- Davis BE, Hammock BG, Kwan N, Pien C, Bell H, Hartman R, Baerwald MR, Schreier B, Gille D, Acuña S, Teh S, Hung T-C, Ellison L, Cocherell DE, and Fangué NA. 2024. "Insights From a Year of Field Deployments Inform the Conservation of an Endangered Estuarine Fish." *Conservation Physiology* Volume 12 (Issue 1). [Article.] Viewed online at: <https://doi.org/10.1093/conphys/coae088>. Accessed: Jan. 2, 2025.
- Davis BE, Hansen MJ, Cocherell DE, Nguyen TX, Sommer T, Baxter RD, Fangué NA, and Todgham AE. 2019. "Consequences of Temperature and Temperature Variability on Swimming Activity, Group Structure, and Predation of Endangered Delta Smelt." *Freshwater Biology* Volume 64 (Issue 12): Pages 2156–2175. [Article.] Viewed online at: <https://doi.org/10.1111/fwb.13403>. Accessed: Feb. 6, 2023.

- Deslauriers D, Chipps SR, Breck JE, Rice JA, and Madenjian CP. 2017. "Fish Bioenergetics 4.0: An R-Based Modeling Application." *Fisheries* Volume 42 (Issue 11): Pages 586–96. [Article.] Viewed online at: <https://doi.org/10.1080/03632415.2017.1377558>. Accessed: Jun. 17, 2025.
- Dhayalan TS, Tran FD, Hung T-C, Senegal TJ, Mora V, Lewis LS, Teh SJ, and Hammock BG. 2024. "Liver Glycogen as a Sensitive Indicator of Food Limitation in Delta Smelt." *Estuaries and Coasts* Volume 47 (Issue 2): Pages 504–518. [Article.] Viewed online at: <https://doi.org/10.1007/s12237-023-01282-y>. Accessed: Mar. 3, 2026.
- Diefenderfer HL, Steyer GD, Harwell MC, LoSchiavo AJ, Neckles HA, Burdick DM, Johnson GE, Buenau KE, Trujillo E, Callaway JC, Thom RM, Ganju NK, and Twilley RR. 2021. "Applying Cumulative Effects to Strategically Advance Large-scale Ecosystem Restoration." *Frontiers in Ecology and the Environment* Volume 19 (Issue 2): Pages 108–17. [Article.] Viewed online at: <https://doi.org/10.1002/fee.2274>. Accessed: Mar. 3, 2026.
- Durand JR, O'Rear TO, and Moyle PB. 2025. "UC Davis Suisun Marsh Fish Study, CA, 1980-2024 Version 1." Environmental Data Initiative. [Article.] Viewed online at: <https://doi.org/10.6073/pasta/8e83d00acabe9754bf87d39f7e18e476>. Accessed: Nov. 18, 2025.
- Enright C, Culberson S, and Burau J. 2013. "Broad Timescale Forcing and Geomorphic Mediation of Tidal Marsh Flow and Temperature Dynamics." *Estuaries and Coasts* Volume 36 (Issue 6): Pages 1319–1339. [Article.] Viewed online at: <https://doi.org/10.1007/s12237-013-9639-7>. Accessed: Apr. 18, 2024.
- Ferrari MCO, Ranaker L, Weinersmith KL, Young MJ, Sih A, and Conrad JL. 2014. "Effects of Turbidity and an Invasive Waterweed on Predation by Introduced Largemouth Bass." *Environmental Biology of Fishes* Volume 97: Pages 79–90. [Article.] Viewed online at: <https://doi.org/10.1007/s10641-013-0125-7>. Accessed: Jan. 12, 2023.
- Feyrer F, Newman K, Nobriga M, and Sommer T. 2011. "Modeling the Effects of Future Outflow on the Abiotic Habitat of an Imperiled Estuarine Fish." *Estuaries and Coasts* Volume 34 (Issue 1): Pages 120–28. [Article.] Viewed online at: <https://doi.org/10.1007/s12237-010-9343-9>. Accessed: Mar. 3, 2026.

- Feyrer F, Newman K, Nobriga M, and Sommer T. 2016. "Delta Smelt Habitat in the San Francisco Estuary: A Reply to Manly, Fullerton, Hendrix, and Burnham's 'Comments on Feyrer et al. Modeling the Effects of Future Outflow on the Abiotic Habitat of an Imperiled Estuarine Fish'." *Estuaries and Coasts* Volume 39 (Issue 1): Pages 287–289. [Article.] Viewed online at: <https://doi.org/10.1007/s12237-015-9987-6>. Accessed: Mar. 3, 2026.
- Feyrer F, Nobriga ML, and Sommer TR. 2007. "Multidecadal Trends for Three Declining Fish Species: Habitat Patterns and Mechanisms in the San Francisco Estuary, California, USA." *Canadian Journal Fisheries & Aquatic Sciences* Volume 64: Pages 723–34. [Article.] Viewed online at: <https://doi.org/10.1139/f07-048>. Accessed: Jan. 3, 2023.
- Fichman RA. 2022. "Interactive Effects of Temperature and Food Availability on Fish Growth, Otolith Accretion, and Otolith Geochemistry in Endangered Delta Smelt (*Hypomesus transpacificus*)." University of California, Davis. Viewed online at: <https://escholarship.org/uc/item/1269h0c8>.
- FLOAT-MAST (Flow Alteration - Management Analysis and Synthesis Team). 2021. "Synthesis of Data and Studies Relating to Delta Smelt Biology in the San Francisco Estuary, Emphasizing Water Year 2017." Interagency Ecological Program. 256. [Report.] Viewed online at: <https://cadwr.app.box.com/v/InteragencyEcologicalProgram/file/838721643382>. Accessed: Feb. 23, 2022.
- Fox J, and Weisberg S. 2019. *An {R} Companion to Applied Regression*, Third Edition. Sage College Publishing.
- Frick H, Chow F, Kuhn M, Mahoney M, Silge J, and Wickham H. 2025. "rsample: General Resampling Infrastructure. Version 1.3.1." [R Package] Viewed online at: <https://doi.org/10.32614/CRAN.package.rsample>. Accessed: Mar. 3, 2026.
- Friedman JH, Hastie T, and Tibshirani R. 2010. "Regularization Paths for Generalized Linear Models via Coordinate Descent." *Journal of Statistical Software* Volume 33 (Issue 1): Pages 1–22. [Article.] Viewed online at: <https://doi.org/10.18637/jss.v033.i01>. Accessed: Jan. 5, 2026.
- Gearty AJ, Ignoffo TR, Slaughter AM, and Kimmerer WJ. 2021. "Growth and Reproductive Rates of the Dominant Copepod *Pseudodiaptomus forbesi* in Response to Environmental Factors and Habitat Type in the Northern San Francisco Estuary." *Aquatic Ecology*. [Article.] Viewed online at: <https://doi.org/10.1007/s10452-021-09863-4>. Accessed: Sep. 8, 2021.
- Gelman A, and Hill J. 2007. *Data Analysis Using Regression and Multilevel/Hierarchical Models*. Cambridge University Press.

- Glibert PM, Dugdale R, Wilkerson FP, Parker AE, Alexander J, Antell E, Blaser S, Johnson A, Lee J, Lee T, Murasko S, and Strong S. 2014. "Major-But Rare-Spring Blooms in 2014 in San Francisco Bay Delta, California, A Result of the Long-term Drought, Increased Residence Time, and Altered Nutrient Loads and Forms." *Journal of Experimental Marine Biology and Ecology* Volume 460: Pages 8–18. [Article.] Viewed online at: <https://doi.org/10.1016/j.jembe.2014.06.001>. Accessed: Jan. 4, 2023.
- Grimaldo LF, Sommer T, Van Ark N, Jones G, Holland E, Moyle PB, Smith P, and Herbold B. 2009. "Factors Affecting Fish Entrainment Into Massive Water Diversions in a Tidal Freshwater Estuary: Can Fish Losses be Managed?" *North American Journal of Fisheries Management* Volume 29: Pages 1253–1270. [Article.] Viewed online at: <https://doi.org/10.1577/M08-062.1>. Accessed: Apr. 18, 2024.
- Hamilton SA, and Murphy DD. 2018. "Analysis of Limiting Factors Across the Life Cycle of Delta Smelt (*Hypomesus transpacificus*)." *Environmental Management* Volume 62 (Issue 2): Pages 365–382. [Article.] Viewed online at: <https://doi.org/10.1007/s00267-018-1014-9>. Accessed: Jan. 3, 2023.
- Hammock BG, Hartman R, Dahlgren RA, Johnston C, Kurobe T, Lehman PW, Lewis LS, Van Nieuwenhuysse E, Ramírez-Duarte WF, Schultz AA, and Teh SJ. 2022. "Patterns and Predictors of Condition Indices in a Critically Endangered Fish." *Hydrobiologia* Volume 849: Pages 675–695. [Article.] Viewed online at: <https://doi.org/10.1007/s10750-021-04738-z>. Accessed: Mar. 3, 2026.
- Hammock BG, Hartman R, Slater SB, Hennessy A, and Teh SJ. 2019. "Tidal Wetlands Associated with Foraging Success of Delta Smelt." *Estuaries and Coasts* Volume 42: Pages 857–867. [Article.] Viewed online at: <https://doi.org/10.1007/s12237-019-00521-5>. Accessed: Sep. 7, 2021.
- Hammock BG, Hobbs JA, Slater SB, Acuña S, and Teh SJ. 2015. "Contaminant and Food Limitation Stress in an Endangered Estuarine Fish." *Science of The Total Environment* Volume 532: Pages 316–326. [Article.] Viewed online at: <http://dx.doi.org/10.1016/j.scitotenv.2015.06.018>. Accessed: Mar. 4, 2026.
- Hammock BG, Moose SP, Solis SS, Goharian E, and Teh SJ. 2019. "Hydrodynamic Modeling Coupled with Long-term Field Data Provide Evidence for Suppression of Phytoplankton by Invasive Clams and Freshwater Exports in the San Francisco Estuary." *Environmental Management* Volume 63: Pages 703–717. [Article.] Viewed online at: <https://doi.org/10.1007/s00267-019-01159-6>. Accessed: Jan. 4, 2023.

- Hammock BG, Ramírez-Duarte WF, Triana Garcia PA, Schultz AA, Avendano LI, Hung T-C, White JR, Bong Y-T, and Teh SJ. 2020. "The Health and Condition Responses of Delta Smelt to Fasting: A Time Series Experiment." *Plos ONE* Volume 15 (Issue 9). [Article.] Viewed online at: <https://doi.org/10.1371/journal.pone.0239358>. Accessed: Jun. 22, 2023.
- Hammock BG, Slater SB, Baxter RD, Fangué NA, Cocherell D, Hennessy A, Kurobe T, Tai CY, and Teh SJ. 2017. "Foraging and Metabolic Consequences of Semi-anadromy for an Endangered Estuarine Fish." *Plos ONE* Volume 12 (Issue 3). [Article.] Viewed online at: <https://doi.org/10.1371/journal.pone.0173497>. Accessed: Mar. 3, 2026.
- Hartig F. 2022. "DHARMA: Residual Diagnostics for Hierarchical (Multi-Level / Mixed) Regression Models." [R Package.] Viewed online at: <https://cran.r-project.org/package=DHARMA>. Accessed: Mar. 3, 2026.
- Hartman R, Burdi CE, Rasmussen NL, Akiyama-Lee C, and Jungbluth M. 2025. "Hidden Complexities in the Base of the Pelagic Food Web: Correlates Between Zooplankton and Chlorophyll Vary by Functional Feeding Group." *Estuaries and Coasts* Volume 48 (Issue 5): Page 129. [Article.] Viewed online at: <https://doi.org/10.1007/s12237-025-01567-4>. Accessed: Mar. 3, 2026.
- Hartman R, Stumpner E, Burdi C, Bosworth D, Maguire A, and IEP Drought Synthesis Team. 2024. "Dry Me a River: Ecological Effects of Drought in the Upper San Francisco Estuary." *San Francisco Estuary and Watershed Science* Volume 22 (Issue 1). [Article.] Viewed online at: <https://doi.org/10.15447/sfews.2024v22iss1art5>. Accessed: Mar. 21, 2024.
- Hasenbein M, Fangué NA, Geist J, Komoroske LM, Truong J, McPherson R, and Connon RE. 2016. "Assessments at Multiple Levels of Biological Organization Allow for an Integrative Determination of Physiological Tolerances to Turbidity in an Endangered Fish Species." *Conservation Physiology* Volume 4 (Issue 1). [Article.] Viewed online at: <https://doi.org/10.1093/conphys/cow004>. Accessed: Jan. 23, 2024.
- Hasenbein M, Komoroske LM, Connon R, Geist J, and Fangué NA. 2013. "Turbidity and Salinity Affect Feeding Performance and Physiological Stress in the Endangered Delta Smelt." *Integrative and Comparative Biology* Volume 53 (Issue 4): Pages 620–634. [Article.] Viewed online at: <https://doi.org/10.1093/icb/ict082>. Accessed: Jan. 12, 2023.

- Hassrick JL, Korman J, Kimmerer WJ, Gross ES, Grimaldo LF, Lee C, and Schultz AA. 2023. "Freshwater Flow Affects Subsides of a Copepod (*Pseudodiaptomus forbesi*) to Low-Salinity Food Webs in the Upper San Francisco Estuary." *Estuaries and Coasts* Volume 46: Pages 450–462. [Article.] Viewed online at: <https://doi.org/10.1007/s12237-022-01142-1>. Accessed: Sep. 1, 2023.
- Hastie T, Tibshirani R, and Friedman J. 2009. *The Elements of Statistical Learning*. Springer Nature Link.
- Hendrix AN, Fleishman E, Zillig MW, and Jennings ED. 2023. "Relations Between Abiotic and Biotic Environmental Variables and Occupancy of Delta Smelt (*Hypomesus transpacificus*) in Autumn." *Estuaries and Coasts* Volume 46 (Issue 1): Pages 149–65. [Article.] Viewed online at: <https://doi.org/10.1007/s12237-022-01100-x>. Accessed: Jan. 23, 2024.
- Hestir EL, Schoellhamer DH, Greenberg J, Morgan-King T, and Ustin SL. 2016. "The Effect of Submerged Aquatic Vegetation Expansion on a Declining Turbidity Trend in the Sacramento-San Joaquin River Delta." *Estuaries and Coasts* Volume 39 (Issue 4): Pages 1100–12. [Article.] Viewed online at: <https://doi.org/10.1007/s12237-015-0055-z>. Accessed: Jan. 4, 2023.
- Hewett SW, and Johnson BL. 1987. "A Generalized Bioenergetics Model of Fish Growth for Microcomputers." University of Wisconsin Sea Grant Institute Sea Grant Document Number: WIS- SG -87-245. [Report.] Viewed online at: <https://repository.library.noaa.gov/view/noaa/44099>. Accessed: Mar. 4, 2026.
- Higham TE, Stewart WJ, and Wainwright PC. 2015. "Turbulence, Temperature, and Turbidity: The Ecomechanics of Predator–Prey Interactions in Fishes." *Integrative and Comparative Biology* Volume 55 (Issue 1): Pages 6–20. [Article.] Viewed online at: <https://doi.org/10.1093/icb/icv052>. Accessed: Dec. 30, 2025.
- Hinton DE, Segner H, Au DW, Kullman SW, and Hardman RC. 2008. "Liver Toxicity." *The Toxicology of Fishes*: Pages 328–352. [Book Section.] CRC Press, Taylor and Francis Group.
- Hobbs JA, Bennett WA, and Burton JE. 2006. "Assessing Nursery Habitat Quality for Native Smelts (*Osmeridae*) in the Low-salinity Zone of the San Francisco Estuary." *Journal of Fish Biology* Volume 69: Pages 907–922. [Article.] Viewed online at: <https://doi.org/10.1111/j.1095-8649.2006.01176.x>. Accessed: Sep. 27, 2021.

- Hobbs JA, Denney C, Lewis L, Willmes M, Schultz A, and Burgess O. 2019. "Exploring Life History Diversity of Delta Smelt During a Period of Extreme Environmental Variability." In: Schultz AA, editor. *Directed Outflow Project: Technical Report 1*. U.S. Bureau of Reclamation, Bay-Delta Office, Mid-Pacific Region. Viewed online at: <https://www.usbr.gov/mp/bdo/docs/directed-outflow-project-tech-report1.pdf>. Accessed: Mar. 3, 2026.
- Hobbs JA, Lewis LS, Willmes M, Denney C, and Bush E. 2019. "Complex Life Histories Discovered in a Critically Endangered Fish." *Scientific Reports* Volume 9 (Issue 1): Page 16772. [Article.] Viewed online at: <https://doi.org/10.1038/s41598-019-52273-8>. Accessed: Mar. 3, 2026.
- Holmes AE, and Kimmerer WJ. 2022. "Phytoplankton Prey of an Abundant Estuarine Copepod Identified in situ Using DNA Metabarcoding." *Journal of Plankton Research* Volume 44 (Issue 2): Pages 316–332. [Article.] Viewed online at: <https://doi.org/10.1093/plankt/fbac002>. Accessed: Mar. 13, 2022.
- Hung T-C, Hammock BG, Sandford M, Stillway M, Park M, Lindberg JC, and Teh SJ. 2022. "Temperature and Salinity Preferences of Endangered Delta Smelt (*Hypomesus transpacificus*, Actinopterygii, Osmeridae)." *Scientific Reports* Volume 12 (Issue 1): Page 16558. [Article.] Viewed online at: <https://doi.org/10.1038/s41598-022-20934-w>. Accessed: Mar. 3, 2026.
- Huntsman B, Brown LR, Wulff M, Knowles N, Wagner RW, and Feyrer F. 2024. "Climate Change Scenarios for Air and Water Temperatures in the Upper San Francisco Estuary: Implications for Thermal Regimes and Delta Smelt." *San Francisco Estuary and Watershed Science* Volume 22 (Issue 2). [Article.] Viewed online at: <http://dx.doi.org/10.15447/sfews.2024v22iss2art1>. Accessed: Mar. 3, 2026.
- Hutton PH, and Roy SB. 2019. "Characterizing Early 20th Century Outflow and Salinity Intrusion in the San Francisco Estuary." *San Francisco Estuary and Watershed Science* Volume 17 (Issue 2). [Article.] Viewed online at: <https://doi.org/10.15447/sfews.2019v17iss2art4>. Accessed: Oct. 5, 2024.
- Hyndman R, Athanasopoulos G, Bergmeir C, Caceres G, Chhay L, Kuroptev K, O'Hara-Wild M, Petropoulos F, Razbash S, Wang E, and Yasmeeen F. 2025. "Forecast: Forecasting Functions for Time Series and Linear Models. Version 8.24.0." [R Package.] Viewed online at: <https://doi.org/10.32614/CRAN.package.forecast>. Accessed: Mar. 3, 2026.

- IEP-MAST, Baxter R, Brown LR, Castillo G, Conrad L, Culberson S, Dekar M, Feyrer F, Grimaldo L, Hunt T, Kirsch J, Mueller-Solger A, Slater S, Sommer T, and Souza K. 2015. "An Updated Conceptual Model for Delta Smelt: Our Evolving Understanding of an Estuarine Fish." Interagency Ecological Program. [Report.] Viewed online at: <https://cadwr.app.box.com/v/InteragencyEcologicalProgram/file/7637441600>. Accessed: Mar. 29, 2024.
- Jeffries KM, Connon RE, Davis BE, Komoroske LM, Britton MT, Sommer T, Todgham AE, and Fangué NA. 2016. "Effects of High Temperatures on Threatened Estuarine Fishes During Periods of Extreme Drought." *The Journal of Experimental Biology* Volume 219 (Issue 11): Pages 1705–1716. [Article.] Viewed online at: <https://doi.org/10.1242/jeb.134528>. Accessed: Jan. 3, 2023.
- Jungbluth MJ, Burns J, Grimaldo L, Slaughter A, Katla A, and Kimmerer W. 2021. "Feeding Habits and Novel Prey of Larval Fishes in the Northern San Francisco Estuary." *Environmental DNA*: Pages 1–22. [Article.] Viewed online at: <https://doi.org/10.1002/edn3.226>. Accessed: Oct. 27, 2021.
- Kayfetz K, Bashevkin SM, Thomas M, Hartman R, Burdi CE, Hennessy A, Tempel T, and Barros A. 2020. "Zooplankton Integrated Dataset Metadata Report. IEP Technical Report 93." California Department of Water Resources. 72 pp. [Report.] Viewed online at: <https://deltacouncil.ca.gov/pdf/science-program/2020-11-09-iep-93-zooplankton-integrated-dataset-metadata.pdf>. Accessed: Mar. 8, 2026.
- Kayfetz K, and Kimmerer W. 2017. "Abiotic and Biotic Controls on the Copepod *Pseudodiaptomus forbesi* in the Upper San Francisco Estuary." *Marine Ecology Progress Series* Volume 581: Pages 85–101. [Article.] Viewed online at: <https://doi.org/10.3354/meps12294>. Accessed: Sep. 7, 2021.
- Killen SS, Costa I, Brown JA, and Gamperl AK. 2006. "Little Left in the Tank: Metabolic Scaling in Marine Teleosts and Its Implications for Aerobic Scope." *Proceedings of the Royal Society B: Biological Sciences* Volume 274 (Issue 1608): Pages 431–438. [Article.] Viewed online at: <https://doi.org/10.1098/rspb.2006.3741>. Accessed: Jan. 6, 2026.
- Kimmerer W. 2004. "Open Water Processes of the San Francisco Bay Estuary: From Physical Forcing to Biological Responses." *San Francisco Estuary and Watershed Science* Volume 2 (Issue 1). [Article.] Viewed online at: <https://doi.org/10.15447/sfew.2004v2iss1art1>. Accessed: Jan. 6, 2023.

- Kimmerer WJ. 2002. "Effects of Freshwater Flow on Abundance of Estuarine Organisms: Physical Effects or Trophic Linkages?" *Marine Ecology Progress Series* Volume 243: Pages 39–55. [Article.] Viewed online at: <https://doi.org/10.3354/meps243039>. Accessed: Sep. 27, 2021.
- Kimmerer WJ, Burau JR, and Bennett WA. 2002. "Persistence of Tidally-oriented Vertical Migration by Zooplankton in a Temperate Estuary." *Estuaries* Volume 25 (Issue 3): Pages 359–371. [Article.] Viewed online at: <https://doi.org/10.1007/BF0269597>. Accessed: Sep. 27, 2021.
- Kimmerer WJ, Gross ES, and MacWilliams ML. 2009. "Is the Response of Estuarine Nekton to Freshwater Flow in the San Francisco Estuary Explained by Variation in Habitat Volume?" *Estuaries and Coasts* Volume 32 (Issue 2): Pages 375–389. [Article.] Viewed online at: <https://doi.org/10.1007/s12237-008-9124-x>. Accessed: Jan. 9, 2023.
- Kimmerer WJ, Gross ES, Slaughter AM, and Durand JR. 2018. "Spatial Subsidies and Mortality of an Estuarine Copepod Revealed Using a Box Model." *Estuaries and Coasts* Volume 42: Pages 218–336. [Article.] Viewed online at: <https://doi.org/10.1007/s12237-018-0436-1>. Accessed: Jan. 3, 2023.
- Kimmerer WJ, Ignoffo TR, Kayfetz KR, and Slaughter AM. 2018. "Effects of Freshwater Flow and Phytoplankton Biomass on Growth, Reproduction, and Spatial Subsidies of the Estuarine Copepod *Pseudodiaptomus forbesi*." *Hydrobiologia* Volume 807 (Issue 1): Pages 113–30. [Article.] Viewed online at: <https://doi.org/10.1007/s10750-017-3385-y>. Accessed: Aug. 7, 2021.
- Kimmerer WJ, Ignoffo TR, Slaughter AM, and Gould AL. 2014. "Food-limited Reproduction and Growth of Three Copepod Species in the Low-salinity Zone of the San Francisco Estuary." *Journal of Plankton Research* Volume 36 (Issue 3): Pages 722–35. [Article.] Viewed online at: <https://doi.org/10.1093/plankt/fbt128>. Accessed: Feb. 28, 2023.
- Kimmerer WJ, and Lougee L. 2015. "Bivalve Grazing Causes Substantial Mortality to an Estuarine Copepod Population." *Journal of Experimental Marine Biology and Ecology* Volume 473: Pages 53–63. [Article.] Viewed online at: <http://dx.doi.org/10.1016/j.jembe.2015.08.005>. Accessed: Mar. 4, 2026.
- Kimmerer WJ, MacWilliams ML, and Gross ES. 2013. "Variation of Fish Habitat and Extent of the Low-salinity Zone with Freshwater Flow in the San Francisco Estuary." *San Francisco Estuary and Watershed Science* Volume 11 (Issue 4): Page 16. [Article.] Viewed online at: <https://escholarship.org/uc/item/3pz7x1x8>. Accessed: Sep. 1, 2023.

- Kimmerer WJ, and Rose KA. 2018. "Individual-Based Modeling of Delta Smelt Population Dynamics in the Upper San Francisco Estuary III. Effects of Entrainment Mortality and Changes in Prey." *Transactions of the American Fisheries Society* Volume 147 (Issue 1): Pages 223–243. [Article.] Viewed online at: <https://doi.org/10.1002/tafs.10015>. Accessed: Mar. 3, 2026.
- Kimmerer WJ, and Thompson JK. 2014. "Phytoplankton Growth Balanced by Clam and Zooplankton Grazing and Net Transport Into the Low-salinity Zone of the San Francisco Estuary." *Estuaries and Coasts* Volume 37: Pages 1202–1218. [Article.] Viewed online at: <https://doi.org/10.1007/s12237-013-9753-6>. Accessed: Jan. 4, 2023.
- Knutson Jr AC, and Orsi JJ. 1983. "Factors Regulating Abundance and Distribution of the Shrimp *Neomysis mercedis* in the Sacramento-San Joaquin Estuary." *Transactions of the American Fisheries Society* Volume 112 (Issue 4): Pages 476–85. [Article.] Viewed online at: [https://doi.org/10.1577/1548-8659\(1983\)112<476:FRAADO>2.0.CO;2](https://doi.org/10.1577/1548-8659(1983)112<476:FRAADO>2.0.CO;2). Accessed: Jan. 3, 2026.
- Komoroske LM, Connon RE, Jeffries KM, and Fangué NA. 2015. "Linking Transcriptional Responses to Organismal Tolerance Reveals Mechanisms of Thermal Sensitivity in a Mesothermal Endangered Fish." *Molecular Ecology*. [Article.] Viewed online at: <https://doi.org/10.1111/mec.13373>. Accessed: Mar. 4, 2026.
- Komoroske LM, Connon RE, Lindberg J, Cheng BS, Castillo G, Hasenbein M, and Fangué NA. 2014. "Ontogeny Influences Sensitivity to Climate Change Stressors in an Endangered Fish." *Conservation Physiology* Volume 2: Page 13. [Article.] Viewed online at: <https://doi.org/10.1093/conphys/cou008>. Accessed: Jun. 22, 2023.
- Komoroske LM, Jeffries KM, Whitehead A, Roach JL, Britton M, Connon RE, Verhille C, Brander SM, and Fangué NA. 2021. "Transcriptional Flexibility During Thermal Challenge Corresponds with Expanded Thermal Tolerance in an Invasive Compared to Native Fish." *Evolutionary Applications* Volume 14 (Issue 4): Pages 931–949. [Article.] Viewed online at: <https://doi.org/10.1111/eva.13172>. Accessed: Mar. 3, 2026.
- Kratina P, and Winder M. 2015. "Biotic Invasions Can Alter Nutritional Composition of Zooplankton Communities." *Oikos* Volume 124 (Issue 10): Pages 1337–1345. [Article.] Viewed online at: <https://doi.org/10.1111/oik.02240>. Accessed: Feb. 28, 2023.

- Kring SA, Figary SE, Boyer GL, Watson SB, and Twiss MR. 2014. "Rapid in situ Measures of Phytoplankton Communities Using the BBE FluoroProbe: Evaluation of Spectral Calibration, Instrument Intercompatibility, and Performance Range." *Canadian Journal of Fisheries and Aquatic Sciences* Volume 71 (Issue 7): Pages 1087–1095. [Article.] Viewed online at: <https://doi.org/10.1139/cjfas-2013-0599>. Accessed: Mar. 4, 2026.
- Kuhn M. 2008. "Building Predictive Models in R Using the Caret Package." *Journal of Statistical Software* Volume 28 (Issue 5): Pages 1–26. [Article.] Viewed online at: <https://doi.org/10.18637/jss.v028.i05>. Accessed: Jan. 5, 2026.
- Lee CY, Smith AG, Hassrick JL, Kalmbach AJ, Sabal MC, Cox DM, Grimaldo L, and Schultz A. 2023. "Flow Augmentations Modify an Estuarine Prey Field." *San Francisco Estuary and Watershed Science* Volume 21 (Issue 2). [Article.] Viewed online at: <http://dx.doi.org/10.15447/sfews.2023v21iss2art1>. Accessed: Dec. 10, 2024.
- Lenth RV, Buerkner P, Herve M, Love J, Riebl H, and Singmann H. 2024. "Package 'emmeans': Estimated Marginal Means, aka Least-Squares Means. Version 1.10.4." [R Package.] Viewed online at: <https://cran.r-project.org/web/packages/emmeans/index.html>. Accessed: Aug. 16, 2025.
- Lewis LS, Denney C, Willmes M, Xieu W, Fichman RA, Zhao F, Hammock BG, Schultz A, Fangue N, and Hobbs JA. 2021. "Otolith-based Approaches Indicate Strong Effects of Environmental Variation on Growth of a Critically Endangered Estuarine Fish." *Marine Ecology Progress Series* Volume 676: Pages 37–56. [Article.] Viewed online at: <https://doi.org/10.3354/meps13848>. Accessed: Mar. 3, 2026.
- Lüdecke D, Ben-Shachar M, Patil I, Waggoner P, and Makowski D. 2021. "Performance: An R Package for Assessment, Comparison and Testing of Statistical Models." *Journal of Open Source Software* Volume 6 (Issue 60): Page 3139. [Article.] Viewed online at: <https://doi.org/10.21105/joss.03139>. Accessed: Mar. 3, 2026.
- Lusardi RA, Hammock BG, Jeffres CA, Dahlgren RA, and Kiernan JD. 2020. "Oversummer Growth and Survival of Juvenile Coho Salmon (*Oncorhynchus kisutch*) Across a Natural Gradient of Stream Water Temperature and Prey Availability: An in situ Enclosure Experiment." *Canadian Journal of Fisheries and Aquatic Sciences* Volume 77 (Issue 2): Pages 413–24. [Article.] Viewed online at: <https://doi.org/10.1139/cjfas-2018-0484>. Accessed: Mar. 4, 2026.

- Mahardja B, Bashevkin SM, Pien C, Khanna S, Pearson D, Davis B, and Basu R. 2025. "Heatwaves and Rising Temperatures in the Upper San Francisco Estuary: Trends and Effects on Ecosystems and Humans." *San Francisco Estuary and Watershed Science* Volume 23 (Issue 1). [Article.] Viewed online at: <http://dx.doi.org/10.15447/sfews.2025v23iss1art4>. Accessed: Mar. 3, 2026.
- Mahardja B, Smith WE, Healy BD, Koizumi C, Nobriga ML, Acuña S, Crawford B, Arend KK, and Runge MC. 2026. "The Effects of Scientific Uncertainty and Values Trade-offs on Flow Management Decisions for an Endangered Fish." *Ecosphere*. [Article.] Viewed online at: <https://doi.org/10.1002/ecs2.70558>. Accessed: Mar. 3, 2026.
- Manly BFJ, Hendrix AN, and Burnham KP. 2015. "Comments on Feyrer et al. "Modeling the Effects of Future Outflow on the Abiotic Habitat of an Imperiled Estuarine Fish"." *Estuaries and Coasts* Volume 38: Pages 1815–1820. [Article.] Viewed online at: <https://doi.org/10.1007/s12237-014-9905-3>. Accessed: Mar. 3, 2026.
- Martin G, Twigg L, and Robinson D. 1996. "Comparison of the Diet of Feral Cats From Rural and Pastoral Western Australia." *Wildlife Research* Volume 23 (Issue 4): Pages 475–484. [Article.] Viewed online at: <https://doi.org/10.1071/WR9960475>. Accessed: Jan. 4, 2026.
- Maunder MN, and Deriso RB. 2011. "A State-space Multistage Life Cycle Model to Evaluate Population Impacts in the Presence of Density Dependence: Illustrated with Application to Delta Smelt (*Hypomesus transpacificus*)." *Canadian Journal Fisheries & Aquatic Sciences* Volume 68: Pages 1285–1306. [Article.] Viewed online at: <https://doi.org/10.1139/f2011-071>. Accessed: Mar. 6, 2026.
- McCormick A, Burdi CE, Mahardja BM, Goodman DM, Mitchell SA, Lee CY, Teh SJ, and Hammock BG. 2025. "The Influence of Zooplankton Availability on Delta Smelt Condition and Foraging Across Habitat Contexts." *San Francisco Estuary and Watershed Science* Volume 23 (Issue 4). [Article.] Viewed online at: <https://doi.org/10.15447/sfews.2025v23iss4art5>. Accessed: Mar. 3, 2026.
- Merz JE, Bergman PS, Simonis JL, Delaney D, Pierson J, and Anders P. 2016. "Long-term Seasonal Trends in the Prey Community of Delta Smelt (*Hypomesus transpacificus*) Within the Sacramento-San Joaquin Delta, California." *Estuaries and Coasts* Volume 39 (Issue 5): Pages 1526–1536. [Article.] Viewed online at: <https://doi.org/10.1007/s12237-016-0097-x>. Accessed: Sep. 7, 2021.

- Merz JE, Hamilton S, Bergman PS, and Cavallo B. 2011. "Spatial Perspective for Delta Smelt: A Summary of Contemporary Survey Data." California Fish & Game Volume 97 (Issue 4): Pages 164–189. [Article.] Viewed online at: <https://nrm.dfg.ca.gov/FileHandler.ashx?DocumentID=46489>. Accessed: Feb. 28, 2023.
- Miller WJ, Manly BF, Murphy DD, Fullerton D, and Ramey RR. 2012. "An Investigation of Factors Affecting the Decline of Delta Smelt (*Hypomesus transpacificus*) in the Sacramento-San Joaquin Estuary." Reviews in Fisheries Science Volume 20 (Issue 1): Pages 1–19. [Article.] Viewed online at: <https://doi.org/10.1080/10641262.2011.634930>. Accessed: Mar. 5, 2026.
- Moyle P, Bennett W, Durand J, Fleenor W, Gray B, Hanak E, Lund J, and Mount J. 2012. "Where the Wild Things Aren't: Making the Delta a Better Place for Native Species." Public Policy Institute of California. [Report.] Viewed online at: <https://www.ppic.org/publication/where-the-wild-things-arent-making-the-delta-a-better-place-for-native-species/>. Accessed: Apr. 18, 2024.
- Moyle PB, Brown LR, Durand JR, and Hobbs JA. 2016. "Delta Smelt: Life History and Decline of a Once-abundant Species in the San Francisco Estuary." San Francisco Estuary and Watershed Science Volume 14 (Issue 2). [Article.] Viewed online at: <http://dx.doi.org/10.15447/sfews.2016v14iss2art6>. Accessed: Jan. 3, 2023.
- Moyle PB, Hobbs JA, and Durand JR. 2018. "Delta Smelt and Water Politics in California." Fisheries Volume 43 (Issue 1): Pages 42–50. [Article.] Viewed online at: <https://doi.org/10.1002/fsh.10014>. Accessed: Feb. 23, 2023.
- Moyle PB, Manfree AD, and Fiedler PL. 2014. Suisun Marsh: Ecological History and Possible Futures. University of California Press.
- Murphy DD, and Weiland PS. 2019. "The Low-salinity Zone in the San Francisco Estuary as a Proxy for Delta Smelt Habitat: A Case Study in the Misuse of Surrogates in Conservation Planning." Ecological Indicators Volume 105: Pages 29–35. [Article.] Viewed online at: <https://doi.org/10.1016/j.ecolind.2019.05.053>. Accessed: Mar. 3, 2026.
- Nobriga ML, Sommer TR, Feyrer F, and Fleming K. 2008. "Long-term Trends in Summertime Habitat Suitability for Delta Smelt (*Hypomesus transpacificus*)." San Francisco Estuary and Watershed Science Volume 6 (Issue 1). [Article.] Viewed online at: <https://doi.org/10.15447/sfews.2008v6iss1art1>. Accessed: Mar. 4, 2026.

- Orsi JJ, and Knutson Jr. AC. 1979. "The Role of Mysid Shrimp in the Sacramento-San Joaquin Estuary and Factors Affecting Their Abundance and Distribution." In: Conomos TJ, editor. *San Francisco Bay: The Urbanized Estuary*. Pacific Division of the American Association for the Advancement of Science. Viewed online at: [https://doi.org/10.1577/1548-8659\(1983\)112%3C476:FRAADO%3E2.0.CO;2](https://doi.org/10.1577/1548-8659(1983)112%3C476:FRAADO%3E2.0.CO;2). Accessed: Mar. 4, 2026.
- Orsi JJ, and Mecum WL. 1996. "Food Limitation as the Probable Cause of a Long-term Decline in the Abundance of *Neomysis mercedis* the Opossum Shrimp in the Sacramento-San Joaquin Estuary." In: Hollibaugh JT, editor. *San Francisco Bay the Ecosystem*. Pacific Division of the American Association for the Advancement of Science. Viewed online at: https://www.waterboards.ca.gov/waterrights/water_issues/programs/bay_delta/docs/cmnt091412/sldmwa/orsi_mecum_1996.pdf. Accessed: Mar. 4, 2026.
- Owens S, Ignoffo TR, Frantzich J, Slaughter A, and Kimmerer W. 2019. "High Growth Rates of a Dominant Calanoid Copepod in the Northern San Francisco Estuary." *Journal of Plankton Research* Volume 41 (Issue 6): Pages 939–954. [Article.] Viewed online at: <https://doi.org/10.1093/plankt/fbz064>. Accessed: Jun. 14, 2020.
- Packard GC, and Boardman TJ. 1988. "The Misuse of Ratios, Indices, and Percentages in Ecophysiological Research." *Physiological Zoology* Volume 61 (Issue 1): Pages 1–9. [Article.] Viewed online at: <https://doi.org/10.1086/physzool.61.1.30163730>. Accessed: Mar. 4, 2026.
- Pasparakis C, Lohroff T, Biefel F, Cocherell DE, Carson EW, Hung T-C, Cannon RE, Fanguie NA, and Todgham AE. 2023. "Effects of Turbidity, Temperature and Predation Cue on the Stress Response of Juvenile Delta Smelt." *Conservation Physiology* Volume 11 (Issue 1). [Article.] Viewed online at: <https://doi.org/10.1093/conphys/coad036>. Accessed: Mar. 3, 2026.
- Pedersen EJ, Miller DL, Simpson GL, and Ross N. 2019. "Hierarchical Generalized Additive Models in Ecology: An Introduction with MGCV." *PeerJ* Volume 7. [Article.] Viewed online at: <https://doi.org/10.7717/peerj.6876>. Accessed: Mar. 3, 2026.
- Pien C, Hartman R, Bush E, Lehman P, and Davis B. 2025. "Thermal Stress and Suitability for Aquatic Species in the San Francisco Estuary." *San Francisco Estuary and Watershed Science* Volume 23 (Issue 2). [Article.] Viewed online at: <http://dx.doi.org/10.15447/sfew.2025v23iss2art3>. Accessed: Mar. 3, 2026.

- Pinkas L, Oliphant MS, and Iverson ILK. 1970. "Fish Bulletin 152. Food Habits of Albacore, Bluefin Tuna, and Bonito In California Waters." UC San Diego: Library – Scripps Digital Collection. [Article.] Viewed online at: <https://escholarship.org/uc/item/7t5868rd>. Accessed: Mar. 4, 2026.
- Polansky L, Mitchell L, and Nobriga ML. 2024. "Identifying Minimum Freshwater Habitat Conditions for an Endangered Fish Using Life Cycle Analysis." *Conservation Science and Practice* Volume 6 (Issue 5). [Article.] Viewed online at: <https://doi.org/10.1111/csp2.13124>. Accessed: Mar. 3, 2026.
- Polansky L, Newman KB, and Mitchell L. 2021. "Improving Inference for Nonlinear State-space Models of Animal Population Dynamics Given Biased Sequential Life Stage Data." *Biometrics* Volume 77 (Issue 1): Pages 352–361. [Article.] Viewed online at: <https://doi.org/10.1111/biom.13267>. Accessed: Mar. 3, 2026.
- Post JR, and Lee JA. 1996. "Metabolic Ontogeny of Teleost Fishes." *Canadian Journal of Fisheries and Aquatic Sciences* Volume 53 (Issue 4): Pages 910–923. [Article.] Viewed online at: <https://doi.org/10.1139/f95-278>. Accessed: Mar. 3, 2026.
- Ramírez-Duarte WF, Hammock BG, Schultz A, Acuña S, and Teh SJ. 2019. "RNA-DNA Ratio as Proxy of Short-Term Growth in Juvenile Delta Smelt in the Sacramento-San Joaquin Delta and San Francisco Estuary." In: Schultz AA, editor. *Directed Outflow Project: Technical Report 1*. U.S. Bureau of Reclamation, Bay-Delta Office, Mid-Pacific Region. Viewed online at: <https://www.usbr.gov/mp/bdo/docs/directed-outflow-project-technical-report1.pdf>. Accessed: Mar. 3, 2026.
- Rasmussen N, Conrad JL, Green H, Khanna S, Caudill J, Gilbert P, Goertler P, Wright H, Hoffmann K, Lesmeister S, Jenkins J, Takata L, Boswort D, Flynn T, Hard E, and Sommer T. 2020. "2017-2018 Delta Smelt Resiliency Strategy Action for Enhanced Control of Aquatic Weeds and Understanding Effects of Herbicide Treatment on Habitat." 332 pp. [Report.] Viewed online at: <https://cadwr.box.com/s/wisajd3e26qhu7t6pmw0g5lpqbor6la>. Accessed: Mar. 3, 2026.
- Riaño D, Khanna S, Lay M, Rasmussen NL, Kato A, and Ustin SL. 2025. "Assessment of the Effect of Management Activities Like a Drought Salinity Barrier and Herbicide Treatments on the Spread of Submersed and Floating Aquatic Estuary Macrophytes." *Science of The Total Environment* Volume 959: Page 178138. [Article.] Viewed online at: <https://doi.org/10.1016/j.scitotenv.2024.178138>. Accessed: Mar. 3, 2026.

- Richardson E, Kraus T, O'Donnell K, Soto-Perez J, Sturgeon C, Stumpner E, and Bergamaschi B. 2025. "Assessing Spatial Variability of Nutrients, Phytoplankton, and Related Water-quality Constituents in the California Sacramento–San Joaquin Delta at the Landscape Scale—Comparison of Four (2018, 2020, 2021, 2022) Spring High-resolution Mapping Surveys." USGS Open File Report 2025-5035. [Report.] Viewed online at: <https://doi.org/10.3133/sir20255035>. Accessed: Mar. 3, 2026.
- Rose KA, Kimmerer WJ, Edwards KP, and Bennett WA. 2013a. "Individual-Based Modeling of Delta Smelt Population Dynamics in the Upper San Francisco Estuary: I. Model Description and Baseline Results." Transactions of the American Fisheries Society Volume 142 (Issue 5): Pages 1238–1259. [Article.] Viewed online at: <https://doi.org/10.1080/00028487.2013.799518>. Accessed: Mar. 3, 2026.
- Rose KA, Kimmerer WJ, Edwards KP, and Bennett WA. 2013b. "Individual-based Modeling of Delta Smelt Population Dynamics in the Upper San Francisco Estuary: II. Alternative Baselines and Good Versus Bad Years." Transactions American Fisheries Society Volume 142: Pages 1260–1272. [Article.] Viewed online at: <https://doi.org/10.1080/00028487.2013.799519>. Accessed: Mar. 3, 2026.
- Schmidt-Nielsen K. 1972. "Locomotion: Energy Cost of Swimming, Flying, and Running." Science Volume 177 (Issue 4045): Pages 222–228. [Article.] Viewed online at: <https://doi.org/10.1126/science.177.4045.222>. Accessed: Mar. 3, 2026.
- Schoellhamer DH. 2011. "Sudden Clearing of Estuarine Waters Upon Crossing the Threshold From Transport to Supply Regulation of Sediment Transport as an Erodible Sediment Pool is Depleted: San Francisco Bay, 1999." Estuaries and Coasts Volume 34 (Issue 5): Pages 885–899. [Article.] Viewed online at: <https://doi.org/10.1007/s12237-011-9382-x>. Accessed: Feb. 6, 2023.
- Schultz AA, editor. 2019. *Directed Outflow Project: Technical Report 1*. U.S. Bureau of Reclamation, Bay-Delta Office, Mid-Pacific Region. Viewed online at: <https://www.usbr.gov/mp/bdo/docs/directed-outflow-project-tech-report1.pdf>. Accessed: Mar. 3, 2026.

- Schultz AA, Grimaldo L, Hassrick J, Kalmbach A, Smith A, Burgess OT, Barnard D, and Brandon J. 2019. "Effect of Isohaline (X2) and Region on Delta Smelt Habitat, Prey and Distribution During the Summer and Fall: Insights into Managed Flow Actions in a Highly Modified Estuary." In: Schultz AA, editor. *Directed Outflow Project: Technical Report 1*. U.S. Bureau of Reclamation, Bay-Delta Office, Mid-Pacific Region. Viewed online at: <https://www.usbr.gov/mp/bdo/docs/directed-outflow-project-tech-report1.pdf>. Accessed: Mar. 3, 2026.
- Schultz AA, and Kalmbach AJ. 2023. "Directed Outflow Project Lower Trophic Study Version 4." Environmental Data Initiative. [Dataset.] Viewed online at: <https://doi.org/10.6073/pasta/86a01140eb3bb756ee9f7f8dab8aefc4>. Accessed: Sep. 19, 2023.
- Shaw CT. 2025. "Interagency Ecological Program Zooplankton Study Version 12." Environmental Data Initiative. [Dataset.] Viewed online at: <https://doi.org/10.6073/pasta/aa49aa972b42cae2d6017aa430914f3f>. Accessed: Mar. 3, 2026.
- Simenstad CA, and Cordell JR. 2000. "Ecological Assessment Criteria for Restoring Anadromous Salmonid Habitat in Pacific Northwest Estuaries." *Ecological Engineering* Volume 15 (Issue 3–4): Pages 283–302. [Article.] Viewed online at: [http://dx.doi.org/10.1016/S0925-8574\(00\)00082-3](http://dx.doi.org/10.1016/S0925-8574(00)00082-3). Accessed: Apr. 18, 2024.
- Slater SB, and Baxter RD. 2014. "Diet, Prey Selection and Body Condition of Age-0 Delta Smelt, *Hypomesus transpacificus*, in the Upper San Francisco Estuary." *San Francisco Estuary and Watershed Science* Volume 14 (Issue 4). [Article.] Viewed online at: <http://dx.doi.org/10.15447/sfews.2014v12iss3art1>. Accessed: Sep. 7, 2021.
- Slater SB, Schultz A, Hammock BG, Hennessy A, and Burdi C. 2019. "Patterns of Zooplankton Consumption by Juvenile and Adult Delta Smelt (*Hypomesus transpacificus*)." In: Schultz AA, editor. *Directed Outflow Project: Technical Report 1*. U.S. Bureau of Reclamation, Bay-Delta Office, Mid-Pacific Region. Viewed online at: <https://www.usbr.gov/mp/bdo/docs/directed-outflow-project-tech-report1.pdf>. Accessed: Mar. 3, 2026.
- Smith WE, and Nobriga ML. 2023. "A Bioenergetics-based Index of Habitat Suitability: Spatial Dynamics of Foraging Constraints and Food Limitation for a Rare Estuarine Fish." *Transactions of the American Fisheries Society* Volume 152 (Issue 5). [Article.] Viewed online at: <https://doi.org/10.1002/tafs.10427>. Accessed: Mar. 3, 2026.

- Smith WE, Polansky L, and Nobriga ML. 2021. "Disentangling Risks to an Endangered Fish: Using a State-space Life Cycle Model to Separate Natural Mortality From Anthropogenic Losses." *Canadian Journal of Fisheries and Aquatic Sciences* Volume 78 (Issue 8): Pages 1008–1029. [Article.] Viewed online at: <https://doi.org/10.1139/cjfas-2020-0251>. Accessed: Jan. 4, 2023.
- Sogard S. 1997. "Size-Selective Mortality in the Juvenile Stage of Teleost Fishes: A Review." *Bulletin of Marine Science* Volume 60 (Issue 3): Pages 1129–1157. [Article.] Viewed online at: <https://www.ingentaconnect.com/content/umrsmas/bullmar/1997/00000060/00000003/art00029>. Accessed: Mar. 3, 2026.
- Sommer T, Hartman R, Koller M, Koohafkan M, Conrad JL, MacWilliams M, Bever A, Burdi C, and Beakes MP. 2020. "Evaluation of a Large-scale Flow Manipulation to the Upper San Francisco Estuary: Response of Habitat Conditions for an Endangered Native Fish." *Plos ONE* Volume 15 (Issue 10). [Article.] Viewed online at: <https://doi.org/10.1371/journal.pone.0234673>. Accessed: Jan. 4, 2023.
- Sommer T, and Mejia F. 2013. "A Place to Call Home: A Synthesis of Delta Smelt Habitat in the Upper San Francisco Estuary." *San Francisco Estuary and Watershed Science* Volume 11 (Issue 2): Page 25. [Article.] Viewed online at: <https://doi.org/10.15447/sfews.2013v11iss2art4>. Accessed: Jan. 3, 2023.
- Sommer T, Mejia FH, Nobriga ML, Feyrer F, and Grimaldo L. 2011. "The Spawning Migration of Delta Smelt in the Upper San Francisco Estuary." *San Francisco Estuary and Watershed Science* Volume 9 (Issue 2): Page 16. [Article.] Viewed online at: <https://doi.org/10.15447/sfews.2014v9iss2art2>. Accessed: Mar. 3, 2026.
- State Water Resources Control Board (SWRCB). 2017. "Scientific Basis Report in Support of New and Modified Requirements for Inflows from the Sacramento River and Its Tributaries and Eastside Tributaries to the Delta, Delta Outflows, Cold Water Habitat, and Interior Delta Flows." 427 pp. [Report.] Viewed online at: https://www.waterboards.ca.gov/bay_delta/docs/2022/201710-bdphaseII-sciencereport.pdf. Accessed: Mar. 3, 2026.
- Stern MA, Flint LE, Flint AL, Knowles N, and Wright SA. 2020. "The Future of Sediment Transport and Streamflow Under a Changing Climate and the Implications for Long-Term Resilience of the San Francisco Bay-Delta." *Water Resources Research* Volume 56 (Issue 9). [Article.] Viewed online at: <https://doi.org/10.1029/2019wr026245>. Accessed: Jan. 4, 2023.

- Stillway ME, Hammock BG, Acuña S, McCormick AR, Hung T-C, Schultz A, Young TM, and Teh SJ. 2024. "Sub-Lethal Responses of Delta Smelt to Contaminants Under Different Flow Conditions." *San Francisco Estuary and Watershed Science* Volume 22 (Issue 2). [Article.] Viewed online at: <https://doi.org/10.15447/sfews.2024v22iss2art5>. Accessed: Mar. 3, 2026.
- Swanson C, Reid T, Young PS, and Cech JJ. 2000. "Comparative Environmental Tolerances of Threatened Delta Smelt (*Hypomesus transpacificus*) and Introduced Wakasagi (*H. nipponensis*) in an Altered California Estuary." *Oecologia* Volume 123: Pages 384–390. [Article.] Viewed online at: <https://doi.org/10.1007/s004420051025>. Accessed: Mar. 3, 2026.
- Swanson C, Young PS, and Cech Jr. JJ. 1998. "Swimming Performance of Delta Smelt: Maximum Performance, and Behavioral and Kinematic Limitations on Swimming at Submaximal Velocities." *The Journal of Experimental Biology* Volume 201: Pages 333–345. [Article.] Viewed online at: <https://doi.org/10.1242/jeb.201.3.333>. Accessed: Mar. 4, 2026.
- Teh SJ, Schultz AA, Duarte WR, Acuña S, Barnard DM, Baxter RD, Garcia PAT, and Hammock BG. 2020. "Histopathological Assessment of Seven Year-classes of Delta Smelt." *Science of The Total Environment*: Volume 726: Page 138333. [Article.] Viewed online at: <https://doi.org/10.1016/j.scitotenv.2020.138333>. Accessed: Mar. 3, 2026.
- Teh SJ, Schultz AA, Ramírez-Duarte W, Acuña S, Barnard DM, Baxter RD, and Hammock BH. 2019. "Histological Analysis of 7 Year-classes of Delta Smelt." In: Schultz AA, editor. *Directed Outflow Project: Technical Report 1*. U.S. Bureau of Reclamation, Bay-Delta Office, Mid-Pacific Region. Viewed online at: <https://www.usbr.gov/mp/bdo/docs/directed-outflow-project-tech-report1.pdf>. Accessed: Mar. 3, 2026.
- Tempel T, Hartman R, Meyer S, Burdi CE, Adams J, Hammock BG, and Davis BE. In Review. "Responses of Delta Smelt in Experimental Enclosures to Different Habitats and Biofouling Mitigation Methods During the Critical Summer–Fall Period " *San Francisco Estuary and Watershed Science*. [Article.]
- Tempel TL, Baerwald M, Schreier BM, Kwan N, Pien C, Davis B, Hartman R, Meyer S, and Burdi CE. 2025. "Delta Smelt Enclosure Studies, North Delta Arc of the Upper San Francisco Estuary, CA, 2019-2024. Version 1." *Environmental Data Initiative*. [Article.] Viewed online at: <https://doi.org/10.6073/pasta/3e168eaf6b33a4e3e276b8d28d29d2a5>. Accessed: Mar. 3, 2026.

- Tibshirani R. 2018. "Regression Shrinkage and Selection Via the Lasso." *Journal of the Royal Statistical Society: Series B (Methodological)* Volume 58 (Issue 1): Pages 267–288. [Article.] Viewed online at: [10.1111/j.2517-6161.1996.tb02080.x](https://doi.org/10.1111/j.2517-6161.1996.tb02080.x). Accessed: Apr. 6, 2026.
- Tillotson M, Lee CY, and Garcia C. 2025. "Association of Delta Smelt with Other Small Pelagic Fishes Suggests the Potential for Competition and Proxy Monitoring." *Endangered Species Research* Volume 56: Pages 117–134. [Article.] Viewed online at: <https://doi.org/10.3354/esr01386>. Accessed: Mar. 3, 2026.
- U.S. Bureau of Reclamation, and California Department of Water Resources. 2023. "Delta Smelt Summer Fall Habitat Seasonal Report for WY 2022." Central Valley Project and State Water Project. Sacramento, CA, 90 pp. [Article.] Viewed online at: <https://www.usbr.gov/mp/bdo/lto/archive/apr.html>. Accessed: Mar. 3, 2026.
- United States Fish and Wildlife Service (USFWS). 2008. "Formal Endangered Species Act Consultation on the Proposed Coordinated Operations of the Central Valley Project (CVP) and State Water Project (SWP). 81420-2008-F-1481-5." United States Fish and Wildlife Service. [Report.] Viewed online at: <https://usbr.contentdm.oclc.org/digital/collection/p15911coll9/id/8737/>. Accessed: Mar. 3, 2026.
- United States Fish and Wildlife Service (USFWS). 2019. "Biological Opinion for the Reinitiation of Consultation of the Coordinated Operations of the Central Valley Project and State Water Project. Service File No. 08FBTD00-2019-F-0164." U.S. Fish and Wildlife Service. [Report.] Viewed online at: <https://www.usbr.gov/mp/bdo/docs/ba-final-biological-assessment.pdf>. Accessed: Feb. 6, 2023.
- USFWS. 2025. "USFWS Delta Smelt HGMP. Appendix 0. Appendix 0. Do Wild-origin Delta Smelt Likely Carry Hatchery Ancestry at This Point?" United States Fish and Wildlife Service, San Francisco Bay–Delta Fish and Wildlife Office. [Report].
- USFWS, Macfarlane C, Goodman D, Erly K, Huber E, Cook J, Bigham C, Peck V, Valdez S, Louwerens E, Speegle J, Hope T, Garcia G, Arrambide A, Higginson P, and Falcon J. 2025. Interagency Ecological Program and US Fish and Wildlife Service: San Francisco Estuary Enhanced Delta Smelt Monitoring Program Data, 2016-2024 ver 12. Environmental Data Initiative. [Dataset] <https://doi.org/10.6073/pasta/ae279e24eef334ee43040e9e4e71941d> Accessed: Mar 5, 2025.

- Wagner RW, Stacey M, Brown LR, and Dettinger M. 2011. "Statistical Models of Temperature in the Sacramento–San Joaquin Delta Under Climate-change Scenarios and Ecological Implications." *Estuaries and Coasts* Volume 34 (Issue 3): Pages 544–556. [Article.] Viewed online at: <https://doi.org/10.1007/s12237-010-9369-z>. Accessed: Feb. 6, 2023.
- Werner I, Deanovic LA, Markiewicz D, Khamphanh M, Reece CK, Stillway M, and Reece C. 2010. "Monitoring Acute and Chronic Water Column Toxicity in the Northern Sacramento–San Joaquin Estuary, California, USA, Using the Euryhaline Amphipod, *Hyalella azteca*: 2006 to 2007." *Environmental Toxicology and Chemistry* Volume 29 (Issue 10): Pages 2190–2199. [Article.] Viewed online at: <https://doi.org/10.1002/etc.281>. Accessed: Mar. 3, 2026.
- Whitledge GW, and Hayward RS. 1997. "Laboratory Evaluation of a Bioenergetics Model for Largemouth Bass at Two Temperatures and Feeding Levels." *Transactions of the American Fisheries Society* Volume 126 (Issue 6): Pages 1030–1035. [Article.] Viewed online at: [https://doi.org/10.1577/1548-8659\(1997\)126<1030:LEOABM>2.3.CO;2](https://doi.org/10.1577/1548-8659(1997)126<1030:LEOABM>2.3.CO;2). Accessed: Mar. 3, 2026.
- Whitley SN, and Bollens SM. 2014. "Fish Assemblages Across a Vegetation Gradient in a Restoring Tidal Freshwater Wetland: Diets and Potential for Resource Competition." *Environmental Biology of Fishes* Volume 97 (Issue 6): Pages 659–674. [Article.] Viewed online at: <http://dx.doi.org/10.1007/s10641-013-0168-9>. Accessed: Sep. 7, 2021.
- Williamshen BO, O'Rear TA, Riley MK, Moyle PB, and Durand JR. 2021. "Tidal Restoration of a Managed Wetland in California Favors Non-native Fishes." *Restoration Ecology* Volume 29 (Issue 5). [Article.] Viewed online at: <https://doi.org/10.1111/rec.13392>. Accessed: Sep. 20, 2023.
- Young MJ, Hartman R, Huntsman BM, Sadro S, Mahardja B, Burdi CE, Smith WE, Smits AP, and Nobriga ML. In Review. "Bioenergetics Modeling Informs Conservation of a "Ghost Fish" in a Hydrodynamically Structured Tidal Ecosystem" *Endangered Species Research*. [Article.]
- Zhang B, Gramacy RB, Johnson LR, Rose KA, and Smith E. 2022. "Batch-sequential Design and Heteroskedastic Surrogate Modeling for Delta Smelt Conservation." *The Annals of Applied Statistics* Volume 16 (Issue 2): Pages 816–842. [Article.] Viewed online at: <https://doi.org/10.1214/21-AOAS1521>. Accessed: Mar. 3, 2026.
- Zhang Y, Ateljevich E, Yu H-C, Wu C-H, and Yu JCS. 2015. "A New Vertical Coordinate System for a 3D Unstructured-grid Model." *Ocean Modelling* Volume 85: Pages 16–31. [Article.] Viewed online at: <https://doi.org/10.1016/j.ocemod.2014.10.003>. Accessed: Mar. 3, 2026.

- Zhang Y, Ye F, Stanev EV, and Grashorn S. 2016. "Seamless Cross-scale Modeling with SCHISM." *Ocean Modelling* Volume 21 (Issue 3): Pages 71–76. [Article.] Viewed online at: <https://doi.org/10.1016/j.ocemod.2016.05.002>. Accessed: Mar. 3, 2026.
- Zierdt Smith EL, Shrader KH, Thompson JK, Parchaso F, Gehrts K, and Wells E. 2023. "Bivalve Effects on the Food Web Supporting Delta Smelt—A Spatially Intensive Study of Bivalve Recruitment, Biomass, and Grazing Rate Patterns with Varying Freshwater Outflow in 2019." USGS Open File Report 2022-1102. 15 pages. [Report.] Viewed online at: <https://doi.org/10.3133/ofr20221102>. Accessed: Mar. 3, 2026.

A. Additional Graphs

A.1 Diagnostic Plots

Figure 58. Diagnostic plots for model of suitable Delta smelt habitat versus X2 actions, SMSCG actions, and season (Table 4, Figure 7).

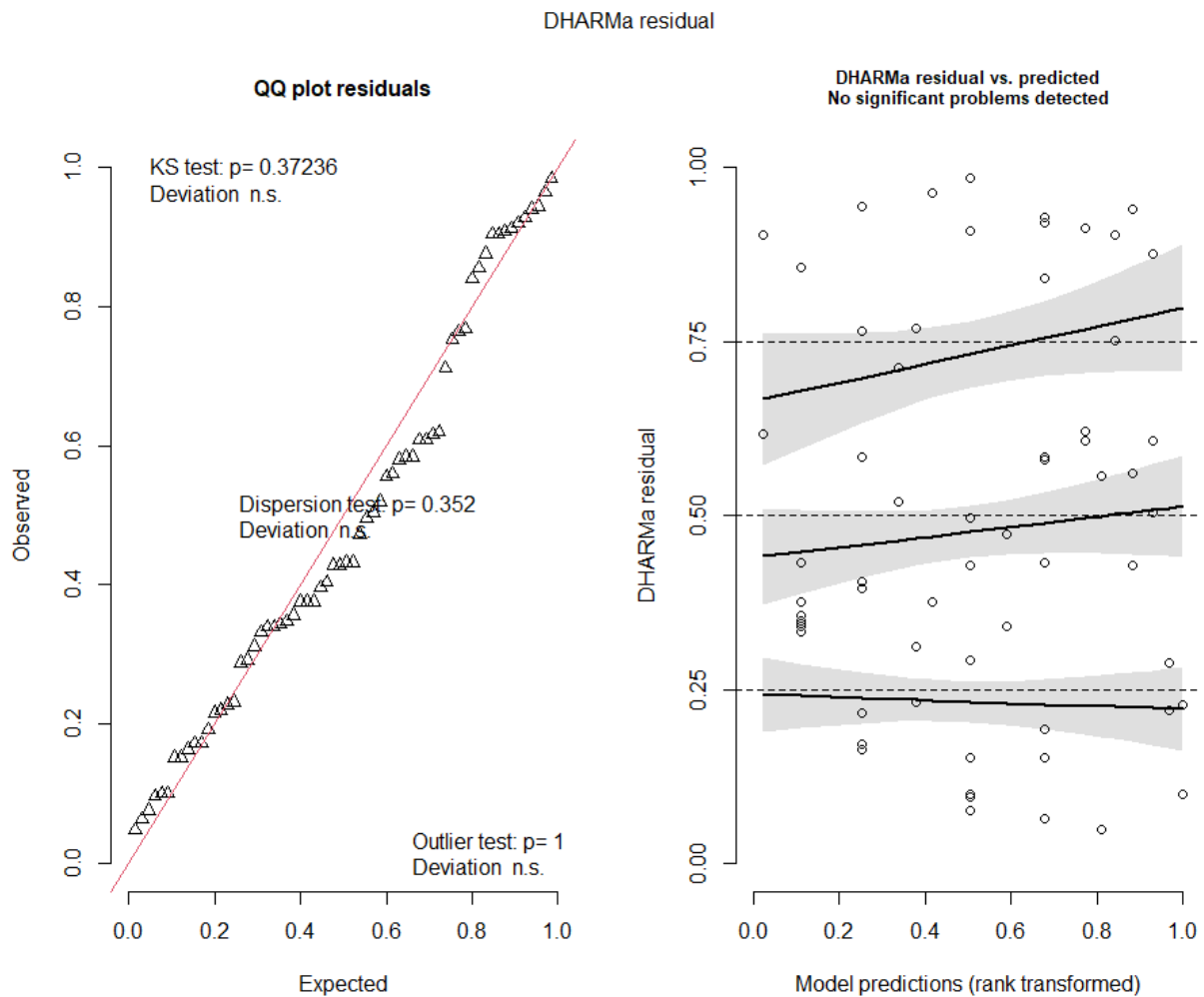


Figure 59. Diagnostic plots for the model of suitable habitat versus X2 (Table 6, Figure 8).

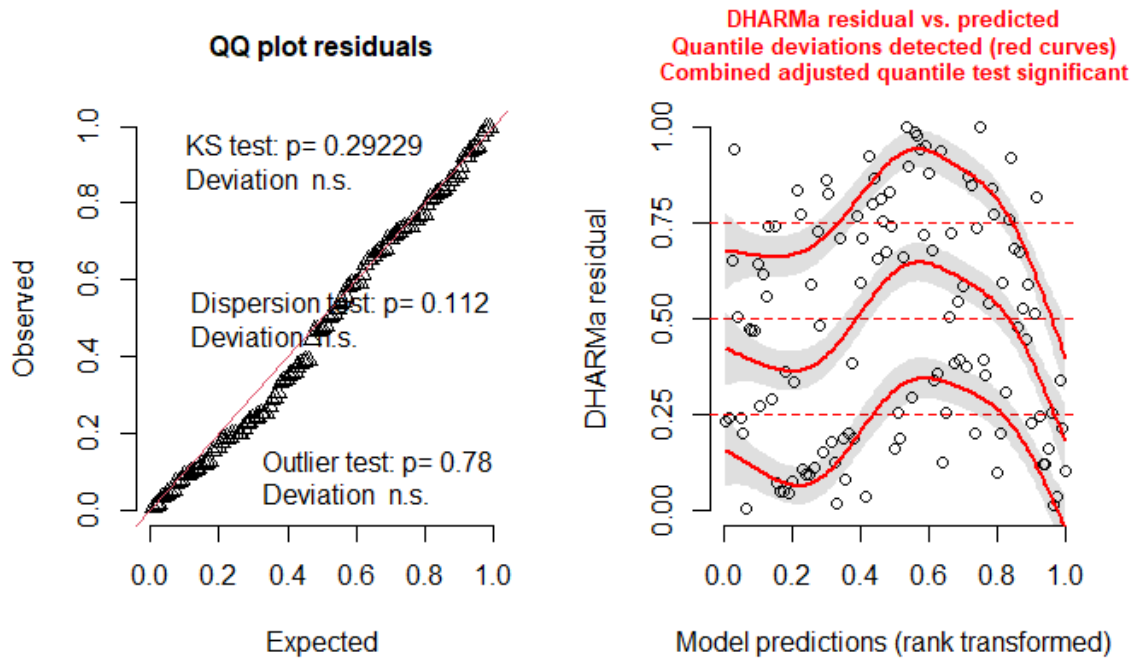


Figure 60. Diagnostic plots for model of chlorophyll fluorescence versus operation of the SMSCG.

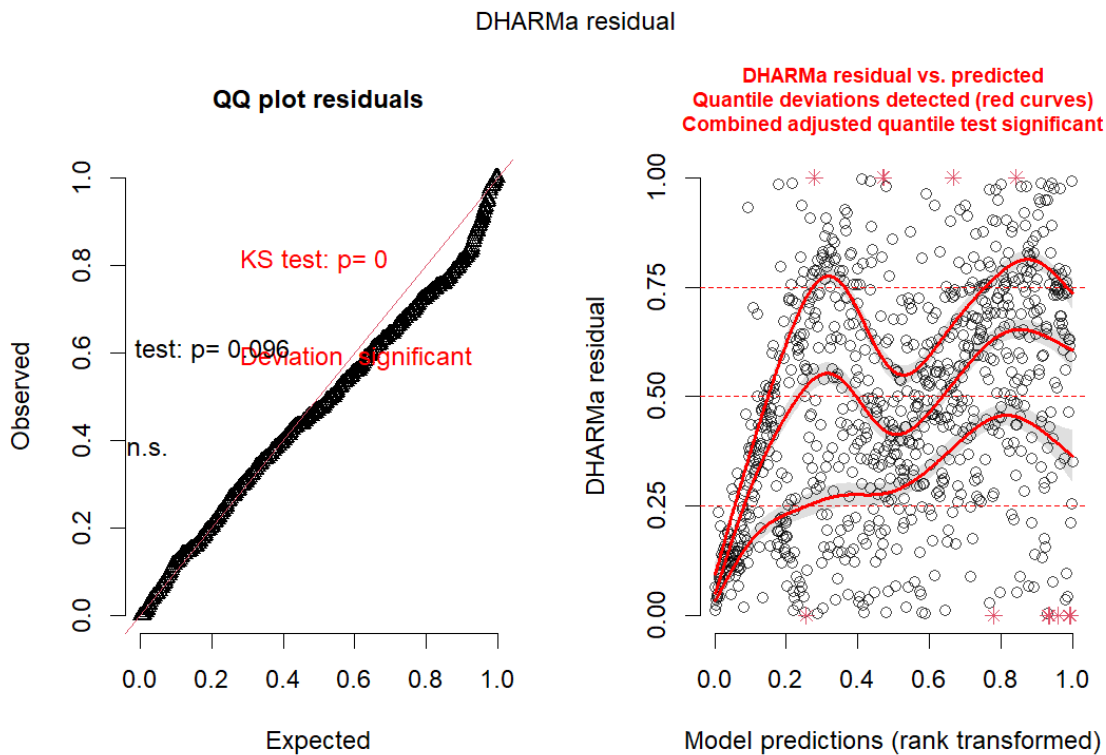


Figure 61. Diagnostic plots for lognormal generalized linear model for *Pseudodiatomus* spp. abundance versus X2 by region and season (Table 8).

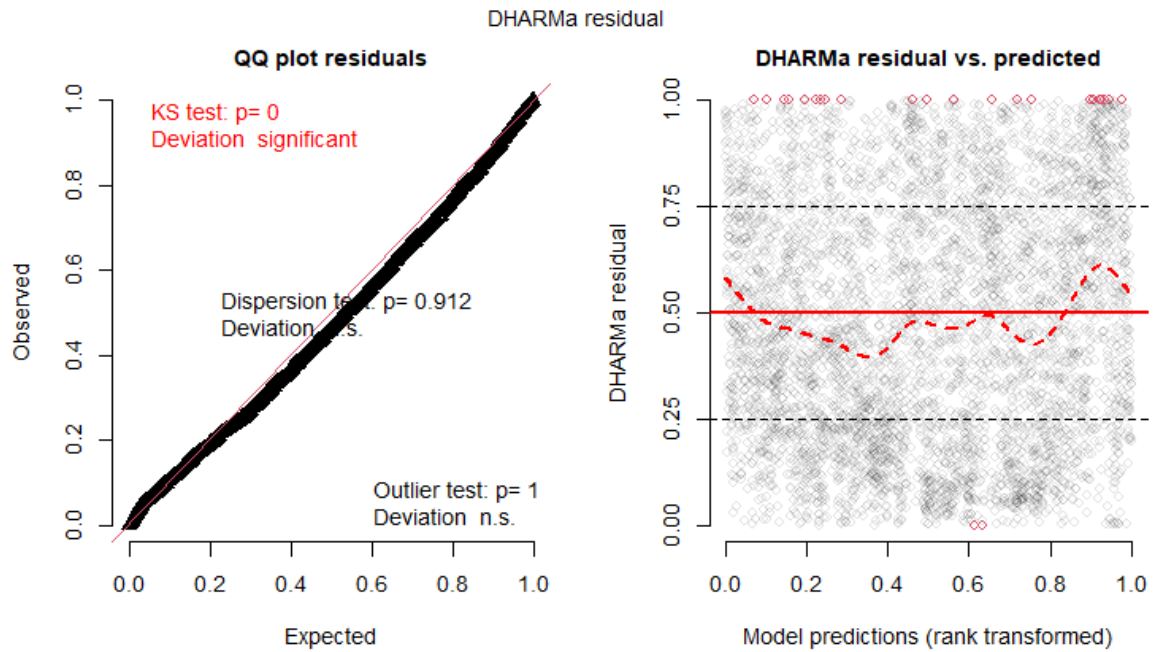


Figure 62. Diagnostic plots for model of *Pseudodiatomus* spp. abundance by salinity bin (Table 9).

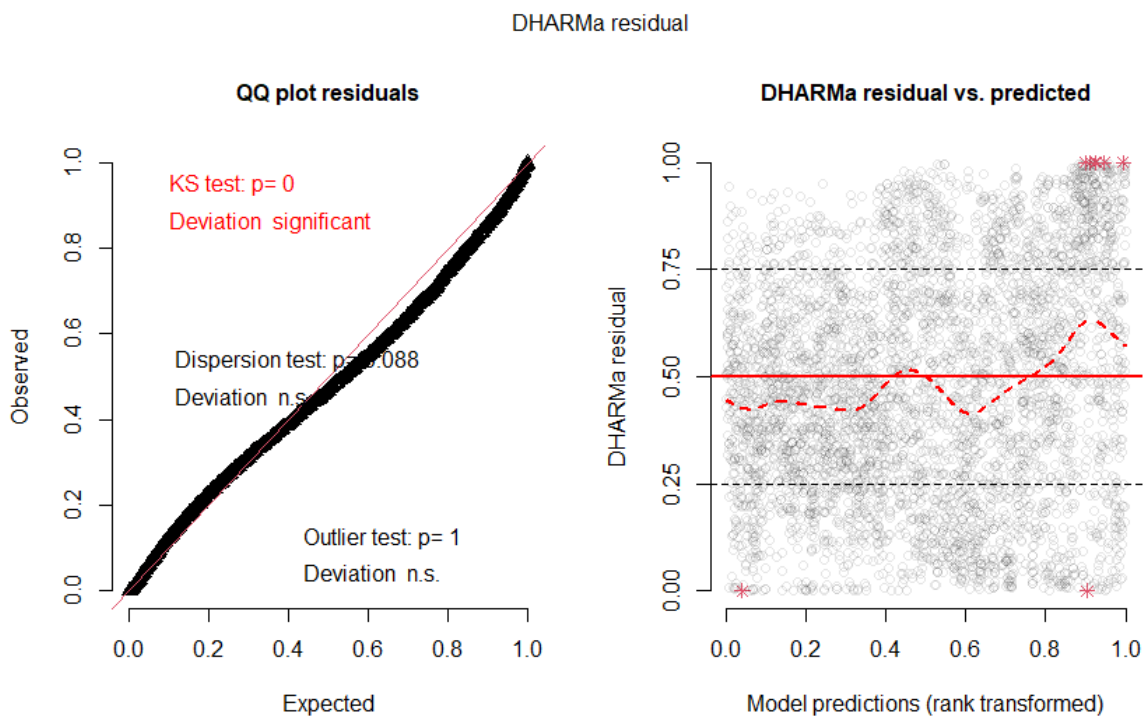


Figure 63. Diagnostic plots for GAM of *Pseudodiaptomus* abundance in Grizzly Bay versus the smooth of salinity and day of year.

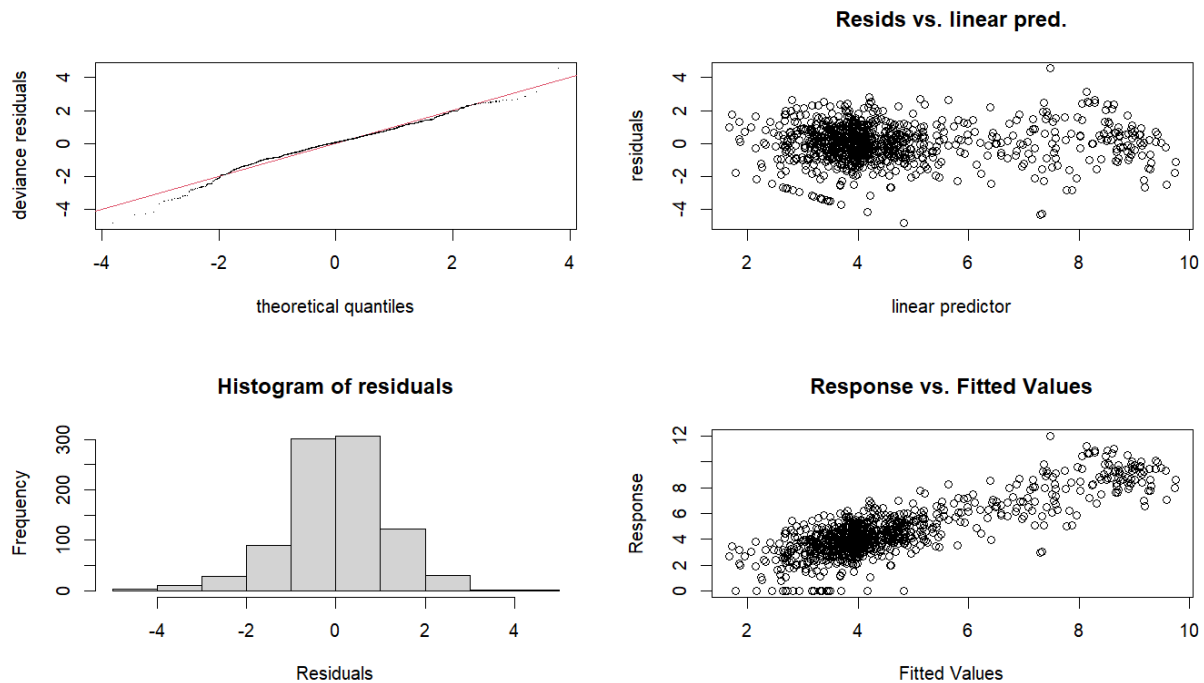


Figure 64. Diagnostic plots for GAM of *Pseudodiaptomus* abundance in Suisun Marsh versus the smooth of salinity and day of year.

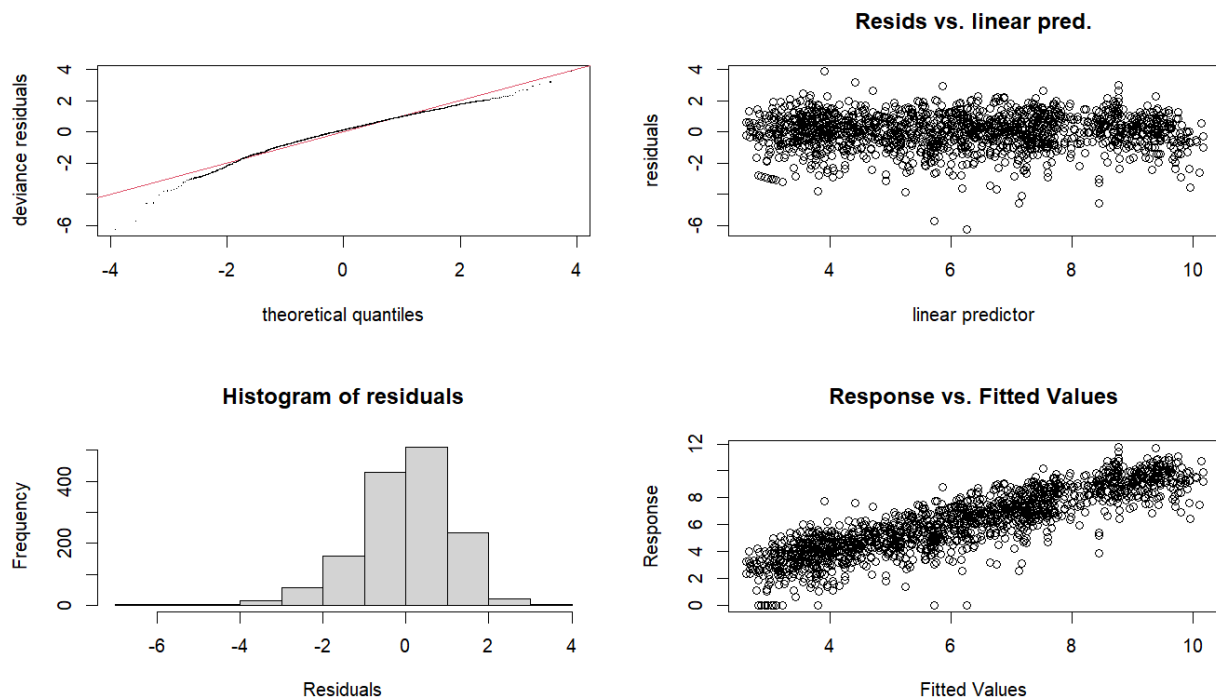


Figure 65. Diagnostic plots for GAM of *Pseudodiaptomus* abundance in Suisun Bay versus the smooth of salinity and day of year.

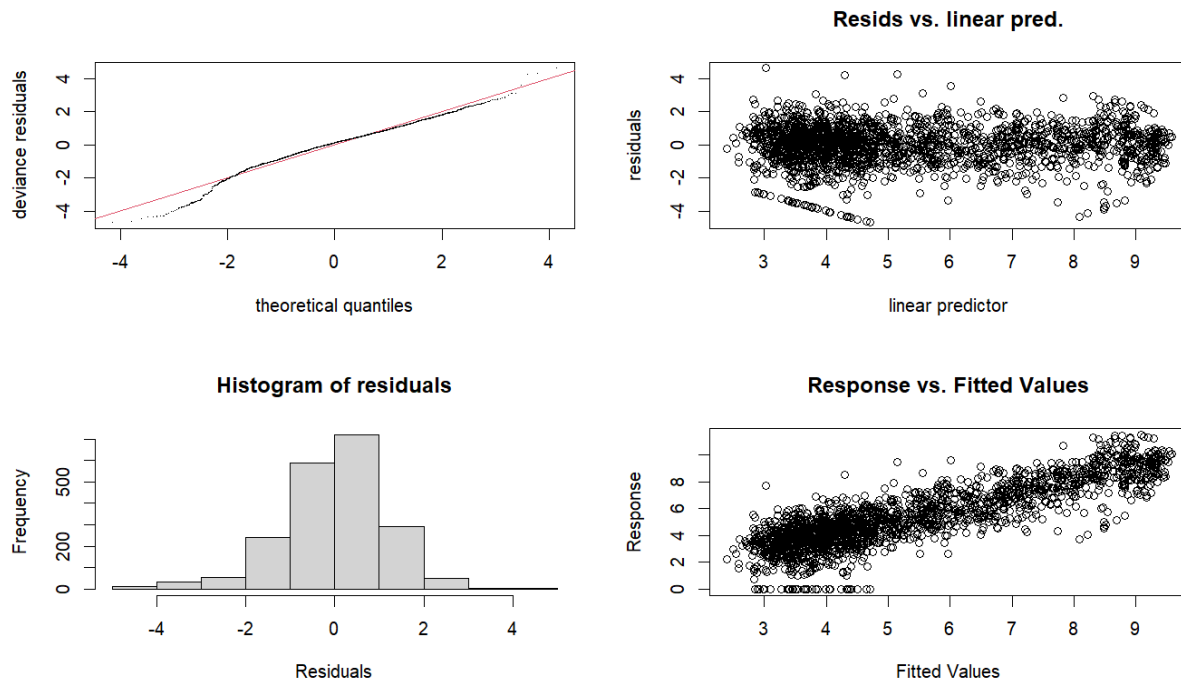
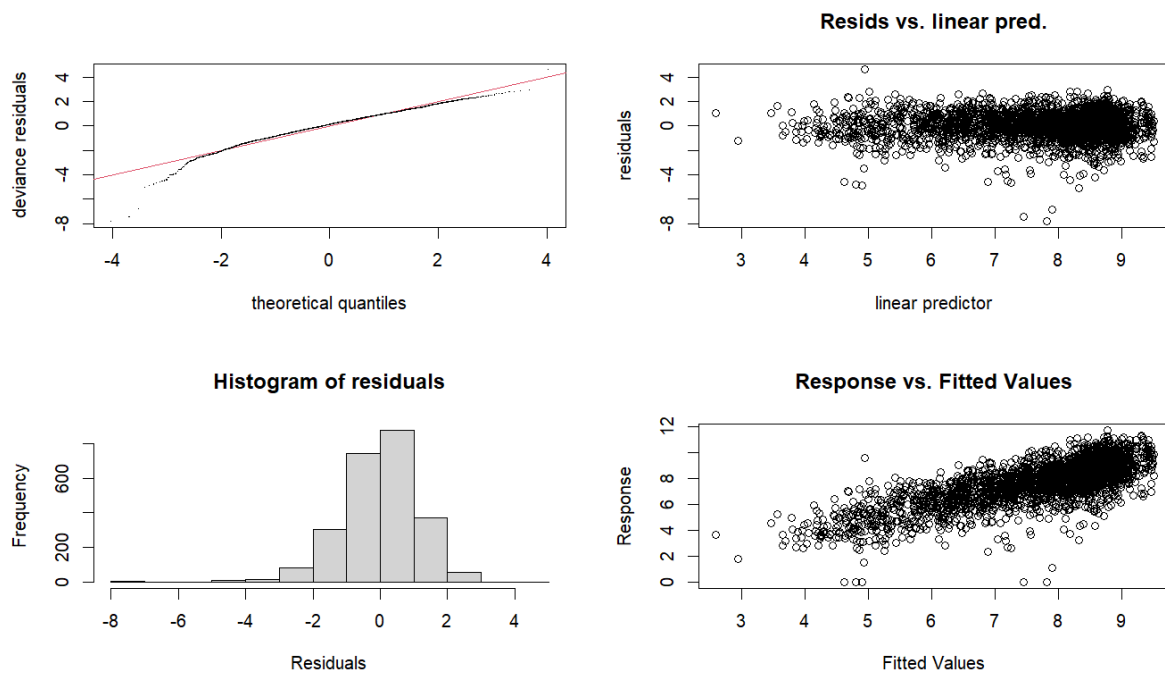
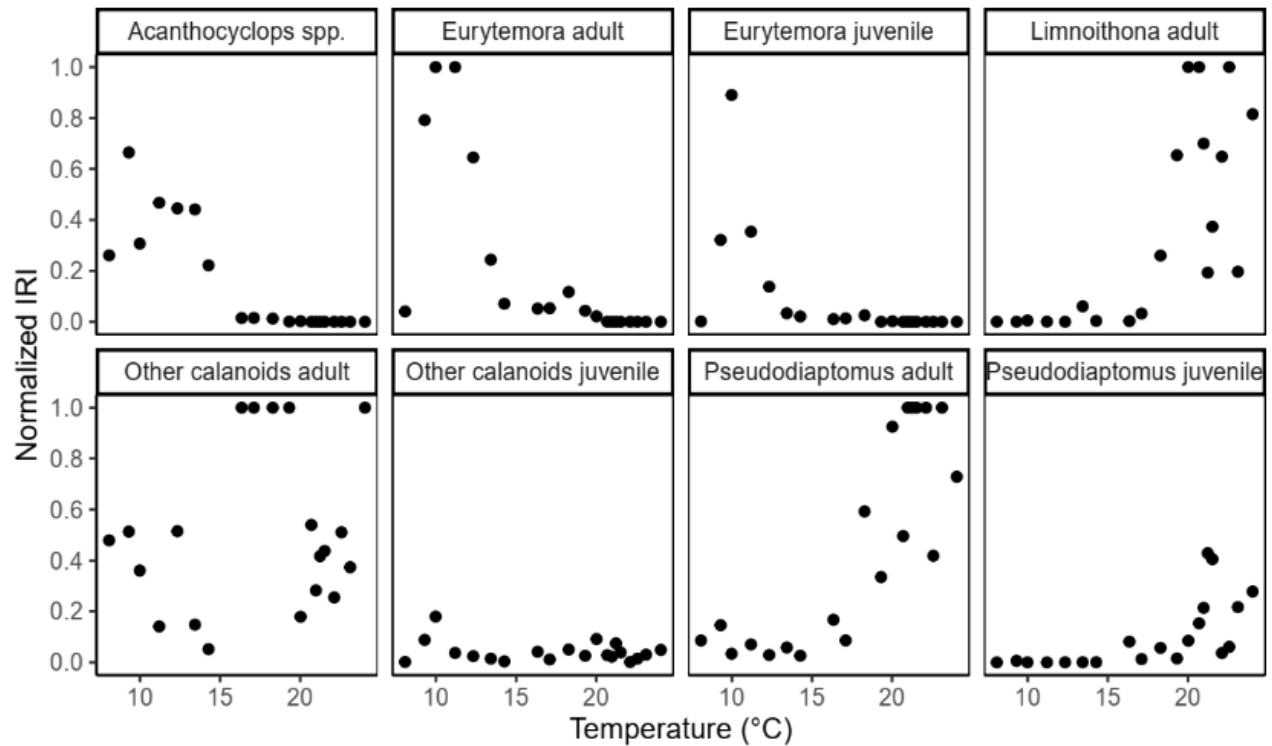


Figure 66. Diagnostic plots for GAM of *Pseudodiaptomus* spp. abundance in the lower Sacramento River versus the smooth of salinity and day of year.



A.2 Additional Diet Graphs

Figure 67. Normalized index of relative importance (Pinkas et al. 1971) of eight zooplankton taxonomic and/or life stage categories enumerated in Delta smelt gut content samples. Normalized IRI is plotted against mean values of 20 quantiles of temperature (top plot), fork length (middle plot) and by turbidity (bottom plot). Normalized IRI is calculated as $IRI/\max(IRI)$ within each quantile or season. Each abiotic quantile represents 75–76 individual DS.



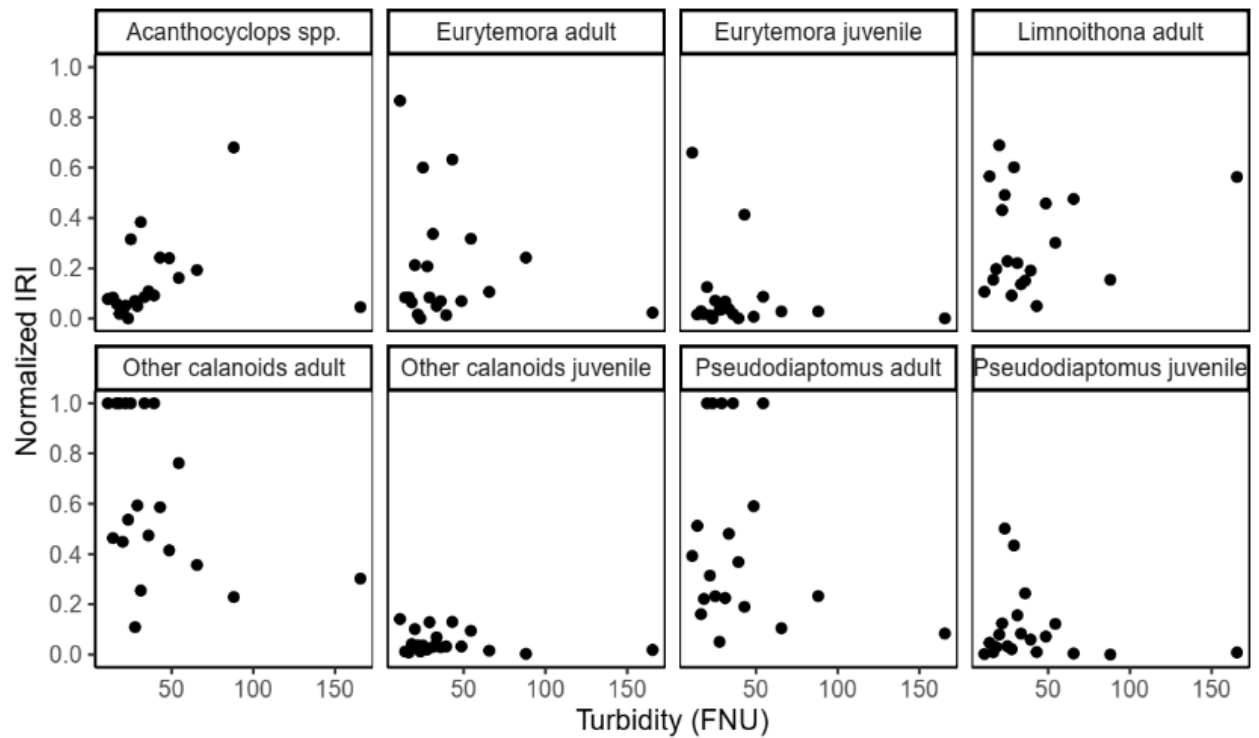
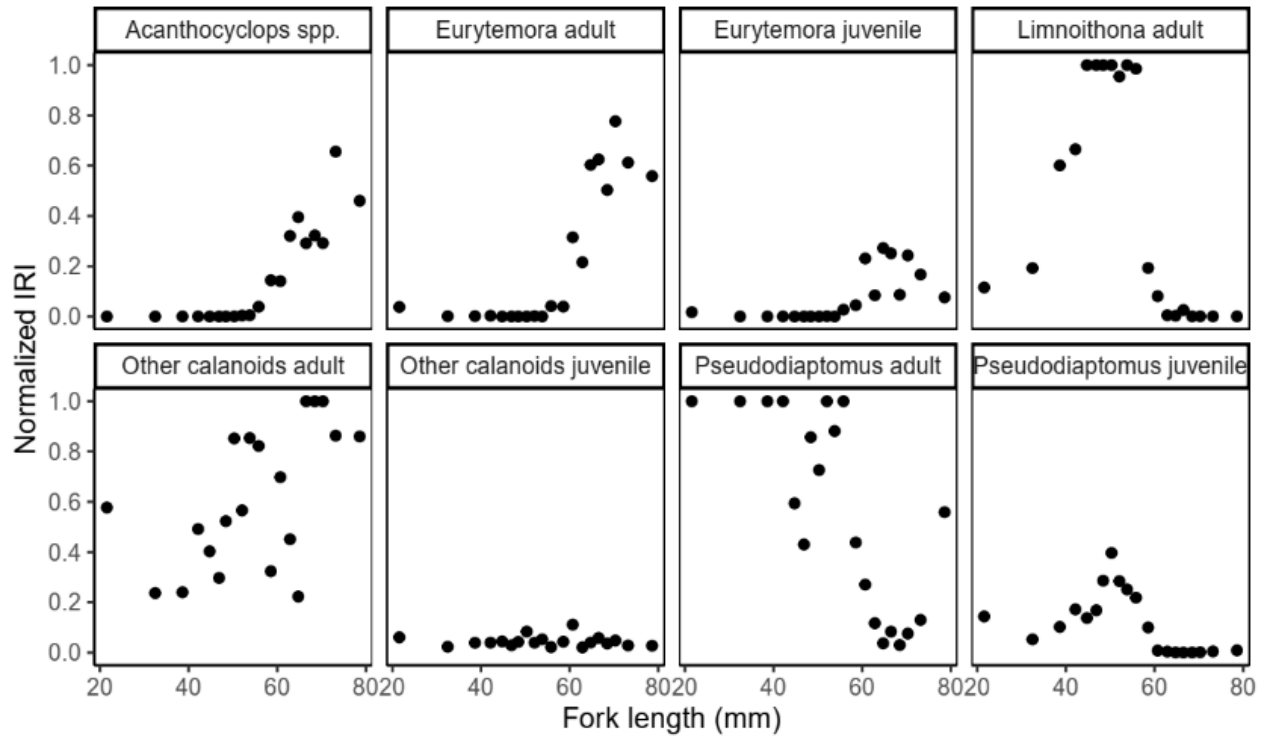


Figure 68. Feeding strategy plots (Amundson et al. 1996). Each point represents an abiotic quantile (N = 20) or season (N = 4), as in the IRI plots in Figure 57. In each panel, the x-axis is the proportion of DS individuals that consumed the indicated prey item within the corresponding quantile or season; the y-axis is the percentage of total biomass (carbon weight, μg) represented by the indicated prey item across all DS that ate at least one of that prey item by quantile or season.

